Novel Immunotherapies for EBV-Associated Cancers

Anna May Swanson

Doctor of Philosophy
The University of Edinburgh

2007

DECLARATION

I declare that all work included in this thesis is my own, except where otherwise stated. No part of this work has been, or will be, submitted for any other degree or professional qualification.

Anna May Swanson
2007

School of Biomedical Sciences
University of Edinburgh
Summerhall
Edinburgh
EH9 1QH

ABSTRACT

Epstein-Barr virus (EBV) is a gamma herpes virus persistently infecting over 90% of the adult population worldwide. It has been aetiologically linked to a number of human malignancies, including more than 90% of post transplant lymphoproliferative disease (PTLD), 50% of Hodgkin's lymphoma (HL), virtually all undifferentiated nasopharyngeal carcinoma (NPC), and approximately 10% of gastric carcinoma (GC). As EBV infection in healthy individuals is mainly controlled by virus specific cytotoxic T lymphocytes (CTLs), we hypothesise that engineering T cells with chimeric T cell receptors (cTCRs) specific for EBV latent membrane proteins (LMPs) will confer on these cells the ability to target and kill the malignant cells of cancers associated with Epstein-Barr virus. Thus, the aim of this project was generate these engineered T cells and to set up a severe combined immunodeficient (SCID) mouse model in which to test their effectiveness.

Three EBV-infected cell lines derived from HL, NPC and GC gave rise to tumours in 11 of 12 (92%), 12 of 12 (100%) and 10 of 10 (100%) SCID mice respectively, when $1x10^7$ cells were injected subcutaneously. Immunohistochemical analysis showed that the HL SCID tumours were CD4-, CD15-, CD20+, CD30+, consistent with a HL Reed-Sternberg cell phenotype, and NPC and GC SCID tumours expressed the epithelial cell marker cytokeratin. Furthermore, all tumours expressed EBV-encoded RNAs (EBERs) and LMP1. This was identical to parent cell line expression patterns, and hence growth *in vivo* did not affect cell phenotype.

T cells were successfully transduced with a retroviral vector encoding a CD19-specific cTCR (CD19-cTCR) with a mean transduction rate of 13%±6%. Transduced cells were cytotoxic for HL-derived L591 cells *in vitro*, with specific lysis of 24%±11% at an effector to target ratio of 20:1. This was significantly higher than specific lysis seen in mock transduced cells ($p>0.05$). At a tumour inoculation dose of $5x10^6$, *in vivo* sc transfer of $5x10^7$ CD19-cTCR transduced cells was able to prevent HL tumour development in 6 of 6 (100%) test mice, whereas 17 of 22 (77%) control mice and 2 of 3 (66%) mice treated with unmodified EBV-specific CTLs developed tumours. Moreover, iv transfer of $5x10^7$ CD19-cTCR transduced cells mediated complete regression of HL SCID tumours in 3 out of 6 (50%) mice.

Phage display selection experiments to isolate a single chain antibody fragment (scFv) specific for viral LMPs for incorporation in a cTCR were performed. Linear, biotinylated and cyclised biotinylated peptides derived from the external reverse turn loops of LMP2 were used as target antigens. Despite extensive testing, no reactive clones specific for the peptides were identified.

The ability of CD19-cTCR transduced cells to specifically lyse HL cells *in vitro*, and clear tumour burden *in vivo*, supports a future role for engineered T cells in the treatment of HL. Despite the lack of success in isolating a scFv for LMP2, the use of viral antigen specific, cTCR redirected T cells remains in principle a valuable therapeutic alternative for EBV-associated malignancies. The SCID models for HL, NPC and GC will provide a useful preclinical tool for investigation of their efficacy *in vivo*.

ACKNOWLEDGEMENTS

To all the people whose contributions helped me on the way to completing this thesis, my heartfelt gratitude. Thanks go to my supervisor Ingo Johannessen, for his advice and support over the course of this PhD, and also for choosing me from halfway around the world and providing me with this wonderful opportunity. Thanks also to Dorothy Crawford, whose insightful comments and suggestions kept the project on track.

Karen McAulay – the Oracle – needs a special mention, for her patience in the face of countless questions and perpetual willingness to help, as does Simon Talbot for discussions on this, that, and everything else. The past and present members of the LCMV have been a constant source of support, both scientific and of the biscuit variety, and I am indebted to them for making my time in Edinburgh so enjoyable. Thursday lunchtime lab meetings were also a source of helpful suggestions and occasional stimulating discussion. A big thank you to my thesis buddy Phoebe Wingate, who celebrated with me when things went right, commiserated when things went wrong, and took me out for coffee when all else failed. I'm glad we made it to the end together.

I am grateful to Bill Smith, Christine Forrest and Anne Woolger in the EPU for all their efforts on my behalf, and also to Shonna Johnston for assistance with flow cytometry.

It goes without saying that I could not have undertaken this PhD without the support of my family. Eternal thanks to my parents - for showing me the world and pointing me in the right direction. Their unfailing love, support and interest always buoyed my spirits. And to Elizabeth, who has achieved so much and yet made me feel like I was doing something special.

Most especially I would like to acknowledge Sam. Everything I could need or want in a friend, he is. This thesis is testament to nothing so much as his belief in me, and his ability to draw out my best efforts. Thank you.

CONTENTS

LIST OF FIGURES

LIST OF TABLES

ABBREVIATIONS

-	Negative
+	Positive
aa	Amino acid
A	Absorbance
Ab	Antibody
AIDS	Acquired immune deficiency syndrome
AP	Alkaline phosphotase
APC	Antigen presenting cell
BART	*Bam*HI A rightwards transcript
BCR	B cell receptor
BL	Burkitt's lymphoma
BMT	Bone marrow transplant
bp	Base pair
BSA	Bovine serum albumin
CAIX	Carboxy anhydrase IX
CAR	Chimeric antigen receptor
CD	Cluster of differentiation
CDR	Complementarity determining region
CML	Chronic myeloid leukaemia
CMV	Cytomegalovirus
Cp	EBV promoter C
Cr	Chromium
CSB	Cell separation buffer
CTAR	C-terminal activation region
cTCR	Chimeric T cell receptor
CTL	Cytotoxic T lymphocyte
CTLA	Cytotoxic T lymphocyte antigen
DC	Dendritic cell
DMEM	Dulbecco's Modified Eagles Medium
DMSO	Dimethyl sulfoxide
DNA	Deoxyribonucleic acid
dsDNA	Double-stranded deoxyribonucleic acid
EA	Early antigen
EBER	EBV-encoded small RNA
eBL	Endemic Burkitt's lymphoma
EBNA	EBV nuclear antigen
EBV	Epstein-Barr virus
E.coli	*Escherichia coli*
EDTA	Ethylenediaminetetraacetic acid
ELISA	Enzyme-linked immunosorbant assay
Fab	Fragment antigen binding
FAP	Fibroblast activation protein
FDA	Food and Drug Administration, USA
FBS	Foetal bovine serum
FITC	Fluorescein isothiocyanate
GC	Gastric carcinoma

GFP	Green fluorescent protein
GM-CSF	granulocyte/macrophage colony-stimulating factor
GVHD	Graft versus host disease
GVL	Graft versus leukaemia
HBSS	Hank's buffered salt solution
HIV	Human immunodeficiency virus
HHV	Human herpes virus
HL	Hodgkin’s lymphoma
HLA	Human leukocyte antigen
HRP	Horse radish peroxidase
HRS	Hodgkin Reed-Sternberg
HSV-TK	Herpes simplex virus thymidine kinase
IHC	Immunohistochemistry
Ig	Immunoglobulin
IL	Interleukin
IM	Infectious mononucleosis
INF	Interferon
ip	Intraperitoneal
IR	Internal repeat
ISH	*In situ* hybridisation
ITAM	Immunoreceptor tyrosine-based activation motif
iv	Intravenous
kb	Kilobase
LC	Langerhans cell
LCL	Lymphoblastoid cell line
LCV	Lymphocryptovirus
LD	Lymphocyte depleted
LMP	Latent membrane protein
LP	Lymphocyte predominant
MA	Membrane antigen
mAb	Monoclonal antibody
MC	Mixed cellularity
MHC	Major histocompatibility complex
MPBS	2% Marvel skim milk powder in PBS
NBF	Neutral buffered formalin
NK	Natural killer
nm	Nanometre
NPC	Nasopharyngeal carcinoma
NS	Nodular sclerosing
NTC	No template control
OD	Optical density
ORF	Open reading frame
oriLyt	EBV lytic origin of replication
oriP	EBV origin of replication
PBL	Peripheral blood leukocytes
PBMC	Peripheral blood mononuclear cell
PBS	Phosphate buffered saline
PE	Phycoerythrin
PEG	Polyethylene glycol

PSMA	Prostate-specific membrane antigen
PTLD	Post transplant lymphoproliferative disease
RBP	Recombinant signal binding protein
RNA	Ribonucleic acid
RPMI	Roswell Park Memorial Institute
SAP	SLAM-associated protein
sBL	Sporadic Burkitt's lymphoma
sc	Subcutaneous
scFv	Single chain variable fragment
SCID	Severe combined immunodeficient
SD	Standard deviation
SLAM	Signalling lymphocytic activation molecule
TAA	Tumour-associated antigen
TARC	Thymus and activation regulated chemokine
TBE	Tris borate EDTA
TBS	Tris buffered saline
TCR	T cell receptor
TGF	Transforming growth factor
Th	T helper
TNF	Tumour necrosis factor
TNFR	Tumour necrosis factor receptor
TR	Terminal repeat
T_{regs}	T regulatory cells
tu	Transducing unit
TY	Tryptone yeast
TYE	Tryptone yeast extract
UV	Ultraviolet
V	Volts
VCA	Viral capsid antigen
VEGF	Vascular endothelial growth factor
V_H	Variable heavy
V_L	Variable light
v/v	Volume per volume
Wp	EBV promoter W
w/v	Weight per volume
XLP	X-linked lymphoproliferative disease

1 Introduction

1.1 Herpesviruses

The family *Herpesviridae* contains over 200 species of virus, isolated from a range of animal hosts as diverse as humans, birds, turtles and oysters, although the viruses are rarely capable of infecting more than one species. This wide distribution and narrow specificity suggests close co-evolution between virus and host. Indeed, herpesviruses are well adapted for survival within their natural host, with virus infection persisting for the life of the host and only very rare fatal illness. Infection in heterologous or immunodeficient hosts can however result in serious disease.

Inclusion with in the herpesvirus family has historically been reliant on the architecture of the virion (see 1.1.2). All herpesviruses also share four principal biologic properties:

1. They encode enzymes used in their own nucleic acid metabolism, DNA synthesis and protein processing.
2. Viral DNA synthesis and capsid assembly occurs in the nucleus, and capsids acquire an envelope as they bud through the nuclear membrane.
3. The production of progeny virus during lytic replication invariably results in host cell death.
4. They are capable of latent infection in their natural hosts. Viral genomes in latently infected cells are maintained as circular episomes, and express a subset of viral genes (Roizman *et al*, 1992).

Despite these common characteristics, herpesviruses also diverge with respect to their biologic characteristics. Host cell range, site and mechanism of latency, and length of replication cycle can all differ (Pellett & Roizman, 2007).

1.1.1 Classification

Herpesviridae is divided into three subfamilies, the *alpha*-, *beta*- and *gammaherpesvirinae*. This classification was based initially on biological

characteristics (Roizman *et al*, 1981), but more recent evaluation of gene content and sequence similarities has upheld the divisions (Roizman & Baines, 1991). Thus far eight human herpes viruses (HHV) have been identified, and are listed in Table 1.1, along with the biological properties that define the herpesvirus subfamilies.

Table 1.1: Classification of herpes viruses, with human examples.
Adapted from Brooks *et al* (2001).

subfamily	biologic properties			human herpesvirus number & common name	
	growth cycle	cytopathology	site of latency		
alpha	short (~18hrs)	cytolytic	sensory neuron ganglia	1	Herpes simplex virus type 1
				2	Herpes simplex virus type 2
				3	Varicella-zoster virus
beta	long (~70hrs)	cytomegalic	salivary glands kidneys lymphocytes	5	Cytomegalovirus
		lymphoproliferative	lymphoid tissue	6	Human herpesvirus 6
				7	Human herpesvirus 7
gamma	variable	lymphoproliferative	lymphocytes	4	Epstein-Barr virus
				8	Kaposi's sarcoma associated herpesvirus

1.1.2 Virus structure

All herpesviruses encode genetic information in a linear double-stranded DNA (dsDNA) genome, which is contained in the toroid-shaped core of the virion (Furlong *et al*, 1972). The surrounding protein coat is made up of 162 capsomeres, and the diameter of the icosahedral nucleocapsid is approximately 125nm (Pellett & Roizman, 2007). Each virion is enclosed in a host-cell derived envelope containing viral glycoproteins. Between the nucleocapsid and the envelope is an amorphous protein tegument, which may be of varying thickness and asymmetrical distribution. The diameter of complete herpesvirus virions range from 120 to 260nm, with variation largely due to the thickness of the tegument (Pellett & Roizman, 2007). A

schematic diagram illustrating common herpesvirus structural elements is shown in Figure 1.1 panel A.

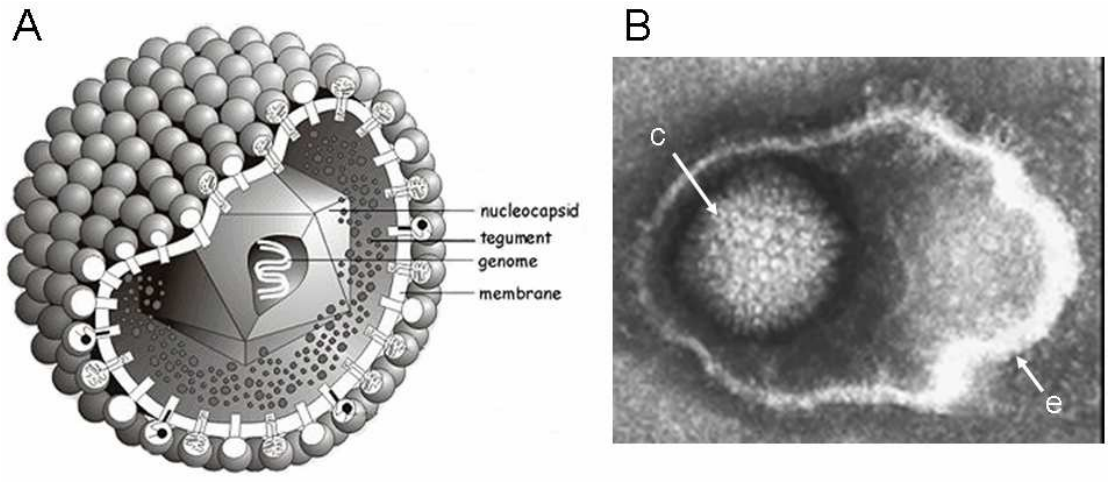

Figure 1.1: The herpesvirus virion.
Schematic diagram of a mature herpesvirus particle, indicating the nucleocapsid, tegument, genome, and membrane of the virion **(A)**. Also, an electron micrograph image **(B)** of a herpesvirus virion, with capsid **[c]** and envelope **[e]** clearly visible. Images from www.biografix.de **(A)** and www.virology.net **(B)**.

1.1.3 Genome

Herpesvirus DNA is packaged as a linear molecule, but upon release from the capsid into the host cell nucleus immediately circularises and is maintained in the cell as a circular episome. Genomes range in size from 120 to 250 kilobase pairs (kb) and encode between 70 and 200 genes. Herpesviruses can contain terminal and/or internal repeated sequences, which may vary in copy number, and some family members undergo genome rearrangements resulting in DNA isomers, for example herpes simplex virus. The majority of herpesvirus genes consist of a single open reading frame, flanked by 5' and 3' nontranslated sequence, a promoter sequence upstream of a TATA box, and a 3' polyadenylation signal. Most, although not all, are transcribed by RNA polymerase II and are unspliced. Approximately 40 'core' genes are conserved across all herpesvirus subfamilies, and all herpesviruses encode at least one gene of host cell origin (Pellett & Roizman, 2007).

1.2 Epstein-Barr virus

Epstein-Barr virus (EBV) was first discovered in 1964 following culture of Burkitt's lymphoma (BL) tumour material. In the 1950s, Dr Dennis Burkitt, a British surgeon working in East Africa, described a childhood malignancy that now bears his name (Burkitt, 1958). He noted a climatically restricted epidemiology for the disease across equatorial Africa, which led him to suggest a mosquito vector and consequently an infectious origin for the disease (Burkitt, 1962). This speculation caught the attention of British virologist Dr Anthony Epstein, who together with Yvonne Barr established the first BL-derived cell lines from tumour samples sent to them by Burkitt (Epstein & Barr, 1964). When examined by electron microscopy, herpesvirus-like particles were clearly present in a proportion of cells (Epstein *et al*, 1964). A similar electron micrograph is shown in Figure 1.1 panel B. EBV has a very narrow host range, as it is able to sustain persistent infection only in humans. However, it is transmitted with ease within the human population, with over 90% of adults being EBV seropositive (IARC, 1997).

Primary infection with EBV generally occurs in young children, and is normally asymptomatic, although infectious mononucleosis (IM) can result when primary infection is delayed until adolescence. EBV has also been aetiologically linked to a number of human malignancies, including BL, post transplant lymphoproliferative disease (PTLD), Hodgkin's lymphoma (HL), nasopharyngeal carcinoma (NPC), and gastric carcinoma (GC). EBV disease associations are covered in more depth in section 1.3.

1.2.1 EBV genome

The EBV genome is 184kb in size, has a guanine-cytosine content of 60% and a characteristic set of repeat sequences. There are tandem reiterated 0.5kb terminal repeat (TR) sequences at both ends of the genome and the unique region is divided by four 3kb reiterated internal repeats (IR) (Kieff & Rickinson, 2007). The circular viral episome is formed by covalent linking of the TRs (Lindahl *et al*, 1976). Each cell infected with EBV contains multiple copies of the episome (Sugden *et al*, 1979).

The prototype EBV, a laboratory strain designated B95-8, was first isolated in 1973 (Miller *et al*, 1973) and fully sequenced in 1984 (Baer *et al*, 1984). Sequencing was carried out using a *Bam*HI fragment library, and as a result genes, promoters, open reading frames (ORF) and polyadenylation sites are often named with reference to the restriction fragment in which transcription begins. For example, BZLF1 refers to a protein situated in the first (1) leftward (L) ORF (F) of the *Bam*HI (B) Z fragment (Z) of the EBV genome. A genome map with *Bam*HI fragments is shown in Figure 1.2.

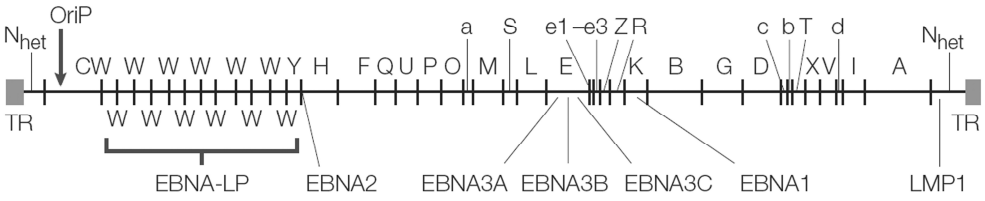

Figure 1.2: *Bam*HI fragments of the EBV genome.
*Bam*HI restriction endonuclease map of the B95-8 EBV genome. Fragments are named by size, with A being the largest and lowercase letters the smallest. Areas within the terminal repeats (TR) are designated Nhet due to the heterogeneity which results from the variable number of TRs in different virus isolates. Image adapted by permission from Macmillan Publishers Ltd: Young LS and Rickinson AB. Nature Reviews Cancer 4:757-768, copyright (2004).

EBV is subdivided into Types 1 and 2. Division is based on genome sequence, with differences in the regions encoding EBV nuclear antigens (EBNA)–LP, 2, 3A, 3B and 3C. Type 2 is more common in African populations, while Type 1 is more common in Western countries (Zimber *et al*, 1986), although both types are present worldwide. Type 1 EBV is more efficient than Type 2 at transforming lymphocytes *in vitro* (Rickinson *et al*, 1987), and delayed infection with Type 1 EBV was significantly more likely to result in IM then a Type 2 infection in a recent epidemiological study (Crawford *et al*, 2006).

1.2.2 EBV encoded transcripts and proteins

There are 84 major unique ORFs contained in the EBV genome (Baer *et al*, 1984). EBV is able to vary the combination of genes expressed in latent and lytic infection through the use of different gene promoters.

1.2.2.1 EBV encoded latent proteins and RNAs

Cells latently infected with EBV constituently express up to nine viral proteins. These are six EBV nuclear antigens (EBNA1, EBNA2, EBNA3A, EBNA3B, EBNA3C, and EBNA-LP), and three latent membrane proteins (LMP1, LMP2A, and LMP2B). Also expressed are two types of viral-encoded, but non-translated RNA, BARTs (BamHI A rightwards transcripts) and EBERs (EBV-encoded RNA). Location of EBV latent genes and promoters on the viral episome is shown in Figure 1.3.

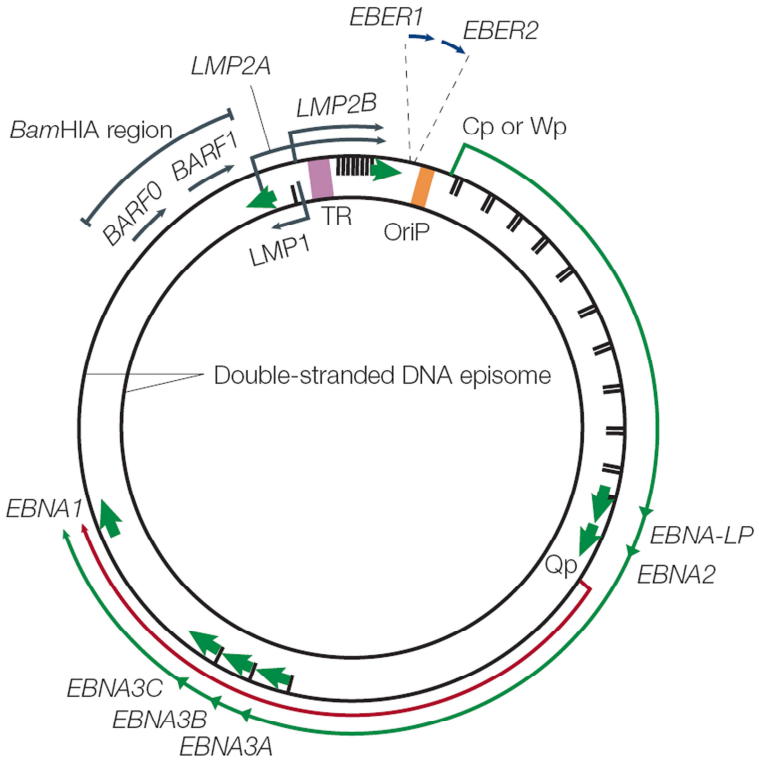

Figure 1.3: The EBV episome.
The double-stranded DNA episome of EBV, showing the location of latent antigens and promoters. Image adapted by permission from Macmillan Publishers Ltd: Young LS and Rickinson AB. Nature Reviews Cancer 4:757-768, copyright (2004).

The role and function of each latent antigen is summarised below and in Table 1.2, and reviewed in several references (Kuppers, 2003; Young & Murray, 2003; Young & Rickinson, 2004; Kieff & Rickinson, 2007).

Table 1.2: EBV latent transcripts.
The open reading frame (ORF), requirement for B cell transformation and main function of EBV antigens expressed during latency. Adapted from Johannessen & Crawford (1999) and Williams & Crawford (2006).

protein	ORF	role in transformation	main function
EBNA1	BKRF1	yes	genome maintenance
EBNA2	BYRF1	yes	viral transactivator
EBNA3A	BLFR3/BERF1	yes	EBNA2 agonist, disrupts cell cycle
EBNA3B	BERF2A/B	no	EBNA2 agonist
EBNA3C	BERF3/4	yes	EBNA2 agonist, disrupts cell cycle
EBNA-LP	BWRF1	no	cooperates with EBNA2
LMP1	BNLF1	yes	viral oncogene, survival factor
LMP2A	BARF1/BNRF1	no	survival factor
LMP2B	BNRF1	no	survival factor
EBERs	BCRF1	no	not known
BARTs	BARF0	not known	not known

EBERs

Two small, non-polyadenylated RNA transcripts, EBER1 and EBER2, are expressed in all forms of EBV latency. They localise to the nucleus, with approximately 10^4 to 10^5 copies per cell (Howe & Steitz, 1986). EBERs are not essential for EBV transformation of B cells (Swaminathan *et al*, 1991), however expression in EBV-negative BL cell lines increases tumourigenicity, promotes cell survival and induces interleukin (IL)-10 expression and thus EBERs may play a role in the pathogenesis of some EBV-associated malignancies, such as BL (Komano *et al*, 1999; Kitagawa *et al*, 2000; Ruf *et al*, 2000).

EBNA1

EBNA1 is the only viral protein translated in all forms of latency (see 1.2.2.2), and also the only EBNA found during lytic infection (Reedman & Klein, 1973). The protein has four components: an internal glycine-alanine repeat flanked by two arginine-rich domains, and a carboxy-terminal DNA binding and dimerisation domain. The two arginine-rich domains facilitate the random association of EBNA1 with chromosomal DNA, whilst the carboxy-terminal binds in a sequence-specific manner to the EBV origin of replication (oriP). These interactions are essential for EBV episome maintenance and partitioning of viral DNA into daughter cells during

mitosis (Yates *et al*, 1985; Lee *et al*, 1999). Expression of EBNA1 in the B cell compartment of transgenic mice leads to development of lymphomas, and thus EBNA1 can be considered a viral oncogene (Wilson *et al*, 1996). EBNA1 also interacts with certain viral promoters, and is thereby involved with transcriptional regulation of LMP1 and the EBNAs, including itself (Kieff & Rickinson, 2007).

Despite being expressed in all virus-infected cells and capable of raising an antibody response (Dillner *et al*, 1984), EBNA1 is a relatively poor target for cytotoxic T cells (CTL) (Rickinson & Moss, 1997). Generally, EBV-positive cells expressing only EBNA1 are resistant to CTL mediated lysis *in vitro* (Levitskaya *et al*, 1995) and CTL responses against EBNA1 are absent *in vivo* (Rickinson & Kieff, 2007). The internal glycine-alanine repeat inhibits degradation of the protein via the ubiquitin/proteosome pathway, which prevents endogenous presentation of EBNA1 peptides by major histocompatibility complex (MHC) class 1 to T cells (Levitskaya *et al*, 1997). However, EBNA1 processed exogenously is capable of eliciting a response from both cluster of differentiation (CD) 4+ and CD8+ T cells, and CTLs responsive to EBNA1 have been detected in EBV seropositive individuals (Blake *et al*, 1997; Voo *et al*, 2002).

EBNA2

EBNA2 is essential for the transformation of B cells into lymphoblastoid cell lines (LCL), inducing proliferation and blocking differentiation (Hammerschmidt & Sugden, 1989). It is a potent transactivator of both cellular and viral genes, upregulating expression of the B cell antigens CD21 and CD23 (Cordier *et al*, 1990; Wang *et al*, 1991), as well as LMP1 and LMP2 (Wang *et al*, 1990b; Zimber-Strobl *et al*, 1991). It also transactivates the viral promoter C (Cp), initiating the switch from promoter W (Wp) to Cp seen early in B cell infection, and thus plays a role in its own transcriptional regulation by this upregulation of its promoter (Puglielli *et al*, 1997). EBNA2 does not bind directly to the transcriptional elements, rather it interacts with the cellular sequence specific DNA binding protein recombinant signal binding protein (RBP)-Jκ, which is partly responsible for targeting EBNA2 to promoters (Grossman *et al*, 1994).

EBNA3

The three members of the EBNA3 family, EBNA3A, 3B and 3C are encoded on tandemly located genes and appear to have a common origin. EBNA3A and 3C are essential for B cell transformation, while EBNA3B is not (Tomkinson *et al*, 1993). All three proteins are transcriptional regulators, binding RBP-Jκ and repressing the effects of EBNA2 upregulation (Le Roux *et al*, 1994; Robertson *et al*, 1996). EBNA3B also upregulates the cytoskeletal protein vimentin and the activation antigen CD40, but down regulates the BL associated antigen CD77 in BL cell lines (Silins & Sculley, 1994). EBNA3C upregulates CD21 and acts with EBNA2 to coactivate the LMP1 promoter (Allday & Farrell, 1994; Marshall & Sample, 1995). EBNA3A and 3C also repress activation of the Cp promoter (Cludts & Farrell, 1998; Radkov *et al*, 1999).

EBNA-LP

The EBNA leader protein (LP) is so named as its coding sequence is included as the leader of each EBNA mRNA transcript (see Figure 1.3). It is not absolutely required for B cell transformation, but it does contribute to the efficient outgrowth of LCLs (Allan *et al*, 1992). EBNA-LP also interacts with EBNA2, coactivating the Cp and LMP1 promoters (Harada & Kieff, 1997).

LMP1

The major transforming protein of EBV, LMP1 is essential for EBV-induced transformation of B lymphocytes *in vitro* (Kaye *et al*, 1993). It is an integral membrane protein with a short amino terminal domain, six hydrophobic transmembrane domains joined by short reverse turns, and a 200 amino acid (aa) carboxy terminus signalling domain (Figure 1.4). The signalling domain contains two functional sequences known as C-terminal activation regions (CTARs), identified by their ability to activate the nuclear factor (NF)-κB pathway (Huen *et al*, 1995). LMP1 post-translationally inserts into cell membranes, primarily the plasma membrane (Hennessy *et al*, 1984). Both terminal domains are cytoplasmic, and at least one of the three outer reverse turn loops is exposed on the cell surface (Liebowitz *et al*, 1986). The protein self-aggregates in the plasma membrane, which appears to be a property of the multiple transmembrane domains, often forming into a single cap-like structure (Liebowitz *et al*, 1986).

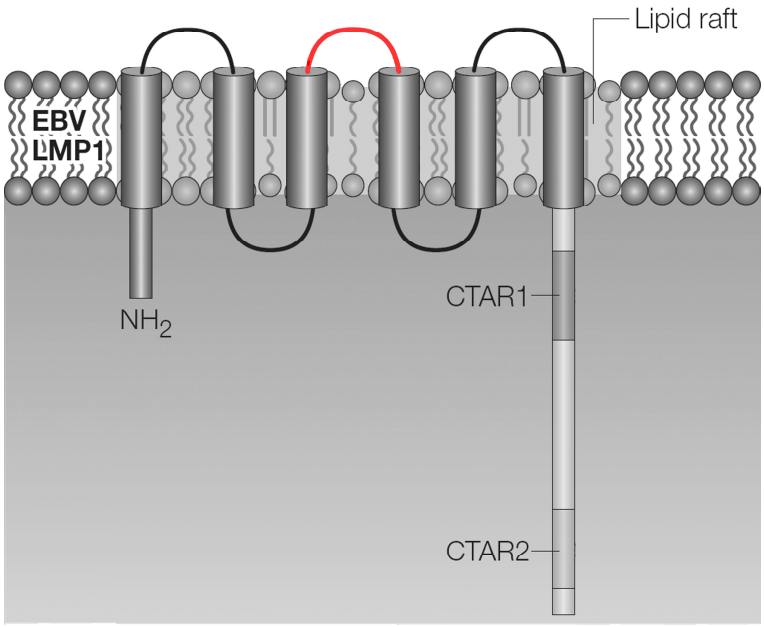

Figure 1.4: Structure of LMP1.
Schematic of LMP1, showing orientation within a cell membrane. LMP1 has a cytoplasmic amino-terminal domain, six hydrophobic transmembrane domains joined by short reverse turns, three of which are extracellular, and a carboxy-terminal cytoplasmic signalling domain containing two C-terminal activation regions (CTARs). The sequence highlighted in red was used as a target peptide in phage display selections (see Figure 5.14). Image adapted by permission from Macmillan Publishers Ltd: Young LS and Rickinson AB. Nature Reviews Cancer 4:757-768, copyright (2004).

Functional studies have shown LMP1 operates as a member of the tumour necrosis factor receptor (TNFR) superfamily. It resembles CD40, another member of the TNFR superfamily, and is able to partially substitute for CD40 *in vivo*, providing activation and differentiation signals to B cells (Uchida *et al*, 1999). LMP1 constituently activates several downstream signalling pathways including the NF-κB pathway, JNK/AP-1, p38/MAPK, and JAK/STAT pathways. It is activation of the NF-κB pathway which contributes to many of the phenotypic consequences of LMP1 expression, such as upregulation of cell surface adhesion molecules (CD11a/CD18, CD54, CD58) and activation antigens (CD21, CD23, CD40) (Wang *et al*, 1990a), and induction of anti-apoptotic proteins (*bcl-2*, *A20*) (Henderson *et al*, 1991). LMP1 also downregulates the pro-apoptotic genes such as *Bax* (Dirmeier *et al*, 2005) and

upregulates cytokine production (IL-6, IL-8, IL-10) (Eliopoulos *et al*, 1999). The LMP1 transmembrane domains, for homoaggregation, and at least one of the two CTARs within the carboxy terminus signalling domain, are required for NF-κB activation (Huen *et al*, 1995; Floettmann & Rowe, 1997). LMP1 also affects the growth of EBV infected epithelial cells, inhibiting differentiation and inducing morphological changes in some cell lines (Dawson *et al*, 1990; Fahraeus *et al*, 1990), although it was able to induce tumourigenicity without inhibiting differentiation in others (Nicholson *et al*, 1997). Expression of LMP1 in the skin of transgenic mice also induced epidermal hyperplasia and altered keratin gene expression (Wilson *et al*, 1990).

LMP1 is transcribed in lytic as well as latent infection. During late lytic infection a truncated LMP1 containing only the last two transmembrane and the intracellular carboxy terminus domain is also transcribed (Hudson *et al*, 1985). This truncated protein does not have the transforming ability of full length LMP1 (Baichwal & Sugden, 1989). Detection of truncated but not full length LMP1 in pure virus preparations and also immediately after infection suggests it is incorporated into virions and thus may have a role to play in newly infected cells (Erickson & Martin, 1997). It has also been suggested that LMP1 functions in the maintenance of latency *in vivo*, as it has been shown to bind the viral transactivating lytic protein BZLF-1 in cells that do not express EBNA2 (Adler *et al*, 2002).

LMP2

The LMP2 gene spans the fused terminal repeats of the EBV episome, and thus can only be transcribed when the genome is circularised (Laux *et al*, 1988). It encodes two distinct proteins, LMP2A and LMP2B, which share 12 hydrophobic transmembrane domains and a 27 aa cytoplasmic carboxy terminal domain (Figure 1.5). LMP2A also contains a 119 aa amino terminal cytoplasmic domain not found in LMP2B (Sample *et al*, 1989). Neither LMP2A nor LMP2B are essential for B cell transformation *in vitro*, although LMP2A is transforming in epithelial cells (Scholle *et al*, 2000). Both LMP2s are under the transcriptional control of EBNA2, although cellular factors can substitute in its absence.

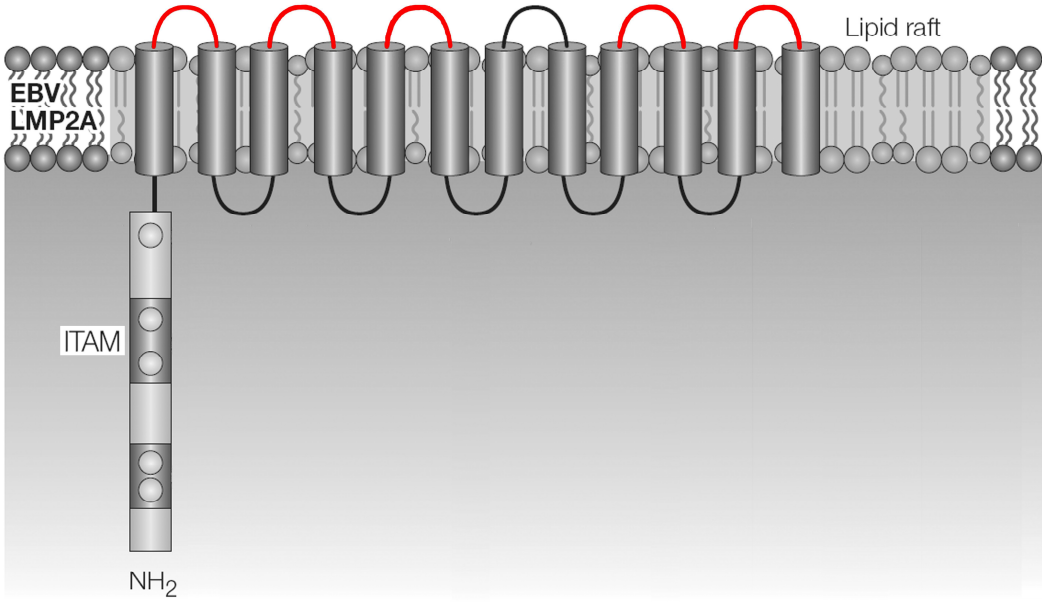

Figure 1.5: The structure of LMP2.
Schematic of LMP2, showing orientation within a cell membrane. LMP2 has twelve hydrophobic transmembrane domains joined by short reverse turns, six of which are extracellular. The amino-terminal cytoplasmic signalling domain is unique to LMP2A, and not present in LMP2B. It contains an immunoreceptor tyrosine-based activation motif (ITAM) which binds lyn and syk tyrosine kinases. Tyrosine residues in the amino-terminal domain are indicated by circles. The sequences highlighted in red were used as target peptides in phage display selections (see Table 5.2). Image adapted by permission from Macmillan Publishers Ltd: Young LS and Rickinson AB. Nature Reviews Cancer 4:757-768, copyright (2004).

The amino terminal cytoplasmic domain unique to LMP2A contains an immunoreceptor tyrosine-based activation motif (ITAM) (Miller *et al*, 1994). The ITAM binds lyn and syk tyrosine kinases, sequestering them from the B cell receptor (BCR) and thus inhibiting antigen stimulated B cell activation and consequently EBV progression into lytic replication (Miller *et al*, 1995). In the absence of the BCR, LMP2A can mimic its actions and provide growth and survival signals to B cells (Caldwell *et al*, 1998; Mancao & Hammerschmidt, 2007). LMP2 forms aggregates in the plasma membrane of B cells, co-localising with LMP1 (Longnecker & Kieff, 1990). It has been suggested that the function of LMP2B may be to modulate spacing of the LMP2A signalling domains in these plasma membrane aggregates (Longnecker & Miller, 1996).

BARTs

Highly spliced polyadenylated RNAs known as BARTs are abundantly expressed during EBV latency. Their function remains unclear, but they have been identified in

NPC (Hitt *et al*, 1989), BL (Tao *et al*, 1998) and HL (Deacon *et al*, 1993), as well as in latently infected healthy individuals (Chang *et al*, 1999) and thus may play a role in viral persistence. BARTs contain three ORFs which could potentially encode protein, but reports on translation of BARTs are inconsistent.

1.2.2.2 Latency programs

Latent infection with EBV is characterised by differential expression of latent proteins, which result from the use of alternative promoters. These expression patterns are termed the latency I or latency program, latency II or default program, and latency III or growth program, and are characteristic of certain EBV-associated diseases (Rowe *et al*, 1992). Latent infection of B cell in healthy seropositive individuals is designated latency program 0. EBV antigen expression, promoter usage and disease associations are shown in Table 1.3.

Table 1.3: EBV latency programs.
The gene expression patterns, EBNA1 promoter and human diseases associated with EBV latency programs. Adapted from Crawford (2001), Rickinson & Kieff (2007), and Straathof *et al* (2003). [*variable EBNA1 expression in healthy seropositive individuals; **expression of LMP2A observed in a proportion of GC cases]

latency program	genes expressed	EBNA1 promoter	disease association
Latency 0	EBERs EBNA1* LMP2A BARTs	Qp	
Latency I ***latency***	EBERs EBNA1 BARTs	Qp	Burkitt's lymphoma Gastric carcinoma **
Latency II ***default***	EBERs EBNA1 LMP1 and/or LMP2A BARTs	Qp	Hodgkin's lymphoma Nasopharyngeal carcinoma T cell lymphomas
Latency III ***growth***	EBERs EBNA1 EBNA2 EBNA3A, 3B, 3C LMP1, 2A, 2B EBNA-LP BARTs	Cp/Wp	Lymphoblastoid cell lines *in vitro* Infectious mononucleosis Post transplant lymphoproliferative disease

1.2.2.3 Lytic replication

The exact conditions needed *in vivo* to initiate a switch from latent to lytic infection remain unclear. *In vitro*, around 2 to 10% of cells in LCL cultures spontaneously enter the lytic cycle (Henle & Henle, 1966). Lytic replication *in vitro* can also be induced by surface immunoglobulin (Ig) crosslinking or phorbol ester treatment. During lytic replication, the EBV genome is amplified 100- to 1000-fold (Hammerschmidt & Sugden, 1988) and progeny virus is released, resulting in host cell death.

EBV lytic replication is controlled by a separate set of genes to those involved with latency. These are expressed consecutively, in groups of immediate early, early and late genes, as outlined below.

Immediate early genes

Immediate early gene products are required for transactivation of lytic replication (Cox *et al*, 1990). The two principle immediate early genes are BZLF1 and BRLF1. Their gene products, the proteins ZEBRA and Rta, coordinately upregulate expression from early EBV promoters (Chevallier-Greco *et al*, 1986). ZEBRA also binds to the lytic origin of replication (oriLyt), inducing viral replication, and can downregulate the latency III promoter Cp (Kenney *et al*, 1989). Rta activates transcription of the viral DNA polymerase, BALF5 (Liu *et al*, 1996).

Early genes

EBV early genes encode at least 30 proteins, most of which are enzymes involved in genome replication. BALF2 is a DNA binding protein important in viral DNA replication (Fixman *et al*, 1992). BHRF1 has homology to the cellular *bcl-2* gene, and potentially works to prevent apoptosis in lytic infection (Henderson *et al*, 1993). The viral DNA polymerase, which is essential for lytic replication of the EBV genome, is also an early gene (Hammerschmidt & Sugden, 1988). Detection of serum antibodies against immediate early and early proteins is used in the diagnosis of IM. Gene products include those of BZLF1, BALF2 and BHRF1, which are collectively termed early antigen (EA).

Late genes

The EBV late genes encode structural glycoproteins as well as proteins involved in cleavage of the progeny virus DNA concatamers, and packaging, envelopment and egress of virions. The major viral structural proteins are the gp350/220 (from ORF BLLF1), and the gp85/25/42 (from ORFs BKRF2, BZLF2 and BXLF2) complexes. These proteins are also involved in attachment and entry of the virion to the host cell, with gp350/220 facilitating virion attachment to B cells via CD21 (Tanner *et al*, 1987), and gp85/25/42 mediating viral fusion via human leukocyte antigen (HLA) class II molecules (Li *et al*, 1995). Detection of serum antibodies against viral capsid antigen (VCA), and membrane antigen (MA), are also used in the diagnosis of IM. VCA is comprised of a range of virus nucleocapsid proteins, while antibodies against MA are generally specific for gp350, and to a lesser extent gp220 and gp85.

1.2.3 EBV infection

1.2.3.1 Cell tropism

In a healthy human host, EBV exhibits a distinct cell tropism, infecting lymphocytes. Lymphocyte infection is generally found in B cells, and although EBV infection of T and natural killer (NK) cells has been seen it is generally restricted to disease states (Kanegane *et al*, 1996; Kanegane *et al*, 1998). There is also evidence for EBV infection of monocytes and macrophages (Shimakage *et al*, 1999; Savard *et al*, 2000). Circulating infected B cells are rare in healthy carriers, with between 1 and 50 EBV-positive cells per million B cells (Khan *et al*, 1996), and are generally of the memory phenotype, that is surface Ig-positive but surface IgD-negative (Babcock *et al*, 1998).

Definitive proof for EBV infection of epithelial cells in healthy individuals has yet to be found. Evidence supporting a role for epithelial infection by EBV includes the presence of viral DNA, mRNA and protein in explant cultures of tonsils from healthy seropositive individuals (Pegtel *et al*, 2004), and the presence of EBV genomes in dysplastic epithelial cells adjacent to gastric adenocarcinomas (Shibata & Weiss, 1992). The presence of EBV in NPC cells and oral hairy leucoplakia (OHL) lesions demonstrates that EBV is capable of epithelial infection under certain conditions

(Klein *et al*, 1974; Greenspan *et al*, 1985). *In vitro*, primary epithelial cells are generally EBV resistant, although some cell lines can be infected.

1.2.3.2 Infection of B cells

EBV preferentially infects resting B cells, attaching to cells via CD21, also known as the C3d complement receptor or complement receptor 2 (Fingeroth *et al*, 1984; Weis *et al*, 1984). The EBV envelope glycoprotein complex gp350/220 acts as the CD21 ligand (Nemerow *et al*, 1987). Monoclonal antibodies to CD21 block viral infection (Fingeroth *et al*, 1984), however EBV BLLF1-deletion mutants which lack gp350/220 are infectious, albeit with reduced efficiency, indicating that gp350/220-CD21 binding is not essential for infection with EBV (Janz *et al*, 2000). The heterotrimer of gp85/25/42 mediates fusion of the virus envelope with the cell membrane (Li *et al*, 1995). Gp42 is an essential component of the trimer, and its association with HLA Class II molecules as coreceptors for fusion plays a critical role in infection (Spriggs *et al*, 1996; Wang & Hutt-Fletcher, 1998; Haan *et al*, 2000). *In vitro* infection of B cells with EBV results in the establishment of LCLs, which are continually cycling and capable of proliferating indefinitely (Pope *et al*, 1968; Steel *et al*, 1977; Tosato *et al*, 1985).

Circularisation of the EBV genome occurs around 12-16 hours post infection when measured during *in vitro* experiments (Kieff & Rickinson, 2007). Of the multiple linear copies released into the cell, only one copy is circularised, resulting in a clonal population of infected cells (Sugden *et al*, 1979). Infection drives the resting B cell into G1, then S-phase, and the circular episome is replicated whilst linear copies are lost. EBNA2 and EBNA-LP are the first viral genes to be expressed, with gene products detectable by about 12 hours post infection (Alfieri *et al*, 1991). Initially, EBNA2 is under the control of the Wp promoter, but a switch to Cp occurs at around 36 hours, concurrent with expression of the remaining EBNAs and LMP1 (Woisetschlaeger *et al*, 1989; Woisetschlaeger *et al*, 1990). LMP2A and 2B are not detected for up to 70 hours post infection, the time when EBERs transcripts also reach substantial levels (Alfieri *et al*, 1991).

Infection of primary B cells with EBV also results in a range of phenotypic changes, similar to those seen with antigen activation of cells, including cell clumping, increased villous projections and increased vimentin expression. There is also upregulation of the cell surface antigens CD21, CD23, CD39, CD40, CD44, and HLA class II; increase in the production of cytokines Il-6, IL-8 and IL-10; and increased expression of the adhesion molecules CD11a/CD18 (LFA-1), CD54 (ICAM-1), and CD58 (LFA-3) (Wang *et al*, 1988; Eliopoulos *et al*, 1999; Kieff & Rickinson, 2007).

1.2.3.3 Infection of epithelial cells

Epithelial cells generally do not express CD21, nor do they have HLA class II molecules on their surface. Therefore, entry of EBV into epithelial cells is evidently via a different method to B cells, although the exact mechanism remains unclear. Using recombinant EBV carrying a neomycin resistant gene, both CD21-dependent and -independent infection of epithelial cell lines has been shown *in vitro* (Yoshiyama *et al*, 1997; Fingeroth *et al*, 1999). Infection is reliant on gp85/25 complexes, which do not include the gp42 component essential for B cell infection (Li *et al*, 1995; Molesworth *et al*, 2000). Interaction between the viral BMRF2 protein and β_1 or $\alpha_5\beta_1$ on the basolateral surface of epithelial cells has also been suggested as an alternative CD21-independent mediator of viral entry (Tugizov *et al*, 2003). *In vitro*, efficient cell to cell infection from EBV-infected LCLs to epithelial cell lines derived from a range of carcinomas has been described (Imai *et al*, 1998), as has transfer of virus from B cell membranes to epithelial cells (Shannon-Lowe *et al*, 2006). This process requires cell to cell contact and is CD21-independent, although induction of CD21 expression enhanced infection efficiency (Chang *et al*, 1999). Once the initial infection is achieved, it is possible that cell to cell spread amongst epithelial cells occurs (Tugizov *et al*, 2003).

1.2.4 EBV primary infection and persistence *in vivo*

EBV infection usually occurs via the oral route, with infectious virus particles shed in saliva (Gerber *et al*, 1972). Primary infection generally occurs in young children, with seroprevalence increasing with age until over 90% of adults are seropositive.

Primary infection is normally asymptomatic, although a self-limiting disease, IM, occurs in 25-50% of cases where primary infection occurs in adolescence (Niederman *et al*, 1970; Sawyer *et al*, 1971; Crawford *et al*, 2006). In IM, primary infection is brought under control by a strong CD8+ CTL response to both latent and lytic antigens (Khanna & Burrows, 2000). The production of EBV-specific antibodies also helps limit the spread of infectious virus. These immune responses are not able to completely eliminate EBV from the body, and a persistent latent infection is established.

The identity of the EBV primary target cell and reservoirs of persistent infection *in vivo* remain controversial. Two hypothetical cycles of infection have been proposed, and are outlined below.

B cell hypothesis

EBV enters the host in saliva and infects naïve B cells. Waldeyer's ring is a band of lymphoid tissue in the throat comprising the palatine, lingual and pharyngeal tonsils. Here the epithelium of the oropharynx dips deeply into the underlying lymphoid tissue to form structures known as crypts, where the epithelial layer is not so tightly knit together and lymphoid cells are able to infiltrate (Perry & Whyte, 1998). This allows EBV in saliva direct access to B cells as a primary target for infection (Faulkner *et al*, 2000; Macsween & Crawford, 2003). Infected naïve B cells undergo clonal expansion and express a latency III phenotype (Babcock *et al*, 2000; Babcock & Thorley-Lawson, 2000). After expansion, cells take on some of the characteristics of germinal centre B cells, expressing the germinal centre-specific marker CD10 and an EBV latency II phenotype (Babcock *et al*, 2000). Under normal conditions, uninfected naïve B cells progress to become germinal centre B cells following antigen-mediated activation, whereupon a minority receive the two survival signals required for transition into memory B cells (Liu & Arpin, 1997). These B cell survival signals are delivered firstly through the BCR via antigen mediated receptor cross-linking, and secondly through the interaction of CD40 on the B cell with CD40 ligand (CD154) on the surface of T helper cells, which are brought together by MHC class II antigen presentation by the B cell. Cells which fail to receive the second survival signal from a helper T cell die by apoptosis. In the absence of antigen, EBV provides infected B cells with these activation and survival signals via LMP1

(replacing CD40) and LMP2 (replacing the BCR) (Caldwell *et al*, 1998; Kilger *et al*, 1998). The infected cells then differentiate into memory B cells, the long term reservoir for EBV. Memory B cells are naturally long-lived, allowing the virus to persist for extended periods, with EBNA1 the only viral protein expressed (Hochberg *et al*, 2004). This latency 0 phenotype prevents detection of infected cells by EBV-specific T cells. Antigen-specific differentiation of EBV infected memory cells into plasma cells causes the virus to progress into lytic phase (Crawford & Ando, 1986; Laichalk & Thorley-Lawson, 2005), resulting in progeny virus, and subsequent infection of naïve B cells to replenish the virus-infected pool (Thorley-Lawson & Gross, 2004). Latently infected memory B cells activated by antigen can also re-circulate back to Waldeyer's ring. The infectious progeny virions released there are thus in a position not only to infect bystander naïve B cells, but also exit to the saliva for transmission. The resistance of individuals with X-linked agammaglobulinaemia, who lack Bruton's thymidine kinase and consequently functional B cells, to EBV infection (Faulkner *et al*, 1999), lends further support for the hypothesis that B cells are both the site of primary as well as persistent infection.

Epithelial cell hypothesis

EBV enters the host in saliva and infects epithelial cells of the oropharynx. Lytic replication results in the spread of infection to B cells present beneath the epithelium. The cycle of infection then continues as outlined in the B cell hypothesis above. Later, infection of the epithelial cells by virus released from plasma cells provides an exit to the saliva for transmission. Corroborating evidence for epithelial to B cell and B cell to epithelial cell EBV infection is provided by the finding that EBV produced in B cells is 'epithelial cell tropic' and EBV produced in epithelial cells is 'B cell tropic', that is they more efficiently infect the opposite cell type (Borza & Hutt-Fletcher, 2002). To elaborate, EBV infection of B cells requires the three part complex of viral glycoproteins gp85/25/42 to bind to HLA class II, whilst infection of epithelial cells requires only gp85/25 two part complex (Li *et al*, 1995). Each virion carries both three-part and two-part complexes, but virions produced by B cells carry relatively more two-part complexes and virions produced by epithelial cells carry relatively more three-part complexes, resulting in greater infection efficiency for the opposite cell type (Borza & Hutt-Fletcher, 2002). *Ex vivo*, cultures of resected tonsils have been shown capable of latent infection (Pegtel *et al*, 2004).

Additionally, chronic low level oro/nasopharyngeal virus shedding is seen in healthy EBV seropositive individuals (Yao *et al*, 1985), which may not be produced by B cells as they yield relatively little infectious virus, thus supporting a role for epithelial infection in amplification of virus to enhance transmission.

A role for other cell types in EBV cycle of infection

Two recent studies have proposed a role for additional cell types in the EBV cycle of infection. In *ex vivo* experiments, Tugizov *et al* (2007) showed that monocytes infected with EBV *in vitro* were able to facilitate the spread of EBV infection to epithelial cells in 9 of 14 tongue and buccal explant cultures, compared with infection of 1 of 20 explants incubated with cell free virus, with EBV-positive langerhans cells (LC) and activated macrophages/LC detected in close proximity to the infected epithelial cells (Tugizov *et al*, 2007). EBV DNA was also detected in CD14+ peripheral blood monocytes of 69% of human immunodeficiency virus (HIV) patients and 47% of healthy volunteers. Furthermore, EBV-infected LCs with a latency 0 or reactivation phenotype were observed *in vivo*, albeit rarely, in oral biopsy tissue from HIV patients (Walling *et al*, 2007). Therefore, since circulating monocyte/macrophage/LCs can migrate to tissue sites including the oral mucosa, these cells may serve as a vehicle for virus transfer between the memory B cell reservoir in the blood compartment and the oral epithelium from whence virus is shed in saliva for transmission.

1.2.5 The immune response to EBV

As the majority of people are EBV seropositive, yet seroconvert silently and sustain an asymptomatic persistent infection, it is clear that the immune system must play an important role in maintaining the balance between virus and host. This key role for the immune system is supported by the presentation of immunocompromised patients with severe EBV-associated disease, such as PTLD. As seroconversion usually goes unnoticed, information on primary infection is principally drawn from the study of IM, and what is known about primary infection in children tends to suggest a broadly similar immune response (Pedneault *et al*, 1996). In IM, EBV elicits both a humoral and cellular response.

1.2.5.1 Humoral response to EBV infection

The humoral response to primary EBV infection is characterised by detectable IgM and IgG to VCA and EA, detectable IgM but relatively weak IgG to MA, and the absence of IgG to EBNA (Moss *et al*, 2001). The composition of VCA, EA and MA is covered in section 1.2.2.3. Antibodies to gp350/220 within the MA complex are neutralising (Thorley-Lawson & Geilinger, 1980). The pattern of antibody expression changes during convalescent IM and for healthy EBV carriers, with stable IgG titres to EBNA, VCA and MA, but undetectable or weak IgG to EA (Moss *et al*, 2001). Approximately 85% of IM patients also have transient serum heterophile antibodies. Heterophile antibodies are IgM molecules reactive with antigens of an unrelated species. In the case of IM, these are antibodies specific for EBV which cross react with epitopes found on equine, ovine and bovine erythrocytes. Detection of heterophile antibodies reactive with horse erythrocytes is the basis of the IM monospot diagnostic test. These heterophile antibodies may be the product of EBV infected B cells (Garzelli *et al*, 1984). EBV specific antibodies could serve to prevent virus superinfection or halt further virus transmission (Thorley-Lawson & Poodry, 1982; Yao *et al*, 1991).

1.2.5.2 Cellular response to EBV infection

NK cells

Higher NK cell numbers have been correlated with lower viral load in IM patients, leading to the suggestion that NK cells may play a role in resolution of primary infection with EBV (Williams *et al*, 2005). However, of themselves NK cells are not sufficient to control initial infection, as shown by outgrowth of EBV-positive lesions in primary infection of immunocompromised post transplant patients who retain NK function.

CD8+ T cells

The CD8+ cytotoxic T cell response to EBV infection is characterised by an antigen driven proliferation of CD8+ T cells displaying an activated phenotype (Callan *et al*, 1996). In IM, these cells are present in both the circulation and the tissues in very high numbers. During acute infection as represented by IM, the CD8+ T cells primarily recognise immediate early and early lytic antigens, whilst cells specific for

latent antigens are relatively few (Steven *et al*, 1997; Hislop *et al*, 2002). The CD8+ T cell response evolves as infection progresses, with numbers of cells specific for lytic antigen dropping as primary infection is resolved, while the numbers of cells specific for latent antigen increase with the establishment of persistent infection (Hislop *et al*, 2002). The immune response to latent antigens is dominated by clones specific for the EBNA3A, 3B and 3C proteins (Khanna *et al*, 1992; Murray *et al*, 1992). The long-term memory T cell compartment maintains cells specific for both EBV lytic and latent epitopes, with lytic antigen specific cells typically more abundant than those specific for latent antigen (Tan *et al*, 1999). EBNA3 immunodominance is preserved amongst those cells specific for latent antigens.

CD4+ T cells

Although the CD4+ T cell response to EBV infection is less well characterised than that of CD8+ T cells, CD4+ cells specific for both lytic and latent antigens have been shown in IM patients, secreting interferon (INF)-γ in a T helper (Th)-like manner (Precopio *et al*, 2003). There is distinct divergence in the capacity of different EBV latent proteins to elicit a CD4+ T cell response, with EBNA1 and EBNA3C the most immunogenic ahead of LMP1 and LMP2 (Leen *et al*, 2001). That is, PBMCs from a higher proportion of EBV-seropositive donors secreted INF-γ in response to peptide stimulation. This is in contrast to the CD8+ cell response, where EBNA3C is the most immunogenic, followed by EBNA1, LMP2 and LMP1 in decreasing order (Leen *et al*, 2001). In addition to their T-helper role, CD4+ cells may also contribute a cytotoxic response, as they have been shown capable of inducing EBV-specific lysis via Fas/FasL interaction (Paludan *et al*, 2002) or granulysin secretion (Sun *et al*, 2002). CD4+ T memory cells are less frequent and of a narrower specific range than their CD8+ counterparts (Leen *et al*, 2001).

1.3 EBV and associated diseases

Although the majority of EBV-infected individuals exhibit no EBV-related illness, primary EBV infection can result in IM and EBV has also been linked with a number of lymphoid and epithelial malignancies. Despite the ubiquitous nature of the virus, EBV-associated malignancies are relatively rare and frequently geographically restricted, indicating that infection is not the only necessary factor in tumourigenesis.

With increases in the number of iatrogenically immunosuppressed transplant and HIV patients there has been a concomitant rise in EBV-associated disease in this setting. A number of these EBV-associated diseases are discussed in the following sections.

1.3.1 Infectious mononucleosis

IM is a self-limiting lymphoproliferative disease which occurs during primary EBV infection of adolescents and young adults. In Western countries, early studies estimated that IM developed in approximately 50% of cases where primary infection was delayed until adolescence (Niederman *et al*, 1970; Sawyer *et al*, 1971), although a more recent study has put this figure closer to 25% (Crawford *et al*, 2006). In developing nations, IM is relatively rare condition, as virtually all children are infected with EBV by the age of two (de-The *et al*, 1978).

Symptoms of IM can include fever, pharyngitis, lymphadenopathy, general malaise and fatigue, and vary in severity from patient to patient. The illness is usually self-resolving within two to four weeks, although fatigue may persist during the convalescent period for up to six months. In rare cases, a chronic IM can develop (Okano *et al*, 1991). Massive lymphocytosis is characteristic of IM, and the proliferating cells are predominantly activated CD8+ T cells, although there is also an expansion of infected B cells (Klein *et al*, 1976; Callan *et al*, 1996). These activated T cells are found in tissues throughout the body, and release proinflammatory cytokines including IL-1, IL-6, and TNF-α (Foss *et al*, 1994), which are thought to result in the immunopathological clinical manifestation of IM.

It is not known why primary EBV infection in adolescence can result in IM when virtually all childhood infections are asymptomatic. One possible explanation is that the dose of virus received via the oral route is much higher in adolescents. This elevated initial exposure results in the numbers of infected B cells exceeding some threshold limit, driving antigen induced T cell proliferation to the point where resulting cytokine levels become pathogenic (Rickinson & Kieff, 2007).

1.3.2 Burkitt's lymphoma

BL typically presents as a tumour of the jaw, although other sites including the ovaries, mammary glands, liver, intestine, and kidneys are not uncommon. Two forms of BL have been described, endemic BL (eBL) and sporadic BL (sBL). eBL is found in equatorial Africa and Papua New Guinea, is EBV associated in 96% of cases, and is one of the most common childhood cancers in equatorial Africa. sBL occurs worldwide with an incidence that is at least 50-fold less than eBL, and an EBV association which falls anywhere between 20 to 70%, depending on the region surveyed (Rickinson & Kieff, 2007).

BL tumours consist of rapidly proliferating cells of B cell origin, which phenotypically resemble germinal centre B cells, and sporadic infiltrating macrophages, resulting in a characteristic 'starry sky' histology (Gregory *et al*, 1987). In EBV-associated BL, the virus is present in all malignant cells in multiple episomal copies, and is clonal, suggesting EBV infection is an early event in tumourigenesis (Neri *et al*, 1991). BL cells display a type I latency, with EBV gene expression limited to EBNA1, EBERs and BARTs. The oncogenic potential of EBNA1 remains a topic of contention, but a possible role in BL cell survival has been suggested (Kennedy *et al*, 2003). EBERs may also contribute to the pathogenesis of BL, as they have been reported to induce IL-10 (Kitagawa *et al*, 2000) and mediate INF-α resistance (Nanbo *et al*, 2002), potentially supporting tumour growth and survival (Ogden *et al*, 2005).

Three key factors in the tumourigenesis of eBL have been identified: EBV infection, c-myc translocation, and malaria. All BL tumour cells contain one of three chromosomal translocations which result in constitutive expression of c-myc, leading to cellular proliferation without differentiation (Rickinson & Kieff, 2007). BL has long been linked with malaria, beginning with Dennis Burkitt himself. Areas of high incidence of holoendemic malaria and eBL in Africa coincide, and where malaria prevalence has fallen due to mosquito eradication, so has the occurrence of eBL (Crawford, 2001). Current theories propose that both malarial stimulation of infected B cells and inhibition of EBV-specific CTLs contribute to the pathogenesis of eBL. Supporting these hypothesises, children with acute malaria have up to five times

more circulating EBV infected cells than those with convalescent malaria (Lam *et al*, 1991), and acute malarial infection results in T cell immune suppression (Whittle *et al*, 1984).

BL is highly sensitive to chemotherapy, with disease free survival rates of 80% after effective treatment. Surgery is rarely necessary to remove tumour bulk. More recently, chemotherapy in combination with the chimeric monoclonal antibody (mAb) Rituximab, which is specific for the B cell antigen CD20 expressed in BL, has been advocated by the Children's Oncology Group (Giulino *et al*, 2007).

1.3.3 Hodgkin's lymphoma

HL is the most common lymphoma of young people in industrialised countries. It has four subtypes; nodular sclerosing (NS), mixed cellularity (MC), and lymphocyte depleted (LD), collectively known as classical HL, and the clinically separate entity lymphocyte predominant (LP) HL. Worldwide, EBV is more likely to be associated with classical rather than LP HL, with around 50% of classical HL EBV-associated in western countries (Rickinson & Kieff, 2007). Within classical HL, it is more commonly associated with the MC and LD rather than the NS subtype (Rickinson & Kieff, 2007). IM has also been shown to be a risk factor for HL (Glaser & Jarrett, 1996).

Incidence of classical HL has traditionally been described as bimodal, with peaks in children and older adults, although this depiction may be somewhat simplistic and subject to regional variations, for example the childhood peak occurs later in affluent compared to non-affluent societies (Macfarlane *et al*, 1995). To more accurately reflect these geographical deviations, a four-disease model of classical HL has been proposed (Figure 1.6; Jarrett, 2006). Based on the age at diagnosis, tumour EBV association and history of IM, classical HL is divided into four subgroups, each with peak of incidence in a different age group, three of which are EBV-associated (peaks a, b, c in Figure 1.6). Of these three EBV-associated peaks, the first subgroup (a) is composed of early childhood disease, which generally occurs before the age of 10 years, and accounts for the majority of childhood cases in developing countries. The second peak (b) represents disease in young adults, which is associated with previous

IM. The final EBV-associated subgroup (c) represents disease in older adults, with HL generally occurring after 55 years of age. The largest subgroup is EBV-negative HL, and accounts for the young adult peak in developed countries. The height and shape of each peak will vary according to the country from which the data are collected.

Figure 1.6: Incidence of Hodgkin's lymphoma. Four disease model of classical HL, divided on the basis of age, EBV-association and history of IM. Subgroups are childhood **(a)**, early adulthood **(b)**, late adulthood **(c)**, and EBV-negative **(d)**. Adapted from Jarrett (2006).

HL is unusual histologically, as less than 2% of the tumour is made up of the malignant mononuclear Hodgkin or multi-nuclear Reed-Sternberg cells (collectively referred to as HRS cells), with the remaining tumour bulk consisting of non-neoplastic infiltrating lymphocytes. As with BL, EBV in HL is clonal, indicating that infection occurs early in tumourigenesis (Anagnostopoulos *et al*, 1989). When present, the virus is carried in HRS cells (Wu *et al*, 1990), with every malignant cell EBV-positive, even in cases with multiple lesions (Rickinson & Kieff, 2007). Rearrangement of Ig genes indicates that these HRS cells are derived from germinal centre B cells (Kanzler *et al*, 1996b). A proportion show obvious 'crippling' mutations in rearranged Ig genes, which under normal conditions should have resulted in apoptosis in the germinal centre, and EBV may play a role in the rescue of these cells (Kanzler *et al*, 1996b). HRS cells display an EBV latency II phenotype, and the expression of LMP1 and LMP2A may promote survival in the pre-apoptotic germinal centre cells. LMP1 likely contributes to the survival and proliferation of

HRS cells through activation of NF-κB (Bargou *et al*, 1997). Although LMP2A has been shown to provide growth and survival signals to B cells (Caldwell *et al*, 1998), its ability to do this in HL is uncertain, as HRS cells have down-regulated many of the components involved in the BCR signalling pathway (Schwering *et al*, 2003).

HL is one of the most treatable adult cancers, with about 80% of patients achieving complete remission, although around one third of patients do relapse. Most treatment strategies involve combinations of chemotherapy and radiotherapy, with Rituximab an option for refractive or recurrent disease, as a proportion of HRS cells express CD20 (Klimm *et al*, 2005).

1.3.4 Nasopharyngeal carcinoma

In contrast to BL and HL, NPC is of epithelial origin and specifically is a tumour of the nasopharyngeal squamous epithelium. Although NPC occurs worldwide, incidence is low except amongst the Inuit peoples, in southeast Asia, and most especially in southern China, where it occurs in up to 3 in 10000 people (Lopes *et al*, 2003). Incidence remains high in males of Cantonese descent irrespective of location, suggesting genetic factors contribute to disease aetiology (Lopes *et al*, 2003). A number of potential environmental cofactors, such as a diet high in salted fish, have also been identified (Armstrong *et al*, 1998).

There are two broadly defined NPC subtypes; differentiated (keratinized), and undifferentiated/poorly differentiated (non-keratinized) NPC. EBV is found in virtually all undifferentiated NPC tumours, but the association with differentiated NPC remains controversial (Rickinson & Kieff, 2007). Undifferentiated NPC lesions are composed of EBV-positive carcinoma cells with a prominent EBV-negative non-neoplastic lymphocyte infiltration (Klein *et al*, 1974). Interactions between these cell types may be important for tumour growth, as tumour cells and infiltrating lymphocytes express molecules, for example CD40 on tumour cells and CD40 ligand on T cells, allowing them to exchange signals involved in cell activation and proliferation (Agathanggelou *et al*, 1995).

As with BL and HL, EBV in NPC is clonal, indicating infection occurs prior to expansion of malignant cells (Raab-Traub & Flynn, 1986). However, pre-malignant genetic events in the absence of EBV infection have also been found, potentially predisposing cells to EBV infection (Lo & Huang, 2002), which is in agreement with data showing that epithelial cells unable to differentiate preferentially support stable EBV infection (Knox *et al*, 1996). To what extent EBV influences the outgrowth of malignant cells remains unclear. At a transcriptional level, NPC displays an EBV latency II phenotype, but this is not maintained through to the level of protein expression. The EBNA1 protein is readily detectable in NPC (Young *et al*, 1988), while LMP1 protein expression is variable, being detected only in around 35% cases (Young *et al*, 1988). Expression of LMP2A has been confirmed by PCR in 94% of NPC tumours and 46% of NPC tumours by immunohistochemistry (Brooks *et al*, 1992; Heussinger *et al*, 2004). NPC patients are also the only group to reproducibly show a serum antibody response to the LMP2 (Frech *et al*, 1990; Lennette *et al*, 1995).

NPC is radiosensitive, and radiotherapy controls disease in 80% of early stage cases. However, early stage tumours often go undetected and treatment of late stage NPC is less reliable and frequently results in refractory or recurrent disease (Wei & Sham, 2005). EBV DNA in serum correlates with tumour burden, and can be used to monitor for disease relapse (Lo *et al*, 1999a; Lo *et al*, 1999b), as can serum concentration of IgA specific for VCA (Chien *et al*, 2001).

1.3.5 Gastric carcinoma

Approximately 10% of gastric carcinomas worldwide are EBV-associated. However, as GC is one of the most common carcinomas the absolute incidence is considerable, with estimates exceeding 50000 cases per year. Both typical adenocarcinomas and carcinoma with prominent lymphocyte infiltration, such as seen in NPC, have been associated with EBV (Shibata & Weiss, 1992; Nakamura *et al*, 1994).

EBV-associated GC has traditionally been classified as expressing a type I latency. However, although EBNA1 is the only latent protein consistently expressed, LMP2

transcripts have also been detected in a proportion of cases (Imai *et al*, 1994; Sugiura *et al*, 1996). EBV in GC is clonal (Imai *et al*, 1994), with almost 100% of cells containing the EBV episome (Zur Hausen *et al*, 2004), suggesting EBV infection is an early event in tumourigenesis. However, conflicting reports of the presence of EBV in preneoplastic dysplastic mucosa means the role of EBV in tumourigenesis has yet to be fully elucidated (Takada, 2000; Zur Hausen *et al*, 2004).

An interdisciplinary approach is used in the treatment of GC, utilising a combination of surgery, chemotherapy and radiotherapy. However, patient outcome remains poor, with frequent disease progression and tumour metastases.

1.3.6 EBV-associated malignancies in the immune compromised

PTLD

The lymphoproliferative disorders that arise post transplant, collectively known as post transplant lymphoproliferative disease (PTLD), are a heterogeneous collection of disorders principally of B cell origin (Hopwood & Crawford, 2000), although T- and NK-derived tumours have also been observed (Nalesnik, 2001). About 90% of PTLD tumours are EBV-positive (Crawford, 2001). The key risk factors for development of PTLD are iatrogenic T cell immunosuppression and primary EBV infection post transplant, with around 50% PTLD associated with a primary EBV infection (Thomas *et al*, 1990). PTLD occurs in up to 10% of all transplant patients, but rates of incidence vary greatly depending on the organ being transplanted, EBV status of the donor and recipient, and choice of immunosuppressive regimen (Burns & Crawford, 2004). PTLD is most likely to occur within one year of transplant, when immunosuppressive therapy is highest, with tumours developing after one year associated with poorer prognosis (Williams & Crawford, 2006). PTLD in bone marrow transplant (BMT) recipients is generally of donor origin, while PTLD in solid organ recipients is of recipient origin.

PTLD tumours usually exhibit a latency III phenotype, although other more restricted patterns have been reported (Young *et al*, 1989a; Cen *et al*, 1993). Decreasing immunosuppressive treatment can lead to an increase in the EBV-specific immune response and tumour regression, at least in early stage disease, and

this evidence, together with the expression of a full range of latent proteins indicates a reliance on EBV to drive the proliferation of malignant cells (Hopwood & Crawford, 2000). EBV in PTLD can be polyclonal, but is generally oligo- or monoclonal, with PTLD arising later than one year post transplant more likely to be monoclonal (Hanto *et al*, 1989). The EBV genome is not necessarily found in all cells within the tumour mass, as infiltrating EBV-negative non-neoplastic lymphocytes often contribute a substantial proportion (Perera *et al*, 1998). Unlike other EBV-associated diseases, the malignant cells of PTLD are able to arise from various points in the B cell differentiation pathway and derivation can include naïve and memory B cells, as well as post-germinal centre B cells with mutations which would normally lead to apoptosis (Timms *et al*, 2003).

First line treatment for solid organ PTLD is reduction in immunosuppression (Gottschalk *et al*, 2005). This is particularly effective against polyclonal tumours, however it is difficult to sustain given the often grave consequences of graft loss, so disease relapse is common. Response rates to reduction of immunosuppression vary from 25 to 63% in adults and 40 to 86% in children (Gottschalk *et al*, 2005; Taylor *et al*, 2005). Chemotherapy had been the second line treatment of choice until the advent of Rituximab, and combination of the two is now generally used with response rates up to 100% (Gottschalk *et al*, 2005). Individually, use of chemotherapy is complicated by increased severity in side-effects due to immune suppression (Oertel *et al*, 2003), and Rituximab monotherapy can lead to CD20- tumour outgrowth (Verschuuren *et al*, 2002). Rituximab alone is the first line treatment for BMT PTLD. Trials of cellular therapy using EBV-specific CTLs for refractive disease have shown promising results in both bone marrow and solid organ PTLD (Rooney *et al*, 1995; Haque *et al*, 2007).

X-linked lymphoproliferative disease

Individuals with a rare genetic disease, X-linked lymphoproliferative (XLP) disease, carry a mutation or deletion in a gene that appears to be important in T and B-cell homeostasis after viral infection (Coffey *et al*, 1998; Sayos *et al*, 1998). The gene product, SLAM-associated protein (SAP), is expressed in activated T and NK cells, and interacts with the signalling lymphocytic activation molecule (SLAM) protein, a member of the Ig superfamily expressed on T, B and dendritic cells (Sayos *et al*,

1998). In healthy individuals, it is thought that the SAP/SLAM interaction acts to maintain equilibrium in Th1/Th2 cytokine production (Williams & Crawford, 2006). Similar to the situation in IM, EBV infection in XLP individuals leads to a massive proliferation of EBV-infected B cells and a concomitant rise in CTLs. Unlike IM, the CTLs of XLP patients apparently cannot limit this B cell expansion, and the resulting cytokine response, primarily of Th1 cytokines such as INF-γ, is thought to result in the extensive organ damage seen in such patients (Williams & Crawford, 2006). Over 50% of XLP patients die in this acute phase, and the majority of survivors go on to develop lymphomas or hypogammaglobulinemia.

AIDS-related lymphomas

The immune deficiency which results from HIV infection means HIV/acquired immune deficiency syndrome (AIDS) patients are at high risk for the development of lymphoproliferative diseases. Like PTLD, AIDS-related lymphomas are a heterogeneous group of disorders. AIDS-related central nervous system lymphomas derive from post germinal centre B cells and almost always contain EBV, while 30 to 50% of peripheral lymphomas are EBV-associated (MacMahon *et al*, 1991). BL in HIV patients is an AIDS-defining illness, but has a less than 50% association with EBV (Hamilton-Dutoit *et al*, 1993). HL also occurs in HIV-infected individuals, with HIV-positive individuals 3 to 7 times more likely to develop HL, and more than 90% of HIV-HL is EBV-associated (Audouin *et al*, 1992; Glaser *et al*, 2003).

1.3.7 Oral hairy leucoplakia

Oral hairy leucoplakia (OHL) is unique amongst EBV-associated disorders in that it alone results from lytic virus replication, confirming that EBV can infect and replicate in non-malignant epithelial cells, at least in an immune compromised setting (Greenspan *et al*, 1985). Benign lesions occur in the superficial layers of the tongue epithelium, with EBV DNA, lytic and some latent proteins found in more differentiated but not basal epithelial cells (Thomas *et al*, 1991). OHL occurs in the immune suppressed, especially late stage AIDS patients, although it has also been seen rarely in non-immunosuppressed individuals (Lozada-Nur *et al*, 1994). Treatment is with the antiviral aciclovir, and results in complete clearance of lesions, attesting to the importance of lytic replication in lesion formation (Greenspan *et al*,

1990). Withdrawal of treatment leads to recurrent disease, although it is not know if this derives from reactivation of epithelial infection or reseeding of the epithelium from the lymphoid reservoir.

1.4 Animal models of EBV-associated malignancies

Although the majority of *in vivo* data collected on EBV have been from latently infected healthy virus carriers, or those with abnormal responses to virus as in IM, there are also a number of animal models available for the study of EBV infection and associated diseases.

1.4.1 Non-human primates

As mentioned previously, herpesviruses generally have a very narrow host range, and initial attempts to study the pathogenesis of EBV by virus inoculation of old world primates revealed little evidence of infection (Frank *et al*, 1976). This was most likely due to presence of cross-reactive immunity to endogenous lymphocryptoviruses (LCVs) (the *gammaherpesvirinae* genus of which EBV is the human representative), or species specific restriction for LCV-induced B cell transformation (Frank *et al*, 1976; Moghaddam *et al*, 1998).

EBV infection of new world primates has proved more successful in providing models for human infection. EBV infection causes an IM-like illness in the common marmoset (*Callithrix jacchus*), with lymphoproliferation and a viral antibody response (Wedderburn *et al*, 1984). Persistent infection ensues, as shown by oropharyngeal virus shedding and EBERs latent transcripts detectable in PBMCs (Cox *et al*, 1996; Farrell *et al*, 1997). Infection does not result in the development of lymphomas, and differs from the human disease in that there is limited B cell involvement (Emini *et al*, 1986). Conversely, EBV infection of the cotton-top tamarin (*Sagunius oedipus*) causes acute B cell lymphoproliferation, with PTLD-like tumours displaying a latency III phenotype (Shope *et al*, 1973; Young *et al*, 1989b). This model has been used for the testing of EBV vaccines (Epstein *et al*, 1985). However, it is not a wholly accurate representation of the human condition, as disease has a rapid onset, lymphoproliferation occurs in 100% of animals infected,

and those which survive this initial disease do not become persistently or latently infected (Shope *et al*, 1973).

Primate models using simian gammaherpesvirus have also been explored. Old world primate endogenous LCVs share a number of common features with EBV including the ability to transform B cells, and their genomes can be arranged collinearly with EBV and show a large degree of homogeneity (Wang *et al*, 2001). Also, the functional mechanisms of latent genes appear to be largely preserved. Rhesus macaques are naturally immune to EBV, but infection via the oral route with a rhesus LCV results in an infection with many similarities to EBV infection in humans, such as lymphadenopathy, latent infection in PBMCs, and persistent virus shedding in oropharyngeal secretions (Moghaddam *et al*, 1997). Co-infection of EBV and simian immunodeficiency virus (SIV) in macaque can also result in the development of B cell lymphomas containing EBV latent transcripts, analogous to the development of EBV-related lymphomas in AIDS patients (Pingel *et al*, 1997).

The drawbacks to use of non-human primates in the study of EBV infection and associated disease are as for any use of such animals. The high expense, specialist facilities, endangered status, and requirement for a high level of security ensure that only limited researchers can afford their use, and then usually only in small numbers. Additionally, primate biology is not as well understood as that of other species, particularly the mouse, and development of transgenic animals is cumbersome. Thus, murine models have been more extensively used, and in particular the SCID mouse.

1.4.2 Mouse models

1.4.2.1 Murine herpesvirus-68

Originally isolated in 1980 from the bank vole (Blaskovic *et al*, 1980), murine herpesvirus-68 (MHV-68) was later classified a gammaherpesvirus based on sequence analysis (Efstathiou *et al*, 1990). Its ability to cause both productive and latent infection in laboratory mice analogous to EBV infection provided the first small animal model for studying immunity and pathogenesis of a gammaherpesvirus

in its natural host (Sunil-Chandra *et al*, 1992a; Sunil-Chandra *et al*, 1992b). However, for the investigation of novel cancer therapies SCID mouse models of EBV-associated malignancies are more appropriate, providing as they do human cells as targets, and so have been more widely used in this application.

1.4.2.2 Models in immunodeficient mice

In 1983, a CB17 mouse mutant was described which lacked functional T and B cells (Bosma *et al*, 1983). The SCID gene was later found to encode the *Prkdc* protein kinase, a component of the recombinase enzyme system needed for dsDNA break repair, which is also essential for correct joining of the V(D)J sequences in B and T cell receptors during lymphocyte maturation (Schuler *et al*, 1986; Fulop & Phillips, 1990). Improper joining leads to non-functional receptors and a block in differentiation. The immunodeficiency is somewhat 'leaky', with 2 to 23% of SCID mice developing a limited number of functional T and B cells (Bosma *et al*, 1988). CB17 SCID mice do have functional NK cells (Dorshkind *et al*, 1985), although development of new SCID strains has led to animals with reduced NK activity, for example non-obese diabetic-SCID mice (Shultz *et al*, 1995).

The first immunodeficient mouse model of cancer was developed in 1977, when athymic nude mice (which lack functional T cells) were shown to support the growth of solid human tumours (Fogh *et al*, 1977). SCID mice also accept xenotransplantation of human cells and tissues, and SCID mice engrafted with cell lines derived from a vast array of human malignancies have been used as *in vivo* models for tumour biology, growth, angiogenesis and metastasis, as well as to test novel cancer therapies. Modelling for EBV-associated disease began when human-SCID chimeras (hu-PBL-SCID) were developed by grafting SCID mice with human PBMCs for studying human immune function (Mosier *et al*, 1988). It was noted that the chimeras often developed EBV-positive lymphomas of B cell origin if the donors were EBV seropositive, (Mosier *et al*, 1988). These tumours were subsequently shown to be immunoblastic lymphomas phenotypically identical to PTLD tumours (Rowe *et al*, 1991). Since then additional SCID models of PTLD have been developed, using LCLs administered by subcutaneous (sc) or intraperitoneal (ip) injection to give rise to tumours (Rowe *et al*, 1991; Lacerda *et al*, 1996).

With respect to EBV-associated malignancies, several HL cell lines, albeit mostly EBV-negative, also form tumours when administered by sc or ip injection in CB17 SCID mice (von Kalle *et al*, 1992). Models of HL with metastasising disease have been established using sc or intravenous (iv) inoculation of HL-derived cell lines (Winkler *et al*, 1994). Xenotransplantation models of EBV-associated NPC and GC are also available (Cheung *et al*, 1999; Oh *et al*, 2007). The use of xenotransplantation SCID mouse models in the testing of novel cancer therapies is well established, and yet some debate remains as to their actual worth, given the variable power of such models to accurately predict how humans will respond to the treatment in the clinic (Sausville & Burger, 2006). The major drawback of murine xenograft models is that, with regard to genetics and histology, the mouse tumours are not always representative of the respective human tumour. An alternative is genetically engineered mouse models, where tumours are histologically and genetically accurate models of human cancer and like the human situation are heterogeneous with regard to frequency, latency, and growth. Indeed, there is a transgenic model of BL in the mouse (Kovalchuk *et al*, 2000). However, BL is unique amongst EBV-associated malignancies in having the well defined genetic mutations needed for the deliberate establishment of a transgenic model. Thus, for the time being at least, the advantages of xenotransplantation - synchronized, easily observable tumours with a high degree of predictability and rapidity of tumour formation, which makes them easy to use – means that it is the preclinical model of choice for the testing of novel therapies against EBV-associated cancer.

1.5 Cancer immunotherapy

Most cancer patients are treated by a combination of surgery, radiation and/or chemotherapy. The term cancer encompasses such a broad spectrum of conditions that it is difficult to treat with a uniform therapy regimen. Complications also arise with conventional treatment of metastatic disease. Immunotherapy of cancer has developed to overcome the limitations of conventional therapy, such as associated toxicities and refractory disease. The human immune system is exceptionally specific once a suitable target is found, and can also provide long term protective memory against disease relapse after initial burden is cleared. The main strategies of

cancer immunotherapy aim at exploiting the potential of tumour-specific antibodies and cellular immune effector mechanisms.

1.5.1 Antibody therapy

The first therapeutic mAb, Orthoclone OKT3, was licensed for clinical use in the 1980s (OrthoGroup, 1985). It was a mouse antibody specific for human CD3 used to treat transplant rejection. Since then, advances such as humanisation, chimerisation and labelling have led to a proliferation in the clinical applications of antibodies. In 2007 there were nine antibody based therapies for the treatment of cancer licensed by the American Food and Drug Agency (FDA), for such diverse malignancies as breast cancer, lymphoma, leukaemia, and colon cancer (FDA Orange Book, 2007), and five antibody based therapies for the treatment of cancer licensed in the UK (British National Formulary, 2007).

Monoclonal antibodies can be directed towards a number of cancer-associated antigens, including vascular growth factors, tumour-associated stroma, host immune checkpoints, and tumour cell surface antigens. Targeting vascular growth factors, for example, can inhibit angiogenesis and prevent tumour growth. Alone, one vascular endothelial growth factor (VEGF)-specific mAb had little direct anti-tumour activity but in combination with chemotherapy it prevented neo-vascularisation and improved survival in patients with metastatic colon cancer (Hurwitz *et al*, 2004). The tumour stroma may also contain components which differ from those in healthy tissue. The fibroblast activation protein (FAP) found on tumour-associated fibroblasts is thought to play a role in tumour formation and metastasis. Whilst a phase I trial of a mAb to FAP in combination with radiotherapy did not result in an objective tumour response, encouragingly the mAb did localise to the tumour site with no uptake by organs, showing successful tumour targeting (Scott *et al*, 2003). Therapeutic antibodies may also have a role to play in immunomodulation, targeting host cells and proteins that act as inhibitory checkpoints in the immune system. Cytotoxic T lymphocyte antigen (CTLA)-4 is expressed mainly on CD4+ T cells and acts as a CD28 antagonist, regulating activation signal 2 to CD8+ T cells (Thompson & Allison, 1997). CTLA-4 antibody blockade has been used to enhance anti-tumour immunity in patients previously treated with anti-cancer vaccines, such as irradiated

tumour cells, dendritic cells engineered to express tumour-associated antigens (TAA), or TAA peptides alone (Hodi *et al*, 2003; Phan *et al*, 2003).

Two of the best known mAbs currently available for the treatment of cancer in the UK are Herceptin, for use in breast cancer, and Rituximab, for the treatment of B cell lymphomas. Herceptin is a humanised IgG1 mAb directed against the extracellular domain of the HER2/neu protein, a member of the epidermal growth factor receptor family. HER2/neu is overexpressed in around 30% of breast cancers (Slamon *et al*, 1987). In combination with chemotherapy, treatment with Herceptin has shown a 52% improvement in event-free survival at three years compared with chemotherapy alone in breast cancer patients (Romond *et al*, 2005). Expression level of HER2/neu is critical to the efficacy of Herceptin, with tumours expressing relatively lower levels of HER2/neu being generally unresponsive to antibody treatment (Vogel *et al*, 2002). Rituximab is also a humanised IgG1 mAb, which targets the mature B cell surface antigen CD20. The mechanism of Rituximab is complex, and includes induction of apoptosis, inhibition of cell growth, complement mediated cell lysis, sensitisation of cells to chemotherapy and radiotherapy, and induction of antibody-dependant cellular cytotoxicity (Smith, 2003). In clinical trials for low grade previously treated B-cell lymphoma, overall response rates of Rituximab alone are around 50% (Berinstein *et al*, 1998; McLaughlin *et al*, 1998; Piro *et al*, 1999), and it is now regularly used alone or in combination with other therapies for the treatment of non-Hodgkin's lymphoma (NHL) and other B cell lymphomas including HL and PTLD, as well as rheumatoid arthritis.

Antibodies also have the potential to deliver cytotoxic agents to tumour cells (Wu & Senter, 2005). Generally, this requires the antibody to bind to a target which will result in the internalisation of the antibody and conjugate, and is likely to be most effective in diffuse malignancies or individual tumours of small volume. The most common conjugate, radioisotopes, can be used for tumour imaging, especially occult tumour deposits, in addition to treatment. In a trial comparing Rituximab with a radiolabelled mAb also specific for CD20 in lymphoma patients whose disease had worsened after chemotherapy, overall response rates were 34% and 80% respectively, with complete response 20% and 34% respectively (Gordon *et al*, 2004). A variety of small molecule toxins have also been linked to mAb, including

the antibiotic calicheamicin, and these conjugated molecules are collectively known as immunotoxins. In a trial for patients with recurrent acute myeloid leukaemia, treatment with a CD33-specific calicheamicin conjugated antibody resulted in an overall response rate of 26%, with a 13% complete response rate (Larson *et al*, 2005). Agents undergoing clinical development for cancer therapy include additional radioisotopes and toxins, as well as drug, cytokine and enzyme alternatives (Wu & Senter, 2005; Shaw *et al*, 2007).

One of the major challenges of antibody drug delivery for cancer therapy is low penetration of antibodies into solid tumours (Jain, 2001). In comparison with whole antibodies (Figure 1.7 A), antibody fragments such as Fab (fragment antigen binding – that section of an antibody which contains the antigen binding site after proteolysis of the molecule; Figure 1.7 B) or scFv (single chain variable fragment – antibody variable heavy [V_H] and variable light [V_L] domains connected by a short DNA sequence encoding a flexible peptide linker; Figure 1.7 C) potentially offer better tumour penetration whilst retaining full antibody binding specificity (Hudson & Souriau, 2003). Additionally, these smaller molecules are more rapidly cleared from the blood, minimising the opportunity for therapeutic side-effects (Holliger & Hudson, 2005). In a phase I trial, an enzyme-linked scFv specific for the oncofetal antigen carcino-embryonic antigen (CEA) expressed on a variety of adenocarcinomas localised to tumour sites, with the enzyme used converting a subsequently administered prodrug to the active form (Mayer *et al*, 2006). The treatment was well tolerated in patients, and a 10% reduction in tumour diameter was seen in one patient by computed tomography imaging.

Fab and scFv fragments are monovalent, which may lead to sub-optimal target affinity and tumour retention. However they do have the potential to be engineered into dimeric, trimeric or tetrameric molecules in order to increase functional affinity. scFv di-, tri-, and tetramers (Figure 1.7 D,E,F, respectively) can be constructed by shortening the peptide linker joining the V_H and V_L domains, facilitating self-assembly. The multimers combine the levels of tumour penetration and blood clearance seen with the monomers, with the tumour retention as a result of higher avidity seen in full antibody molecules (Holliger & Hudson, 2005). Similarly, Fab dimers with improved avidity and stability can also be engineered, usually by

chemical conjugation (Figure 1.7, G) A Fab dimer also specific for CEA has been shown to localise to tumours and deliver radioisotopes in a preclinical trial for colorectal cancer (Casey *et al*, 2002). Alternatively, molecules with multiple specificities can be engineered (Figure 1.7 D,G), with the potential to cross-link two different antigens or localise effector molecules to specific targets.

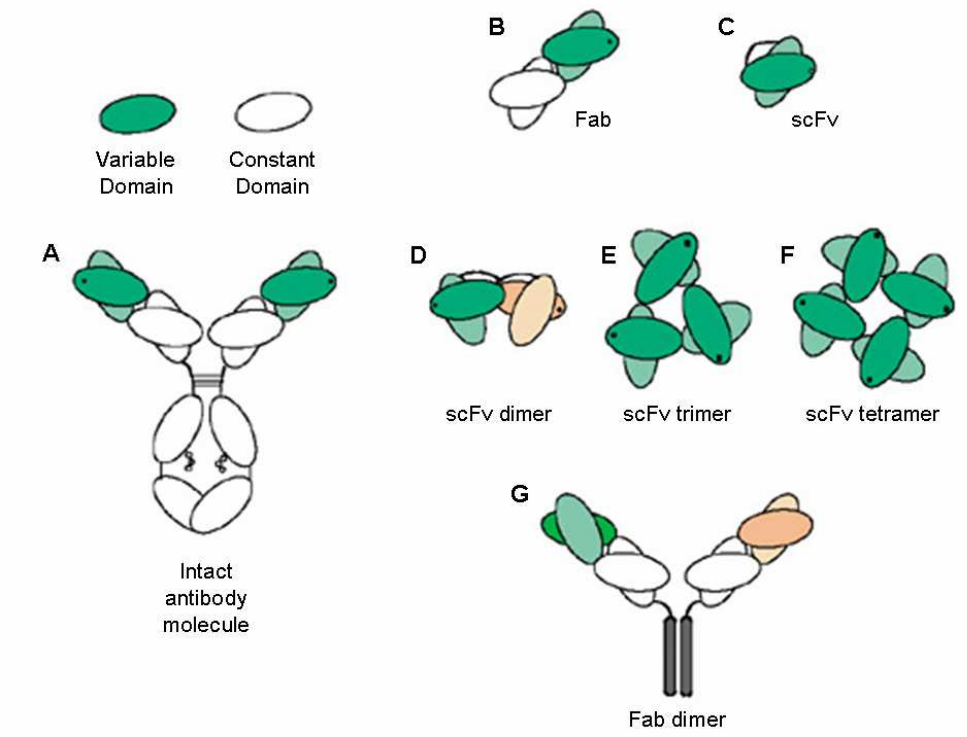

Figure 1.7: Antibody molecule with Fab and scFv fragments.
Schematic representation of an intact antibody molecule (IgG; **A**) together with antibody fragments Fab **(B)** and scFv **(C)**. The engineered recombinant fragments scFv dimer **(D)**, trimer **(E)**, and tetramer **(F)**, and a Fab dimer **(G)** are also shown. Variable domains are represented by coloured ovals with antigen-binding sites indicated by dots. Constant domains are represented by uncoloured ovals. Colours also represent different specificities in the scFv and Fab dimmers **(D,G)**. Image reprinted by permission from Macmillan Publishers Ltd: Hudson PJ and Souriau C. Nature Medicine 9:129-134, copyright (2003).

The engineering of antibodies to produce scFv as outlined above has generally been performed in a human or murine setting. From a therapeutic standpoint, human derivatives are currently superior as they have a lower immunogenicity, although as research continues it may eventually be possible to identify and remove

immunogenic epitopes on molecules. Nevertheless, in recent years much interest has focused on the immunoglobulin-like molecules of the camelids (camels and llamas) and cartilaginous fish (wobbegong and nurse sharks) species, which have evolved naturally single-domain variable regions. The requirement for relatively short complementarity determining regions (CDR) (short amino acid sequences within the variable domains of an antibody which come into contact with antigen during antibody-antigen interactions) in human and murine antibodies limits target antigens to predominantly flat or concave topologies (Hudson & Souriau, 2003). Camelid and shark variable domains can stably incorporate longer CDR loops, and are thus also able to access convex surfaces or cavities (Dooley & Flajnik, 2005). Examples of these include the binding sites of enzymes and narrow cavities in surface antigens of viruses which have evolved to bind their cognate receptor while remaining generally inaccessible to intact antibodies and thus immunosilent (Holliger & Hudson, 2005). This makes antibody fragments derived from camelid and shark variable domains potentially very useful as targeting agents, especially against pathogenic organisms. Their inherent stability and solubility currently suit them to *in vitro* diagnostic use until methods for reducing their immunogenicity in humans can adapt them for therapeutic use.

Although mAb therapy has many promising applications in cancer therapy, cancer is a diverse range of illnesses, and what is applicable in one setting may not be appropriate in another. Harnessing the cellular immune system may provide effective therapies where antibodies alone cannot. The role of the cellular immune response in cancer immunotherapy, with particular emphasis given to CD8+ CTLs, is outlined in the next section.

1.5.2 Cellular therapy

To date, the majority of clinical cellular immunotherapy has been directed against viruses, specifically CMV and EBV. In pioneering work, Riddell *et al* (1992) prophylactically administered CMV-specific CTL clones derived from donor peripheral blood mononuclear cells (PBMCs) to a small number of at risk BMT patients, who were protected from CMV-related disease. The first treatment of virus-associated cancer occurred soon after, when donor PBMCs were used to treat

EBV-associated PTLD in BMT patients (Papadopoulos *et al*, 1994). Three of five patients responded well to therapy, however all three also developed graft versus host disease (GVHD). The following year, 10 BMT patients were infused with donor derived polyclonal EBV-specific CTLs (Rooney *et al*, 1995). Three patients with EBV-related lymphoproliferation responded to treatment, and EBV DNA in PBMCs fell to normal levels. None of the remaining seven patients developed PTLD. Preparation of virus-specific cells *ex vivo* appeared to deplete the alloreactive T cells seen in the earlier trial, and GVHD was not observed in any patient (Papadopoulos *et al*, 1994; Rooney *et al*, 1995). In an extended trial by the same group, EBV-specific CTLs prevented development of PTLD in all of 39 treated patients compared with seven of 61 (11.5%) controls, and five of six (83.3%) patients treated for overt lymphoma achieved complete remission (Rooney *et al*, 1998). In a trial of 33 solid organ transplant patients, EBV-specific CTLs have also been used to successfully treat PTLD, with an overall response rate of 52% (Haque *et al*, 2007). Donor PBMCs are not usually available in this setting, so allogeneic or autologous strategies for EBV-specific CTL manufacture have been established for the treatment of PTLD (Haque *et al*, 1998; Khanna *et al*, 1999). Cellular therapy has also been tested against other EBV-associated cancers including HL and NPC. However, as these tumours arise in immunocompetent hosts and express a more restricted pattern of viral antigens, they are less responsive to EBV-specific therapy. In small-scale trials, three of six patients with refractory NPC and three of 11 relapsed HL patients achieved a measurable response to treatment with EBV-specific CTLs (Bollard *et al*, 2004; Straathof *et al*, 2005a).

With respect to cancers not associated with viral infection, early therapies using donor PBMCs re-induced remission in BMT patients with relapsed chronic myeloid leukaemia (CML) (Kolb *et al*, 1990). This is a graft versus leukaemia (GVL) effect and not transferable for general cancer therapy, although it showed proof of principle that the immune system could combat tumours. However, the majority of TAA are weakly immunogenic self-antigens and natural T cells against these antigens are low in frequency, have low T cell receptor (TCR) avidity or are anergic, and thus a more robust cellular therapy is needed (Tey *et al*, 2006). To this end, leukaemia-specific CTLs have been generated from PBMCs by loading dendritic cells with antigen derived from whole leukaemic blasts, capable of lysing tumour cells *in vitro*

(Montagna *et al*, 2001). Anti-leukaemic CTLs have also been shown to mediate tumour regression of CML *in vivo* (Falkenburg *et al*, 1999). In the autologous setting, CTLs specific for melan-A peptide could be generated from the PBMCs of melanoma patients using dendritic cells pulsed with tumour peptide epitopes as antigen presenting cells (APCs), and clinical responses were seen in some patients (Meidenbauer *et al*, 2003). However, this approach is limited to patients carrying the HLA haplotype required to bind the previously defined immunogenic epitope. Alternatively, lines of tumour infiltrating lymphocytes (TILs) can be cultured from individual patients and screened for specific clones reactive with autologous tumours cells, which can then be re-infused into the patient. In one trial of metastatic melanoma refractory to standard therapies, objective responses to TIL therapy were seen in six of 13 patients, and mixed responses in four others (Dudley *et al*, 2002).

The strategies mentioned above are highly labour intensive and clinical trials of cancer cellular immunotherapy have, virus-associated malignancies aside, shown modest and variable response rates. Effective therapies require T cells to persist, expand, traffic and home to tumours and mediate effector function. One approach to target weakly immunogenic TAA is to engineer T cell specificity by gene modification, which will be covered in the next section.

1.5.3 Engineered T cells

There are two strategies by which T cells can be genetically engineered with a defined tumour specificity, or 're-targeted'. The α and β chains of a TCR define a T cells antigen specificity, and thus the first approach is simply to transfer native α and β TCR chains with the required specificity into T cells HLA matched with the target. This has been accomplished with TCRs specific for TAA, and engineered cells (those containing the transferred genes) against TAAs such as the melan-A protein expressed in melanoma are capable of *in vitro* antigen-specific anti-tumour activity (Clay *et al*, 1999). The strategy by which engineered T cells are employed in the treatment of patients is outlined in Figure 1.8. The first clinical trial using transferred native TCRs resulted in tumour regression in two of 15 patients with progressive metastatic melanoma (Morgan *et al*, 2006). Issues associated with this method include mispairing of the introduced and endogenous α and β TCR chains and low

surface expression of the introduced TCR (Morgan *et al*, 2006). Steps to overcome these limitations are being undertaken, including modification of the introduced TCR chains to prevent mispairing and potentially also increase surface expression (Cohen *et al*, 2007). However, as each TCR is specific for a peptide-MHC complex, this therapy remains restricted to patients that share both MHC allele and tumour antigen.

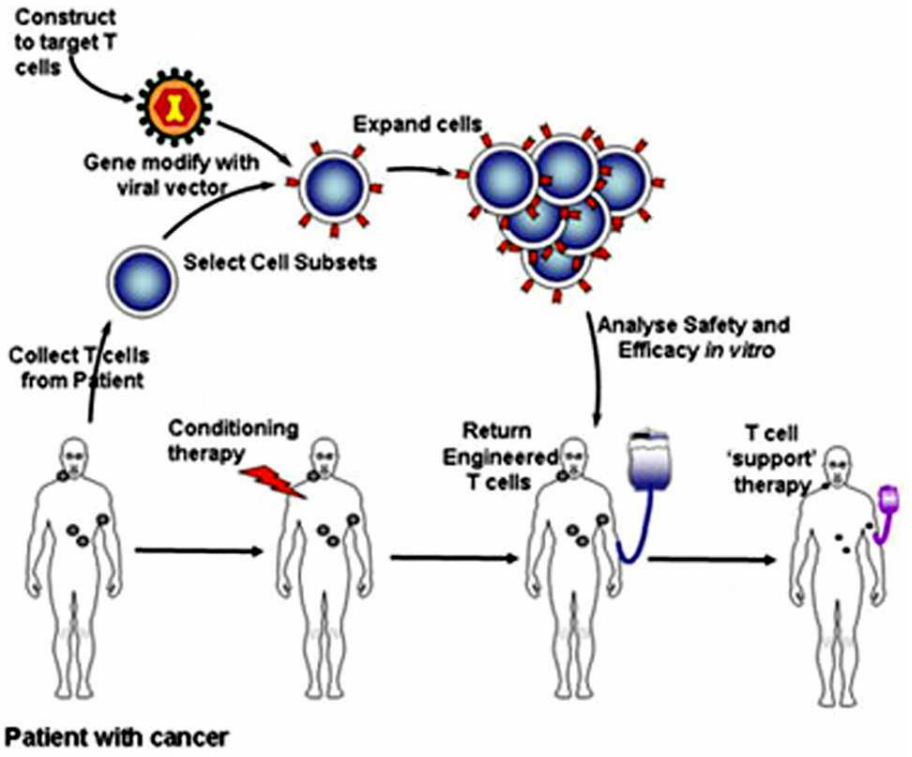

Figure 1.8: Treatment using engineered T cells.
An outline of the process by which T cells are taken from a suitable cancer patient, engineered to express tumour-specific cTCRs, expanded and re-infused into the patient as treatment. Adapted with permission from the ATTACK Project website (www.attack-cancer.org).

The second strategy by which T cells can be re-targeted is by transfer of a chimeric TCR (cTCR), also known as a chimeric antigen receptor (CAR) or 't-body' (Eshhar *et al*, 1993). These molecules generally contain an antibody based external domain such as a scFv (see Figure 1.7), and the internal domain of a TCR for signal transduction and T cell activation (Eshhar *et al*, 2001). They are expressed on the surface of the T cell as a single gene-encoded homodimer, enabling MHC-independent recognition of native TAA. Cells engineered with cTCRs specific for a range of TAA, including CD19, CD30, HER2/neu and prostate-specific membrane

antigen (PSMA), have been shown capable of specific tumour cell lysis *in vitro* (Gong *et al*, 1999; Haynes *et al*, 2002; Cheadle *et al*, 2005; Savoldo *et al*, 2007), and are listed with other TAAs targeted by cTCRs in Table 1.4.

Table 1.4: Tumour associated antigens targeted by cTCR engineered T cells. [FBP; folate-binding protein: CEA; carcino-embryonic antigen: NCAM; neural cell adhesion molecule: PSMA; prostate-specific membrane antigen]

targeted antigen	target cells	reference
CD19	B cell lymphoma	Brentjens *et al* (2003)
CD20	B cell lymphoma	Jensen *et al* (2003b)
CD30	Hodgkin's lymphoma	Hombach *et al* (2001)
CD171	neuroblastoma	Park *et al* (2007)
CEA	gastrointestinal tumours	Gilham *et al* (2002)
FBP	ovarian carcinoma	Kershaw *et al* (2002)
ErbB-2	breast, ovarian carcinoma	Haynes *et al* (2002)
carboxy anhydrase IX	renal cell carcinoma	Weijtens *et al* (2000)
MAGE-A1	melanoma	Willemsen *et al* (2000)
NCAM	neuroblastoma	Gilham *et al* (2002)
PSMA	prostate cancer	Gong *et al* (1999)

Engineering chimeric receptors for T cells is still an evolving field, and technical challenges remain to be resolved. One problem involves the binding of engineered cells to targets. The scFv-TAA association must be specific yet permit disengagement for efficient killing of multiple target cells (Kalergis *et al*, 2001). Thus, to allow serial killing as well as to limit potential cross-reactivity with healthy tissue, scFv and target antigens must be chosen with care. Another challenge is the optimal transduction of signals through the cTCR. Early cTCR constructs contained the intracellular CD3ζ moiety, which delivered a potent signal 1 to the engineered cell upon antigen binding, but the downregulation of T cell costimulation molecules on most tumours result in a lack of signal 2, leading to apoptosis or anergy of the engineered cell (Maher & Davies, 2004). The two signal model of T cell activation is illustrated in Figure 1.9. Initial research focused on incorporating CD28 into the cTCR, fusing the signalling domain of this costimulatory protein in series with the CD3ζ domain, to create receptors capable of delivering both signal 1 and signal 2 for T cell activation (Finney *et al*, 1998; Eshhar *et al*, 2001; Maher *et al*, 2002). Additional activation signal domains including lck tyrosine kinase and OX40 are now also being investigated (Geiger *et al*, 2001; Pule *et al*, 2005).

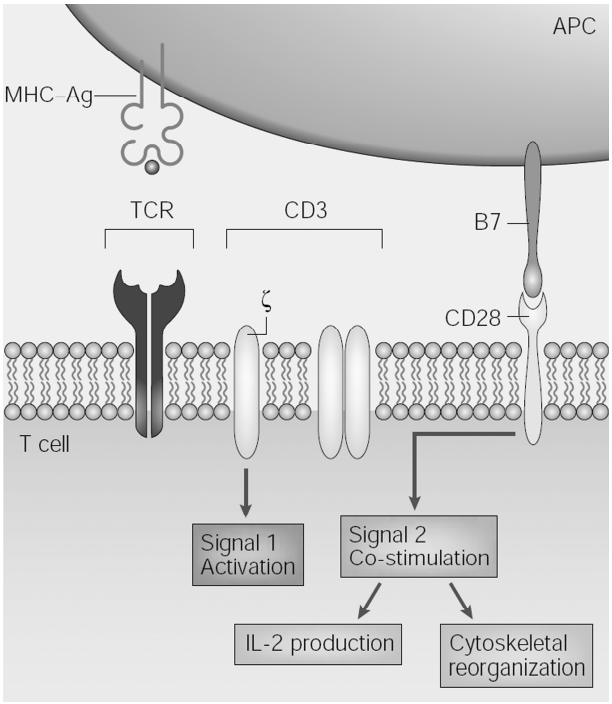

Figure 1.9: Two signal model of T cell activation.
T cells require two signals to become fully activated. Signal 1 [activation] is initiated by the binding of the TCR complex (including CD3) to the antigenic peptide presented by MHC. Signal 2 [co-stimulation] is antigen independent and is also delivered by the antigen presenting cell (APC) via a B7-CD28 interaction. The second signal promotes T cell activation and proliferation, increasing expression of IL-2.

Binding of a native TCR to its cognate peptide/MHC complex results in the phosphorylation of ITAMs within the intracellular CD3 molecules, and transduction of an activation signal via Lyk and Fyn kinases recruited primarily to CD3-ζ (Pitcher & van Oers, 2003). How precisely peptide/MHC binding induces this transduction remains unclear, although several factors are thought to play a role, including conformational changes in the TCR and receptor aggregation. The TCR/CD3-ε complex undergoes a conformational change that uncovers a proline-rich sequence in the CD3-ε cytoplasmic tail, allowing it to bind the ubiquitously expressed adapter protein Nck, which may recruit further effector molecules to the CD3 ITAMs (Buday, 1999; Gil *et al*, 2002). Aggregation of TCR complexes following multimeric peptide/MHC binding brings individual CD3 cytoplasmic domains into close proximity, facilitating transphosphorylation of the ITAMs (Minguet *et al*, 2007). Aggregation of receptors also draws the membranes of target and effector cells together, excluding large molecules such as CD45 with its intracellular phosphotases, allowing CD3 ITAMs to remain phosphorylated (Rudolph *et al*, 2006). Correspondingly, the BCR (which incorporates surface-bound antibody) also transduces signals using a combination of conformational changes and aggregation. It is likely signal transduction by cTCRs is accomplished in a similar way to native

TCRs, utilising the aggregation of receptors, although if conformational change plays a role it has yet to be elucidated, as cTCRs do not incorporate CD3-ε.

With the inclusion of a second signal, engineered T cells can be repeatedly activated by antigen *in vitro*, with each round of stimulation resulting in specific lysis of target cells and IL-2 driven proliferation (Maher *et al*, 2002). Engineered T cells have also been shown capable of controlling tumour growth in animal models (Haynes *et al*, 2002; Brentjens *et al*, 2003). Recent phase I clinical studies have proved the therapy well tolerated for the treatment of metastatic ovarian cancer and neuroblastoma (Kershaw *et al*, 2006; Park *et al*, 2007). Although tumour regression was not observed, bearing in mind the heavy and refractory disease burden of patients in such trials, these were overall positive results. Persistence of therapeutic cells *in vivo* remains an issue; both trials saw rapid clearing of cells carrying cTCRs, as measured by vector specific PCR of PBMCs. It should be noted that neither of the cTCRs used carried a domain for signal 2 transduction within the TCR. However, the cells used to treat ovarian cancer patients were alloreactive via their native TCR, due to engineered PBMCs being co-cultured with irradiated allogenic PMBCs prior to cTCR transduction, as it had been shown that this strategy provided proliferation signals in response to subsequent immunisation with allogeneic PBMCs (Kershaw *et al*, 2002).

One issue likely to affect further development of cTCR engineered T cell is the vector used to transport the receptor into cells. Currently, the majority of research is carried out using retroviral vectors. However, as seen in a gene therapy trial for X-linked severe combined immune deficiency (SCID), this carries the risk of viral insertional mutagenesis and subsequent cellular transformation (Hacein-Bey-Abina *et al*, 2003). Experimental results indicate that lentiviral vectors are less prone to insertional mutagenesis than retroviral vectors, at least in mouse models (Montini *et al*, 2006), and as such are an alternative option, although a large amount of *in vivo* data needs to be collected to more accurately determine their overall safety. A further option is the inclusion of conditional suicide genes in the vector. An example is herpes simplex virus thymidine kinase (HSV-TK), which has been used in phase II trials for BMT patients with relapsed haematological malignancies receiving infusions of donor lymphocyte transduced with HSV-TK (Ciceri *et al*, 2007).

Tumour regression was concurrent with GVHD, which abated after ganciclovir administration tripped the suicide switch. This approach would guard against potential inappropriate responses to therapy.

Research into cTCR engineered T cells is still in its infancy, but it is a field with vast potential for application in the therapy of cancer. Although there are many issues still to address, it holds great promise for treatments applicable to refractory or recurrent malignancies.

1.6 Antibody phage display

1.6.1 Background

Antibodies have such a wide range of applications, medically and scientifically, that their use has become near ubiquitous in biotechnology. Beyond the treatment of cancer, antibody technology has been exploited for diagnostic testing, *in vivo* radioimaging, labelling of cells for experimental purposes, and treatment of non-malignant illnesses, to name but a few examples. In the early period of their use, serum containing polyclonal antibodies was collected from immunised animals. With the advent of hybridoma technology it was possible to reliably produce mAbs (Kohler & Milstein, 1975). However, there remained a number of limitations to hybridoma technology. As animals still needed to be immunised in the initial stage, it was not possible to produce antibodies against toxic, pathogenic, non-immunogenic or some self antigens (Winter & Milstein, 1991). Importantly for clinical uses, the antibody molecule was murine, leading to the generation of human anti-mouse antibodies in patients, especially with repeated dosing. Generation of hybridomas was also costly and time consuming. In groundbreaking work, Dr George Smith established a method by which polypeptides could be presented on the surface of filamentous phage, a virus able to infect the common laboratory bacteria *E.coli* and capable of replication and assembly without host cell lysis (Smith, 1985). This method was subsequently adapted for antibody presentation (McCafferty *et al*, 1990).

The filamentous phage particle has a thread-like shape approximately 6.5 nm in diameter and 1 µm in length (Paschke, 2006). Its circular single-stranded DNA

genome is encased in a cylindrical protein coat, predominantly composed of the major coat protein, pVIII. At one end, the phage particle incorporates about five copies of the minor coat proteins pVII and pIX. At the other end, three to five molecules of the remaining minor coat proteins pIII and pVI are displayed. A schematic diagram of a filamentous phage is shown in Figure 1.10. Antibodies displayed on filamentous phage are not entire IgG molecules, but rather scFv or Fab antibody fragments (see Figure 1.7). A comparison of Fab and scFv formats for antibody phage display is given in Table 1.5.

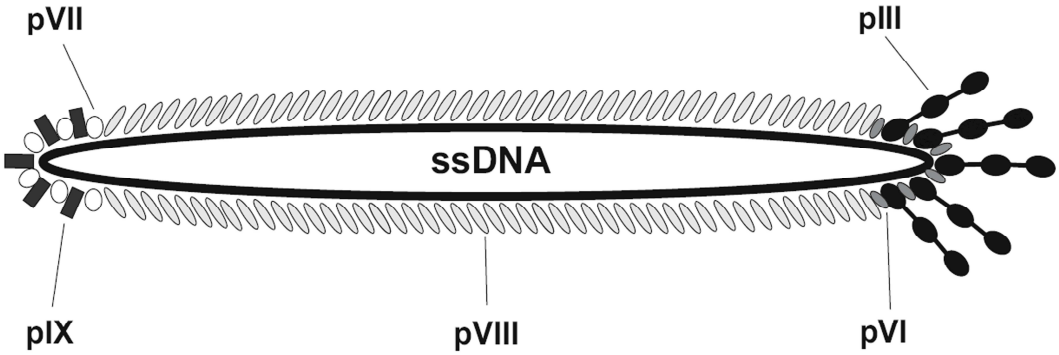

Figure 1.10: Filamentous phage particle.
Schematic of a filamentous phage particle, showing the major coat protein pVIII encasing the single-stranded DNA genome, with minor proteins pIII, pVI, pVII and pIX incorporated into the coat at either tip. Image adapted from Paschke M. Applied Microbiology and Biotechnology 70:2-11, copyright (2006), with kind permission from Springer Science and Business Media.

Table 1.5: Comparison of scFv and Fab formats in antibody phage display.

scFv	Fab
Better tolerated by bacteria	More difficult to synthesise
Less likely to be degraded	More likely to be degraded
Can form dimers	No dimerisation
Single protein molecule	Two protein molecules
Peptide linker can shorten	No such problems
Less stable	More stable
A fraction of expressed scFv can be non-functional	Tends to be more functional
DNA insert 700 bp	DNA insert >1500 bp

1.6.2 Phage and phagemids

The principle underlying all phage display systems is the physical linkage of a polypeptide's phenotype to its corresponding genotype. For antibody phage display, antibody fragments are fused to a minor coat protein, usually pIII. The C terminus of the pIII protein inserts into the coat, and is essential for the structural integrity of the phage, whilst the antibody fragment is presented on the surface of the phage particle. As the genetic information encoding the fusion protein is contained in the phage genome packaged inside the phage particle, identification of a desirable clone by fragment binding allows simultaneous recovery of the gene encoding the selected antibody fragment. These fragments can then be cloned into vectors encoding intact Ig molecules, or alternative targeted immunotherapy frameworks, such as chimeric receptors (Willemsen *et al*, 2001; Nagy *et al*, 2002).

There are two genetic systems used in antibody phage display, the first being phage vectors and the second phagemid vectors. The properties of each system are outlined in Table 1.6. In phage vectors, the antibody-pIII fusion gene is inserted directly into the phage genome (McCafferty *et al*, 1990). The major advantage of this is that all copies of the pIII protein contain the antibody fragment. However, the disadvantages are consequent low transduction efficiency and a negative selection pressure on phage carrying the fusion product, as replication and pIII expression is linked to the genome. In the second method, the antibody-pIII fusion gene is contained in a phagemid vector (Hoogenboom *et al*, 1991). A phagemid is a plasmid that bears a phage-derived origin of replication in addition to its plasmid origin of replication. The additional proteins necessary for replication and packaging of the phagemid vector into a phage particle are encoded in a second 'helper' phage, with which the bacteria are superinfected, a process know as 'phage rescue'. The helper phage is also able to replicate itself, and thus two types of phage particles are produced carrying either phagemid or helper phage DNA. The fraction of phage containing the helper phage genome can be reduced significantly by using a helper phage with a defective origin of replication or packaging signal, leading to preferential packaging of the phagemid DNA over the helper phage genome (Russel *et al*, 1986). Wildtype pIII expressed by the helper phage is also preferentially incorporated into the phage particle. This can lead to the production of 'bald phage' which display no antibody

fragments. The frequency of bald phage can be reduced using helper phage with mutated, trypsin-sensitive pIII protein (Kristensen & Winter, 1998). The cleaved pIII molecule is non-infectious, preventing bald phage being amplified during rescue.

Table 1.6: Comparison of phage and phagemid systems for antibody display libraries.

phage	phagemid
Three to five copies of antibody per phage	Only 1 –10% of phagemids have one copy of the displayed antibody
Difficult to transfect and make DNA	Easy to handle
Faster to select and easier to use	Slower to select (helper phage needed)
Must subclone to make soluble Ab	Soluble Ab made directly
Phenotypic and genotypic homogeneity	Phenotypic and genotypic heterogeneity
Genetically less stable (deletions)	More stable genetically
Greater diversity of antibodies selected	Lower diversity of antibodies selected
Lower affinity antibodies also selected due to avidity effects	Higher affinity antibodies selected due to monomeric display
Not suitable for affinity maturation due to avidity effects	Better for affinity maturation

1.6.3 Antibody libraries

Antibody phage libraries are divided into four categories depending on the type and source of the antibody fragment: immune, naïve, semi- and fully-synthetic. Immune libraries are constructed using B cells from an immunised animal or immune patient, and are thus pre-enriched for antigen-specific clones, making it possible to isolate high affinity antibodies from relatively small libraries. The disadvantage of immune libraries is that they require immunogenicity of the target antigen in either humans or animals, and immunisation and library construction is required for each antigen.

Naïve libraries, as the name suggests, are constructed using PBMCs or splenocytes from unimmunised animals or human donors. The libraries are constructed using antibody V_H and V_L domains, which are amplified from cytoplasmic RNA (as B cells are highly enriched in Ig mRNA) or synthesised *de novo*. The two variable domains

are combinatorially assembled to create a large and diverse array of antibodies. Semi-synthetic libraries are derived from unrearranged V-genes from germline B cells, or from a single antibody framework, with at least one CDR genetically randomised, while fully synthetic libraries use a single framework with randomly integrated CDR cassettes. The greatest advantage of synthetic libraries is the ability to isolate antibodies specific for self antigens, which is not always possible with immune or naïve libraries.

Naïve, semi-synthetic and fully synthetic libraries are collectively know as 'single pot' libraries, as they are not be biased towards any particular antigen, and theoretically contain antibody fragments which will bind to virtually every antigen. Thus one library can be used for the isolation of high affinity clones against multiple targets. Libraries with a theoretical diversity of up to 10^{10} independent clones have been generated (Paschke, 2006).

1.6.4 The process of selection

Selection from phage display libraries is a cyclic process of discriminating enrichment and amplification. The phage library is exposed to antigen, allowing specific phage to bind to their targets. Antigen-bound phage are then recovered and subsequently amplified by infection in *E.coli*. This process is known as 'panning', in the same sense that historically prospectors panned for gold. The amplified phage population is then subjected to the next round of panning. Generally, two to four rounds of panning are completed before the selected phage are individually analyzed to identify specific binders. If affinity for the antigen is sufficiently high for the intended purpose, the selected antibody fragment can be used directly in immunotherapy applications. Otherwise, affinity maturation techniques, for example site-specific or combinatorial mutagenesis of the CDRs, can be used to enhance the binding properties of the fragment (Wu *et al*, 1998; Boder *et al*, 2000).

An extensive range of methodologies exists for the isolating of specific clones from phage libraries (Bradbury & Marks, 2004). At its most basic, selection involves immobilisation of the protein antigen on a solid base such as an immunotube or ELISA plate. More complex variations on this theme include the fixing of whole

cells to solid supports or enrichment on tissue sections (de Kruif *et al*, 1995). Another alternative is biotinylation of the antigen, allowing retrieval of phage/antigen using streptavidin coated magnetic beads for example. Phage can also be selected on whole cells grown in monolayers or in solution, with cells lysed to release internalised specific binders (Griffiths *et al*, 1993). Alternatively, phage selection on whole cells can be performed by fluorescence associated cell sorting (FACS), using labelled monoclonal antibodies specific for the phage particle and a selectable marker co-expressed on target cells within a heterogeneous population (de Kruif *et al*, 1995).

Over the course of successive rounds of panning, several assays can be employed to monitor selection. These include polyclonal enzyme-linked immunosorbant assays (ELISA), which measure the increases in specific binders, PCR screening, which monitors selection pressure by examining the presence of antibody fragment inserts, and restriction mapping of the antibody fragments, which assesses diversity within the phage population. The analysis of target specificity in individual clones at the end of selection can also be assayed in several ways. Monoclonal phage ELISA is often used in the first instance as it is a rapid and relatively sensitive test. Following this initial screen, other assays can be employed, including sequencing of antibody fragments, and expression of soluble antibody fragments from the phage vector. The majority of phage libraries are engineered so that soluble expression of antibody fragments includes a peptide tag such as myc or Flag, to facilitate the use of soluble fragments in screening ELISAs, FACs, Western blots or immunohistochemistry.

1.7 Project aims

EBV-associated malignancies have been successfully treated using virus-targeted immunotherapy. However, the majority of EBV-associated malignancies display a restricted set of viral latent antigens, and there remain a proportion of patients who respond to neither conventional nor experimental therapies.

The aim of this project was to investigate the following hypothesis:

> *'Engineering with a chimeric T cell receptor directed against the Epstein-Barr virus latent membrane 2 will confer upon T cells the ability to target and kill the malignant cells of cancers associated with Epstein-Barr virus.'*

In order to test this hypothesis, three main projects were undertaken: (1) SCID mouse models for EBV-associated HL, NPC and GC were set up to provide a framework in which to test engineered cells; (2) PBMCs were engineered with a cTCR specific for the B cell antigen CD19, and their effect against HL derived cell lines examined, and (3) a novel scFv specific for the extracellular sections of EBV LMP2 was sought from phage display libraries, for incorporation in a cTCR and eventual use as an alternative therapy for EBV-associated malignancies.

2 Materials and Methods

2.1 Materials

2.1.1 Equipment

Automatic pipettor	‘Pipetboy acu’, Integra Biosciences ‘Powerpette plus’, Jencons
Balances	fine: ‘AE163’, Mettler medium: ‘BP310P’, Sartorius gross: ‘EK-200G’, AND
Centrifuges	‘1-15K’, Scientific Laboratory Supplies ‘3K18C’, Sigma Laboratory Centrifuges ‘Falcon 6/300’, MSE ‘J2-21’, Beckman Coulter ‘Micro Centaur’, MSE ‘Mistral 3000E’, MSE ‘Mistral 3000i’, MSE
Flow cytometers	‘FACScan’, Becton Dickinson ‘FACSCalibur’, Becton Dickinson
Fume hood	Lynwood Installations
Gamma counter	‘1480 Wizard’, Perkin Elmer
Gel Documentation System	UVP transilluminator and camera with a ‘UP-D895’ Synoptics printer and UVP ‘Labworks Image Acquisition and Analysis’ software

Gel electrophoresis system	Scotlab tank with Stratagene 'Feather Volt 500' power pack
Haemocytometer	Scientific Laboratory Supplies
Heating block	'DB.3', Techne
Histology Image Capture	'BX51' Olympus microscope with Polaroid 'PDMC-2' camera and 'DMC le' software
Humidity chamber	Sandrest
Incubators	30°C: Hearson 37°C: Gallenkamp, Sandrest 37°C humidified: Leec, Forma Scientific 37°C shaking: '4536', Forma Scientific 55°C: Hybaid
Microbiological safety cabinets (Class II)	Medical Air Technology Envair Arrowmight Biosciences
Microscopes	'Laborlux K', Leitz 'TMS', Nikon
Microwave	'SM18', Proline
PCR machine	'T3 Thermocycler', Biometra
pH meter	'HI 8521', Hanna Instruments
Pipettes	'Pipetman', Gilson 'Nichipet', Nichiryo
Plate reader	'MRX', Dynex Technologies

Real time PCR machine	‘R-3000’, Rotor-Gene
Refrigeration	4°C: Electrolux -20°C: Labcold -70°C: ‘Ultra 85’, Assab
Roller Mixer	‘SRT1’, Stuart Scientific
Shakers	‘Orbital shaker’, Denly ‘R/100/TW’, Luckham
Spectrophotometer	‘GeneQuant II’, Pharmacia Biotech ‘CE 272’, Cecil Instruments
Stirrer	‘Magnetic Stirrer Hotplate’, Stuart Scientific
Vortex	‘MS2 Minishaker’, IKA
Waterbaths	Clifton Grant Instruments

2.1.2 Suppliers

AbD Serotec	Endeavour House, Kidlington, Oxford, OX5 1GE, UK. www.ab-direct.com
Barloworld Scientific	Beacon Road, Stone, ST15 0SA, UK. www.barloworld-scientific.com
Becton Dickinson	21 Between Towns Road, Cowley, Oxford, OX4 3LY, UK. www.bdeurope.com

Clonetec	2 Avenue du President Kennedy, 78100 Saint-Germain-en-Laye, France. www.clontech-europe.com
Dako	Denmark House, Angel Drive, Ely, CB7 4ET, UK. www.dako.co.uk
Fisher Scientific	Bishop Meadow Rd, Loughborough, LE11 5RG, UK. www.fisher.co.uk
GE Healthcare	Amersham Place, Little Chalfont, HP7 9NA, UK. www.amershambiosciences.com
Geneservice Ltd	Cambridge Science Park, Milton Road, Cambridge, CB4 0FE, UK. www.geneservice.co.uk
Greiner Bio-One	Brunel Way, Stroudwater Business Park, Stonehouse, GL10 3SX, UK. www.greinerbioone.com
Invitrogen	Inchinnan Business Park, 3 Fountain Drive, Paisley, PA4 9RF, UK. www.invitrogen.com
Marligen Biosciences	Stirling Road, High Wycombe, HP12 3ST, UK. www.marligen.com
Miltenyi Biotec	Almac House GU24 9DR Surrey, UK. www.miltenyibiotec.com
New England Biolabs	75-77 Knowl Piece, Wilbury Way, Hitchen, SG4 0TY, UK. www.neb.uk.com

Nunc Brand	Supplied by Fisher Scientific.
Perbio	Unit 9, Atley Way, North Nelson Industrial Estate, Cramlington, NE23 1WA, UK. www.perbio.com
Promega	Delta House, Southampton Science Park, Southampton, SO16 7NS, UK. www.promega.com/uk
Qiagen	Qiagen House, Fleming Way, Crawley, RH10 9NQ, UK. www1.qiagen.com
Sigma Aldrich	The Old Brickyard, New Road, Gillingham, SP8 4XT, UK. www.sigmaaldrich.com
StemCell Technologies	60 rue des Berges, Miniparc Polytec, batiment Tramontane Grenoble 38000, France. www.stemcell.com
Thistle Scientific	DFDS House, Goldie Road, Uddingston, G71 6NZ, UK. www.thistlescientific.co.uk
UDP	Amber Park, Berristow Lane, South Normanton, DE55 2FH, UK. www.udg.co.uk
Vector Laboratories	3 Accent Park, Bakewell Road, Peterborough PE2 6XS, UK. www.vectorlabs.com

Vision BioSystems	Balliol Business Park, West Benton Lane, Newcastle Upon Tyne, NE12 8EW, UK. www.vision-bio.com
VWR	Hunter Boulevard, Magna Park, Lutterworth, LE17 4XN, UK. uk.vwr.com

2.1.3 Solutions

CBS	PBS with: 2% FBS 1mM EDTA
H-top agar	1% (w/v) tryptone 0.8% (w/v) NaCl 0.6% (w/v) bacto-agar
Minimal agar	7.6mM $(NH_4)_2SO_4$ 0.1% (w/v) dextrose 1.7mM $Na_3C_6H_5O_7.2H_2O$ 1.5% (w/v) bacto-agar 1mM $MgSO_4$ 0.0005% (w/v) Thiamine-HCl 33.1mM KH_2PO_4 60.1mM K_2HPO_4
PBS pH 7.4	137mM NaCl 2.7mM KCl 4.3mM Na_2HPO_4 1.4mM KH_2PO_4

PBSA	PBS with: 1% w/v BSA 0.1% w/v sodium azide 0.2% w/v EDTA
TBE buffer pH 8.3	0.44M Tris 0.44M Boric acid 12mM EDTA
TBS	25mM Tris 137mM NaCl 27.7µM KCl
2xTY medium	1.6% (w/v) tryptone 1% (w/v) yeast extract 0.5% (w/v) NaCl
2xTY AG	2xTY medium with: 100µg/ml ampicillin 1% (w/v) glucose
2xTY AKG	2xTY medium with: 100µg/ml ampicillin 50µg/ml kanamycin 0.1% (w/v) glucose
TYE agar	1% (w/v) tryptone 0.5% (w/v) yeast extract 0.8% (w/v) NaCl 1.5% (w/v) bacto-agar
TYE AG	TYE agar with: 100µg/ml ampicillin 1% (w/v) glucose

2.2 Tissue culture techniques

2.2.1 Maintenance of cell lines

Cell lines were cultured in sterile plastic-ware and maintained at 37°C in 5% humidified CO_2 in the appropriate medium as listed in Table 2.1.

Table 2.1: Media and cell lines used for tissue culture.
[RPMI; Roswell Park Memorial Institute, FBS; foetal bovine serum, DMEM; Dulbecco's Modified Eagles Medium]

culture medium	media	supplements	cell lines	reference
complete medium-20	RPMI	FBS to 20% (v/v)	CTLs	
		2mM L-glutamine	HDLM2	(Drexler *et al*, 1986)
		100U/ml penicillin	L540	(Diehl *et al*, 1981)
		100U/ml streptomycin	L591	(Diehl *et al*, 1982)
			PG13	(Miller *et al*, 1991)
complete medium-10	RPMI	FBS to 10% (v/v)	AGS	(Barranco *et al*, 1983)
		2mM L-glutamine	B95-8	(Miller *et al*, 1972)
		100U/ml penicillin	K562	(Lozzio & Lozzio, 1975)
		100U/ml streptomycin	L1236	(Wolf *et al*, 1996)
			LCLs	
			NUGC3	(Akiyama *et al*, 1988)
			Raji	(Pulvertaft, 1964)
complete medium-8	RPMI	FBS to 8% (v/v)	C666.1	(Cheung *et al*, 1999)
		2mM L-glutamine		
		100U/ml penicillin		
		100U/ml streptomycin		
DMEM	DMEM	FBS to 10% (v/v)	HT1080	(Rasheed *et al*, 1974)
		2mM L-glutamine		
		100U/ml penicillin		
		100U/ml streptomycin		

Cell lines HDLM2, L1236, L540 and L591 were a gift from Professor Ruth Jarrett, LRF Virus Centre, University of Glasgow; AGS and NUGC3 a gift from Professor Kenzo Takada, Institute for Genetic Medicine, Hokkaido University, Japan; and C666.1 a gift from Professor Paul Farrell, School of Medicine, Imperial College, London, UK. RPMI, DME, L-glutamine, penicillin, and streptomycin were supplied by Invitrogen. FBS was supplied by Perbio. Plastics for cell culture were supplied by Barloworld Scientific, Becton Dickinson, Fisher Scientific and Greiner Bio-One.

2.2.2 Passaging adherent cell lines

Culture medium was removed from the cell monolayer and cells were washed with 0.02% versene (0.5mM EDTA, 0.001% phenol red in PBS) then incubated with a 1:1 solution of versene and 0.25% (w/v) trypsin (Invitrogen) at 37°C until the cells detached from the plastic. The cells were either seeded directly into a new culture flask, or centrifuged at 180g for 7 minutes and the resulting pellet resuspended in fresh medium and seeded into a new flask.

2.2.3 Freezing and thawing cells

For long term storage of cell lines, viable cells were centrifuged at 180g for 7 minutes and resuspended in freeze medium (70% RPMI, 20% FBS and 10% DMSO) at cell concentrations between $5x10^6$ and $2x10^7$ cells/ml. Volumes of 1ml were aliquoted into cryovials and placed in a cryo 1°C freezing container (VWR) for overnight slow freezing at -70°C before being transferred to liquid nitrogen.

Frozen cell lines were thawed quickly in a 37°C incubator and washed twice by centrifugation in Hank's buffered salt solution (HBSS) (Invitrogen), or in RPMI with 20% FBS for CTLs and transduced cells, at 180g for 7 min. Pelleted cells were resuspended at the appropriate concentration and media for the line

2.2.4 Cell separation by centrifugation

Ficoll-hypaque density centrifugation was used to separate PBMCs from whole blood and to remove dead cells from cultures. Cell suspensions were layered into an equal volume of Histopaque-1077 (Sigma) and centrifuged at 600g and 4°C for 20 minutes. Viable cells were removed from the Histopaque/medium interface and resuspended in HBSS (Invitrogen) and centrifuged at 180g for 7 minutes. Cell pellets were resuspended in an appropriate volume of media or buffer, as required.

2.2.5 Cell separation by antibody-coated magnetic beads

EasySep systems (StemCell Technologies) were used to separate cell populations on the basis of cell surface antigen expression, following the manufacturer's

instructions. Briefly, cells were washed in cell separation buffer (CSB) at 180g for 7 minutes and resuspended at $1x10^8$ cells/ml in CSB. The appropriate EasySep positive selection cocktail (bi-specific tetrameric antibody complexes directed against the selection antigen and dextran) was added at a concentration of 100µL/ml cells for CD56 selection and 200µL/ml cells for CD34 selection, and the mixture incubated for 15 minutes at room temperature. Nanoparticles (magnetic dextran iron particles in water) were added at a concentration of 50µL/ml, and the mixture incubated for 10 minutes at room temperature. Total volume was brought to 2.5ml with CBS and the tube placed in an EasySep magnetic for 5 minutes. The supernatant was poured off, the tube removed from the magnet, 2.5ml CSB added to the remaining cells, and the tube placed back in the magnet. The separations were repeated a total of 4 times for CD34 selection and 3 times for CD56 selection. Both the positively selected fraction and the depleted fraction were retained, counted, and resuspended at $1x10^6$ cells/ml in complete medium-20 for further culture.

2.2.6 Counting cells

An aliquot of cells was diluted 1:1 with 0.4% (w/v) trypan blue (Sigma) and applied to a haemocytometer. Stained and unstained cells were counted to determine the percentage of viable cells and total cell number.

2.3 DNA Extraction

2.3.1 Extraction of phagemid DNA from bacteria

Single colonies of bacteria infected with phage growing on agar plates or clones stored in 15% glycerol at -70°C were inoculated into 5ml 2xTY AG and incubated overnight, shaking at 37°C. An aliquot of 1ml was pelleted by centrifugation at 11600g for 5 minutes and the DNA extracted using the Rapid Plasmid Miniprep System (Marligen Bioscience Inc) according to the manufacturer's instructions. Briefly, the cells were resuspended in 250µl buffer G1, to which 250µl Buffer G2 was added to lyse the bacteria and the mixture incubated for 5 minutes at room temperature. Following lysis, 350µl Buffer M3 was added, the tube inverted several times and centrifuged at 12000g for 10 minutes. The supernatant was applied to a

spin cartridge which was subsequently centrifuged at 12000g for 1 minute. The cartridge was washed with 700µl Buffer G4 at 12000g for 1 minute and the DNA eluted by addition of 50µl H_2O, incubation at room temperature for 1 minute and centrifugation at 12000g for 2 minutes. DNA was stored at -20°C.

2.3.2 Extraction of viral and genomic DNA from cell lines

DNA from cultured cells was extracted using a QIAamp DNA Mini Kit (Qiagen) according to the manufacturer's instructions. Briefly, 2-5x10^6 cells were pelleted by centrifugation at 180g for 7 minutes and resuspended in 200µl PBS. To this was added 20µl Proteinase K (600mAU/ml) and 200µl Buffer AL. The solution was vortexed for 15 seconds then incubated at 56°C for 10 minutes. 200µl ethanol was added and the mixture vortexed again for 15 seconds. The mixture was applied to a spin column which was subsequently centrifuged at 6000g for 1 minute. The column was washed with 500µl Buffer AW1 at 6000g for 1 minute, followed by 500µl Buffer AW2 at 20000g for 3 minutes, and the DNA eluted by addition of 50µl H_2O, incubation at room temperature for 1 minute and centrifugation at 6000g for 1 minute. DNA was stored at -20°C.

2.3.3 Ethanol precipitation

0.1 volume 3M NaOAc (Sigma) pH 4.6 and 2.5 volumes 95% (v/v) ethanol at -20°C (Sigma) were added to 1 volume DNA. The mixture was vortexed, incubated on ice for 20 minutes then centrifuged for 30 minutes at 13000g and 4°C. The pellet was rinsed in 70% (v/v) ethanol then centrifuged for 15 minutes at 13000g and 4°C. The supernatant was aspirated and the DNA pellet air dried for 1 hour before resuspension in H_2O and storage at -20°C.

2.3.4 Determination of DNA concentration

DNA concentration was measured using a spectrophotometer, with water used to reset the machine. The OD_{260} of the DNA was measured and the concentration calculated using the following formula:

DNA concentration (µg/ml) = OD_{260} x dilution factor x 50

2.4 *Molecular Techniques*

2.4.1 Restriction digests

PCR amplified phagemid DNA was digested with the restriction enzyme BstNI (New England Biolabs), at approximately 1 unit per µg DNA, in the supplied reaction buffer with 100µg/ml BSA, in a total volume of 24µl. Reactions were incubated at 60°C for 2 hours and visualised on a 2% (w/v) agarose gel.

2.4.2 Standard PCR

Standard PCR was used to screen phage clones for the presence of 935 bp full length inserts, as per the supplier's instructions (Geneservice). The reaction mix contained 1.5mM Mg^{2+} (Promega), 200µM dNTPs (GE Healthcare), 10pmoles of each primer, 10µl 5x Green GoTaq Flexi Buffer (Promega), 1.5U GoTaq Flexi DNA Polymerase (Promega) and DNA in a final volume of 50µl. DNA was added either to a total amount of approximately 50ng, or as bacteria picked directly from an agar plate. A negative reaction with dH_2O in place of template DNA was included in all runs.

Primers (synthesised by Sigma) were;

LMB3: 5' - CAGGAAACAGCTATGAC - 3' and
pHEN seq: 5' - CTATGCGGCCCCATTCA - 3'.

PCR were carried out on a T2 Thermocycler (Biometra). The reaction consisted of an initial denaturation step (95°C, 2 minutes), followed by 30 cycles of denaturation (95°C, 30 seconds), annealing (55°C, 30 seconds) and elongation (72°C, 2 minutes). A final elongation step (72°C, 5 minutes) was followed by cooling to 4°C before visualisation on a 2% (w/v) agarose gel.

2.4.3 Real time PCR

Real time PCR was used to assay EBV viral load (Leung *et al*, 2002). After DNA extraction a section of the viral polymerase was amplified and the levels of product determined using a 6-carboxyfluorescein (FAM) and 6-carboxy-tetramethylrhodamine (TAMRA) dual-labelled fluorogenic hybridisation probe. A

section of the housekeeping gene β-globin was also amplified from each sample in order to normalise DNA calculations. The reaction mix contained 3mM Mg^{2+} (Promega), 200µM dNTPs (GE Healthcare), 100pmoles each primer, 200pmol probe, PCR reaction buffer (10mM Tris-HCl pH 9.0, 50mM KCl, 0.1% TritonX), 1.25U Taq DNA polymerase (Promega), 275ng TaqStart antibody (Clonetec) and 1µg DNA in a volume of 25µl. A negative reaction with dH_2O in place of template DNA was included in all runs.

Oligonucleotides for the EBV polymerase amplification were;

forward: 5' - AGTCCTTCTTGGCTACTCTGTTGAC - 3',
reverse: 5' - CTTTGGCGCGGATCCTC - 3', and
probe: 5' - FAM-CATCAAGAAGCTGCTGGCGGCC-TAMRA - 3'.

Primers for β-globin amplification were;

forward: 5' - GGCACCCCTAAGGTGAAGGC - 3',
reverse: 5' - GGTGAGCCAGGCCATCACTA - 3' and
probe: 5' - FAM-CATGGCAAGAAAGTGCTCGGTGCCT-TAMRA - 3'.

All oligonucleotides for real time PCR were synthesised by Sigma. PCRs were carried out on an R-3000 Real Time Thermal Cycler (Rotor-Gene). The reaction consisted of an initial denaturation step (95°C, 10 minutes), followed by 60 cycles of denaturation (95°C, 20 seconds) and annealing and elongation (58ºC 60 sec). An initial standard curve was generated from serially diluted DNA extracted from Raji cells, which contain approximately 50 copies of the EBV genome per cell (Glaser & Nonoyama, 1974), and imported during analysis for calculation of DNA copy number. Several standards of known copy number were amplified during each run for comparison with the imported curve.

2.4.4 Agarose gel electrophoresis

Agarose was dissolved in the appropriate volume of TBE buffer by heating in a microwave. Ethidium bromide to a final concentration of 100µg/l was added to the molten gel to allow visualisation of the DNA. Samples were loaded into the set gel,

and run at 100V in TBE for 1 hour. The nucleic acid bands were visualised on a UV transilluminator.

2.4.5 DNA sequencing

Between 300-500ng of DNA was resuspended in nuclease-free water to a total volume of 5µl. Samples were sent to Jill Lovell at the School of Biological Sciences Sequencing Service, University of Edinburgh, for sequencing using the BigDye Terminator Cycle Sequencing System and an ABI Sequencer (Applied Biosystems).

2.4.6 HLA typing

DNA was resuspended in nuclease-free water to a final concentration of 100-300µg/ml. Samples were sent to Professor Anthony Dodi, the Anthony Nolan Bone Marrow Trust, Royal Free Hospital, London, UK, for HLA typing at the A, B or C loci, and Karen Stewart at the Scottish National Blood Transfusion Service Tissue Typing Laboratory, Royal Infirmary, Edinburgh, UK, for typing at the A, B, C, DR and DQ loci.

2.5 Virus Techniques

2.5.1 Production and titration of EBV

B95-8 cultures in complete medium-10 were grown to appropriate volumes, and then culture vessels sealed and incubated at 37°C to drive virus into the lytic phase. After 7-10 days, supernatant was centrifuged at 490g for 10 minutes then passed through a 0.8µ filter. The virus stock was used immediately or stored at -70°C. For titration, 10-fold dilutions of the virus stock was added to $2x10^6$ EBV negative PBMCs in complete medium-10, which were then transferred to 10 replicate wells per dilution in a 96-well flat bottomed culture plate at $2x10^5$cells per well. Cells were incubated at 37°C in 5% humidified CO_2 for four weeks, with additional media added to the plates as necessary. After four weeks, each dilution was scored for outgrowth of transformed cells, with the lowest dilution having ≥50% positive wells taken as the virus titre.

2.5.2 *In vitro* infection with EBV

For infection of the EBV-negative HL cell lines HDLM2, KMH2, L1236, and L540, a pellet of 10^7 cells was resuspended in 100µL virus preparation and the volume made up to 1ml in culture medium, before incubation at 37ºC in 5% humidified CO_2 for 1 hour. Cells were washed with HBSS then plated at a density of $2x10^6$ cells per well in a 24-well plate for continuing culture. Samples were collected at 3, 14, and where necessary 49 days post infection for DNA extraction.

2.5.3 Production and titration of retrovirus

PG13 producer cell lines (Miller *et al*, 1991) for a retrovirus encoding either a chimeric TCR specific for CD19 with a truncated CD34 molecule as a marker of transduction, or the empty vector with green fluorescent protein (GFP) as a marker of transduction, were provided by Dr Eleanor Cheadle, Paterson Institute for Cancer Research, University of Manchester (Cheadle *et al*, 2005). As a cell monolayer approached 70% confluence the supernatant was aspirated and fresh media added. After overnight incubation at 37°C the supernatant was passed through a 0.45µ filter and used immediately or stored at -70°C. For titration, 10-fold dilutions of the virus stock and approximately 4µg/ml polybrene (Sigma) was added to HT1080 cells which had been seeded 24 hours previously in a 24-well culture plate at a density of $1x10^4$ cells per well. Cells and virus were incubated overnight at 37°C, then the virus was removed and fresh media added. Following a further 5 days incubation the cells were harvested and stained with anti-CD34-fluorescein isothiocyanate (FITC) for FACS analysis. The titre was calculated as follows;

$$\text{titre (tu/ml)} = \frac{\text{frequency positive cells (\%)}}{100} \times \text{initial cell number} \times \text{dilution factor}$$

2.6 Phage library techniques

2.6.1 Phage libraries used

Tomlinson I+J

The Tomlinson phage library is in phagemid/scFv format, with a diversity of $2.8x10^8$ (Goletz *et al*, 2002). It is a synthetic library based on a single human framework for

V_H (V3-23/DP-47 and J_H4b) and V_κ (O12/O2/DPK9 and J_κ1). The canonical structure encoded by this structure is the most common in the human antibody repertoire. pIT2 was used as the phagemid vector. The CDR3 of the heavy chain was designed to be as short as possible while still forming an antigen binding surface. Side-chain diversity was incorporated in CDR3 and CDR2 regions in both V_H and V_κ at positions which make contacts to the antigens. CDR1 regions were kept constant. Additional diversity was generated by PCR using partially degenerate primers designed to introduce random sequences into the V_H and V_κ CDR3 loops. The library was preselected on Protein A and Protein L, favouring the retention of functional scFv. HIS6 and myc tags were included for the identification of soluble scFv. The Tomlinson I+J human single fold scFv phage libraries were supplied by Geneservice Ltd. Included with the libraries were control clones specific for ubiquitin and BSA, T-phage resistant *E.coli* strain TG1 for phage propagation and KM13 helper phage (Kristensen & Winter, 1998) for library rescue

ETH2Gold

The ETH2Gold phage library is in phagemid/scFv format, with a diversity of $3x10^9$ (Silacci *et al*, 2005). It is a synthetic library, and uses one V_H and two V_κ regions for the scFv framework (DP47/DPL16 and DP47/DPK22). pHEN1 was used as the phagemid vector. Diversity was generated by PCR using partially degenerate primers designed to introduce random sequences into the V_H and V_κ or V_λ CDR3 loops. The library was preselected on Protein A and Protein L, favouring the retention of functional scFv. A myc tag was included for the identification of soluble scFv.

RotMar

The RotMar library was constructed using an identical method as the de Haard library (de Haard *et al*, 1999). It is in phagemid/Fab format, with a diversity of $5.36x10^9$. The RotMar is a naïve library, with PBL from two donors and spleen from two donors used as a source of RNA for amplification of V_H and V_L regions. Primers were designed as to allow amplification of all commonly used V-gene segments. V_H and V_L regions were combined by cloning V_H regions into a vector already containing V_L. 70% of clones contain a κ light chain and 30% a λ light

chain. pCES1 was used as the phagemid vector. A single CH1 domain was used. HIS6 and myc tags were included for the identification of soluble Fab.

2.6.2 Growing *E.coli* TG1

Frozen TG1 stock in 15% glycerol was streaked onto minimal agar plates and incubated 24-48 hours at 37°C. Single colonies were picked into 5ml 2xTY medium and grown shaking overnight at 37°C. The overnight culture was diluted 1:100 in fresh 2xTY medium and grown shaking at 37°C until the OD at 600nm (OD_{600}) reached 0.4-0.5, and the bacteria were in an exponential growth phase.

2.6.3 Preparing helper phage KM13

TG1 at an OD_{600} of 0.4-0.5 was added to 100-fold dilutions of the KM13 helper phage. After incubation at 37°C in a waterbath for 30 minutes, cultures were added to molten H-top agar at 42°C and the mixture immediately poured onto pre-warmed TYE plates, then incubated overnight at 37°C. A small plaque was picked into 5ml fresh TG1 at an OD_{600} of 0.4-0.5 and the culture grown shaking at 37°C for 2 hours. The culture was then diluted 1:100 in fresh 2xTY medium and grown shaking at 37°C. After 1 hour, kanamycin was added to a final concentration of 50µg/ml to select for bacteria infected with helper phage, as KM13 carries a kanamycin resistance gene, and the culture grown shaking overnight at 30°C. The overnight culture was centrifuged at 10800g for 15 minutes and one part polyethylene glycol (PEG)/NaCl (20% (w/v) PEG 6000 in 2.5M NaCl) added to four parts of the supernatant to precipitate the helper phage. The mixture was incubated on ice for 1 hour, then the helper phage pelleted by centrifugation at 10800g for 30 minutes. The phage was resuspended in PBS and the precipitation repeated. The resuspended helper phage was then centrifuged at 11600g for 10 minutes to remove any bacterial debris, and stored at 4°C for the short term or -70°C in 15% glycerol for the long term. To titre the helper phage stock, TG1 at an OD_{600} of 0.4-0.5 was added to 100-fold dilutions of phage, as well as 100-fold dilutions of phage which had been treated with 1mg/ml trypsin (Sigma) for 30 minutes at 37°C. Following incubation at 37°C in a waterbath for 30 minutes, cultures were plated in H-top agar as above, and then incubated overnight at 37°C. If the titre of the trypsin-treated phage was 10^5-10^8

lower than the titre of the non-trypsin treated phage, the preparation was deemed acceptable.

2.6.4 Rescuing phage libraries

Phage libraries in TG1 were grown in 2xTY with 100µg/ml ampicillin to select for bacteria infected with phage clones, which carry an ampicillin resistance gene, and 1% (w/v) glucose as the scFv gene is under the control of a lacZ promoter and the glucose inhibits expression of soluble scFv fragments. For library rescue, phage stock in TG1 was grown shaking at 37°C until the OD_{600} reached 0.4-0.5. A 10-fold excess of KM13 was added to an aliquot of the library large enough to ensure library diversity was not compromised and incubated without shaking in a 37°C waterbath for 30 minutes. The bacteria were pelleted by centrifugation at 3000g for 10 minutes, resuspended in 2xTY AKG, and grown shaking overnight at 30°C. The overnight culture was centrifuged at 3300g for 30 minutes and one part PEG/NaCl added to four parts of the supernatant to precipitate the phage. The mixture was incubated on ice for 1 hour, then the phage pelleted by centrifugation at 3300g for 30 minutes. The phage was resuspended in PBS, centrifuged at 11600g for 10 minutes to remove any bacterial debris, and then stored at 4°C for the short term or at -70°C in 15% glycerol for the long term. To titre library stock, TG1 at an OD_{600} of 0.4-0.5 was added to 100-fold dilutions of phage. After incubation at 37°C in a waterbath for 30 minutes, cultures were spotted onto TYE AG plates and incubated overnight at 37°C.

2.6.5 Selection on immunotubes

In early selection experiments, immunotubes (Nunc) were coated directly with the peptide being used as capture antigen. In later experiments, immunotubes were coated with either streptavidin or avidin and biotinylated peptides added subsequently. Finally, a negative selection step was incorporated into the protocol in which the phage were passed through two immunotubes coated with streptavidin or avidin, added to the biotinylated peptide in solution and then the mixture applied to a third immunotube coated with streptavidin or avidin. All peptides were manufactured by Thistle Scientific. Protocols for selection were as follows:

1. Unmodified peptides

Immunotubes were coated overnight at 4°C with 100µg/ml peptide in PBS. The following day the tubes were washed three times with PBS and blocked for 2 hours at room temperature with 2% marvel skim milk powder in PBS (MPBS). The tubes were washed three times with PBS, phage in MPBS was added and the tubes incubated at room temperature for 1 hour rolling and 1 hour standing. The tubes were washed 10 (round 1) or 20 (rounds 2 and 3) times with PBS containing 0.1% Tween 20 (PBS-Tween) and the phage eluted using 1mg/ml trypsin and a rolling incubation for 10 minutes at room temperature.

2. Biotinylated peptides

Immunotubes were coated overnight at 4°C with 500ng/ml streptavidin or avidin in 0.1M $NaHCO_3$ pH 8.2. Streptavidin was used in rounds 1 and 3, avidin in round 2. The following day the tubes were washed twice with PBS and twice with PBS-Tween and blocked for 2 hours at room temperature with MPBS. The tubes were washed twice with PBS and twice with PBS-Tween, 100µg/ml biotinylated peptide in MPBS was added and the tubes incubated for 1 hour at room temperature. Tubes were washed twice with PBS and twice with PBS-Tween, phage in MPBS was added and the tubes incubated at room temperature for 1 hour rolling and 1 hour standing. The tubes were washed 5 and 5 (round 1) or 10 and 10 (rounds 2 and 3) times with PBS-Tween 20 and PBS and the phage eluted using 1mg/ml trypsin and a rolling incubation for 10 minutes at room temperature.

3. Biotinylated peptides with negative selection

Immunotubes were coated overnight at 4°C with 500ng/ml streptavidin or avidin in 0.1M $NaHCO_3$ pH 8.2. Streptavidin was used in round 1, avidin in round 2. The following day the tubes were washed twice with PBS and twice with PBS-Tween and blocked for 2 hours at room temperature with MPBS. The tubes were washed twice with PBS and twice with PBS-Tween, phage in MPBS added and the tube incubated rolling for 15 minutes. The phage mixture was then decanted into a fresh coated tube and incubated standing for 15 minutes. The phage mixture was next added to 100µg/ml biotinylated peptide in MPBS and incubated 1 hour shaking and 1 hour standing at room temperature. The phage-peptide mixture was decanted in to a final fresh coated tube and incubated 15 minutes rolling and 15 minutes standing. The

tubes were washed 5 and 5 (round 1) or 10 and 10 (round 2) times with PBS and PBS-Tween and the phage eluted using 1mg/ml trypsin and a rolling incubation for 10 minutes at room temperature.

In the above protocols, eluted phage was rescued by addition of TG1 at an OD_{600} of 0.4-0.5. After incubation in a 37°C waterbath for 30 minutes, 10-fold dilutions of the culture were spotted onto TYE AG plates to titre the selection output and the remaining bacteria pelleted by centrifugation at 11600g, resuspended in a small volume of 2xTY and spread on a BioAssay dish (Nunc) containing TYE AG (round 1 only) or TYE AG plate. Titre plates were incubated overnight at 37°C, pellet plates incubated overnight at 30°C.

2.6.6 Amplifying selected phage

After overnight growth of pellet plates, 2xTY with 15 % glycerol was added to plates and the cells loosened with a disposable spreader then collected into a tube. Aliquots of the harvested bacteria were added to 2xTY AG until the OD_{600} reached approximately 0.1, then the culture grown shaking at 37°C until an OD_{600} of 0.4-0.5 was reached. A 10-fold excess of KM13 was added to an aliquot of the culture and incubated without shaking in a 37°C waterbath for 30 minutes. The bacteria were pelleted by centrifugation at 3000g for 10 minutes, resuspended in 2xTY AKG and grown shaking overnight at 30°C. The overnight culture was centrifuged at 3300g for 30 minutes and one part PEG/NaCl added to four parts of the supernatant to precipitate the phage. The mixture was incubated on ice for 1 hour and then the phage pelleted by centrifugation at 3300g for 30 minutes. The pellet was resuspended in PBS, centrifuged at 11600g for 10 minutes to remove any bacterial debris, and then stored at 4°C for the short term or -70°C in 15% glycerol for the long term.

2.6.7 Rescuing monoclonal phage

Phage eluted from selection tubes was rescued by addition of TG1 at an OD_{600} of 0.4-0.5. After incubation at 37°C in a waterbath for 30 minutes, 10-fold dilutions of the culture were spread onto TYE AG plates to titre the selection output and ensure

well separated colonies, then incubated overnight at 37°C. Individual colonies were inoculated into 2xTY AG in 96-well flat bottomed plates (Nunc) and grown shaking overnight at 37°C. The next day 5µl of the culture was transferred to fresh 2xTY AG in 96-well plates and grown shaking at 37°C. After 2 hours, 10^9 KM13 per well were added and the cultures shaken at 37°C for a further hour. The plates were then centrifuged at 1800g for 10 minutes, the supernatant aspirated, and the bacterial pellet resuspended in 2xTY AKG before being incubated shaking overnight at 30°C. The next day, the plate was centrifuged at 770g for 10 minutes and the supernatant reserved for analysis by ELISA.

2.6.8 Phage ELISA

Coating and blocking of the 96-well assay plate (Nunc) was carried out using the same concentration of target antigen and identical conditions to those used for coating and blocking the immunotubes during the selection of the phage to be assayed. Once this was complete, phage in 2% MPBS was added and the plate incubated for 1 hour at room temperature. Generally, 10µl PEG precipitated polyclonal phage (see 2.6.6) or 50µl monoclonal phage supernatant (see 2.6.7) was used. The phage solution was then discarded and the plate washed twice with PBS-Tween and twice with PBS. A 1:5000 dilution of HRP-anti-M13 (GE Healthcare) in 2% MPBS was then added and the plate incubated for 1 hour at room temperature, then washed twice with PBS-Tween and twice with PBS. A substrate solution of 100µg/ml 3,3',5,5'-tetramethylbenzidine (Sigma) in 100mM sodium acetate pH 6.0 with 0.006% (v/v) hydrogen peroxide was added to each well and the plate incubated for 10 minutes at room temperature before the reaction was stopped with 1M sulphuric acid and the $OD_{(450-650)}$ for each well read.

2.7 Preparation of therapeutic cells

2.7.1 PBMC activation

Fresh or frozen PBMCs were washed twice by centrifugation in RPMI, first at 800g for 8 min, then 400g for 7 min. Pelleted cells were resuspended at $1x10^6$ cells/ml in complete medium-20 supplemented with 1µg/ml anti-CD3 (Becton Dickinson) and

1µg/ml anti-CD28 (Becton, Dickinson), and incubated at 37°C in 5% humidified CO_2 for 72 hours.

2.7.2 Retrovirus transduction

Activated PBMCs were resuspended in undiluted supernatant from a PG13 retrovirus producer cell line (see 2.5.3). 6ug/ml polybrene (Sigma) was added to the suspension, which was then centrifuged at 1200g and 4°C for 3 hours. Transduced cells were resuspended at approximately $5x10^5$ cells/ml in complete medium-20 supplemented with 100IU/ml IL-2 (UDG) and incubated overnight at 37°C in 5% humidified CO_2. Transduction was repeated the following day. Transduced cells were cultured for up to 2 weeks in complete medium-20, with IL-2 to a concentration of 100IU/ml added to the culture three times a week.

2.7.3 Establishing an LCL

PBMCs were resuspended in undiluted EBV preparation (see 2.5.1) and incubated at 37°C with occasional agitation. After 1 hour the suspension was centrifuged at 180g for 7 minutes, the pellet resuspended at $2x10^6$ cells/ml in complete medium-10 supplemented with 1µg/ml cyclosporin A (Sigma), and the cells seeded into a 48-well plate. Culture plates were incubated at 37°C in 5% humidified CO_2 until outgrowth of immortalised clones signalled establishment of a cell line.

2.7.4 Reviving CTLs

All CTLs and HLA matched LCLs were sourced from a cell bank created in our laboratory (Wilkie *et al*, 2004). Frozen CTLs were thawed and washed twice by centrifugation in complete medium-20 at 180g for 7 min. Pelleted cells were resuspended at $2x10^6$ cells/ml in complete medium-20 supplemented with 20U/ml IL-2 and incubated at 37°C in 5% humidified CO_2 overnight before use.

2.7.5 Flow cytometric analysis

Cells to be analysed were added to polystyrene round bottom tubes (Becton Dickinson) and washed twice in PBSA (1% w/v BSA, 0.1% w/v sodium azide, 0.2% w/v EDTA) by centrifugation at 120g for 5 minutes. The supernatant was decanted and cells resuspended in residual liquid. 10µL of the appropriate antibody (see Table 2.2) was added and the tubes incubated for 20 minutes at 4°C in the dark. Cells were washed twice in PBSA then resuspended in 1x CellFix (Becton Dickinson) and stored at 4°C in the dark for up to one week until FACS evaluation on either a FACScan (Becton Dickinson) or FACSCalibur (Becton Dickinson) flow cytometer. At least 10000 events were acquired for each sample. Data was subsequently analysed using the CellQuest software.

Table 2.2: Antibodies used in flow cytometric analysis.
[FITC: fluorescein isothiocyanate; PE: phycoerythrin]

antibody	clone	isotype	conjugate	supplier
CD4	RPA-T4	IgG_1, κ	PE	Becton Dickinson
CD8	RPA-T8	IgG_1, κ	PE	Becton Dickinson
CD19	HIB19	IgG_1, κ	PE	Becton Dickinson
CD34	581	IgG_1, κ	FITC	Becton Dickinson
CD56	B159	IgG_1, κ	PE	Becton Dickinson

2.7.6 Chromium release assay

Cytotoxic activity *in vitro* was measured using a standard chromium (Cr) release assay (Haque *et al*, 1998). Cells from each target cell line were labelled with ^{51}Cr for 1 hour at 37°C before plating with effector cells at an effector:target ratio of 20:1, 10:1 and 5:1. After incubation at 37°C for 4 hours the release of ^{51}Cr from lysed cells was measured on a gamma counter. Spontaneous release was calculated by incubating target cells without effector cells, and maximum release calculated by incubating target cells with 1% Triton-X (Sigma). Percent specific lysis was calculated as follows;

$$\% \text{ specific lysis} = \frac{(\text{test release} - \text{spontaneous release})}{(\text{maximum release} - \text{spontaneous release})} \times 100$$

2.8 Animal Models

CB17 SCID mice (Bosma *et al*, 1983) were maintained in a specific pathogen free unit and housed in microinsulator caging. Procedures were carried out under Project Licences 60/2766 and 60/3530, and Personal Licence 60/10062.

2.8.1 Tumour induction in SCID mice

Cells for injection were washed once in HBSS then resuspended in complete medium-10. A volume of 100µl was administered for each injection. Mice injected by the subcutaneous (sc) route received injections in one or both flanks. Mice injected by the intraperitoneal (ip) route received one injection in the abdomen. For tumour prophylaxis or treatment, intravenous (iv) injections of cells were given into a tail vein.

2.8.2 Monitoring tumour growth and collection of samples

Mice were observed three times a week for illness or tumour formation. Upon showing signs of illness, appearance of skin necrosis at the tumour site, tumour growth exceeding 18mm in any plane, or at a predetermined time point, mice were culled by cervical dislocation and examined post mortem. Any macroscopic tumour tissue or organs of interest were removed and samples fixed in neutral buffered formalin (NBF).

2.9 Immunohistochemistry

2.9.1 Preparation of slides

To create slides of cultured cells, approximately $1x10^8$ cells were washed in HBSS at 180g for 7 minutes and then fixed in 5ml NBF for 2 hours at room temperature. Fixed cells were pelleted at 180g for 7 minutes and resuspended in cooled 2% (w/v) agarose in PBS.

Cell pellets and mouse tissue fixed in NBF were embedded in paraffin wax blocks. Sections of 6µm were cut from the blocks and mounted on polysine coated

microscope slides (VWR). This work was carried out by Mrs Grace Grant, School of Biomedical Sciences, University of Edinburgh.

2.9.2 Rehydration of sections

Paraffin wax-embedded sections were dewaxed by immersion in xylene for 5 minutes, and then rehydrated by sequential immersion in 100%, 90%, 70%, and 30% (v/v) ethanol for 5 minutes each. The slides were washed in distilled water for 5 minutes and left to air dry.

2.9.3 Antibody retrieval

Dewaxed slides were immersed in Target Retrieval Solution (Dako) in a coplin jar which had been preheated to approximately 95°C for 20 minutes. The entire jar was removed to the bench and allowed to cool for a further 20 minutes. The slides were then washed twice with distilled water and left to air dry.

2.9.4 Antibody staining using AP

Visualisation of antibody staining using alkaline phosphotase (AP) was performed using the EnVision Detection System (Dako) according to the manufacturer's instructions. Briefly, after dewaxing and antibody retrieval, sections were incubated with primary mouse anti-human mAb (see Table 2.3) at the appropriate dilution for 30 minutes at room temperature. Antibodies were diluted in block buffer (0.05mol/l Tris-HCl pH7.2-7.6, 1% w/v BSA). Slides were washed twice in TBS, and then incubated with an AP-labelled polymer specific for mouse immunoglobulin for 30 minutes at room temperature. The slides were washed again with TBS, and then the AP label developed using a Fast Red solution (naphtol AS-Mx phosphate in Tris buffer) with levamisole to inhibit endogenous AP. The slides were then washed twice in distilled water and counterstained with Gill's formula haematoxylin (Vector Laboratories) for 5 minutes before mounting with Faramount aqueous mounting medium (Dako).

Table 2.3: Antibodies used in immunohistochemistry.

antibody	clone	isotype	dilution	supplier
BZLF1	BZ.1	IgG_1, κ	1:20	Dako
CD4	4B12	IgG_1, κ	1:20	Vision BioSystems
CD8	1A5	IgG_1	1:20	Vision BioSystems
CD15	HI98	IgM, κ	1:150	Becton Dickinson
CD19	LE-CD19	IgG_1	1:200	AbD Serotec
CD20	L26	IgG_{2A}, κ	1:400	Dako
CD30	BerH8	IgG_1, κ	1:150	Becton Dickinson
cytokeratin	AE1/AE3	IgG_1, κ	1:100	Dako
EBNA2	PE2	IgG_1, κ	1:25	Dako
LMP1	CS.1-4	IgG_1, κ	1:100	Dako

2.9.5 Antibody staining using HRP

Visualisation of antibody staining using horse radish peroxidase (HRP) was performed using the Novolink Polymer Detection System (Vision BioSystems) according to the manufacturer's instructions. Briefly, after dewaxing and antibody retrieval, sections were incubated with a peroxidase block for 5 minutes to neutralise endogenous peroxidases, washed twice with TBS, incubated with a protein block for 5 minutes, washed twice with TBS and then incubated with primary mouse anti-human mAb (see Table 2.3) at the appropriate dilution for 30 minutes at room temperature. Antibodies were diluted in Antibody Dilutant (Dako). Slides were washed twice in TBS, then incubated with a post primary block for 30 minutes, washed twice again in TBS, then incubated with a HRP-labelled polymer specific for mouse immunoglobulin for 30 minutes at room temperature. The slides were washed twice with TBS, and then the HRP label developed using a 1.74% 3,3-diaminobenzidine (DAB) solution. The slides were then washed twice in distilled water and counterstained with haematoxylin for five minutes before mounting with Faramount.

2.9.6 EBER *in situ* hybridisation

EBER ISH was carried out using a PNA ISH Detection Kit (Dako). Dewaxed slides were rehydrated by sequential immersion in 100%, and 95% ethanol and double processed water (Sigma) for 5 minutes each. Sections were then incubated with

15µg/ml Proteinase K (Sigma) in 50mM Tris-HCl pH 7.6 for 30 minutes at 37°C in a humidity chamber, then washed twice in double processed water and dehydrated by immersion in 95% ethanol for 10 seconds. An EBV (EBER) PNA Probe (Dako) labelled with FITC was added to each section, covered with a coverslip, and incubated at 55°C for 3 hours in a humidity chamber. Coverslips were removed during immersion in the supplied stringent wash solution for 25 minutes at 55°C. Slides were washed once in TBS, and then incubated for 30 minutes at room temperature with the supplied AP-labelled anti-FITC detection antibody, before being washed twice with TBS and twice with distilled water. AP was developed using a 5-bromo-4-chloro-3-indolylphosphate/nitroblue tetrazolium (BCP/NBT) Alkaline Phosphotase Substrate Kit (Vector Laboratories), with slides being incubated with substrate solution for 45 minutes at room temperature in a humidity chamber, and then washed in 100mM Tris-HCl pH 9.5 and running tap water. Sections were counterstained with haematoxylin for five minutes before mounting with Faramount.

2.9.7 Haematoxylin and eosin staining

Dewaxed and rehydrated slides were immersed in haematoxylin for 10 minutes, washed with running tap water for 5 minutes, immersed in 1% w/v eosin Y (Sigma) for 15 minutes then washed again in running tap water for 5 minutes. Sections were mounted with Vectamount permanent mounting medium (Vector). Histological examination was assisted by Dr Christopher Bellamy, Department of Pathology, Royal Infirmary, Edinburgh.

2.10 Statistical analysis

Data is presented as mean ± standard deviation (SD). The non-parametric Mann Whitney t test was used to compare levels of specific lysis in chromium release assays. Fisher's exact test for comparison of proportions, and Wilcoxon rank sum test for comparison of two groups, was used to analyse immunotherapy data. In all cases, $P<0.05$ was accepted as indicating a significant difference. Tests were carried out using Prism 4.0 for Windows (GraphPad Software, San Diego California USA).

3 Animal Models for EBV-Associated Malignancies

The modelling of human diseases in animals provides researchers with essential tools for studying disease pathogenesis and offers valuable insight into the mechanism and effect of new treatments. Small animal models, especially murine, are routinely used to test novel cellular therapies (Brentjens *et al*, 2003; Zeng *et al*, 2005; Savoldo *et al*, 2007). I*n vitro* techniques such as the chromium release assay are able to test the effector mechanism of therapeutic cells, as will be seen in Chapter 4. I*n vivo* models are able to investigate other characteristics, such as the ability of cells to traffic to tumour sites and exert an effect over an extended period of time. These abilities are essential if therapeutic cells are to be effective in a patient setting. Thus, in order to test our hypothesis that engineered T cells could target and kill the malignant cells of cancers associated with EBV, an *in vivo* model was desirable. To provide *in vivo* models for HL, NPC and GC, SCID mice were inoculated sc with cell lines derived from these EBV-associated malignancies. The cell lines and resulting SCID tumours were evaluated for histology, immunophenotype, viral gene expression and growth characteristic for comparison with parent tumours.

3.1 Histology of cell lines

In order to characterise the HL (HDLM2, L1236, L540, L591), NPC (C666.1) and GC (AGS, NUGC3, NUGC3-EBV) cell lines (see Table 2.1) prior to use *in vivo*, cells from *in vitro* culture were pelleted, fixed in NBF, and embedded in 2% w/v agarose. Sections were mounted on slides and stained with haematoxylin and eosin to examine cell morphology. Photomicrographs of HL cell lines are shown in Figure 3.1 and NPC and GC cell lines in Figure 3.2.

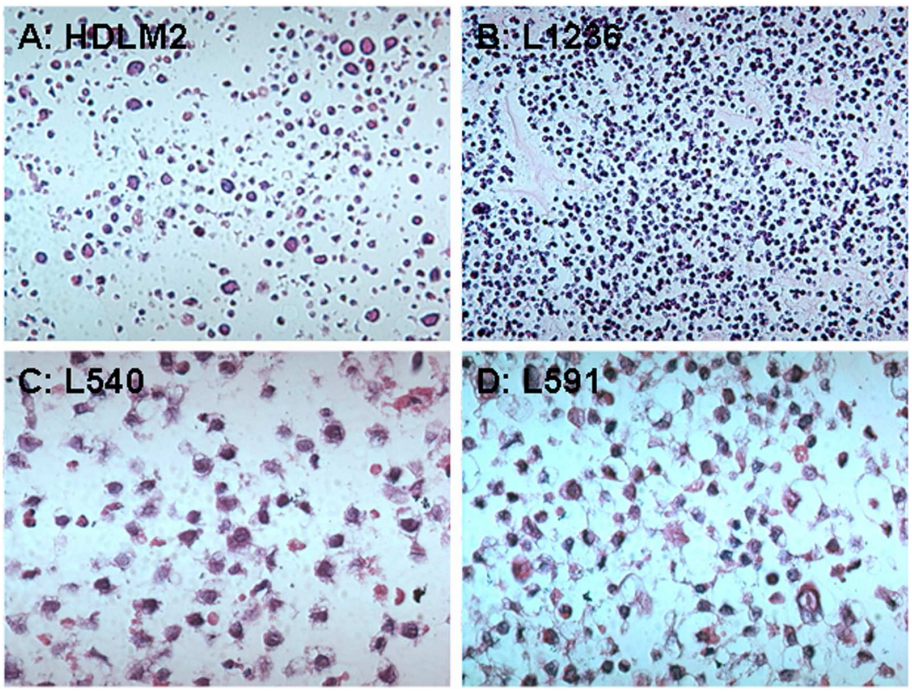

Figure 3.1: Haematoxylin and eosin staining of HL cell lines.
HL cell lines HDLM2 **(A)** and L1236 **(B)** at x200 magnification, and L540 **(C)** and L591 **(D)** at x400 magnification, with blue nuclear and pink cytoplasmic staining.

Histologically, the four HL cell lines (HDLM2, L1236, L540, L591) displayed a pleiomorphic phenotype in culture (Figure 3.1). The majority of cells were small and lymphoid in appearance, with occasional, large, bi- and multi-nuclear blastoid cells, which is consistent with a HRS cell phenotype. The carcinoma cell lines (AGS, NUGC3, NUGC3-EBV, C666.1) were also pleiomorphic in culture, with an undifferentiated malignant phenotype (Figure 3.2).

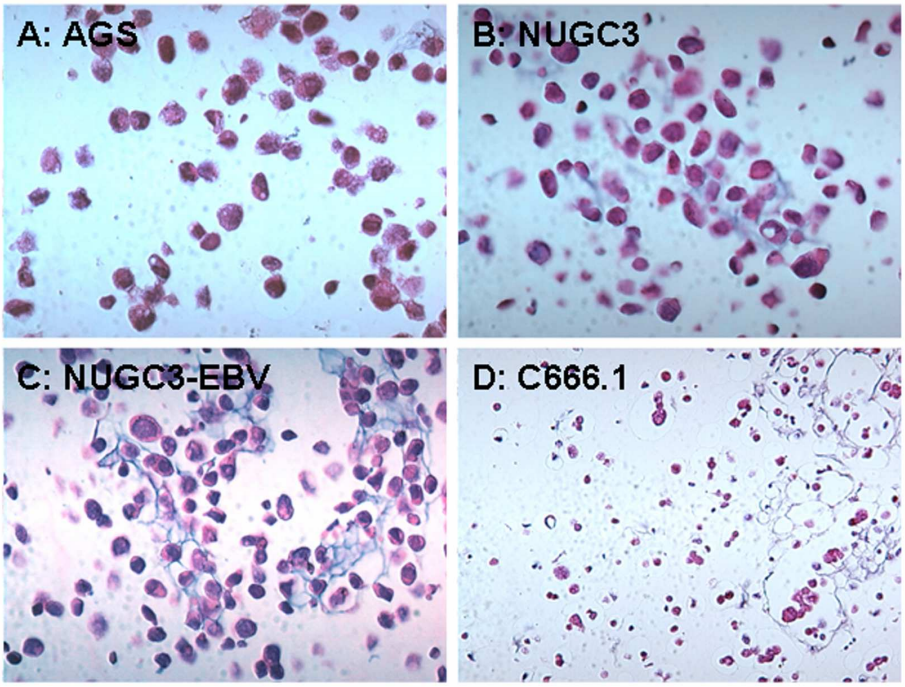

Figure 3.2: Haematoxylin and eosin staining of carcinoma cell lines.
GC lines AGS **(A)**, NUGC3 **(B)** and NUGC3-EBV **(C)** at x400 magnification, and NPC line C666.1 **(D)** at x200 magnification, with blue nuclear and pink cytoplasmic staining.

3.2 *In vitro* infection of EBV-negative HL cell lines

As L591 is the only naturally EBV-positive HL cell line (Diehl *et al*, 1982), an attempt was made to infect the remaining HL cell lines (HDLM2, L1236, L540) with EBV *in vitro*, with the aim of expanding the available range of EBV-positive targets for later use in SCID mice. Cells were incubated with EBV for one hour at 37°C in 5% humidified CO_2 and then maintained in culture (see 2.2.1), with samples taken at 3, 14, and 49 days post infection for DNA extraction. Real time PCR was used to assay viral load (see 2.4.3; Leung *et al*, 2002). An EBV-positive L591 sample and a no template control (NTC) were included.

DNA from L591 cells was amplified by PCR, and no product was present in the NTC sample. The three cell lines (HDLM2, L1236, L540) were infected with EBV, showing DNA amplification on at least one time point. However, the infection was transient in all three cell lines, with no EBV DNA detected at 14 (L540) or 49

(HDLM2, L1236) days post infection (Table 3.1). Therefore, L591 remained the only EBV-positive HL in the following experiments.

Table 3.1: Viral load of HL cells after infection *in vitro* with EBV.

cell line	time point (days)	EBV copies/10^6 cells
L591	-	$3.5x10^6$
HDLM-2	3	$2.3x10^5$
	14	$1.5x10^4$
	49	0
L1236	3	$5.6x10^5$
	14	$5.4x10^4$
	49	0
L540	3	$1x10^2$
	14	0

3.3 Tumour outgrowth

To set up animal models for EBV-associated malignancies, a panel of four HL cell lines (HDLM2, L1236, L540, L591), one NPC cell line (C666.1) and four GC cell lines (AGS, AGS-EBV, NUGC3, NUGC3-EBV) were used (see Table 2.1). SCID mice were injected sc into the flank with $1x10^7$ cells and monitored for tumour formation and subsequent growth (see 2.8.1 and 2.8.2). Additional cell doses of $5x10^6$, $2x10^6$ and $1x10^6$ were used for the L591, NUGC3-EBV and C666.1 cell lines to determine optimum cell dose for tumour formation.

3.3.1 Time to tumour onset

Time to onset following sc injection was defined as the day at which tumours became macroscopically apparent. Experiments were terminated at a predetermined time limit of 100 days (Johannessen *et al*, 2000).

All four HL cell lines tested formed tumours in SCID mice (Table 3.2). At a dose of $1x10^7$ cells, at least 80% of mice injected with HDLM2, L1236, L540, or L591 developed tumours, with median time to tumour onset ranging between 14 days for L1236 and 44 days for HDLM2. As the only EBV-positive HL cell line, L591 was selected for further titration experiments to determine the minimum dose required for reliable engraftment.

Table 3.2: Tumour incidence following sc inoculation of SCID mice with HL cell lines.

cell line	cell dose	number of tumours/ site injected (%)	time to tumour onset median	range
HDLM2	$1x10^7$	8 / 10 (80)	44	41-53
L1236	$1x10^7$	9 / 10 (90)	14	14-20
L540	$1x10^7$	11 / 12 (92)	22	19-44
L591	$1x10^7$	11 / 12 (92)	28	14-37
	$5x10^6$	17 / 22 (77)	20	16-28
	$2x10^6$	9 / 16 (56)	32	32-54

In the L591 titration experiment, a cell dose of $2x10^6$ did not result in reliable tumour formation, as tumour outgrowth was seen in only 9 of 16 cases (56%). Although engraftment rates dropped from 11 of 12 (92%) to 17 of 22 (77%) between doses of $1x10^7$ and $5x10^6$ respectively, there was a narrower range in time to tumour onset, 14-37 days compared with 16-28 days. This allowed for more accurate estimations of time to tumour formation and hence facilitating the planning of immunotherapy experiments. Thus it was decided that a dose $5x10^6$ cells per injection would be used in immunotherapy experiments.

Next, the ability of carcinoma cell lines (AGS, AGS-EBV, NUGC3, NUGC3-EBV, C666.1) to cause tumour outgrowth in SCID mice was assessed. All carcinoma cell lines formed tumours in SCID mice, with the exception of AGS-EBV (Table 3.3). At least 70% of mice injected with AGS, NUGC3, NUGC3-EBV, or C666.1 at a dose of $1x10^7$ cells developed tumours, with median time to tumour onset ranging between 8 days for C666.1 and 71 days for AGS. As the sole EBV-positive representatives for their respective tumours, NUGC3-EBV for GC and C666.1 for NPC were selected

for further titration experiments to determine the minimum dose required for reliable engraftment.

In titration experiments with NUGC3-EBV and C666.1, cell doses of $1x10^6$ cells and $2x10^6$ respectively resulted in tumour formation in 100% of mice. The range in time to tumour onset remained relatively narrow at 23-26 days for NUGC3-EBV and 17-24 days for C666.1. Thus it was decided that a dose $1x10^6$ cells per injection for NUGC3-EBV, and $2x10^6$ cells per injection for C666.1, would be used in immunotherapy experiments.

Table 3.3: Tumour incidence following sc inoculation of SCID mice with CG and NPC cell lines.

cell line	cell dose	number of tumours/ sites injected (%)	time to tumour onset median	range
AGS	$1x10^7$	7 / 10 (70)	71	60-95
AGS-EBV	$1x10^7$	0 / 10 (0)	-	-
NUGC3	$1x10^7$	10 / 10 (100)	21	18-21
NUGC3-EBV	$1x10^7$	12 / 12 (100)	18	11-18
	$5x10^6$	4 / 4 (100)	13	13
	$2x10^6$	4 / 4 (100)	13	13
	$1x10^6$	4 / 4 (100)	25	23-26
C666.1	$1x10^7$	10 / 10 (100)	8	8
	$5x10^6$	4 / 4 (100)	17	17-21
	$2x10^6$	4 / 4 (100)	23	17-24

In order to assess the suitability of ip tumours to model EBV-associated malignancies in SCID mice, a study of tumour engraftment via ip administration was undertaken. All cell lines (HDLM2, L1236, L540, L591, AGS, AGS-EBV, NUGC3, NUGC3-EBV, C666.1) were injected at a dose of $1x10^7$ cells per mouse. Time to onset was defined as time from injection of cells to termination of mice showing signs of distress (hunched back, poor grooming, lethargy, panting).

Although each group contained only three mice, engraftment rates were generally poor compared with sc injection, with L1236 alone engrafting in 100% of mice

(Table 3.4). L540 and NUGC3 engrafted in 2 of 3 mice (67%), L591, AGS, NUGC3-EBV, and C666.1 engrafted in 1 of 3 mice (33%), and HDLM2 and AGS-EBV injected mice did not develop tumours. In light of these results, and due to difficulty in determining tumour onset before mortality (as death rapidly followed initial clinical symptoms of illness, usually within 8 hours), it was decided not to pursue this model any further.

Table 3.4: Tumour incidence following ip inoculation of SCID mice with HL, GC and NPC cell lines.

cell line	derivation	number of tumours/ number of mice (%)
HDLM2	HL	0 / 3 (0)
L1236		3 / 3 (100)
L540		2 / 3 (67)
L591		1 / 3 (33)
AGS	GC	1 / 3 (33)
AGS-EBV		0 / 3 (0)
NUGC3		2 / 3 (67)
NUGC3-EBV		1 / 3 (33)
C666.1	NPC	1 / 3 (33)

3.3.2 Growth rate

Following sc tumour onset, SCID mice from the experiments in 3.3.1 were followed over time to monitor tumour growth and assess suitability for use as EBV-associated malignancy models for testing immunotherapies. Tumours were measured in the cranial/caudal and ventral/dorsal planes, with tumour size taken as the product of these two measurements (Haynes *et al*, 2002). Experiments were terminated upon tumours exceeding 18mm in any plane, in order to sample tumour tissue, or when the pre-set time limit of 100 days was reached.

Once established, all HL tumours (HDLM2, L1236, L540, L591) continued to increase in size over time. Growth curves from mice injected sc with $1x10^7$ cells are shown in Figure 3.3. There were no cases of complete spontaneous tumour regression. After a delayed onset compared to other cell lines, HDLM2 tumours

grew very slowly, with only one tumour exceeding 10mm in length prior to the 100 day time point. In light of this it was decided that HDLM2 was not a suitable *in vivo* model, as differences in growth rate between treated and untreated groups could be difficult to discern. In comparison, L1236 and L540 tumours engrafted earlier and displayed much faster growth, capable of doubling tumour size in an average of 2 or 5 days respectively. This rapid growth rate, especially in L1236 tumours, contributed to the decision not to pursue these cell lines for further modelling, as therapeutic cells might not be capable of an effective response in such a short time frame. L591 tumours displayed slow but constant growth, and as such were deemed most suitable for future use, as therapeutic cells would be given sufficient time to mount an effective response against tumour cells, and differences in tumour growth rate between treated and control animals could be detected.

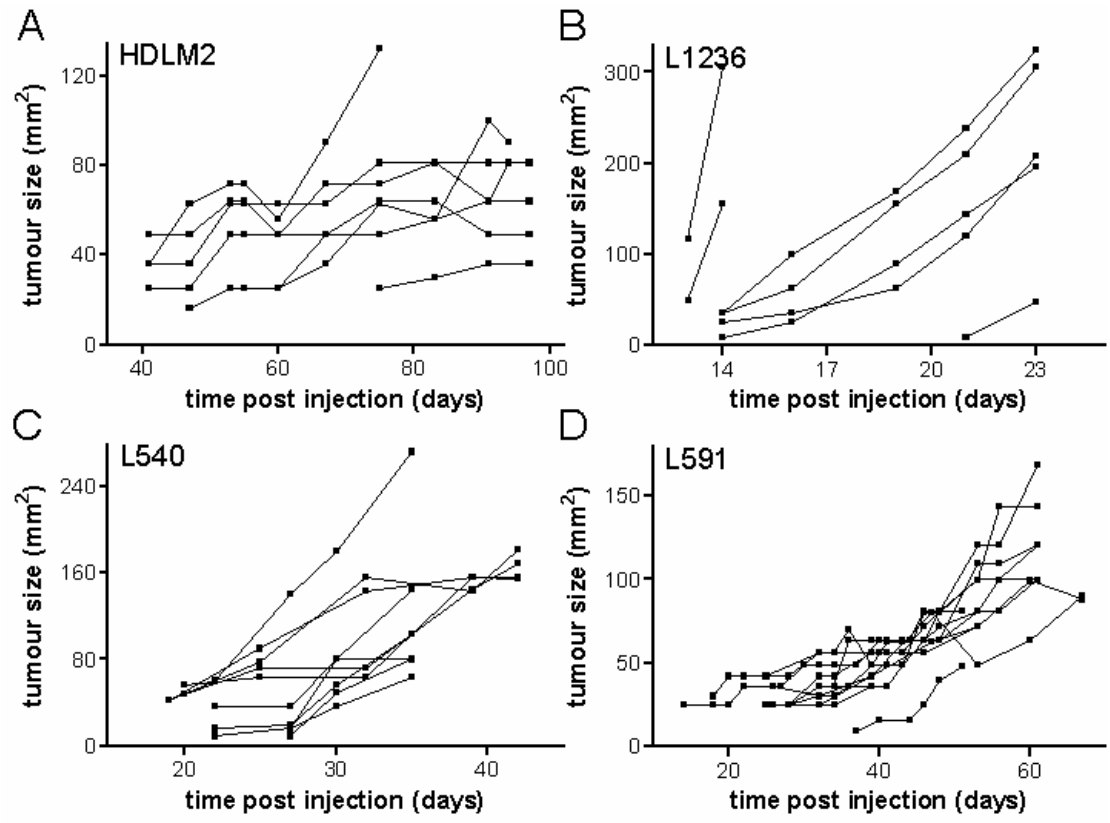

Figure 3.3: Tumour growth curves of HL cell lines in SCID mice.
Cell lines HDLM2 **(A)**, L1236 **(B)**, L540 **(C)** and L591 **(D)** were injected sc at a dose of $1x10^7$. Each line represents an individual tumour.

Once engrafted, all tumours from carcinoma cell lines (AGS, NUGC3, NUGC3-EBV, C666.1) continued to increase in size over time. Growth curves from mice injected with $1x10^7$ cells are shown in Figure 3.4. There were no cases of complete spontaneous tumour regression. Tumours in mice injected with AGS cells developed tumours after a long period of time, with a wide range of onset, 60-95 days post injection. This model was subsequently deemed not suitable for further modelling due to the consequent difficulty in planning immunotherapy experiments. NUGC3, NUGC3-EBV, and C666.1 all engrafted early after inoculation, at a median of 21, 18 and 8 days post inoculation, respectively. Growth was also rapid, with tumours from all three cell lines capable of doubling in size in an average of 4 days, leading to the decision to titrate cell dose (Table 3.3).

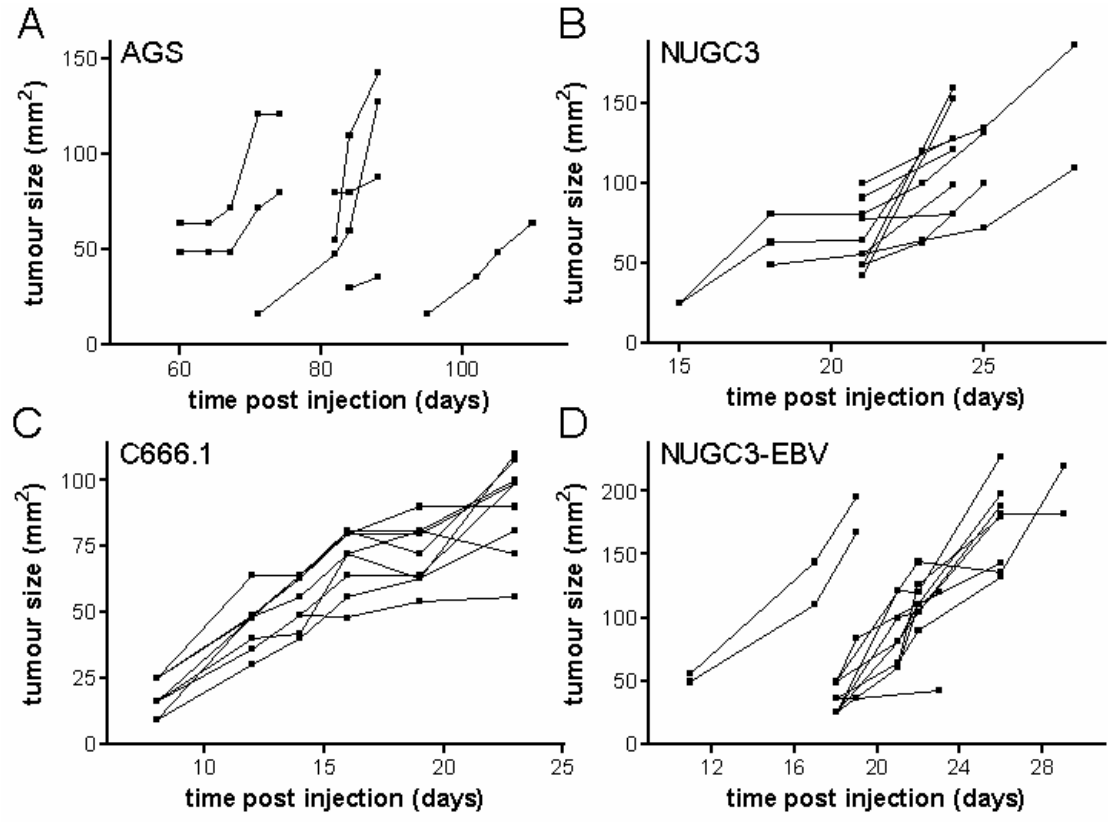

Figure 3.4: Tumour growth curves of carcinoma cell lines in SCID mice.
GC cell lines AGS **(A)**, NUGC3 **(B)**, and NUGC3-EBV **(D)**, and NPC cell line C666.1 **(C)** were injected sc at a dose of $1x10^7$. Each line represents an individual tumour.

3.4 Characterisation of HL, NPC and CG SCID tumours

To characterise HL, NPC and GC SCID malignancies, samples of tumours were fixed in NBF and embedded in paraffin wax. Sections were stained with haematoxylin and eosin for histological analysis. HL tumours were immunostained with a panel of mAbs for cell surface markers to differentiate between tumour types and confirm parent cell line identity. NPC and GC tumours were immunostained for cytokeratin to demonstrate epithelial derivation. Finally, tumours were immunostained for a range of EBV latent and lytic antigens to verify EBV infection and latency state.

3.4.1 Histology

Sections of tumours derived from EBV-positive tumour cell lines were stained with haematoxylin and eosin to determine the histology of the tumours. Photomicrographs of HL tumours are shown in Figure 3.5, and GC and NPC in Figure 3.6.

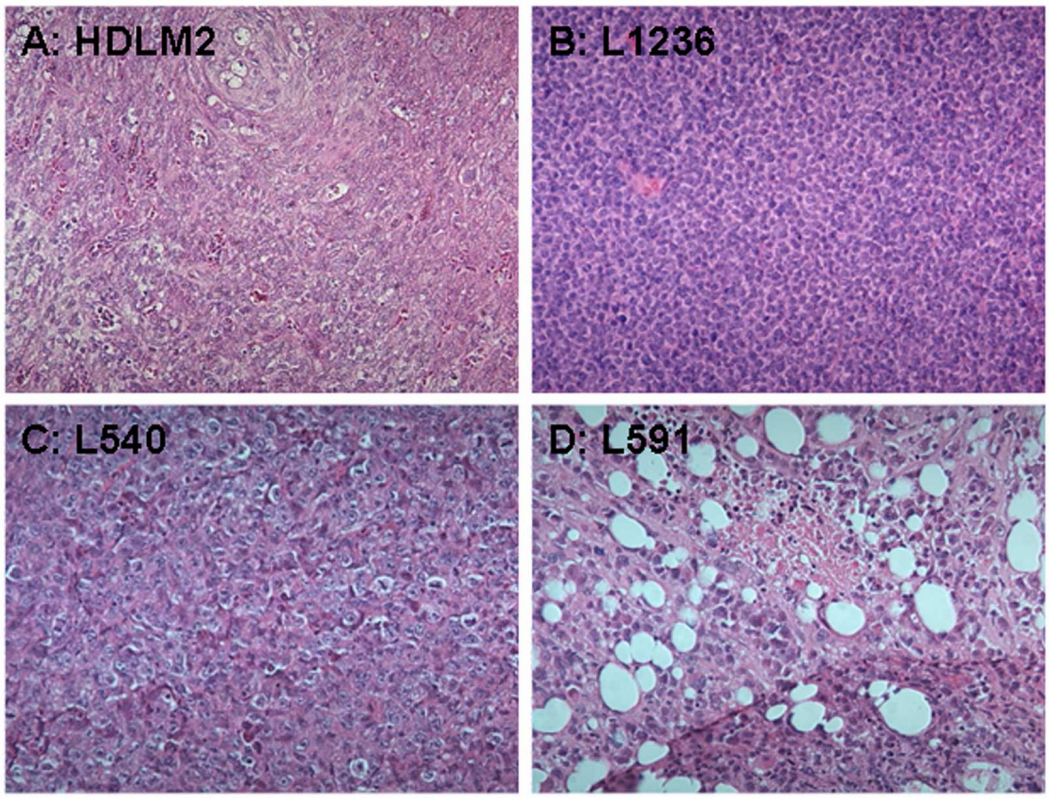

Figure 3.5: Haematoxylin and eosin staining of HL SCID tumours.
HL cell lines HDLM2 **(A)**, L1236 **(B)**, L540 **(C)** and L591 **(D)** at x200 magnification, with blue nuclear and pink cytoplasmic staining.

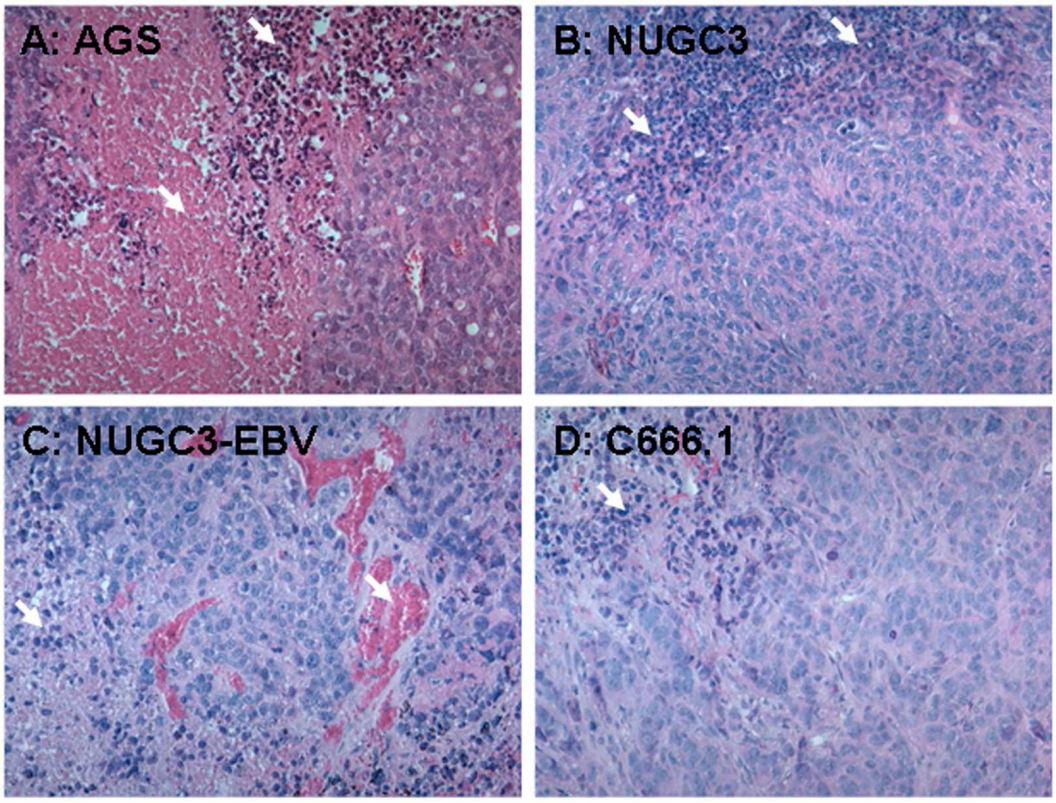

Figure 3.6: Haematoxylin and eosin staining of GC and NPC SCID tumours.
GC lines AGS **(A)**, NUGC3 **(B)** and NUGC3-EBV **(C)**, and NPC line C666.1 **(D)**, at x200 magnification, with blue nuclear and pink cytoplasmic staining. White arrows indicate areas of necrosis.

Three of the HL cell lines (HDLM2, L1236, L540) gave rise to relatively homogeneous tumours, despite cells in culture displaying a more heterogeneous phenotype, with haematoxylin and eosin staining of sections showing sheets of blast cells (Figure 3.5 panels A,B,C). Tumours derived from L591 cells retained their culture heterogeneity, with sections showing a polymorphic population of large bi- and multi-nuclear blast cells, again consistent with a HRS cell phenotype (Figure 3.5 panel D). Tumours derived from carcinoma cell lines (AGS, NUGC3, NUGC3-EBV, C666.1) showed sheets of undifferentiated malignant cells (Figure 3.6).

3.4.2 Immunophenotype

In order to characterise the cell surface phenotype of SCID tumours derived from HL cell lines (HDLM2, L1236, L540, L591), immunostaining for a panel of human CD antigens was performed. Panel mAb were directed against: CD4 (T-lineage antigen),

CD15 (myeloid/HL-associated antigen), CD20 (B-cell marker), and CD30 (activation/HL-associated antigen). Antibodies were selected for their combined ability to differentiate between tumour types and confirm parent cell line identity. At least five tumours derived from each cell line were evaluated. Expression was assessed on a qualitative basis, and positively stained cells were not quantitated.

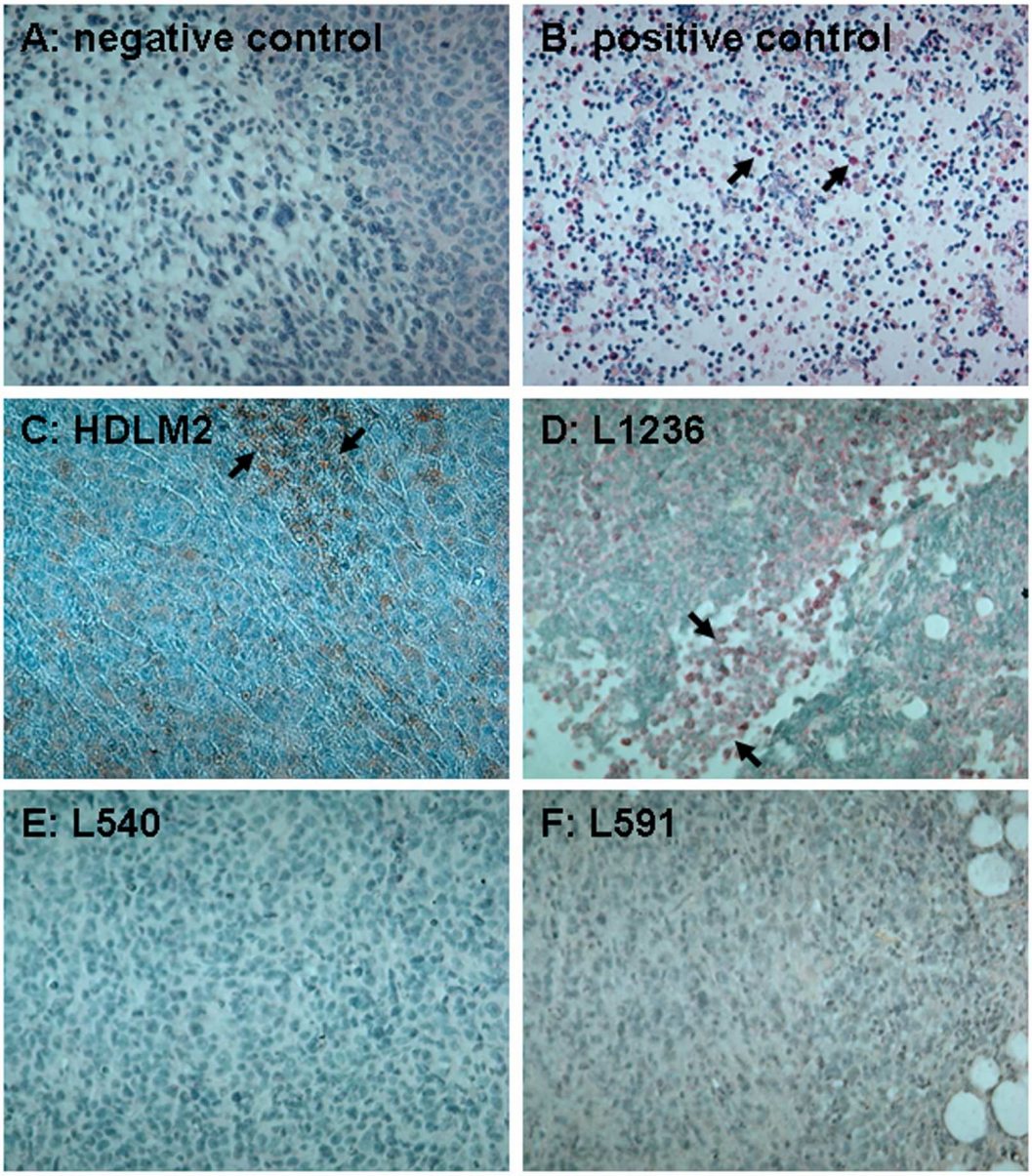

Figure 3.7: CD4 expression on HL SCID tumours.
HL tumours derived from HDLM2 **(C)**, L1236 **(D)**, L540 **(E)** and L591 **(F)** at x200 magnification, stained for CD4 expression. AP detection system shows positive red membrane staining **(B,D)**. HRP detection system shows positive brown membrane staining **(C)**. Negative control was GC SCID tumour **(A)**, positive control was a CTL line **(B)**. Black arrows indicate areas of positive staining **(C,D)**, or single positive cells **(B)**. Sections were counterstained with haematoxylin.

Expression of CD4 was seen in sections of HDLM2 and L1236 tumours, but not L540 or L591 tumours (Figure 3.7). Expression of CD15 was seen in sections of HDLM2 and L540 tumours, but not L1236 or L591 tumours (Figure 3.8). L591 alone expressed CD20 (Figure 3.9), while all tumours expressed CD30 (Figure 3.10). A summary of these results is shown in Table 3.5. The immunophenotype of tumours was consistent with that of the parental cell line.

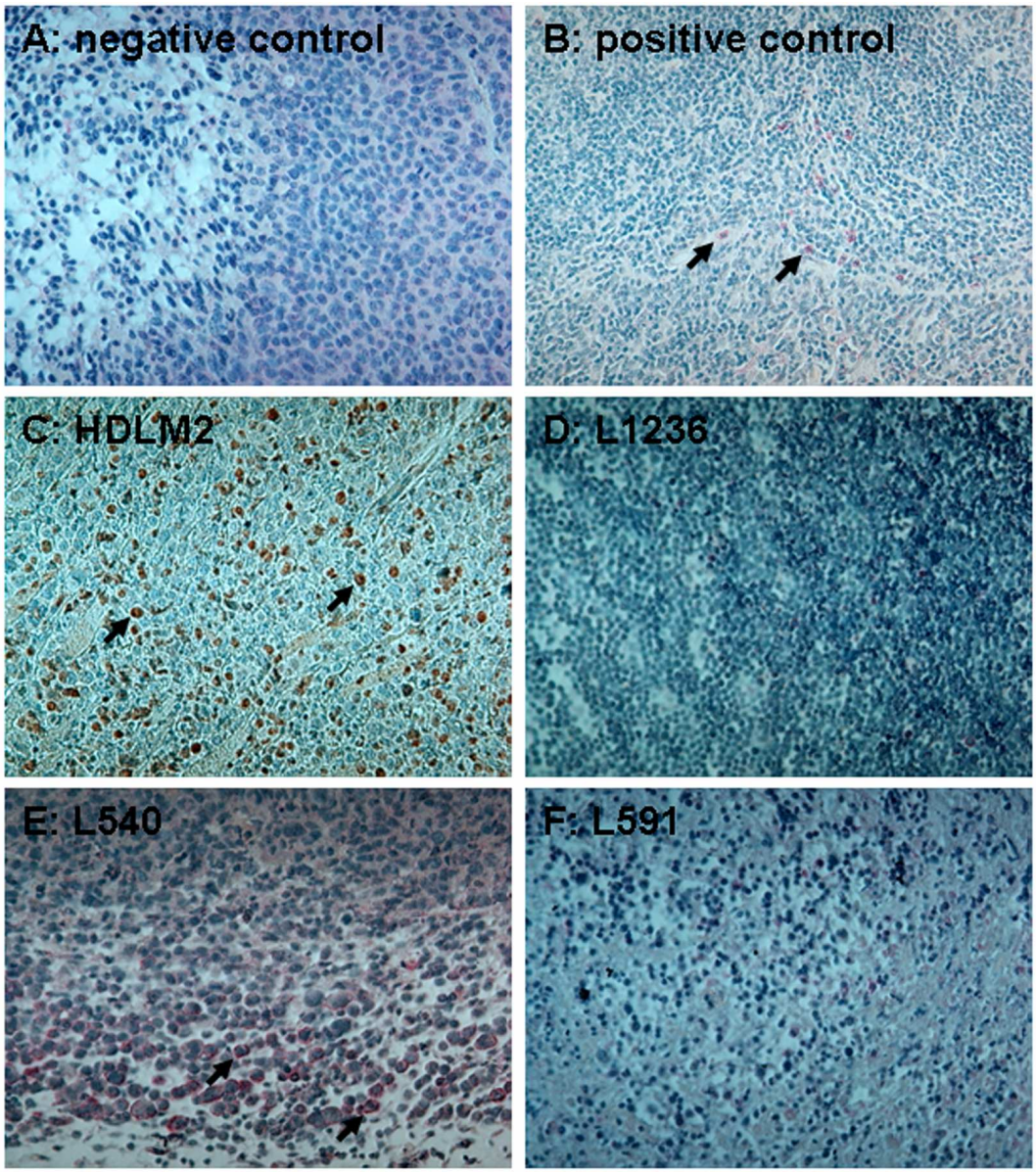

Figure 3.8: CD15 expression on HL SCID tumours.
HL tumours derived from HDLM2 **(C)**, L1236 **(D)**, L540 **(E)** and L591 **(F)** at x200 magnification, stained for CD15 expression. AP detection system shows positive red membrane staining **(B,E)**. HRP detection system shows positive brown membrane staining **(C)**. Negative control was GC SCID tumour **(A)**, positive control was human tonsil **(B)**. Black arrows indicate individual positive cells. Sections were counterstained with haematoxylin.

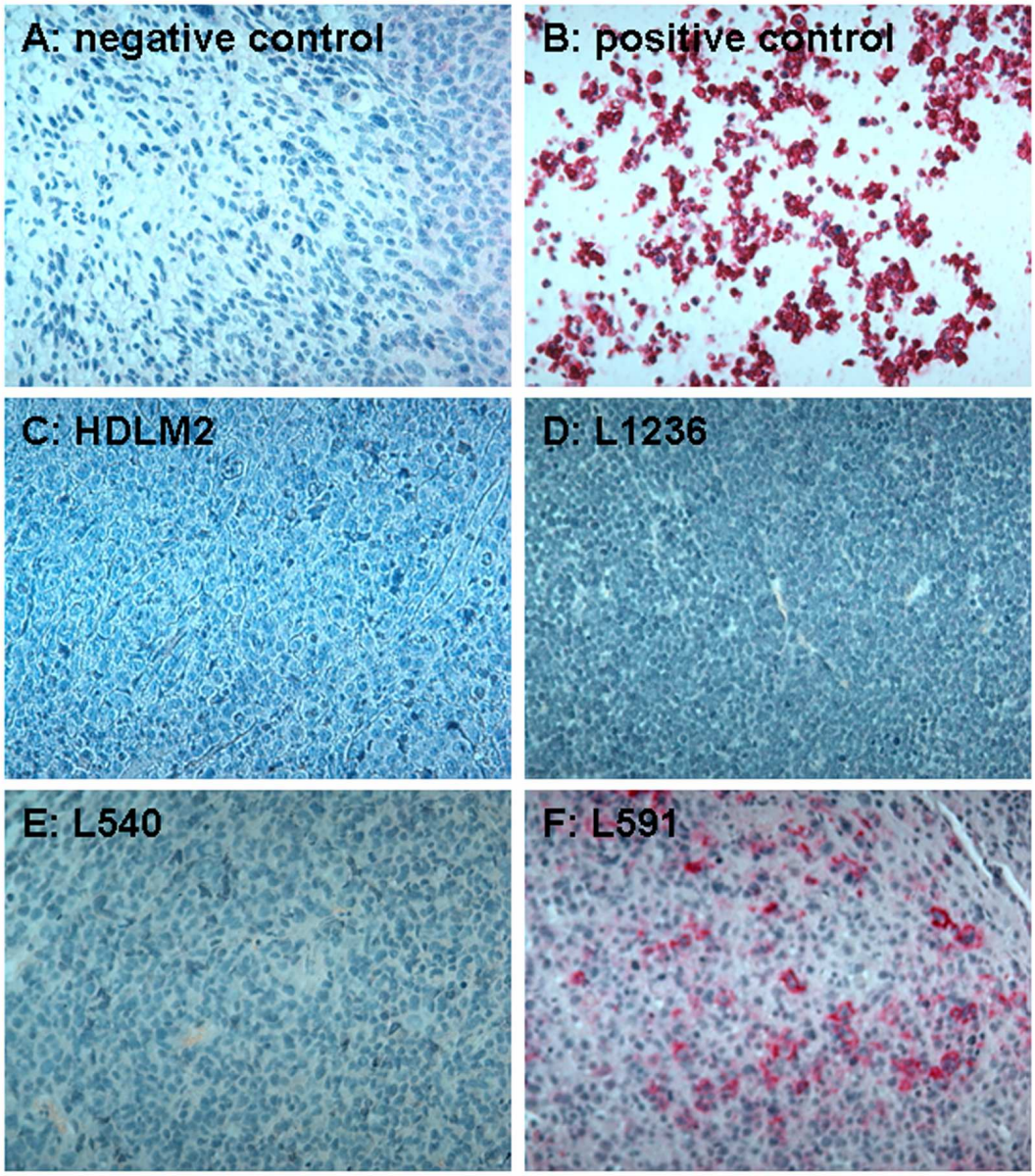

Figure 3.9: CD20 expression on HL SCID tumours.
HL tumours derived from HDLM2 **(C)**, L1236 **(D)**, L540 **(E)** and L591 **(F)** at x200 magnification, stained for CD20 expression. AP detection system shows positive red membrane staining **(B,F)**. Negative control was GC SCID tumour **(A)**, positive control was an LCL **(B)**. Sections were counterstained with haematoxylin.

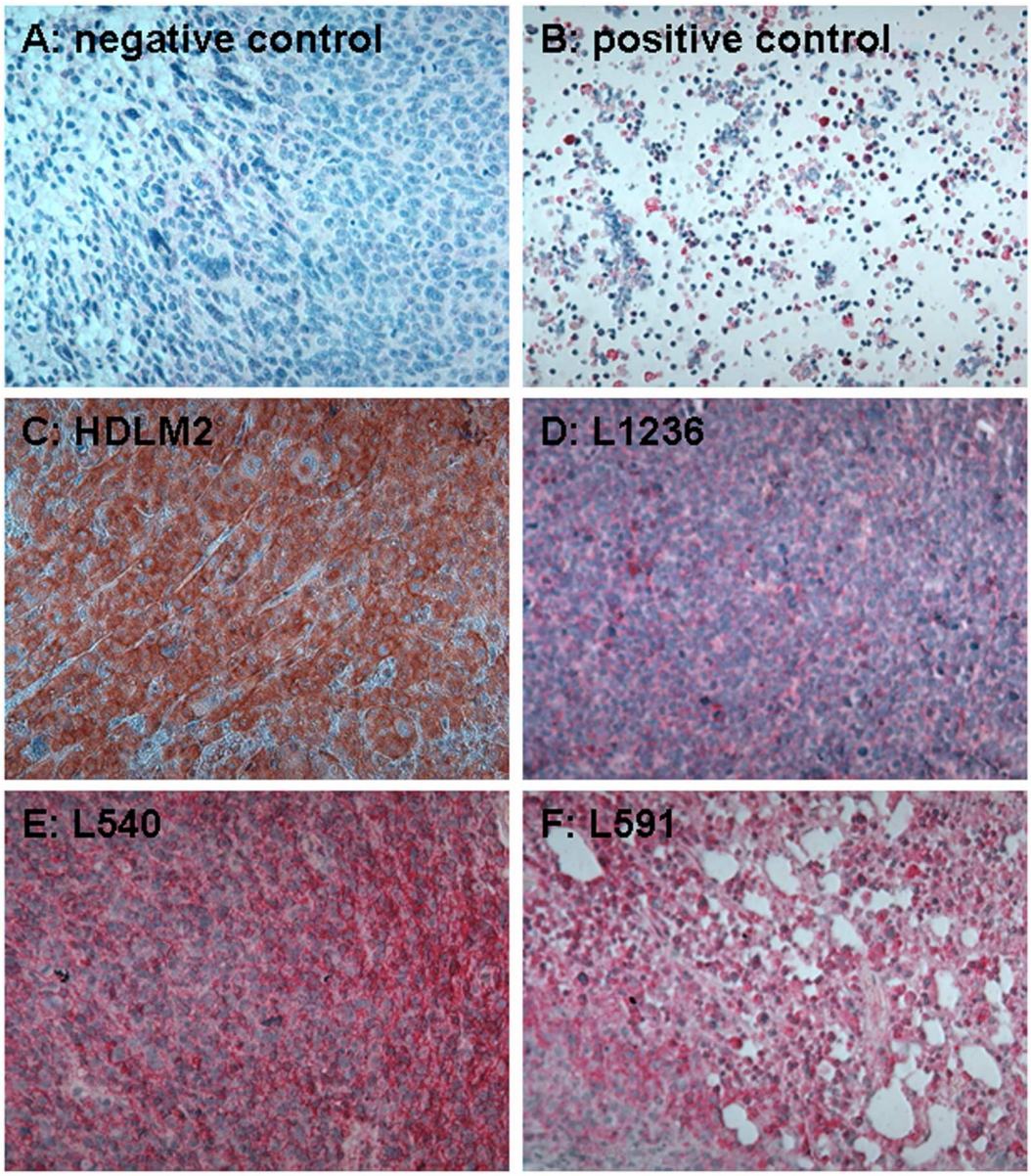

Figure 3.10: CD30 expression on HL SCID tumours.
HL tumours derived from HDLM2 **(C)**, L1236 **(D)**, L540 **(E)** and L591 **(F)** at x200 magnification, stained for CD30 expression. AP detection system shows positive red membrane staining **(B,D,E,F)**. HRP detection system shows positive brown membrane staining **(C)**. Negative control was GC SCID tumour **(A)**, positive control was a CTL line **(B)**. Sections were counterstained with haematoxylin.

Table 3.5: Cell surface phenotype of HL SCID tumours.

SCID tumour	antigen expression			
	CD4	CD15	CD20	CD30
HDLM2	+	+	-	+
L1236	+	-	-	+
L540	-	+	-	+
L591	-	-	+	+

In order to confirm epithelial origin, SCID tumours derived from GC cell lines AGS, NUGC3 and NUGC3-EBV, and NPC cell line C666.1 were stained for human cytokeratin of both Type I and II (Woodcock-Mitchell *et al*, 1982). As shown in Figure 3.11, all tumours expressed cytokeratin.

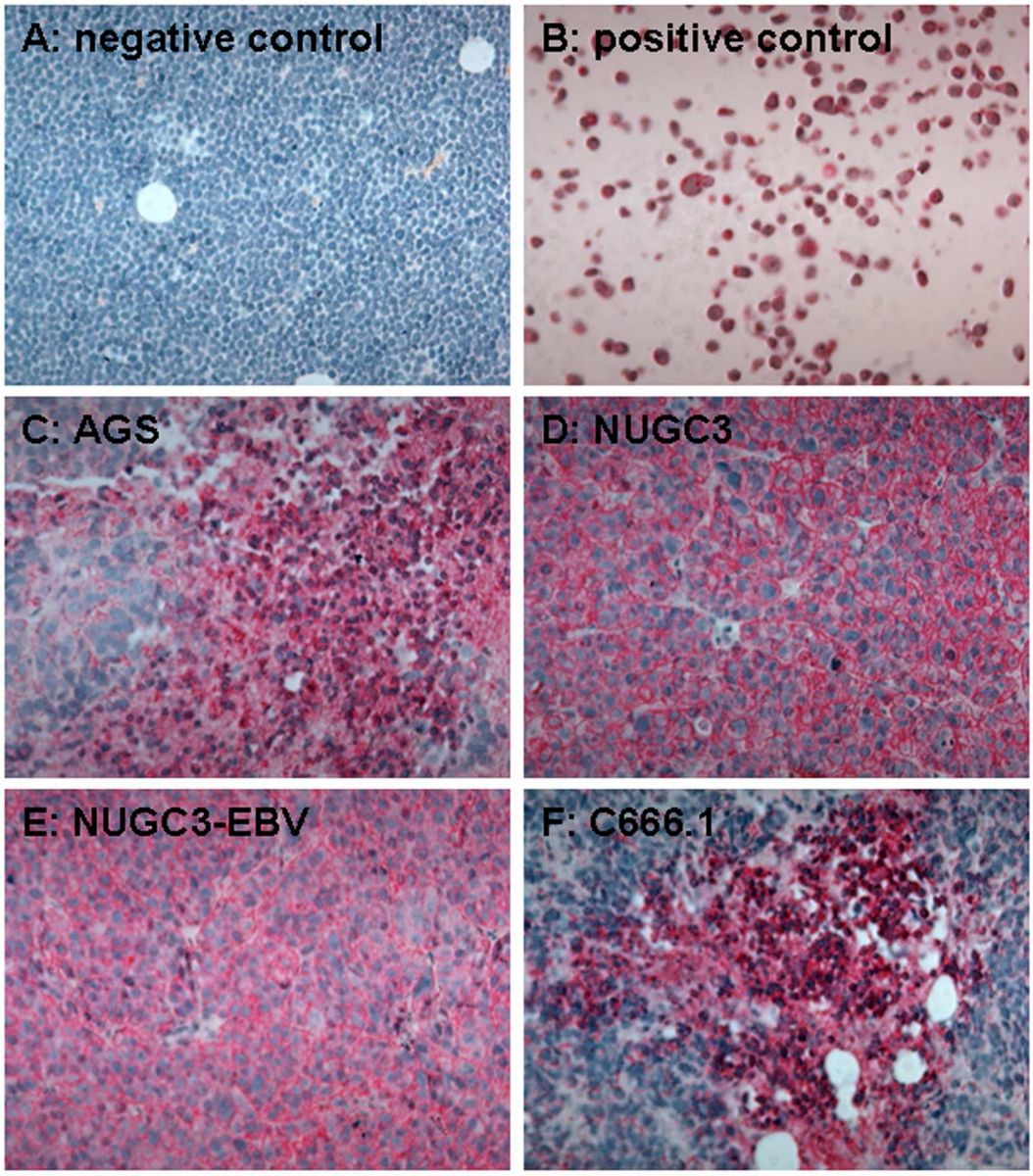

Figure 3.11: Cytokeratin expression in GC and NPC SCID tumours.
GC tumours derived from AGS **(C)**, NUGC3 **(D)**, and NUGC3-EBV **(E)**, and NPC tumour derived from C666.1 **(F)** at x200 magnification, stained for cytokeratin expression. AP detection system shows positive red cytoplasmic staining **(B,C,D,E,F)**. Negative control was a T cell lymphoma SCID tumour **(A)**, positive control was NUGC3 cell line **(B)**. Sections were counterstained with haematoxylin.

3.4.3 EBV infection

To confirm the EBV status of cell lines (L1236, L540, L591, NUGC3-EBV, C666.1), tumour sections were probed for EBERs expression using *in situ* hybridisation. At least five tumours derived from each cell line were evaluated. Results are shown in Figure 3.12.

The EBV-positive cell lines L591, NUGC3-EBV and C666.1 expressed EBERs, with characteristic nuclear staining evident in 100% of tumour cells (Figure 3.12). The EBV-negative cell lines L1236 and L540 showed no EBERs expression.

In order to assess the level of latent and lytic replication in the infected cells, tumours derived from the EBV-positive cell lines (L591, NUGC3-EBV, C666.1) were subsequently immunostained for three EBV latent and lytic antigens. Antigens were EBNA2, expressed in latency III, LMP1, expressed in latency II and III, and the immediate early lytic protein BZLF1. At least three tumours derived from each cell line were evaluated. Expression was assessed on a qualitative basis, and positively stained cells were not quantitated.

EBNA2 protein was expressed in L591 and C666.1 tumours, but not NUGC3-EBV tumours (Figure 3.13). All three tumour types expressed the latent protein LMP1 (Figure 3.14), although this was only seen in 1 of 3 (33%) NUGC3-EBV tumours. BZLF1 was not expressed at all in NUGC3-EBV or C666.1 tumours, but the occasional BZLF1-positive cell was observed in L591 tumours (Figure 3.15). A summary of these results is shown in Table 3.6.

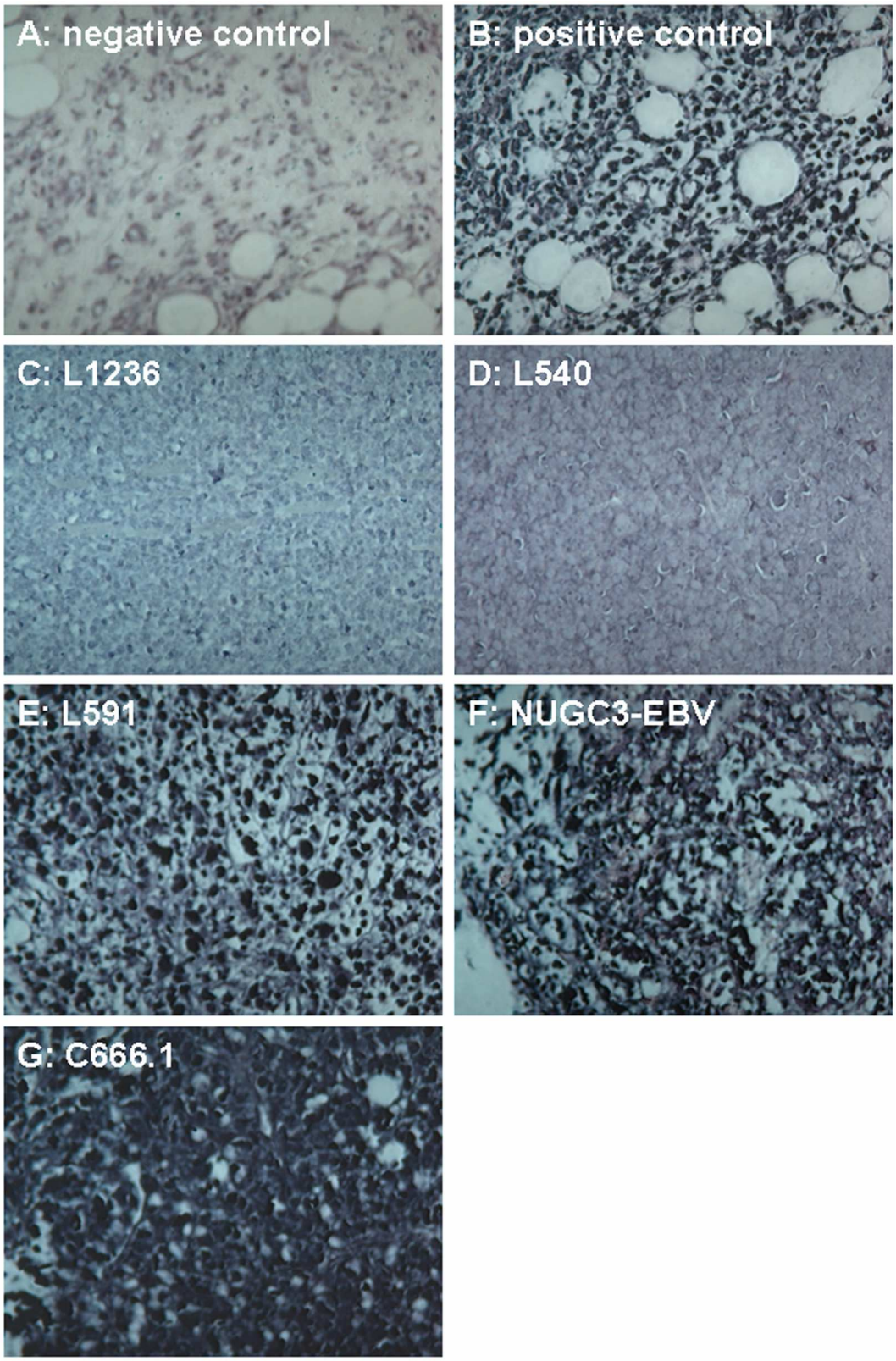

Figure 3.12: EBERs expression in HL, GC and NPC SCID tumours.
HL tumours derived from L1236 **(C)**, L540 **(D)**, and L591 **(E)**, and GC derived NUGC3-EBV **(F)**, and NPC derived C666.1 **(G)**, all at x200 magnification, probed by *in situ* hybridisation for EBERs expression. AP and BCP/NBT detection system shows positive black nuclear staining **(B,E,F,G)**. Negative control is human bowel lymphoma with negative control probe **(A)**, positive control is human bowel lymphoma with EBERs probe **(B)**. Sections were counterstained with haematoxylin.

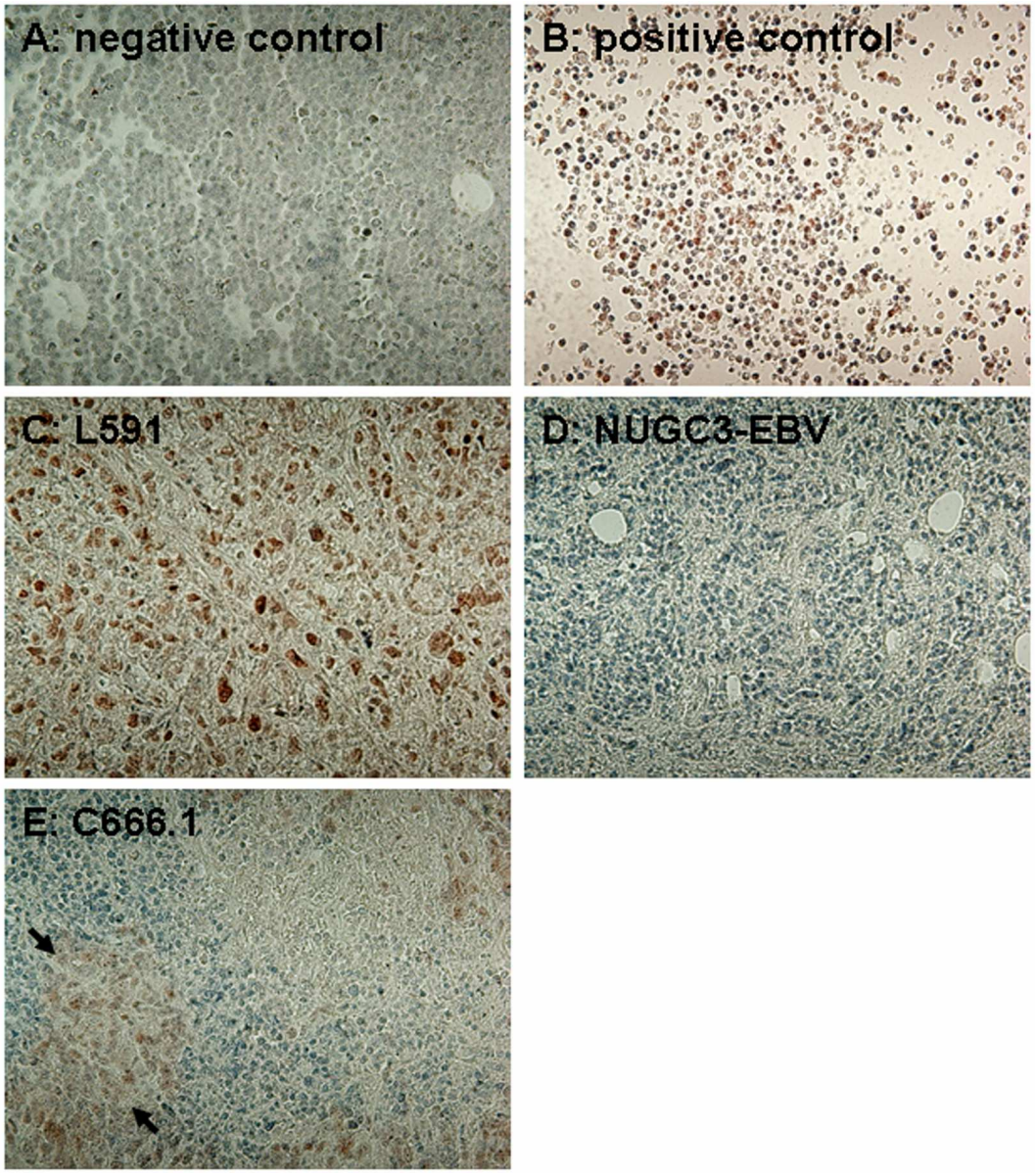

Figure 3.13: EBNA2 expression in EBV-positive SCID tumours.
HL cell line L591 **(C)**, GC cell line NUGC3-EBV **(D)**, and NPC cell line C666.1 **(E)**, at magnification x200, stained for EBNA2 expression. HRP detection system shows positive brown nuclear staining **(B,C,E)**. Negative control was EBV-negative HL SCID tumour **(A)**, positive control was LCL **(B)**. Black arrows indicate areas of positive staining. Sections were counterstained with haematoxylin.

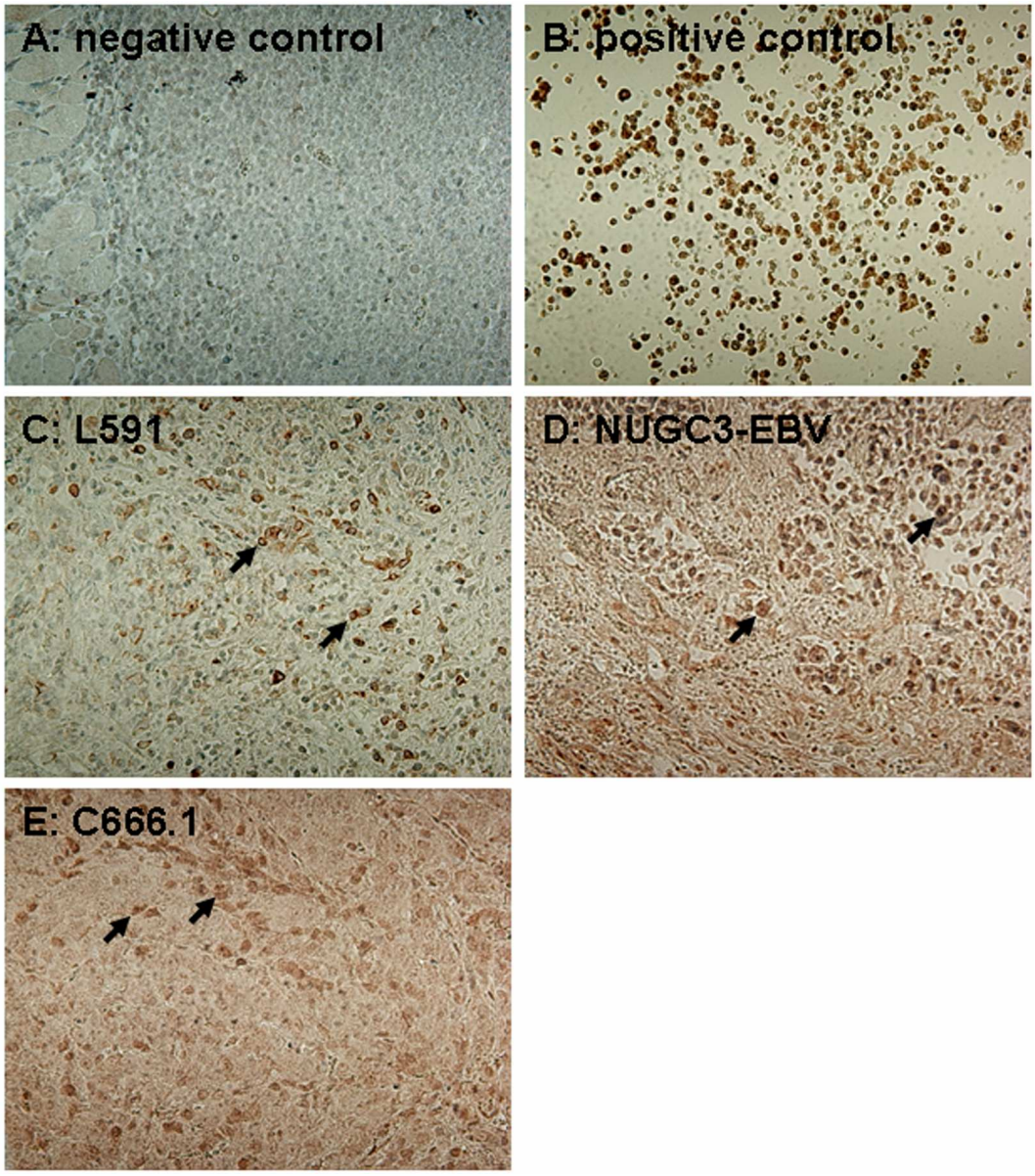

Figure 3.14: LMP1 expression in EBV-positive SCID tumours.
HL cell line L591 **(C)**, GC cell line NUGC3-EBV **(D)**, and NPC cell line C666.1 **(E)**, at magnification x200, stained for LMP1 expression. HRP detection system shows positive brown membrane staining **(B,C,D,E)**. Negative control was EBV-negative HL SCID tumour **(A)**, positive control was LCL **(B)**. Black arrows indicate individual positive cells. Sections were counterstained with haematoxylin.

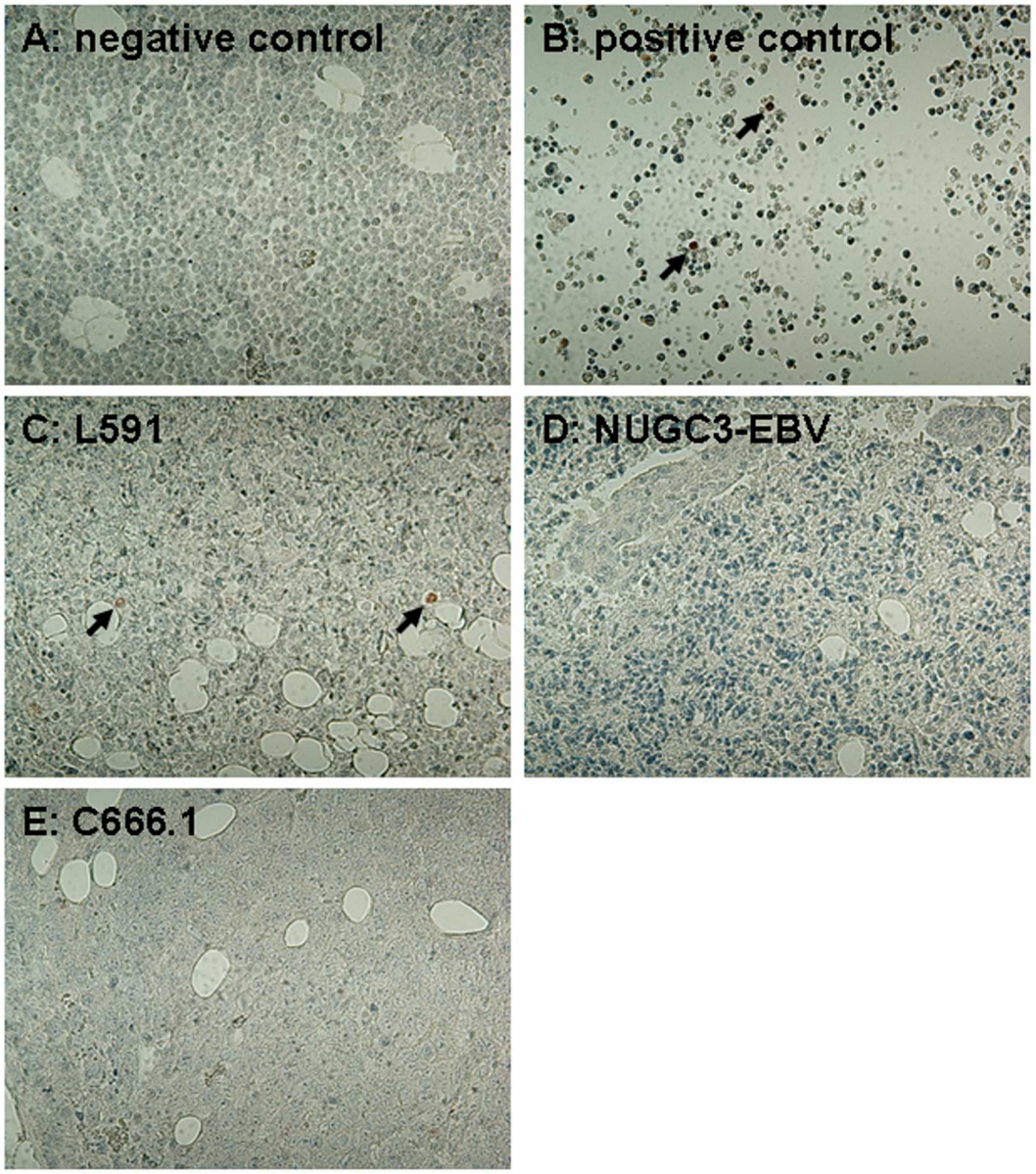

Figure 3.15: BZLF1 expression in EBV-positive SCID tumours.
HL cell line L591 **(C)**, GC cell line NUGC3-EBV **(D)**, and NPC cell line C666.1 **(E)**, at magnification x200, stained for BZLF1 expression. HRP detection system shows positive brown cytoplasmic staining **(B,C)**. Negative control was EBV-negative HL SCID tumour **(A)**, positive control was LCL **(B)**. Black arrows indicate individual positive cells. Sections were counterstained with haematoxylin.

Table 3.6: Viral antigen expression in EBV-positive SCID tumours.
(+): rare positive cells -/+: expression in 1 of 3 samples

SCID tumour	human derivation	antigen expression EBNA2	LMP1	BZLF1
L591	HL	+	+	(+)
NUGC3-EBV	GC	-	-/+	-
C666.1	NPC	+	+	-

3.5 Summary of results

Hodgkin's lymphoma cell lines

In vitro:

- Cell lines (HDLM2, L1236, L540, L591) displayed a heterogeneous phenotype in culture. The majority of cells were small and lymphoid in appearance. Occasional large bi- and multi-nuclear blastoid cells, consistent with a HRS cell phenotype, were also present.
- Three EBV-negative cell lines (HDLM2, L1236, L540) were infected with EBV *in vitro*. However, infection was not sustained.

In vivo:

- HL cell lines (HDLM2, L1236, L540, L591) injected sc in SCID mice formed tumours which displayed sustained growth over time.
- Titration of the L591 cell line determined that $5x10^6$ cells was the minimum cell number for consistent sc tumour formation, and this dose was used in subsequent immunotherapy experiments.
- Injection of cell lines ip in SCID mice resulted in poor outgrowth of tumours. Furthermore, it was difficult to determine tumour onset *in vivo*. This model was not utilized in further experiments.
- Histology of sc SCID tumours derived from three HL cell lines (HDLM2, L1236, L540) showed homogeneous sheets of blast cells. SCID tumours derived from L591 consisted of a heterogeneous population of large bi- and multi-nuclear blast cells, consistent with a HRS cell phenotype.
- The immunophenotype of sc SCID tumours derived from HL cell lines (HDLM2, L1236, L540, L591) was consistent with that of parental cell lines.
- EBER ISH of L591 sc SCID tumours confirmed EBV infection, with immunostaining showing a viral latency III gene expression pattern.

Carcinoma cell lines

In vitro:

- Cell lines (AGS, NUGC3, NUGC3-EBV, C666.1) were a pleiomorphic population in culture, displaying an undifferentiated malignant phenotype.

In vivo:

- Cell lines (AGS, NUGC3, NUGC3-EBV, C666.1) injected sc in SCID mice formed tumours which displayed sustained growth over time, with the exception of one cell line (AGS-EBV) which did not form tumours *in vivo*.
- Titration of the NUGC3-EBV and C666.1 cell lines determined that $1x10^6$ and $2x10^6$ cells, respectively, were the minimum cell dose for consistent sc tumour formation, and these doses were used in subsequent immunotherapy experiments.
- Histology of sc SCID tumours derived from carcinoma cell lines (AGS, NUGC3, NUGC3-EBV, C666.1) showed sheets of undifferentiated malignant cells.
- Immunostaining for cytokeratin in SCID tumours derived from carcinoma cell lines (AGS, NUGC3, NUGC3-EBV, C666.1) confirmed their epithelial origin.
- EBER ISH of NUGC3-EBV and C666.1 sc SCID tumours confirmed EBV infection, with immunostaining showing a viral latency II/I expression pattern for NUGC3-EBV and latency III for C666.1.

3.6 Discussion

Although much information can be gathered from *in vitro* experiments, investigations into the safety and efficacy of new therapeutic agents are best carried out using relevant *in vivo* models. Interactions between agent and subject are complex and not always predictable, therefore testing in a situation akin to that of the clinic is likely to provide a more accurate view of therapeutic effect and limit unforeseen events. Thus, the initial aim of the project was to establish mouse models of the EBV-associated malignancies HL, NPC and GC in which to test novel immunotherapies.

The malignant cells of HL, the HRS cells, have a heterogeneous phenotype both morphologically and immunophenotypically (Gruss & Kadin, 1996). Reed-Sternberg cells are multi-nucleated, while Hodgkin cells are mono-nucleated. The antigenic profile of HRS cells varies between tumours, although a panel of antigens common to most primary HRS cells has been identified. This panel includes the surface antigens CD15, CD25, CD30, CD40, CD54, CD70, CD71, MHC class II and the nuclear proliferation antigen Ki-67 (Gruss & Kadin, 1996). No individual cell line is able to model all possible manifestations of a HRS cell, and thus a panel of HL cell lines was assembled in order to represent more accurately the clinical situation. As the bulk of a HL tumour consists of infiltrating lymphocytes with only a small proportion of HRS cells, attempts to propagate HRS cell lines *in vitro* have often resulted in the outgrowth of EBV-positive LCLs rather than true HRS cell lines. This situation can also occur *in vivo*, as SCID mice implanted with HL lymph node biopsy samples can develop EBV-positive tumours derived from virus infected B cells rather than HRS cells (Meggetto *et al*, 1996). Equally, it is possible that during initial attempts to propagate HL samples *in vitro*, EBV-positive HRS cell lines may have been discarded, as EBV infection of a cell line was considered a contamination in the past. Given the difficulties encountered in establishment of these early HL cell lines, it is now virtually impossible to prove that three lines used in the current project (HDLM2, L540, L591) are derived from HRS cells. Nevertheless, they display characteristics not inconsistent with HRS cells, including expression of cell surface markers from the panel common to primary HRS listed above, polynuclearity and morphological heterogeneity (Drexler, 1993), and continue to be used widely as cell lines representative of HL (Baumforth *et al*, 2005; Savoldo *et al*, 2007). Furthermore, the L1236 cell line has been identified definitively as being derived from HRS cells, as identical Ig gene rearrangement sequences were demonstrated in L1236 cells and HRS cells in the bone marrow of the patient from whom the cell line was established originally (Kanzler *et al*, 1996a).

To test EBV-targeted immunotherapies, EBV-positive cell lines are required. Three EBV-negative HL cell lines (HDLM2, L1236, L540) were initially infected with the B95-8 laboratory strain of the virus. Although none of these cell lines express the EBV receptor CD21 (Diehl *et al*, 1981; Drexler *et al*, 1989; Kis *et al*, 2005), it has been shown that CD21 is not absolutely required for EBV infection of either B

lymphocytes or epithelial cells (Janz *et al*, 2000). The cell lines harboured EBV DNA as demonstrated by PCR three days after *in vitro* infection (Table 3.1). However, EBV copy number declined over time until EBV DNA could no longer be amplified from the infected cells. This is in line with other reports of transient EBV infection in susceptible cell lines, including the HL-derived KMH2 cell line (Kis *et al*, 2005). As these cells are already transformed, there is not likely to be any survival advantage accorded by EBV infection *in vitro* and so negative selection pressure may cause EBV-positive cells to be lost from culture.

For lasting EBV infection of cell lines *in vitro*, recombinant EBV carrying a selectable marker is generally used until stably infected sublines are established (Shimizu *et al*, 1996; Imai *et al*, 1998; Baumforth *et al*, 2005; Kis *et al*, 2005). One such HL cell line (KMH2-EBV), and two GC cell lines (AGS-EBV, NUGC3-EBV), were acquired together with their parent lines (Shimizu *et al*, 1996; Imai *et al*, 1998; Kis *et al*, 2005). At a dose of $1x10^7$ cells, sc injection of KMH2 or KMH2-EBV in SCID mice resulted in tumour formation on 4 of 10 (40%) and 0 of 5 (0%) occasions, respectively. In light of this poor rate of tumour outgrowth no further experiments were performed with the KMH2 cell lines. As stated in the project aims, the original intention was to model EBV-associated malignancies so as to have a framework within which to test novel LMP2-targeted therapies. The generation of target cell lines expressing a range of EBV latent antigens more reflective of the restricted virus gene expression characteristic of HL is an ongoing issue for researchers developing EBV-targeted therapies for HL. Cell lines currently used are LCLs expressing the full set of latent antigens, or EBV-negative cell lines transduced with recombinant vaccinia constructs encoding individual EBV genes (Murray *et al*, 1990; Murray *et al*, 1992). Interestingly, the *in vitro* infected subline of the AGS GC cell line also failed to form tumours in SCID mice, while 70% AGS injections gave rise to tumours (Table 3.3). In the NUGC3 GC setting, the EBV infected subline and the EBV-negative parent were equally as efficient in forming tumours. The SCID model is known to be 'leaky', that is 2 to 23% of mice develop some functional T and B cells in addition to their native NK cell activity (Bosma *et al*, 1988). It is possible that infection with recombinant EBV caused the KMH2 and AGS cell lines to become more 'visible' to the residual SCID immune system, although why this should occur in only two of three cell lines is not clear. However, the low level

immune function, if present, is unlikely to affect the SCID models in which tumour formation was observed, as no spontaneous tumour regression was seen in any case.

EBER ISH confirmed EBV infection in three cell lines; L591 derived from HL, NUGC3-EBV from GC and C666.1 from NPC (Figure 3.12). EBV-associated HL expresses a latency II phenotype, which is not seen in L591. In contrast, the observed EBV expression pattern for L591 is type III (Vockerodt *et al*, 2002), with positive immunostaining seen for EBNA2 (Table 3.6). As such, it more closely resembles an LCL, and the presence of occasional lytically infected cells as detected by BZLF1 immunostaining supported this.

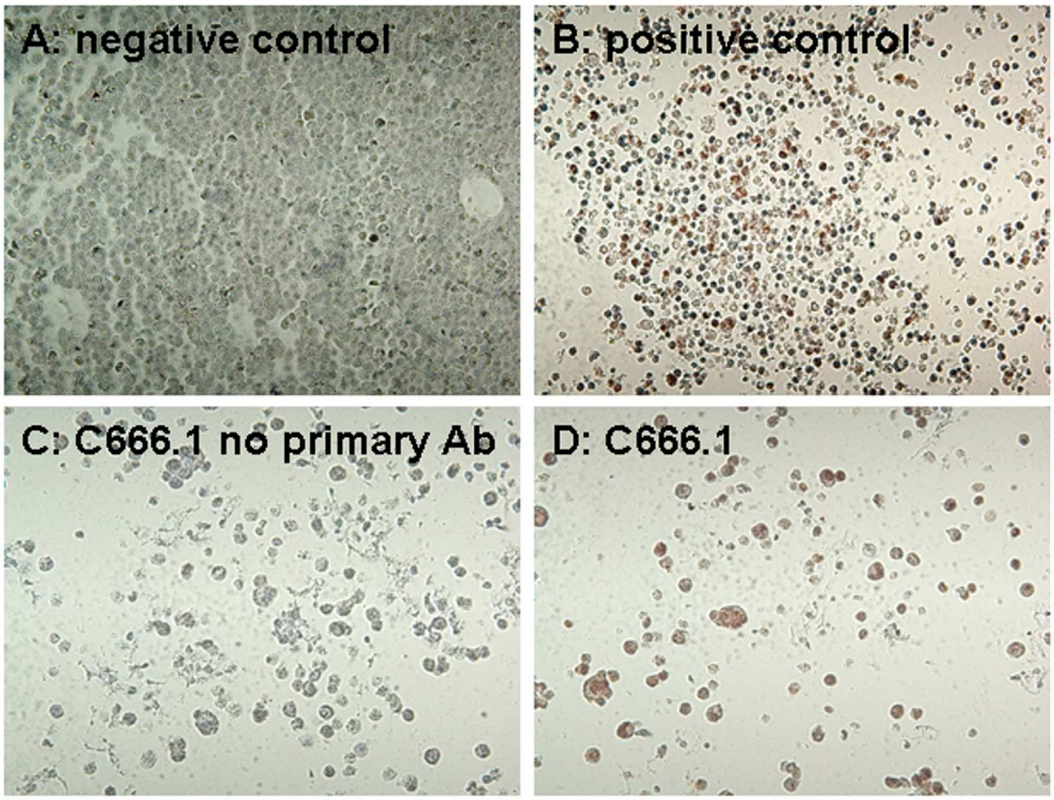

Figure 3.16: EBNA2 expression in the C666.1 NPC cell line.
NPC cell line C666.1, at magnification x400, without primary antibody **(C)** and stained for EBNA2 expression **(D)**. HRP detection system shows positive brown nuclear staining **(B,D)**. Negative control was EBV-negative HL SCID tumour **(A)**, positive control was LCL **(B)**. Sections were counterstained with haematoxylin.

Tumours derived from C666.1 were also positive for EBNA2 expression by immunohistochemistry, which is also not consistent with the expected latency II EBV expression pattern of NPC, and contradicts the findings of the laboratory in

which the cell line was established (Cheung *et al*, 1999). A drift from latency I to latency III expression has been seen in some BL cell lines after prolonged *in vitro* culture, and a similar event may have occurred here. Immunostaining of C666.1 cells embedded in agarose confirmed EBNA2 expression in the NPC cell line (Figure 3.16).

In some respects, the discrepancy between EBV latency phenotypes in HL and NPC models compared with the *in vivo* human situation does not affect the use of these models for testing targeted cellular therapies. That is, provided expression levels of the target protein remain largely unaffected by changes in latency state. As will be discussed in Chapter 4, cells engineered with a CD19-specific cTCR were tested using EBV-positive HL cells as targets. Expression of CD19 was the only requirement of these targets, and the presence of EBV antigens extraneous. If the therapeutic cells target EBV proteins, the issue may become more complicated. However, expression of the full range of EBV latent antigens does not prevent lysis of LCLs by CTLs specific for the subdominant viral protein LMP2 (Lalonde *et al*, 2007). Again, as expression of the target protein is the only requirement, until *in vitro* and *in vivo* model systems with restricted viral gene expression analogous to EBV latency II are developed, models with full EBV latent antigen expression will remain useful for testing novel targeted therapies.

In conclusion, the SCID models of HL, NPC and GC characterised here will be useful in the future for pre-clinical testing of novel immunotherapies, in particular those targeting EBV within the cancerous cell. Within the scope of this project, the HL SCID model provided a framework within which to gauge the ability of CD19-specific engineered T cells to prevent or treat CD19 positive HL tumours.

4 Immunotherapy Using Engineered T Cells

In recent years, immunotherapy with infusions of allogeneic, EBV-specific CTLs has been used to successfully treat PTLD tumours (Haque *et al*, 2002). However, the EBV infected cells of HL, NPC and GC lack expression of immunodominant viral antigens, and similar therapies in these malignancies have resulted in a less potent CTL anti-tumour response (Bollard *et al*, 2004; Straathof *et al*, 2005a). To increase CTL effectiveness, T cells can be genetically engineered to express cTCR directed against tumour antigens.

The overall aim of this project was to engineer a cTCR specific for the EBV LMP2 protein. As cTCRs are modular, generally the scFv extracellular portion from an existing cTCR is exchanged for a new scFv as a starting point for the engineering of cTCRs with novel specificity. To this end, whilst a suitable scFv specific for LMP2 was being sought (see Chapter 5), the cytotoxic potential of a cTCR specific for the B cell signalling molecule CD19 was assessed. Additionally, HRS cells can express CD19, so T cells engineered with a CD19-specific cTCR could in the future be used for treatment of HL.

CD19-specific cTCR (CD19-cTCR) engineered T cells have been shown to specifically lyse the CD19+ve Raji BL cell line, as well as non-Hodgkin's lymphoma (NHL) lymph node tumour biopsy cells *in vitro* (Cheadle *et al*, 2005), but have not been tested on HL cells. The aim of these experiments was to engineer T cells to express this CD19-cTCR, kindly supplied by Dr Eleanor Cheadle, and to test their effectiveness against HL cells *in vitro* and in the HL SCID model established in Chapter 3.

4.1 Engineering therapeutic T cells

To engineer T cells, a retroviral vector encoding the CD19-cTCR was centrifuged with PBMCs previously activated with anti-CD3 and -CD28, for three hours at 4°C on two sequential days, then cultured in media supplemented with IL-2 for up to 14 days (see 2.7.1 and 2.7.2). As the vector expression cassette contained a truncated CD34 gene (a haematopoietic stem cell marker not expressed on any other cell types utilized in these experiments), CD34 expression was used as a surrogate marker of transduction and hence also cTCR expression. PBMCs were also transduced with mock virus containing the vector backbone with GFP substituted for the CD19-cTCR expression cassette as a negative control.

4.1.1 PBMC donors

All frozen PBMCs used to generate CD19-cTCR T cells were sourced from a cell bank created in our laboratory, as were unmodified EBV-specific CTLs and matched LCLs (Wilkie *et al*, 2004). It was planned that therapy with unmodified CTLs would be used as a comparison standard for treatment with engineered T cells. In order to select the best match donor from the bank, HLA typing of cell lines was carried out at the Anthony Nolan Bone Marrow Trust, London, UK, or the Scottish National Blood Transfusion Service Tissue Typing Laboratory, Edinburgh, UK (see 2.4.6).

Tissue typing results are shown in Table 4.1. After typing, donor A was selected for L591, with matching loci A1 and B35; donor B was selected for NUGC3, with matching loci A24 and B52; and donor C was selected for C666.1, with matching locus B57. However, in addition to the HLA Class I, CTL-C and C666.1 also had a HLA Class II locus in common, DR1. Donor D was selected as a complete mismatch for L591 cells, with no common alleles at the loci typed.

Table 4.1: HLA typing of target cell lines for immunotherapy, and best match donors.

		HLA type					
cell line	L591	*A1*	*A33*	*B8*	*B35*		
	NUGC3	*A24*		*B52*			
	C666.1	*- **		*B57*	*B58*	*DR1*	*DR3*
donor	A	*A1*	*A3*	*B35*	*B57*		
	B	*A21*	*A24*	*B7*	*B52*		
	C	*A1*	*A2*	*B8*	*B57*	*DR1*	*DR7*
	D	*A11*	*A24*	*B18*	*B44*		

* no specific product determinable.

4.1.2 Virus titration

The first CD19-cTCR virus preparation collected from the PG13 producer cell line was titred on HT1080 cells in duplicate wells of a 24-well tissue culture plate. Cells were incubated overnight with neat, 1:10, 1:100, and 1:1000 dilutions of virus and transduction was assessed by FACS using an anti-CD34 antibody after five days culture (Figure 4.1).

At a 1:10 dilution, 38% of cells expressed CD34 (Figure 4.1), which equated to a titre of 1.9×10^5 tu/ml. This figure was in line with previous virus preparations both in our laboratory and that of Dr Cheadle. For transduction of PBMCs, 15ml of undiluted PG13 supernatant was used per 2×10^6 PBMCs, and thus the multiplicity of infection (MOI) was approximately 1.5.

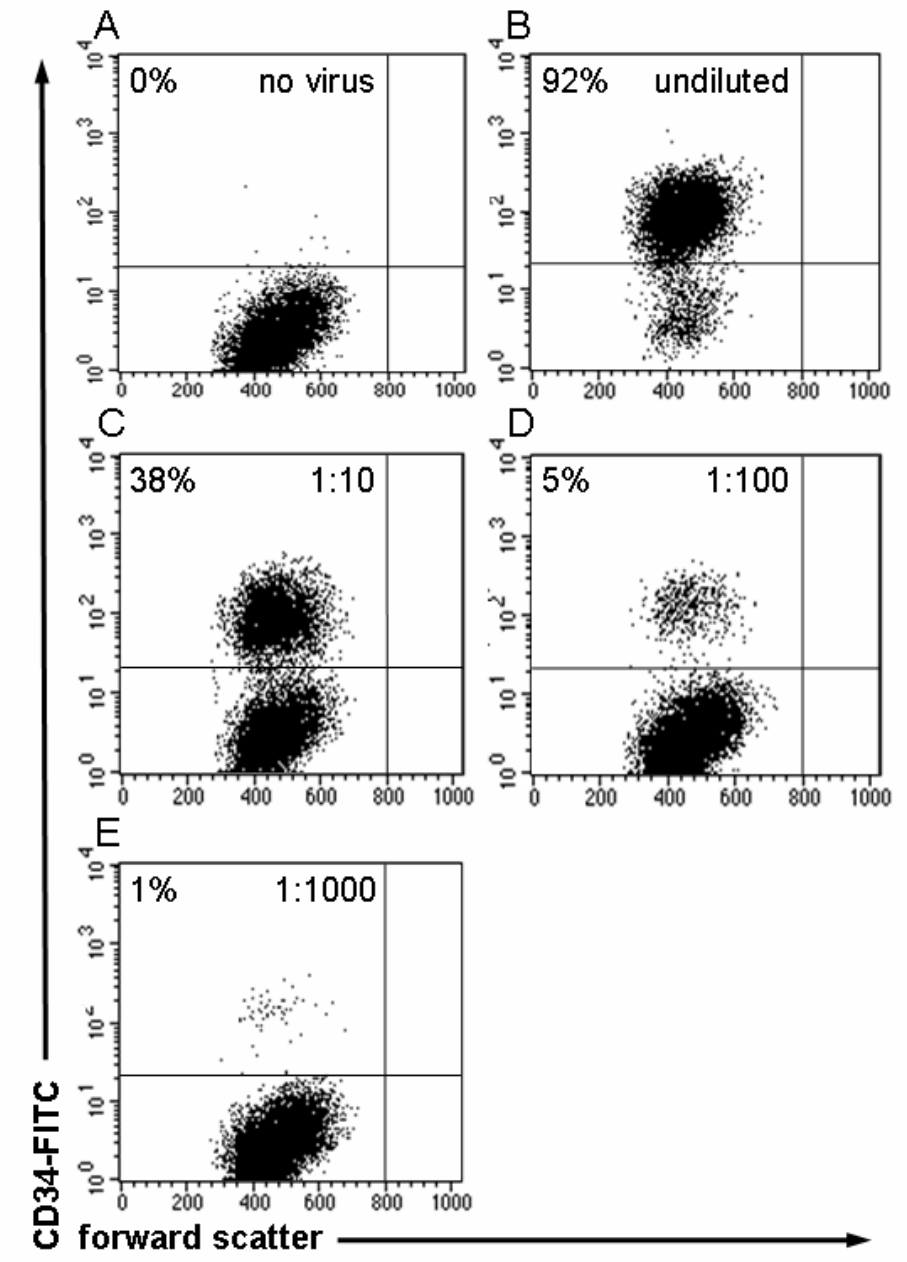

Figure 4.1: CD19-cTCR virus titration.
FACS plots of CD19-cTCR titration on HT1080 cells, showing CD34 expression as a marker of transduction, with undiluted **(B)**, 1:10 **(C)**, 1:100 **(D)**, and 1:1000 **(E)** dilutions of virus, and a virus free negative control **(A)**.

4.1.3 Transduction of fresh and frozen PBMCs

In order to assess if frozen stocks of PBMCs could be used to generate engineered T cells, the transduction rates between fresh and frozen PBMCs were compared. A total of $6x10^6$ cells from each source were transduced with virus or media in place of

virus (subsequently designated untransduced), then cultured for 13 days (see 2.7.2). Cell viability and absolute live cell number in the total culture volume were assessed at 4, 8, 11 and 13 days post transduction (Figure 4.2).

At all time points in the four cultures cell viability remained above 75%. There was no apparent difference in cell expansion between any of the cultures, with final absolute live cell number on day 13 slightly higher for fresh cells (untransduced - $5.1x10^8$; CD19cTCR - $5.7x10^8$) compared with frozen cells (untransduced - $2.8x10^8$; CD19cTCR - $3x10^8$) (Figure 4.2).

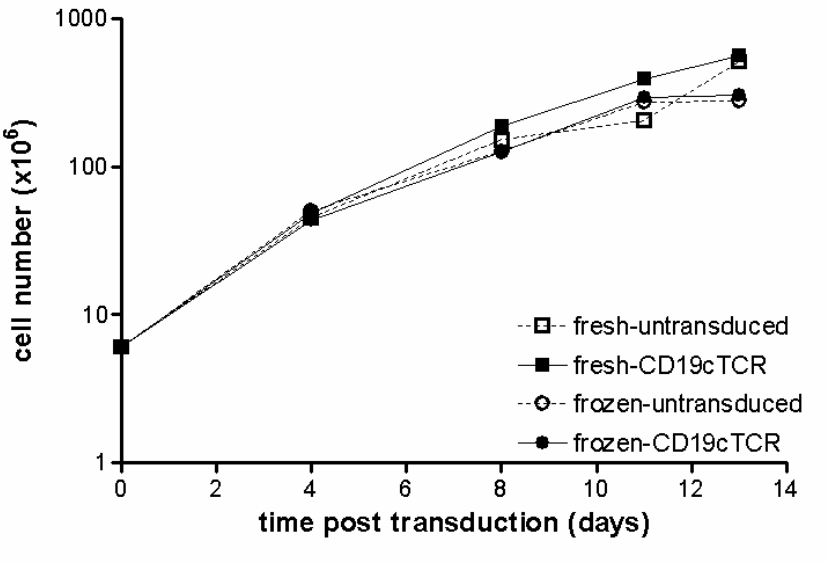

Figure 4.2: Growth of PBMCs post transduction.
Absolute live cell numbers of PBMCs after transduction with a retrovirus encoding a CD19-specific cTCR, or untransduced PBMCs subjected to the transduction protocol with culture medium in place of virus.

After 11 days in culture, the level of transduction in fresh and frozen cultures was assessed by anti-CD34 FACS analysis. Fresh and frozen PBMCs gave very similar transduction rates, with 18% of fresh PBMCs expressing CD34, compared with 19% frozen PBMCs (Figure 4.3). In light of these results, frozen PBMCs were used in subsequent transductions as the bank provided a more convenient and uncomplicated source of PBMCs than colleagues.

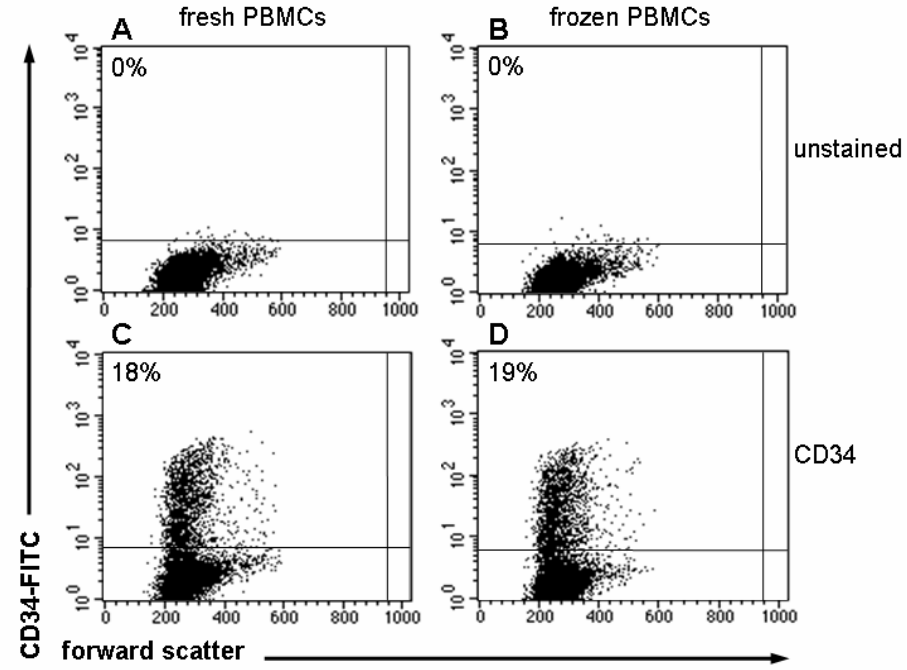

Figure 4.3: Transduction of fresh and frozen PBMCs with a CD19-cTCR. FACS plots of CD19-cTCR transduced PBMCs, showing CD34 expression as a marker of transduction in 18% of fresh **(C)** and 19% of frozen **(D)** cells, with unstained fresh **(A)** and frozen **(B)** cells as negative controls.

4.1.4 Transduction rates of CD19-cTCR and GFP virus

In total, transduction experiments with two viruses (GFP and CD19-cTCR) and three donors (donors A and D, and fresh PBMCs from a colleague) were completed, with mean transduction rates of 5%±3% for the GFP virus and 13%±6% for the CD19-cTCR virus. Results are shown in Figure 4.4. Transduction rates for individual experiments ranged from 2-8% for the GFP virus and 6-20% for the CD19-cTCR virus. Cells from some of these experiments were subsequently used for *in vivo* studies (see 4.3.1 and 4.3.2).

A

virus	GFP	CD19-cTCR
transduced	2.3	6.4
cells	3.3	7.6
(%)	4.3	8.6
	8.1	17.9
		18.9
		20.3
mean	4.7	13.27
SD	2.5	6.39

B

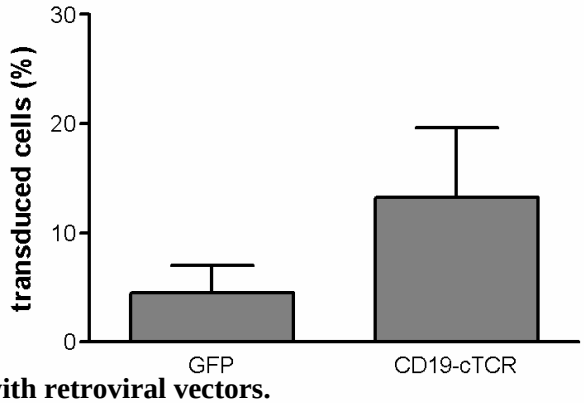

Figure 4.4: Transduction rates of PBMCs with retroviral vectors. The transduction rates of retroviral vectors containing GFP or a CD19-cTCR in PBMCs, assayed by FACS analysis of GFP or CD34 expression. A table of results from all experiments **(A)** and a graphical summary with mean±SD **(B)** is shown.

4.1.5 Transgene expression over time

Extended culture of transduced T cells may result in loss of transgene expression and hence reduced efficacy of T cell therapy (Eshhar *et al*, 2001; Morgan *et al*, 2006). In order to assess the optimum time frame for use of PBMCs transduced with CD19-cTCR, expression of the GFP and CD19-cTCR transgenes was assayed at days 2, 4, 6, 9, 10 and 11 post transduction using FACS analysis.

Expression of GFP continued to increase over the entire measurement period, from 1.4% to 3.4% of total cells (Figure 4.5). In contrast, expression of CD34 as a marker for CD19-cTCR expression peaked on day nine at 9.0% then fell slightly over the following two days to 8.6% of total cells on day 11. In light of these results, transduced cells were cultured for between 10 and 14 post transduction before use in cytotoxicity experiments or *in vivo* models.

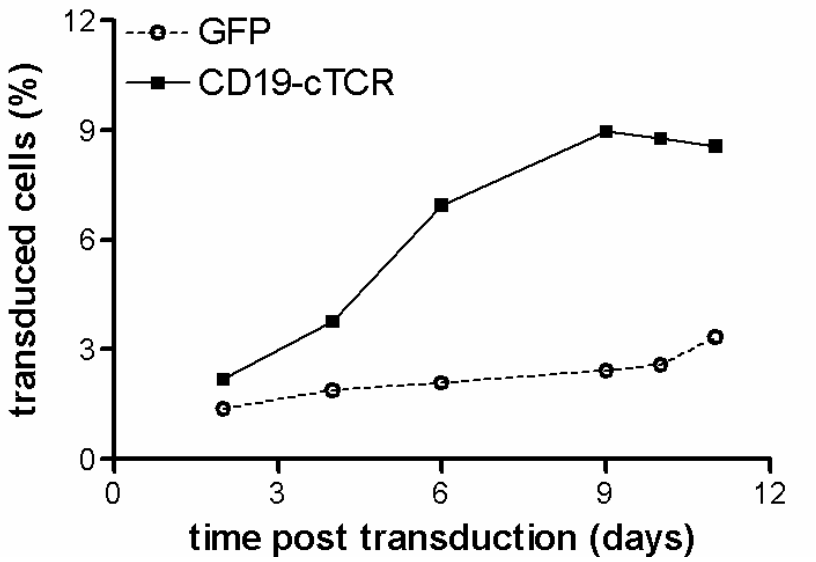

Figure 4.5: Transgene expression over time.
Level of transgene expression over an 11 day culture period in PBMCs transduced with a retroviral vector containing GFP or CD19-cTCR, as assessed by FACS analysis.

4.1.6 Immunophenotype of transduced PBMCs

In order to define cell subpopulations within the CD19-cTCR transduced cell culture, expression of cell surface antigens was assayed by FACS. CD4 and CD8 immunostaining was used to determine T cell subsets, CD19 immunostaining was used to detect B cells, and CD56 immunostaining was used to identify NK cells. The results of four transduction experiments using PBMCs from donors A and D are shown in Figure 4.6.

CD8+ T cells made up 57%±6% of the total population, and CD4+ T cells 39%±4% (Figure 4.6). Less than 1% of cultured cells expressed CD19. CD56+ NK cells comprised 14%±4% of the total population.

A

antigen	CD4	CD8	CD19	CD56
positive	34.0	61.0	0.37	16.6
cells	36.4	61.0	0.00	18.1
(%)	44.2	58.1	0.02	10.4
	40.0	48.1	0.00	11.4
mean	38.7	57.1	0.10	14.1
SD	4.4	6.2	0.18	3.8

B

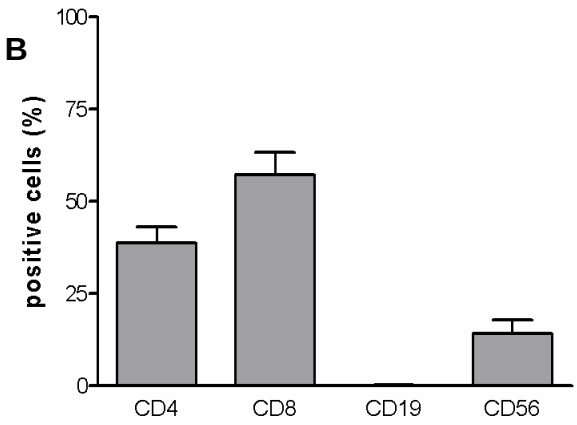

Figure 4.6: Immunophenotype of PBMCs transduced with CD19-cTCR.
Expression of cell surface antigens CD4, CD8, CD19 and CD56 on PBMCs transduced with CD19-cTCR, assayed by FACS analysis. A table of results from all experiments **(A)** and a graphical summary **(B)** is shown.

4.2 *In vitro* killing by engineered T cells

To gauge the cytotoxic potential of T cells engineered with CD19-cTCR, standard 4 hour ^{51}Cr release assays were performed (Haque *et al*, 1998). The targets used in these assays were L591, donor A derived LCL, L1236, and NK cell sensitive K562. CD19 expression on target cells was assessed using flow cytometry. Briefly, target cells were labelled with ^{51}Cr then incubated with effector cells (PBMCs from donor A or D transduced with GFP [mock] or CD19-cTCR virus) at effector to target ratios of 20:1, 10:1 and 5:1. After 4 hours, the amount of ^{51}Cr released from lysed cells was measured on a gamma counter, and the level of specific lysis calculated, as described in 2.7.6.

4.2.1 CD19 expression on target cell lines

In order to confirm the expression of CD19 on the target cell lines (L591, donor A derived LCL, L1236, K562), FACS analysis was carried out prior to performing ^{51}Cr release assays (Figure 4.7). Immunostaining of SCID tumours resulting from sc injection of L591 and LCLs was used to verify maintenance of expression patterns *in vivo* (Figure 4.8).

Both the HL cell line L591 and donor A LCLs expressed CD19, as analysed by FACS, with 100% and 80% of cells respectively staining positive (Figure 4.7). SCID tumours derived from L591 and LCLs also expressed CD19 (Figure 4.8). Neither the K562 nor the L1236 cell line expressed CD19. Consequently, in ^{51}Cr release assays the K562 cell line was used as a control for levels of NK cell killing, and L1236 was used as a negative control.

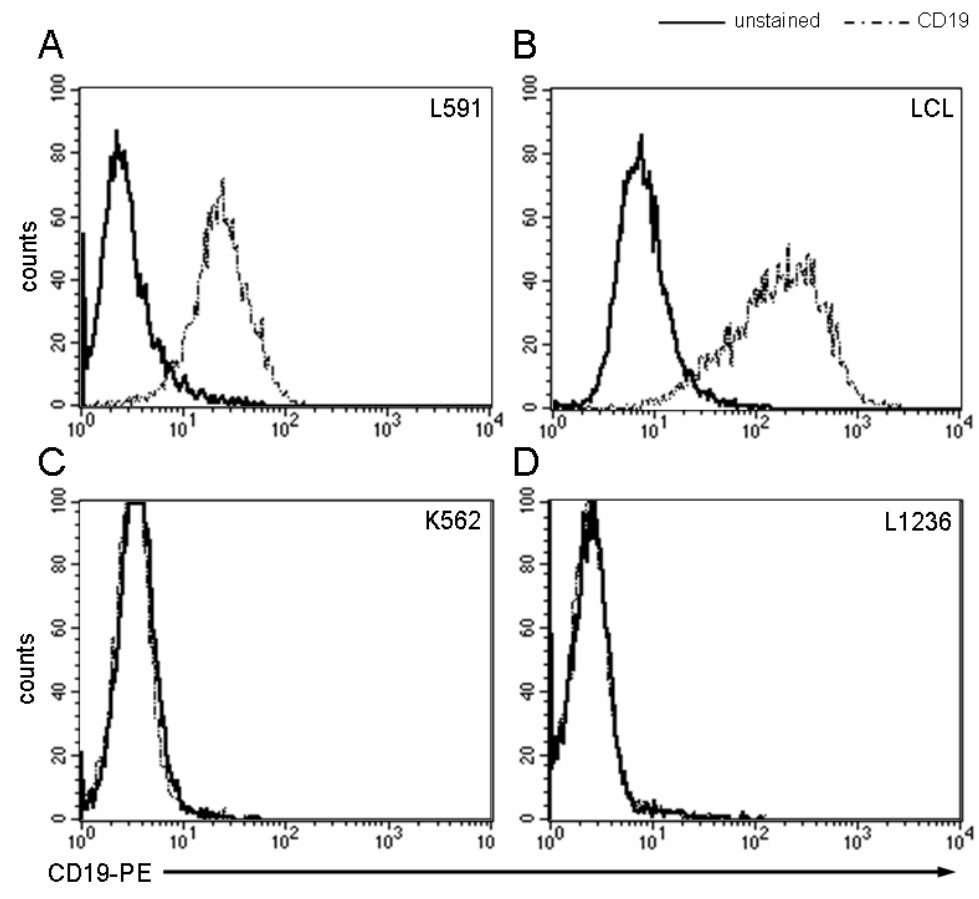

Figure 4.7: CD19 expression on ^{51}Cr release assay target cell lines.
FACS analysis shows expression of CD19 on the HL cell line L591 **(A)** and an LCL **(B)**, but no expression on the NK sensitive K562 **(C)** or HL L1236 **(D)** cell lines.

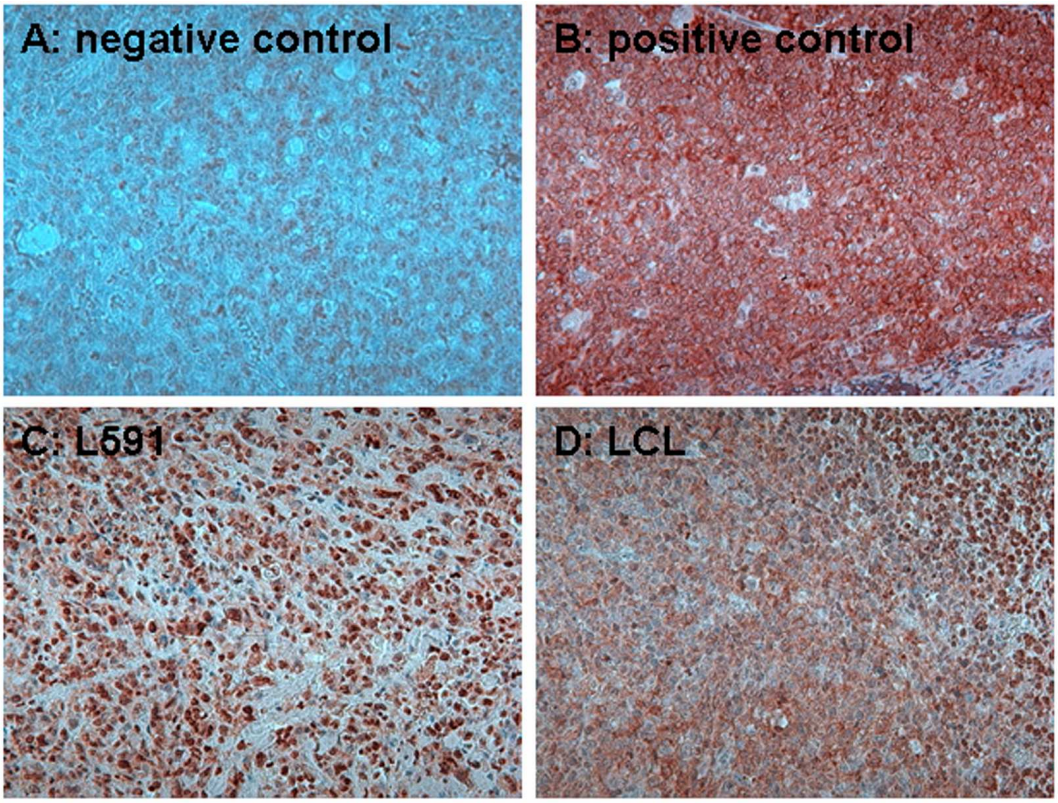

Figure 4.8: CD19 expression on SCID tumours.
Tumours derived from HL L591 **(C)** and an LCL **(D)** at x200 magnification, stained for CD19 expression. HRP detection system shows positive brown membrane staining **(B,C,D)**. Negative control was GC derived SCID tumour **(A)**. Positive control was human tonsil **(B)**. Sections were counterstained with haematoxylin.

4.2.2 Chromium release assays using engineered T cells

For each transduction experiment the cytotoxicity of CD19-cTCR transduced PBMCs, and mock GFP transduced PBMCs was assessed using a ^{51}Cr release assay. L591 and donor A LCLs were used as target cell lines, with K562 and L1236 as control targets. The effector to target ratios used were 20:1, 10:1 and 5:1. Results shown are from five (L591, LCL, K562) and three (L1236) experiments (Figure 4.9).

Specific lysis was seen at all effector to target ratios against L591 and LCLs. At an effector to target ratio of 20:1, PBMCs expressing CD19-cTCR lysed the target cells at a significantly higher rate than mock transduced PBMCs (Figure 4.9). Specific lysis for L591 target cells was 24%±11% (range 12-35%) for CD19-cTCR transduced cells compared with 5%±3% (range 2-9%) for mock-transduced cells

(Mann Whitney, p=0.0079), and for LCLs was 29%±13% (range 12-44%)for CD19-cTCR transduced cells compared with 3%±2% (range 1-6%) for mock-transduced cells (Mann Whitney, p=0.0079). This significant difference between CD19-cTCR and mock transduced cells continued at effector to target ratios of 10:1 and 5:1 for both L591 and LCL target cell lines. Mean % specific lysis and Mann Whitney p values are shown in Table 4.2.

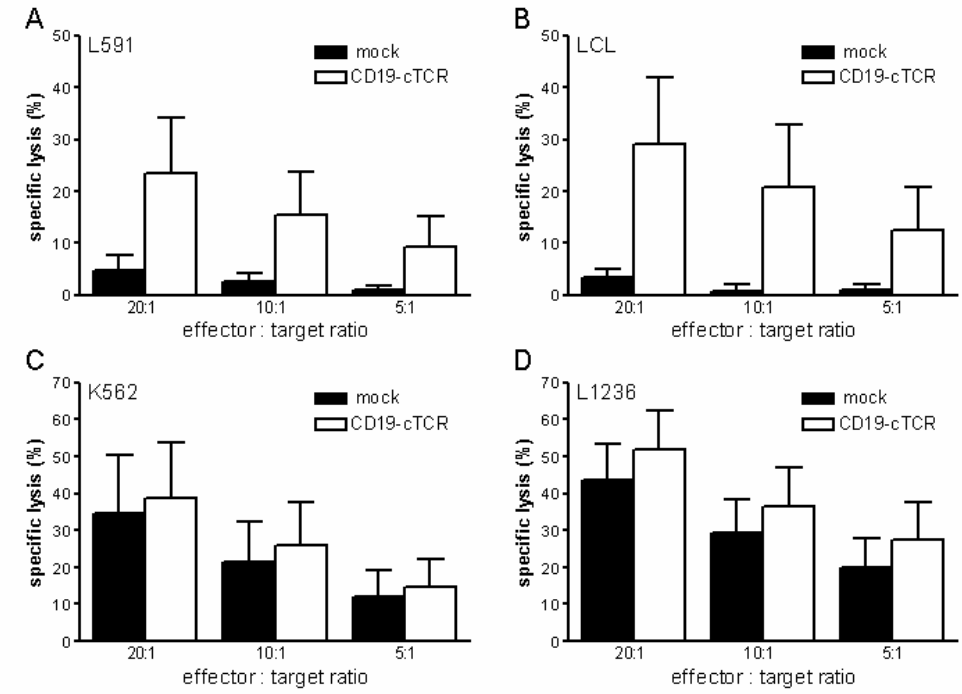

Figure 4.9: Specific lysis of target cells by engineered T cells.
Cytotoxicity of CD19-cTCR transduced PBMCs and mock GFP transduced PBMCs in an *in vitro* ^{51}Cr release assay, against target cell lines L591 **(A)**, donor A derived LCLs **(B)**, K562 **(C)** and L1236 **(D)**. Specific lysis was seen against L591 and LCLs **(A,B)**, but not K562 and L1236 **(C,D)**. Bars show mean±SD for five **(A,B,C)** and three **(D)** experiments.

There was no significant difference in the ability of mock or CD19-cTCR transduced cells to lyse the K562 or L1236 target cell lines, with both effector lines capable of high levels of cytotoxicity (Figure 4.9). Specific lysis at an effector to target ratio of 20:1 for K562 target cells was 39%±15% (range 25-57%) for CD19-cTCR transduced cells, compared with 35%±16% (range 18-53%) for mock-transduced cells (Mann Whitney, p=0.8413); and for L1236 was 52%±11% (range 40-50%) for CD19-cTCR transduced cells, compared with 44%±10% (range 32-51%) for mock-transduced cells (Mann Whitney, p=0.4000). This non-significance between CD19-

cTCR and mock transduced cells continued at effector to target ratios of 10:1 and 5:1 for both K562 and L1236 target cell lines. Mean % specific lysis and Mann Whitney p values are shown in Table 4.2. Given the similarities in the patterns of specific lysis of L12356 and K562, which is an NK sensitive target, and the presence of NK cells in transduced cultures (mean 14.1% of total population CD56+, Figure 4.6), the effect of NK activity on *in vitro* cytotoxicity was examined.

Table 4.2: Mean specific lysis (%) of target cells by engineered T cells.
Comparison of specific lysis between CD19-cTCR and mock transduced PBMCs on effector cell lines L591, LCL, K652 and L1235, with Mann Whitney P values. [* indicates significant difference]

effector:target ratio	20:1		10:1		5:1	
effector cells	mock	CD19-cTCR	mock	CD19-cTCR	mock	CD19-cTCR
L591	5	24	3	15	1	9
	p=0.0079*		p=0.0079*		p=0.0079*	
LCL	3	29	1	21	1	13
	p=0.0079*		p=0.0079*		p=0.0079*	
K562	35	39	21	26	12	15
	p=0.8413		p=0.6905		p=0.6905	
L1236	44	52	30	36	2	28
	p=0.4000		p=0.7000		p=0.4000	

4.2.3 Effect of NK cells on *in vitro* cytotoxicity

To assess the role of CD56+ NK cells in the ^{51}Cr release assays, a depletion experiment was performed. CD56+ cells were separated from a population of donor A PBMCs transduced with CD19-cTCR three days previously using anti-CD56 coated magnetic beads. Enriched and depleted fractions were maintained in culture for a further seven days and the number of CD56+ cells remaining in each fraction was then analysed by FACS (Figure 4.10). The cytotoxic potential of each fraction, as well as unfractionated CD19-cTCR transduced cells and GFP mock transduced cells, was then assessed by ^{51}Cr release assay.

Before separation, CD56+ cells made up 18% of the total population (Figure 4.10). After separation, the NK-depleted fraction contained 11% CD56+ cells, and the NK-enriched population 73% CD56+ cells.

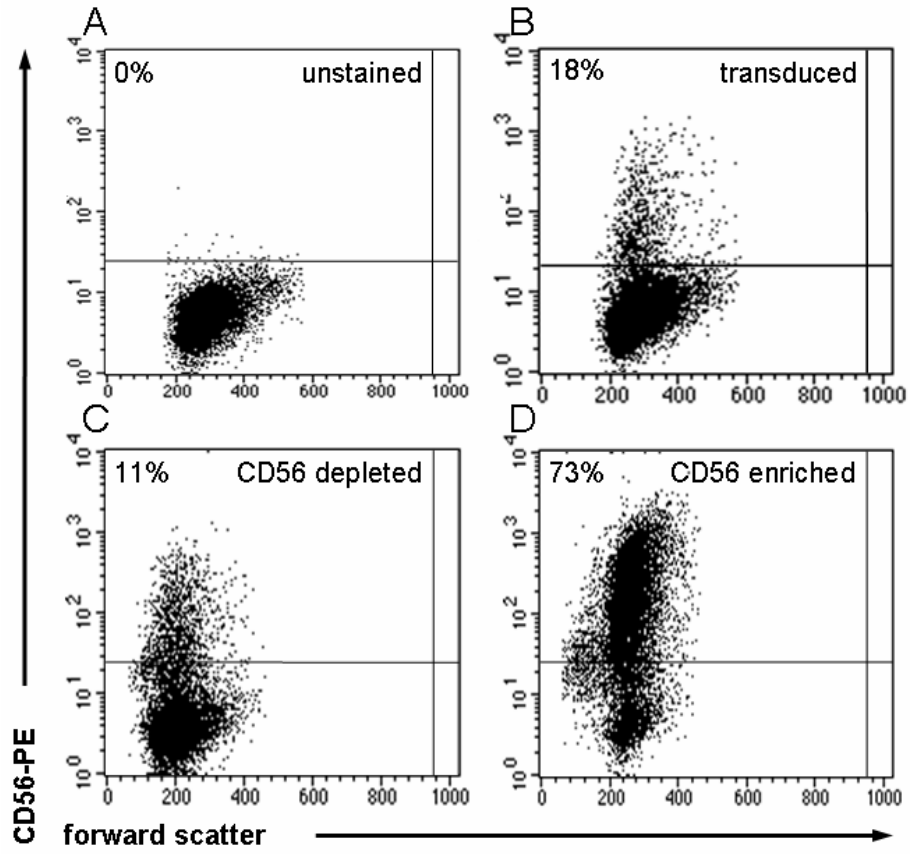

Figure 4.10: Percentage of NK cells in a population of CD19-cTCR transduced cells before and after CD56 separation.
FACS analysis in PBMCs transduced with CD19-cTCR **(B)** and following CD56-depletion **(C)** or CD56-enrichment **(D)**. Unstained cells are shown in **(A)**.

The number of transduced cells before separation was 8%. This number remained the same in the NK-depleted fraction, but was reduced in the NK-enriched fractions to 3% (Figure 4.11).

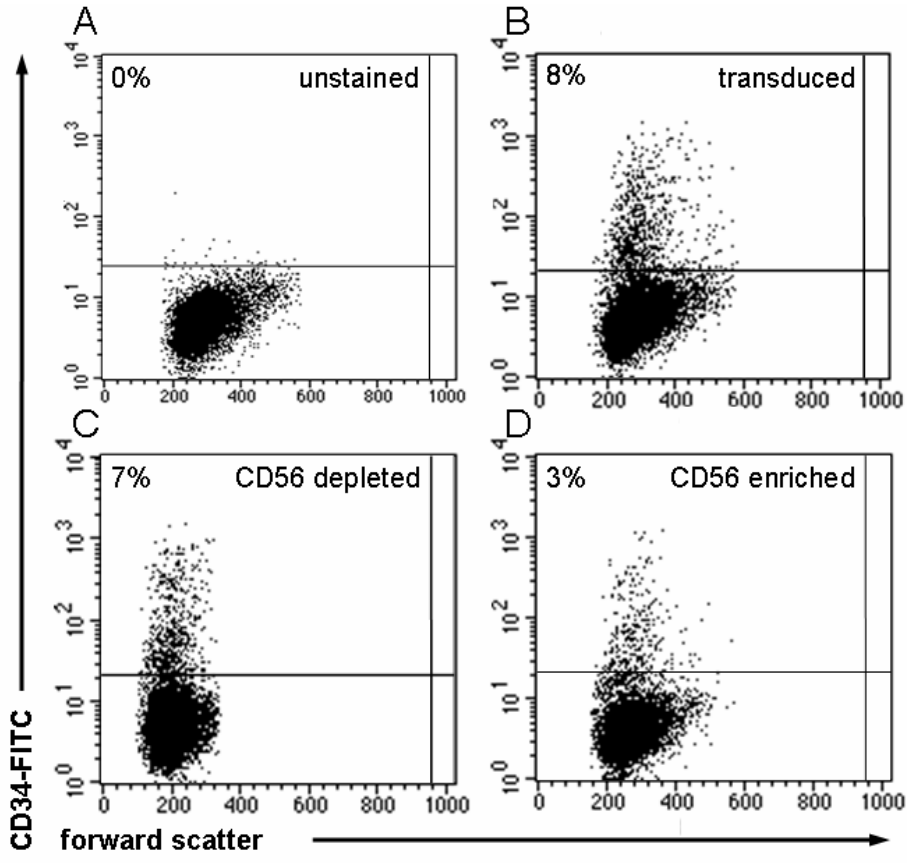

Figure 4.11: Percentage of transduced cells before and after CD56 separation. FACS analysis of CD34 expression as a marker of transduction in PBMCs transduced with CD19-cTCR **(B)** and following CD56-depletion **(C)** or CD56-enrichment **(D)**. Unstained cells are shown in **(A)**.

In a ^{51}Cr release assay, specific lysis of K562 and L1236 was dramatically reduced when CD56+ cells were depleted from the effector cell population, and increased when CD56+ cells were enriched at all effector to target ratios (Figure 4.12). Specific lysis at an effector to target ratio of 20:1 for K562 target cells was 52% for CD19-cTCR transduced cells, compared with 53% for mock-transduced cells; and for L1236 was 40% for CD19-cTCR transduced cells, compared with 47% for mock-transduced cells; whilst for CD56-depleted and CD56-enriched populations it was 9% and 78% for K562 and 20% and 82% for L1236, respectively. Killing of L591 and LCL targets was minimally affected. This suggests that NK cells are principally responsible for the high levels of L1236 killing observed previously (see 4.2.2).

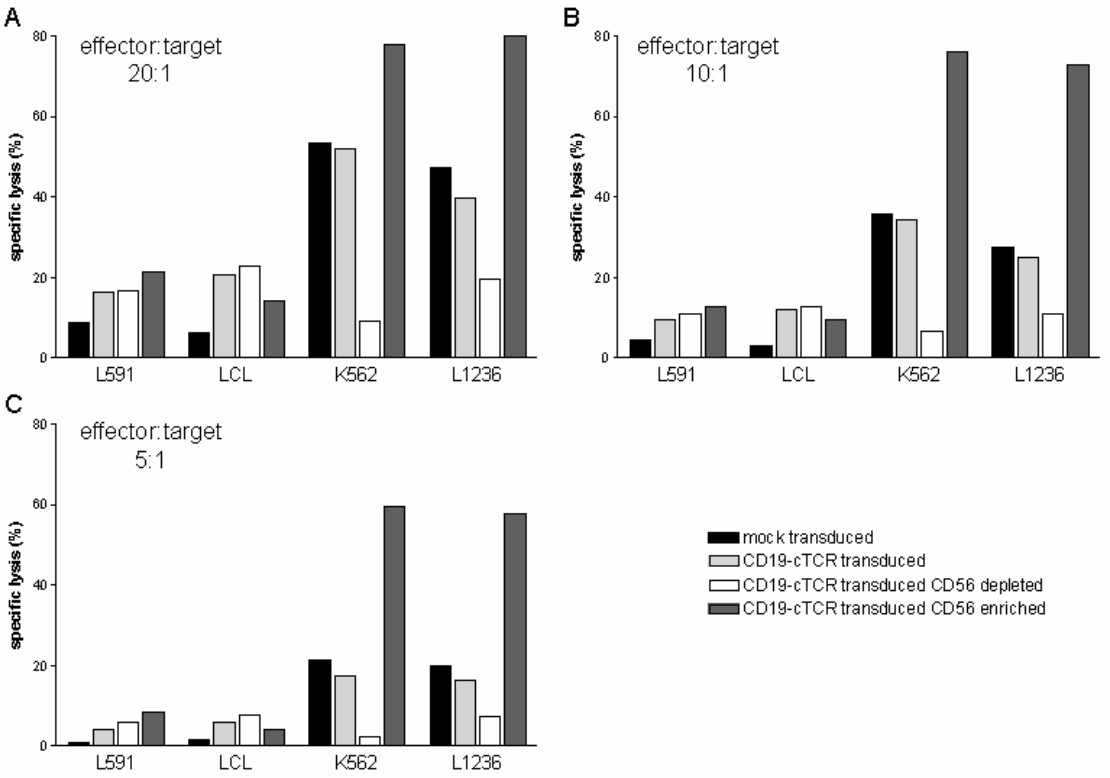

Figure 4.12: Effect of NK cells on *in vitro* cytotoxicity.
^{51}Cr release assays using mock, transduced, transduced CD56-depleted and transduced CD56-enriched effector cells at effector to target ratios of 20:1 **(A)**, 10:1 **(B)** and 5:1 **(C)** show lysis of the K562 and L1236, but not L591 and LCL target cell lines is dependent on NK cells.

4.2.4 Selection of CD34+ transduced cells

The final fraction of cells expressing the CD34 transgene after transduction with the CD19-cTCR vector ranged from 6-20% (see 4.1.4). With such low transduction efficiencies in some experiments, it was decided to enrich a population of CD19-cTCR transduced cells using the truncated CD34 molecule as a selection marker. This would increase the fraction of cells expressing CD19-cTCR and potentially also enhance specific lysis of L591 cells. CD34+ cells were selected from a population of PBMCs which had been transduced with the CD19-cTCR vector nine days earlier, using anti-CD34 coated magnetic beads. CD34-enriched and CD34-depleted fractions were cultured overnight, then the number of CD34+ cells remaining in each fraction as well as in unfractionated CD19-cTCR transduced cells was analysed by FACS (Figure 4.13). The cytotoxic potential of each fraction, unfractionated CD19-cTCR transduced cells, and GFP mock transduced cells was then assessed by ^{51}Cr release assay (Figure 4.14).

Before separation, CD34+ cells made up 8% of the total population (Figure 4.13). After separation, the transduced CD34-depleted fraction contained 1% CD34+ cells, and the transduced CD34-enriched population contained 82% CD34+ cells.

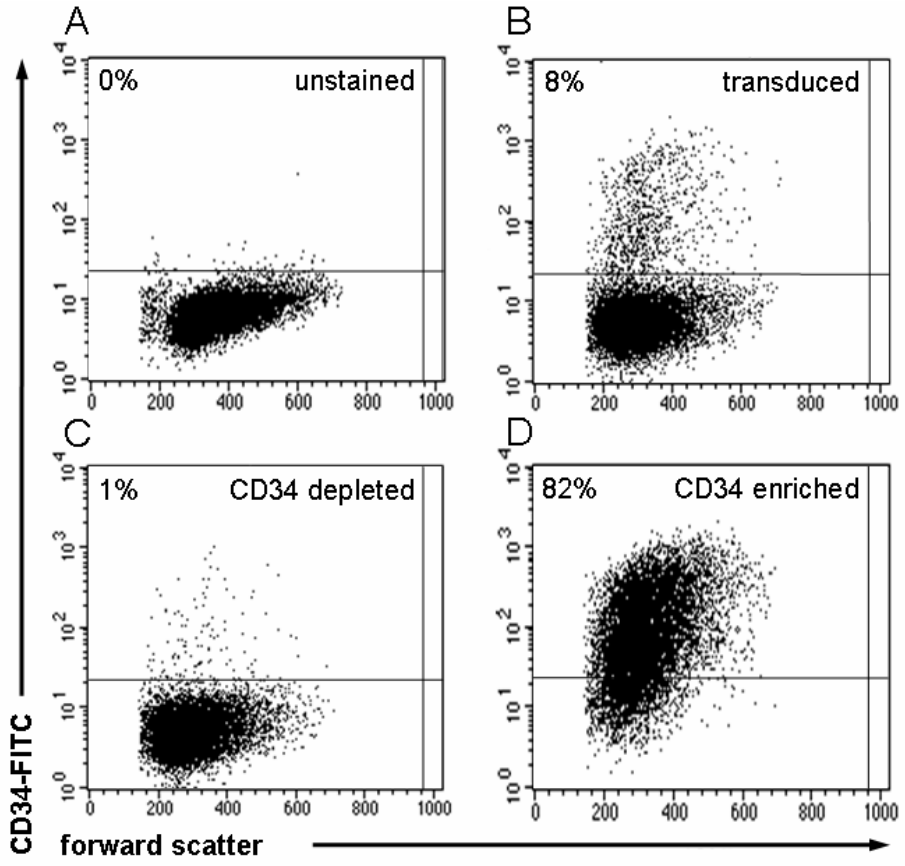

Figure 4.13: Percentage of transduced cells before and after CD34 separation. FACS analysis of CD34 expression as a marker of transduction in PBMCs transduced with CD19-cTCR **(B)** and following CD34-depletion **(C)** or CD34-enrichment **(D)**. Unstained cells are shown in **(A)**.

In a ^{51}Cr release assay, specific lysis of L591 and LCL cell lines was increased when number of transduced cells increased (Figure 4.14). When the percentage of CD34+ cells in CD19-cTCR transduced cells, the CD34-depleted fraction, and the CD34-enriched fraction was 8%, 1% and 82%, respectively, specific lysis at an effector to target ratio of 20:1 of L591 cells was 12%, 10%, and 21%, respectively, while specific lysis of LCLs was 12%, 7%, and 41%, respectively. In contrast, specific lysis of the NK target K562 cell line decreased when the number of transduced effector cells increased. With CD19-cTCR transduced cells, the CD34-depleted fraction, and the CD34-enriched fraction as effectors, specific lysis at an effector to target ratio of 20:1 was 57%, 47% and 10% respectively (Figure 4.14). Thus,

increasing the fraction of cells specific for CD19 enhanced specific lysis of L591 and LCL target cells.

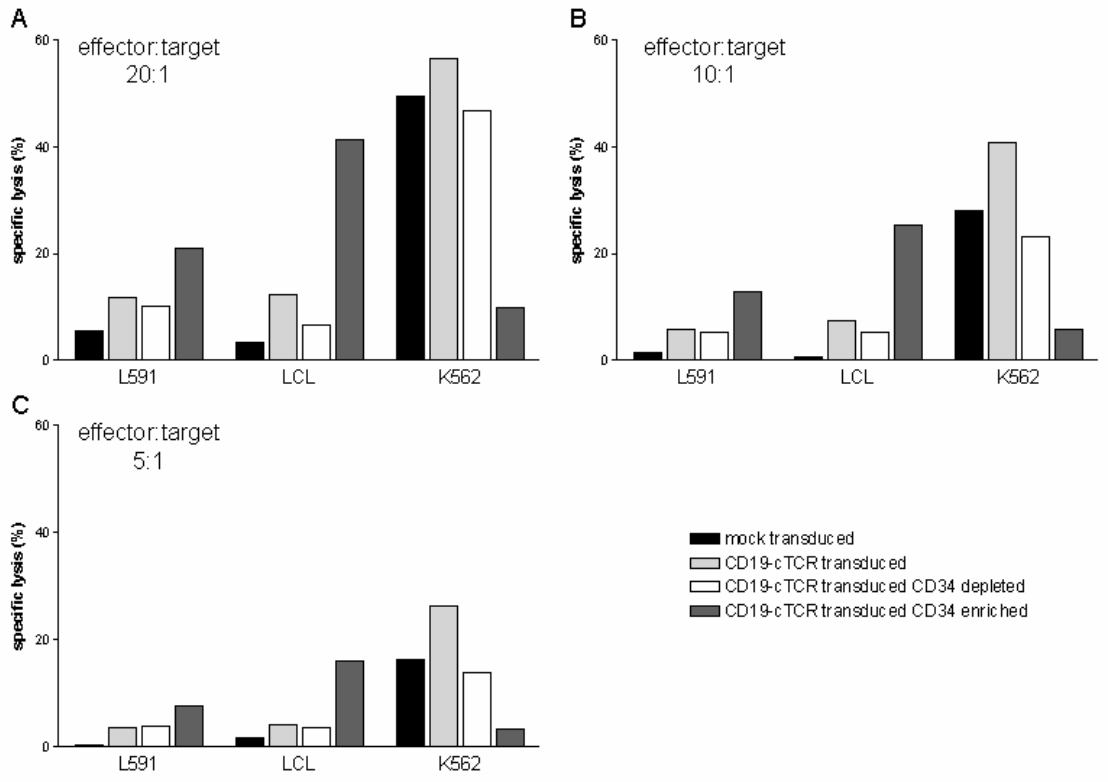

Figure 4.14: Effect of transduced cell numbers on *in vitro* cytotoxicity.
^{51}Cr release assays using mock, transduced, transduced CD34-depleted and transduced CD34-enriched effector cells at effector to target ratios of 20:1 **(A)**, 10:1 **(B)** and 5:1 **(C)** show lysis of L591 and LCL but not NK target K562 is dependent on cells transduced with CD19-cTCR.

4.2.5 Freezing and thawing of transduced cells

In order to assess whether frozen stocks of CD19-cTCR transduced PBMCs could be utilised, an experiment was conducted to test if specific lysis was affected by the freeze/thawing process. Cells were frozen and stored at -70°C for nine days, then thawed and cultured overnight in complete medium-20 supplemented with IL-2. A test sample where IL-2 in the overnight culture medium was replaced with the activation antibodies anti-CD3 and -CD28 was also included. Results of a ^{51}Cr release assay are shown in Figure 4.15.

Although specific lysis of L591 cells fell slightly after freezing from 16% to 13%, in LCLs specific lysis remained steady at 21% and 20%; suggesting that storage of transduced cells is a viable option (Figure 4.15). Freeze/thawing seemed to inhibit the

ability of NK cells to lyse their K562 targets with specific lysis falling from 52% before freezing to 19% after thawing. Reactivation with anti-CD3 and -CD28 increased the specific lysis of all three targets to 31%, 39% and 78% for L591, LCL and K562 respectively. These results were consistent for an effector to target ratio of 10:1 (Figure 4.15 panel B). At an effector to target ratio of 5:1 (Figure 4.15 panel C), specific lysis was below 8% for targets L591 and LCL and all effectors except restimulated frozen cells, where it was 17% and 18% respectively. For K562, target lysis at an effector to target ratio of 5:1 was as for higher effector to target ratios, with similar levels seen with mock transduced and freshly transduced effector cells, and a reduction or increase in lysis for frozen and restimulated cells, respectively. Restimulation with anti-CD3 and -CD28 appears therefore, to enhance NK as well as T cell activity, and thus is not suitable for improving specific activity of T cells in *ex vivo* mixed cultures when NK activity is not also desired.

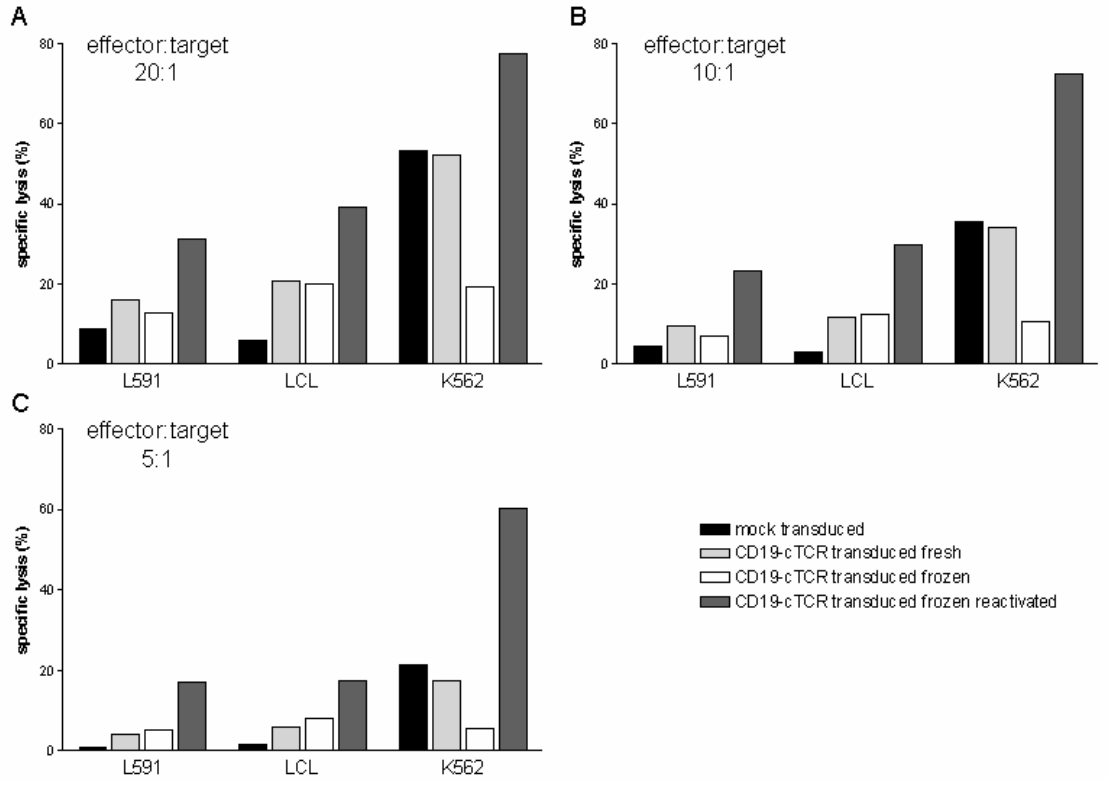

Figure 4.15: Effect of freezing and thawing of CD19-cTCR transduced PBMCs on *in vitro* cytotoxicity.
^{51}Cr release assays using mock, fresh CD19-cTCR transduced, frozen and thawed CD19-cTCR transduced, and frozen, thawed restimulated CD19-cTCR transduced PBMCs at effector to target ratios of 20:1 **(A)**, 10:1 **(B)** and 5:1 **(C)** show freeze/thawing had no effect on the L591, LCL or K562 target cell lines. Reactivation increased lysis in a non-specific manner.

4.2.6 EBV-specific CTLs

^{51}Cr release assays were performed in order to gauge the ability of EBV-specific CTLs generated from PBMCs of donors A, B and C (CTL-A, -B, -C) to lyse their respective matched targets, (HL - L591, GC - NUGC3-EBV and NPC - C666.1 [see 4.1.1]). Effector to target ratios of 20:1, 10:1 and 5:1 were used, and autologous LCLs and K562 were also employed as targets.

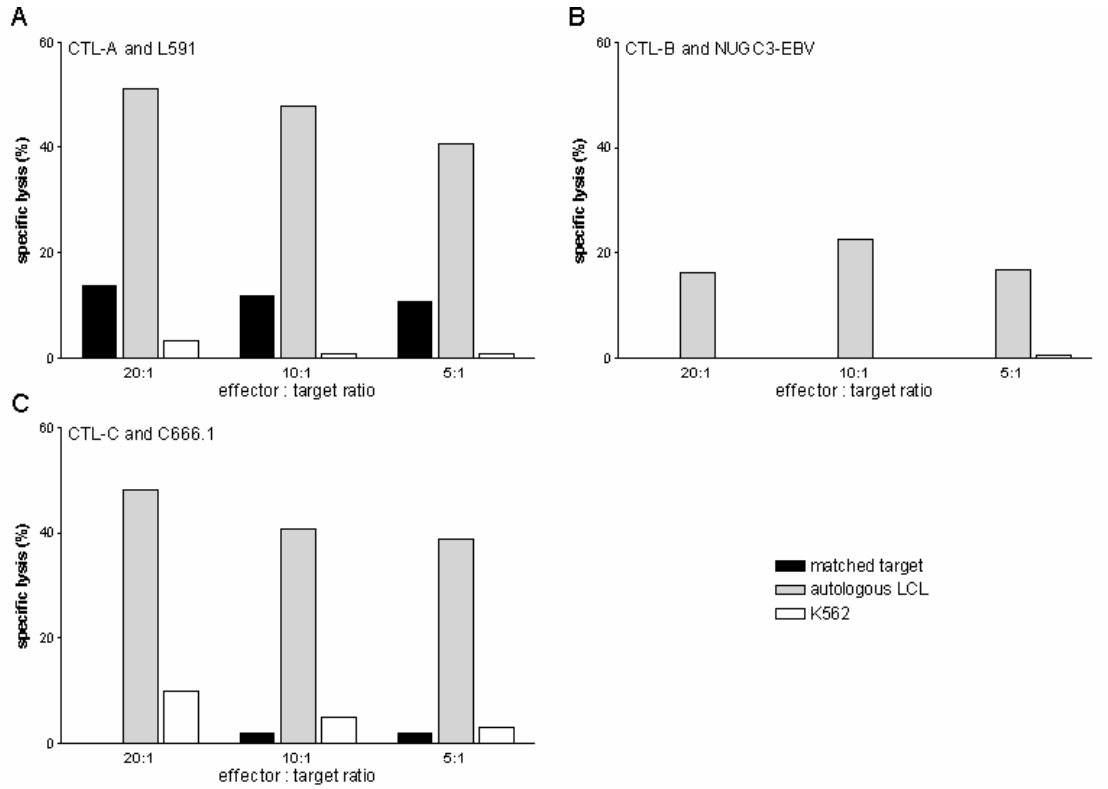

Figure 4.16: *In vitro* cytotoxicity of EBV-specific CTLs against HLA best match target cell lines.
^{51}Cr release assays with effector/target matches of donor A CTLs and L591 **(A)**, donor B CTLs and NUGC3-EBV **(B)**, and donor C CTLs and C666.1 **(C)** show specific lysis against autologous LCL for all combinations, with comparatively less **(A,C)** or no **(B)** lysis against best match EBV-associated malignancy targets.

All three CTL lines showed cytotoxicity against autologous LCLs, with specific lysis at all effector to target ratios above 40%, 16%, and 39% for CTL-A, CTL-B and CTL-C, respectively (Figure 4.16). Matched CTLs showed little or no cytotoxicity against carcinoma cell lines NUGC3-EBV and C666.1, with specific lysis not exceeding 2% at any effector to target ratio. In comparison, L591 cells were lysed by matched CTLs, with specific lysis of 14%, 12%, and 11% at effector to target

ratios of 20:1, 10:1 and 5:1, respectively. As mentioned previously (see 1.2.2.2), the restricted viral antigen expression seen in GC, HL and NPC (Table 1.3) protects tumour cells from targeting by T cells when compared with autologous EBV-infected cells expressing the full range of latent antigens, and this data supports that observation.

4.3 Immunotherapy of tumours *in vivo*

In parallel experiments, prevention of tumour formation by EBV-specific CTLs and engineered T cells was evaluated in the SCID mouse model described in Chapter 3. Two strategies were tested: a prophylactic strategy where EBV-specific CTLs were injected simultaneously with tumour cells lines, either with both tumour and therapeutic cells sc, or with tumour cells sc and therapeutic cells iv; and a treatment strategy with administration of therapeutic cells iv after sc tumour onset.

4.3.1 Prophylactic immunotherapy of SCID HL

To assess the ability of therapeutic cells to prevent tumour formation in the L591 HL *in vivo* model, three strategies were tested. Firstly, $5x10^6$ L591 cells were injected sc into three SCID mice simultaneously with $3.5x10^7$ CTL-A. Secondly, $5x10^6$ L591 cells were injected sc into six SCID mice simultaneously with $5x10^7$ PBMCs transduced with CD19-cTCR. Finally, $5x10^7$ PBMCs transduced with CD19-cTCR were injected iv into five SCID mice coincident with sc injection of $5x10^6$ L591. Time to onset and subsequent tumour growth was monitored.

Results of prophylactic therapy of SCID HL are shown in Table 4.3. Administration of CTL-A sc or CD19-cTCR transduced cells iv made no significant difference to tumour formation, with 2 of 3 (67%) CTL-A treated mice (Fisher's exact, p=1.0) and 4 of 6 (67%) iv administered CD19-cTCR treated mice (Fisher's exact, p=0.6219) developing tumours. None of 6 (0%) mice administered CD19-cTCR sc developed tumours, which was a significant effect (Fisher's exact, p=0.001). Median time to tumour in untreated mice was 20 days, compared with 29 days in iv administered CD19-cTCR treated mice, which was not a significant difference (Wilcoxon rank sum test, p=0.0625).

Table 4.3: Tumour incidence in HL SCID mice given prophylactic immunotherapy. Tumour formation following sc injection of HL L591 cells and coincident treatment with CTL-A administered sc, or CD19-cTCR transduced PBMCs administered sc or iv. [* indicates significant effect p=0.001]

treatment cells			number of tumours/		time to tumour onset (days)	
cell line	cell number	route	number of mice (%)		median	range
untreated	-	-	17 / 22	(77)	20	16-28
CTL-A	$3.5x10^7$	sc	2 / 3	(67)	27	26-28
CD19-cTCR	$5x10^7$	sc	0 / 6*	(0)	-	-
CD19-cTCR	$5x10^7$	iv	4 / 6	(67)	29	21-33

Tumour growth in untreated, sc administered CTL-A treated mice and iv administered CD19-cTCR transduced PBMC treated mice is shown in Figure 4.17. Tumours in sc administered CTL-A treated mice showed sustained growth from time of onset until termination of the experiment at day 70. Of the four iv administered CD19-cTCR transduced PBMC treated mice which developed tumours, three showed sustained tumour growth, and one had completely cleared tumour burden by day 64 post L591 injection.

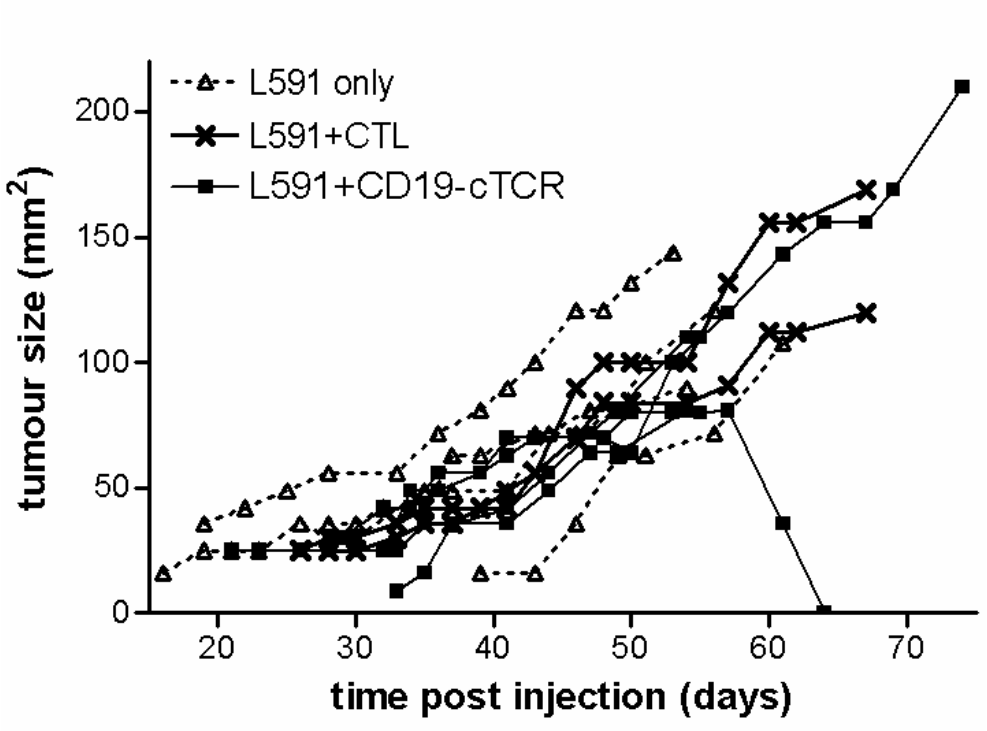

Figure 4.17: HL SCID tumour growth following prophylactic immunotherapy. Prophylactic immunotherapy with either EBV-specific CTLs or CD19-cTCR transduced PBMCs did not prevent formation of sc HL tumours in SCID mice. Each line represents an individual mouse.

4.3.2 Immunotherapy of established HL SCID tumours

The ability of PBMCs transduced with CD19-cTCR to treat established sc L591 tumours was also tested. Six tumour-bearing SCID mice were injected iv with $5x10^7$ PBMCs transduced with CD19-cTCR between three and nine days after tumour formation, and subsequent tumour growth observed (Figure 4.18).

Three mice were culled prior to the conclusion of the experiment due to tumour necrosis. These lesions displayed sustained tumour growth up to time of culling. The remaining three mice had completely cleared their tumour burden by 65, 69 and 83 days post L591 injection (Figure 4.18). This was a significant effect when compared with 17 untreated mice with established tumours from doses of $5x10^6$ and $2x10^6$ L591 cells who showed no tumour regression (Fisher's exact, p=0.011). In a time course experiment to confirm trafficking of transduced cells to tumours, five tumour-bearing SCID mice were injected iv with $5x10^7$ PBMCs transduced with a CD19-cTCR. At each of 1, 4, 7, 11, and 18 days post treatment a single mouse was culled and immunohistochemistry performed on tumour sections. An anti-CD8 antibody was used as an indirect marker to detect CD19-cTCR cells infiltrating the tumours. Infiltrating cell presence was assessed on a qualitative basis, and positively stained cells were not quantitated. CD8+ cells were seen in tumours on day 11 and 18 post treatment, but not days 1, 4 or 7 (Figure 4.19).

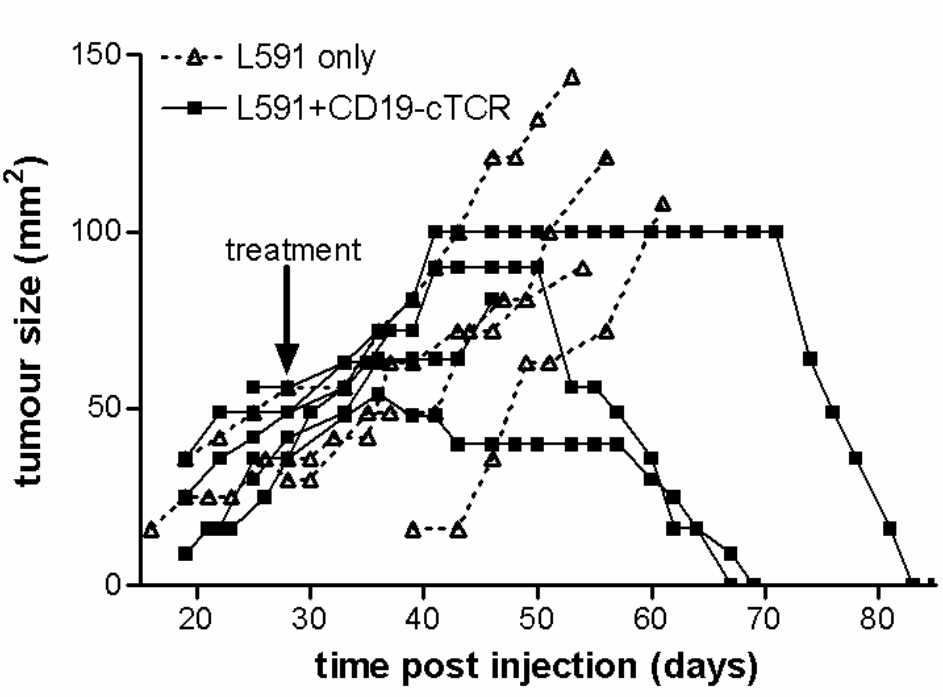

Figure 4.18: HL SCID tumour growth following immunotherapy.
Tumour growth curves of SCID mice bearing sc tumours derived from HL L591 cells treated with CD19-cTCR transduced PBMCs, showing complete regression in three of six mice. Each line represents an individual mouse.

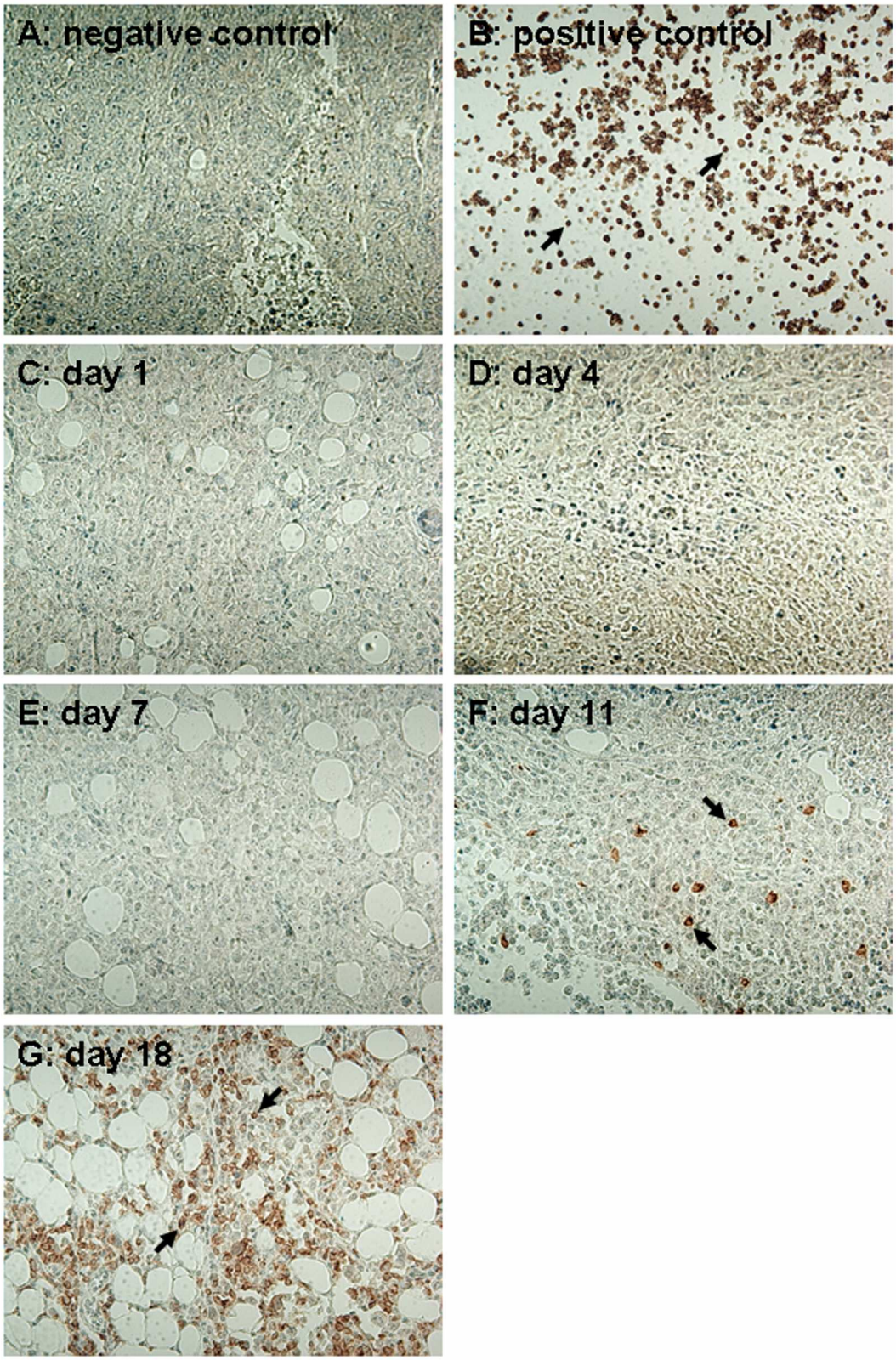

Figure 4.19: Infiltration of CD8+ T cells in HL SCID tumours.
Immunostaining showing CD8+ cells in L591 tumours treated with CD19-cTCR transduced PBMCs at days 11 **(F)** and 18 **(G)**, but not days 1 **(C)**, 4 **(D)** or 7 **(E)** post treatment. HRP detection system shows positive brown membrane staining **(B,F,G)**. Negative control was GC derived SCID tumour **(A)**. Positive control was a CTL line **(B)**. Black arrows indicate individual positive cells. Sections were counterstained with haematoxylin.

4.3.3 Prophylactic immunotherapy of SCID NPC

To assess the ability of donor C CTLs to prevent tumour formation *in vivo*, $2x10^6$ C666.1 cells were mixed with $4.5x10^7$ CTL-C and injected sc into five SCID mice. Time to tumour formation and subsequent tumour growth was observed.

Treatment with CTLs did not prevent C666.1 tumour formation as 5 of 5 (100%) mice injected developed tumours (Table 4.4). Median time to tumour in untreated mice was 19 days, compared with 13 days in treated mice, which was not a significant difference (Wilcoxon rank sum test, p=0.25). All tumours showed sustained growth from time of onset until termination of the experiment (Figure 4.20).

Table 4.4: Tumour incidence following sc inoculation of SCID mice with the NPC cell line C666.1 alone, or mixed with partially HLA matched, EBV-specific CTLs.

cell line	cell dose	CTL dose	number of tumours/ number of mice (%)	time to tumour onset (days) median	range
C666.1	$2x10^6$	-	7 / 7 (100)	19	12-24
C666.1	$2x10^6$	$4.5x10^7$	5 / 5 (100)	13	10-17

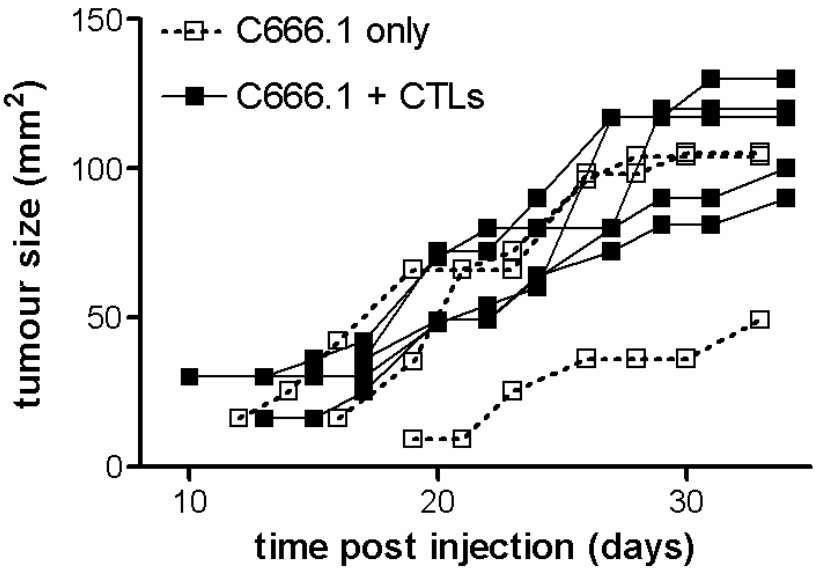

Figure 4.20: Tumour growth after prophylactic therapy of NPC SCID tumours with EBV-specific CTLs.
Tumour growth curves of sc injected C666.1 cells in SCID mice, with and without partially matched, EBV-specific CTLs. Each line represents an individual mouse.

Mice were culled at day 34 post injection and immunohistochemistry performed on tumour sections. An anti-CD8 antibody was used as a direct marker of tumour infiltrating CTLs. Infiltrating cell presence was assessed on a qualitative basis, and positively stained cells were not quantitated. In 5 of 5 treated mice (100%), but 0 of 3 untreated mice (0%), CD8+ cells were present in the tumour (Figure 4.21).

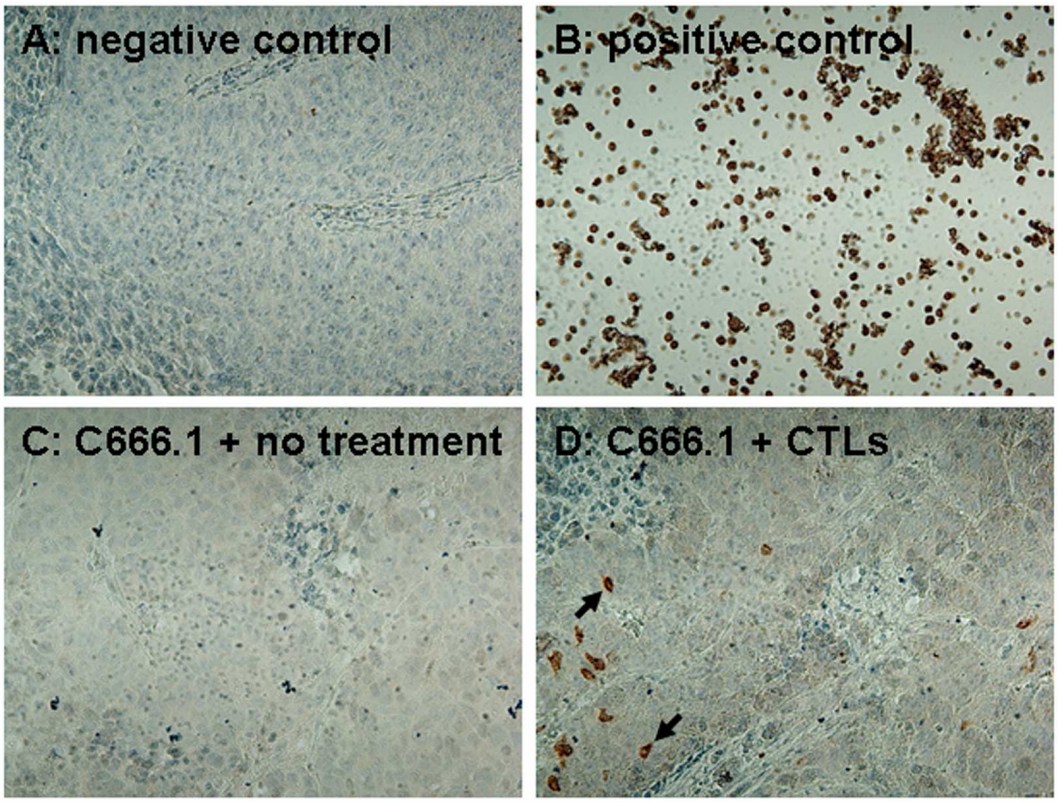

Figure 4.21: Infiltration of CD8+ cells in NPC SCID tumours.
Immunostaining showing CD8+ cells in C666.1 tumours treated with partially HLA matched, EBV-specific CTLs **(D)**, which are not present in untreated tumours **(C)**. HRP detection system shows positive brown membrane staining **(B,D)**. Negative control is GC derived SCID tumour **(A)**. Positive control is a CTL line **(B)**. Sections were counterstained with haematoxylin.

4.4 Summary of results

- Activated PBMCs were transduced with a retroviral vector encoding a cTCR specific for CD19. Mean transduction rate was 13%±6%, with a range of 6-20%.
- Optimum transgene expression levels were achieved between 9 and 11 days post transduction.

- 48-60% of cells in CD19-cTCR transduced cultures were CD8+ T cells, with 34-44% of the population CD4+ T cells. CD56+ NK cells made up 10-18% of the total culture.
- Transduced T cells were able to kill CD19+ L591 and LCLs at a significantly higher rate than mock transduced T cells.
- The CD56+ NK cell fraction within the transduced population was responsible for high levels of lysis of the CD19- L1236 and K562 target cells when both transduced and mock transduced effector cells were used.
- CD34-enrichment of transduced cells enhanced specific lysis of L591 and LCL target cells, but not K562 target cells.
- Freezing had a minimal effect on the ability of transduced cells to lyse L591 and LCL target cells.
- Reactivation of transduced cells improved lysis of L591 and LCL target cells, as well as lysis of K562 target cells.
- EBV-specific HLA matched CTL lines lysed autologous LCLs and the HL cell line L591, but not the GC cell line NUGC3-EBV or the NPC cell line C666.1.
- HLA matched CTLs administered sc or CD19-cTCR transduced cells administered iv did not significantly halt sc outgrowth of L591 cells in SCID mice.
- CD19-cTCR transduced cells administered sc were able to completely prevent L591 tumour formation in SCID mice, which was a significant treatment effect ($p=0.001$).
- CD19-cTCR transduced cells administered iv to SCID mice with established sc L591 tumours were able to mediate complete tumour regression in 50% of cases, which was a significant treatment effect ($p=0.011$).
- HLA matched CTLs administered sc did not prevent tumour formation in SCID mice injected with C666.1 cells.
- CD19-cTCR transduced T cells in L591 injected mice and EBV-specific CTLs in C666.1 injected mice were able to traffic to the tumours.

4.5 Discussion

In addition to the HL cell killing observed in the current project, CD19-specific cTCR expressing T cells have shown cytotoxic potential against B cell NHL, B-CLL and B-ALL (Brentjens *et al*, 2003; Cooper *et al*, 2003; Cheadle *et al*, 2005). In contrast to B cell NHL, expression of CD19 is not consistently observed in HL, although a variable percentage of classical HL biopsies (0 to 75%) and cell lines (20 to 30%) express the marker (Herbst *et al*, 1989; Schmid *et al*, 1991; Drexler, 1992; Drexler, 1993). Thus, a proportion of HL patients are eligible for treatment with CD19-specific therapies. This project demonstrated that activated PBMCs transduced with a retroviral vector express a cTCR specific for CD19, are capable of specific lysis of CD19+ target cells in an *in vitro* cytotoxicity assay, and can mediate tumour regression in an *in vivo* model of HL.

It has been reported previously that transgene expression in therapeutic T cells decreases after 10 to 14 days *in vitro* culture (Eshhar *et al*, 2001). Transgene expression levels were measured for 11 days post transduction, and peak expression was not seen immediately following transduction, but instead increased steadily over the first nine days and then remained relatively stable on days 10 and 11 when the experiment was terminated (Figure 4.5). This indicates that there may be a window of opportunity for therapeutic use of such cells, when transgene expression is at its height. An additional consideration when planning treatment using therapeutic cells is the time required to expand cells *in vitro* in order to obtain sufficient numbers for therapeutic use. Delayed treatment resulting from the initial use of conventional therapy may reduce impact of the therapeutic cells in some cases. Thus, in order to best meet requirements for large numbers of cells available on demand, the ability of therapeutic cells to withstand storage at -70°C with their cytotoxic potential intact was tested. The freeze/thawing process had minimal effect on the ability of transduced cells to lyse CD19+ target cells (Figure 4.15), and thus it may be possible to either store a patient's own cells that have been transduced and expanded against possible need, or create a bank of allogeneic therapeutic cells available on a best HLA match basis (to prevent host killing of the therapeutic cells).

Levels of retrovirus transduction varied between 6-20%, with a mean 13%±6% cells expressing CD34 as a marker of transduction (Figure 4.4). This was slightly lower

than the mean 27%±12% (range 12-43%) transduction rates reported by our collaborators using the same virus construct (Cheadle *et al*, 2005). However, fresh virus was made for each transduction experiment, and although every effort was made to standardise virus production techniques, titrations were not routinely performed. It is therefore possible that the disparity in transduction rates was partly a result of variations in virus concentration.

Increasing the fraction of transduced cells in the total population by selection with anti-CD34 coated magnetic beads improved levels of specific lysis (Figure 4.14), however it was not a simple relationship between number of CD34+ cells and level of specific lysis. Others have also observed that levels of T cell transduction do not correlate with absolute levels of target cell lysis (Cheadle *et al*, 2005). It may not be necessary to achieve expression of the cTCR on as many as the 82% of cells seen after CD34 selection (Figure 4.13), and optimisation to improve transduction rates may suffice. The bearing of low transduction rates and specific lysis in ^{51}Cr release assays on the *in vivo* effect of engineered cells is unclear. A recent trial using EBV-specific CTLs to treat PTLD showed no correlation between levels of specific lysis as measured by ^{51}Cr release assays and tumour response (Haque *et al*, 2007). Equally, such a correlation was not observed in experiments investigating CTL treatment in SCID models of PTLD (personal communication, Dr Ingolfur Johannessen). It remains to be seen if the weighted importance of *in vitro* results is maintained when the therapeutic cells are directed against a single epitope via a cTCR compared with the multiple specificities of the CTLs used in previous trials.

As reactivation has been shown to counteract the loss of transgene expression over time during *in vitro* culture (Eshhar *et al*, 2001), thawed cells were reactivated with anti-CD3 (to provide activation signal 1) and anti-CD28 (signal 2) antibodies to offset the potential detrimental effect of freeze/thawing on cTCR expression. Reactivation improved levels of specific lysis above and beyond those seen with unfrozen effector cells for both L591 and LCL target cells (Figure 4.15). Therefore, incubation of therapeutic cells with anti-CD3 and anti-CD28 antibodies immediately prior to administration may improve anti-tumour effects. Additionally, as similar increases in lysis were also seen for the K562 NK target cell line, NK cells may need to be removed prior to reactivation.

Much work has been done to discover the optimum combination of activation and stimulation signals for T cells in order to enhance their cytotoxic effect. Culture medium for CTLs is generally supplemented with IL-2 for T cell survival and proliferation (Morgan *et al*, 1976; Miyazaki *et al*, 1995), but other cytokines have been used both individually and in combination to achieve peak T cell activation and proliferation, including IL-7, IL-15 and IL-21 (Schluns *et al*, 2000; Brentjens *et al*, 2003; Zeng *et al*, 2005). Where CTLs have been engineered to express cTCRs, other techniques to enhance T cell activation have also been tested, such as restimulation of engineered cells through their endogenous TCR. This has applications not only when tumour cells express both the cTCR target (TAA) and the native TCR target (viral antigen) (Savoldo *et al*, 2007), but also where engineered APC presenting the native TCR target can be co-administered with the therapeutic T cells (Cooper *et al*, 2005). As the exact rules governing signal propagation through cTCRs have not yet been fully deciphered, additional attention has been given to providing improved signal 1 and 2 transduction from within the cTCR itself. Addition of lck tyrosine kinase or OX40 signalling domains to cTCR constructs already containing CD28 and ζ moieties did not compromise the effector function of engineered cells, and may improve long term proliferation and activation of engineered T cells (Geiger *et al*, 2001; Pule *et al*, 2005).

The persistence and proliferation of engineered T cells *in vivo* is advantageous in cellular immunotherapy. Therapeutic cells should ideally have immediate effect in reducing tumour burden and also be able to localise to metastatic cells and protect against disease relapse. The conditions used to activate T cells are crucial in determining therapeutic outcome (Brentjens *et al*, 2003). Until the optimum culture environment for engineered T cells is established, an alternative approach entails *in vivo* proliferation of administered T cells rather than reliance on *ex vivo* expansion. For the treatment of cancer, administration of an excess of therapeutic cells risks tumour lysis syndrome, which results from the rapid destruction of malignant cells and consequent release of intracellular ions, nucleic acids, proteins and their metabolites into the extracellular space, overwhelming the body's normal homeostatic mechanisms and potentially leading to life-threatening complications such as renal failure, arrhythmias, and seizures. In contrast, a paucity of transferred cells risks inadequate clinical response. Cells capable of expanding in the patient to

meet individual need are therefore a major asset. Such *in vivo* expansion may also clarify why tumours in the SCID treatment model continued to increase in size for up to 10 days after infusion of engineered cells before beginning to regress (Figure 4.18), and why CD8+ T cells were not detectable in tumours by immunostaining until day 11 post infusion (Figure 4.19). Although the engineered cells used to treat established SCID tumours had the highest transduction levels seen during this project, the transduced cells still needed to traffic to the tumour site and expand before reaching sufficient numbers to effect a clinical response. Cells engineered with a CD19-specific cTCR were able to effect complete tumour regression in 50% of SCID mice carrying an established HL tumour, a significant treatment effect ($p=0.011$) (Figure 4.18). The animals which did not respond to treatment were culled due to necrosis of the skin at the tumour site, as opposed to excessive tumour growth. It is possible that a more rapid treatment effect may avoid this complication. Delays in tumour regression have been observed in other cellular therapy models. During experiments in which *Rag*$^{-/-}$ mice (targeted mutations of the recombination-activating genes result in mice with complete ablation of functional T and B cells) bearing murine thymomas engineered to express the influenza epitope NP(366-374) were treated with NP(366-374)-specific engineered T cells, tumour growth continued for an average of eight days following T cell administration before initiation of regression (Kessels *et al*, 2001). Increasing the number of transduced cells, either by improving transduction rates or manually enriching transduced cells based on a selectable marker may produce a more immediate effect. This could in turn improve overall treatment responses in the SCID HL model.

Immunophenotyping of activated PBMC cultures following transduction with a CD19-cTCR revealed a population of predominately CD8+ T cells (mean 57%±6%), with CD4+ T cells contributing the next largest fraction (39%±4%) (Figure 4.6). Addition of IL-2 to the culture medium, which is standard procedure for *in vitro* culture of T cells, does tend to favour the establishment of majority CD8+ CTL lines (Wilkie *et al*, 2004). B cells constituted less than 1% of the total population. A substantial fraction of NK cells was also detected in all cultures tested, averaging 14%±4% of the total population. This is consistent with CTL lines at early time points in their development into specific effectors (Vanhoutte, 2006). High levels of K562 lysis mediated by NK cells has also been seen in PBMCs transduced with an

unmodified LMP2-specific TCR (Orentas *et al*, 2001). For patient use, CTL expansion *in vitro* involves multiple rounds of antigenic stimulation, which increases cell line specificity but also has the effect of substantially decreasing the NK fraction (Wilkie *et al*, 2004; Comoli *et al*, 2005; Straathof *et al*, 2005a). It has also been shown previously that transduction does not alter the CD3, CD4, CD8 or CD56 immunophenotype of CTL lines (Savoldo *et al*, 2007).

The presence of NK cells in the therapeutic cell cultures is interesting in light of their involvement in the lysis of the HL L1236 cell line in ^{51}Cr release assays (Figure 4.12). As mentioned previously, the L1236 cell line has been definitively identified as derived from EBV-negative HRS cells (Kanzler *et al*, 1996a). However, in their native HL environment HRS cells utilise a number of mechanisms to avoid killing by NK cells. The extensive inflammatory infiltrate characteristic of classical HL consists primarily of Th2 and T regulatory cells (T_{regs}) and is generally devoid of Th1 cells, CD8+ T cells and NK cells (Poppema, 2005). HRS cells appear to maintain this composition by the secretion of Th2 type chemokines such as the thymus and activation regulated chemokine (TARC) (van den Berg *et al*, 1999), as well as cytokines that inhibit Th1 responses for example IL-10 (Herbst *et al*, 1996), leading to a decreased anti-tumour immune response. An association between areas in the HLA class I region of the genome and EBV-positive HL suggests polymorphisms in this area may affect proper EBV peptide presentation to CD8+ T cells facilitating immune escape (Diepstra *et al*, 2005). HRS cells in EBV-negative HL can lose HLA class I expression, thus escaping CTL detection but potentially becoming NK targets. However, expression of HLA-G in HL has been associated with EBV-negative, MHC class I-negative status (Poppema, 2005), and HLA-G expression has been implicated in evasion of CTL- and NK cell-mediated cytotoxicity (Carosella *et al*, 2003). L1236 was derived from a patient with EBV-negative HL, and FACS analysis indicates surface expression of HLA class I (Wolf *et al*, 1996). Thus, NK-mediated killing occurs through an alternative mechanism, possibly indicating a role for NK cells in cellular immunotherapy of HL. Although NK cells are inhibited by self-HLA molecules, they hold cytotoxic potential for cancer cells (Ruggeri *et al*, 2002), and NK cells expressing cTCRs are capable of specific lysis of leukaemia cells *in vitro* (Imai *et al*, 2005).

In conclusion, the results presented in this chapter showing the ability of CD19-cTCR engineered T cells to specifically lyse CD19+ HL target cells supports the central hypothesis of this thesis, and is in line with the data of others in the field (Brentjens *et al*, 2003; Cooper *et al*, 2003; Cheadle *et al*, 2005). Given these encouraging results, it is to be hoped that phase I trials of CD19-cTCR engineered T cells will soon commence, with a view to CD19-cTCR engineered T cells becoming a future treatment option for CD19+ leukaemia and lymphoma patients who relapse or are refractory to conventional therapies.

5 Identification of LMP2-Specific scFv Using Phage Display

In Chapter 4, T cells were redirected against HL cells with a cTCR specific for the B cell marker CD19. Due to the modular nature of cTCR construction, the CD19-specific scFv could potentially be replaced with a scFv specific for any cell surface antigen. To utilise this feature, a scFv specific for LMP2 was required, as the EBV latent protein was selected as a suitable target for redirecting T cells to EBV-associated malignancies. Antibody phage display technology was chosen as the method by which to isolate this LMP2-specific scFv. Phage libraries displaying antibody fragments have been used to select scFv or Fab specific for a range of targets. Indeed, a TNFα-specific antibody derived from a fragment isolated by phage display has been approved for use in autoimmune arthritis (Hoogenboom, 2005). Therefore, scFv specific for the extracellular peptide loops of LMP2 (Figure 1.5) were sought for the creation of an LMP2-specific cTCR to direct T cells against EBV-associated malignancies. Initially, selections were performed using the Tomlinson I+J human single fold scFv phage library, although later experiments employed the ETH2Gold scFv and RotMar Fab libraries.

5.1 Standardisation experiments

5.1.1 Library characterisation

Initially, frozen aliquots of the Tomlinson I+J libraries (Geneservices) were thawed and amplified to create working stocks. To confirm the presence of full length scFv inserts, 10 clones from each library were screened using PCR. Agarose gel electrophoresis of the PCR products is shown in Figure 5.1.

For Library I, three reactions amplified no product and the remaining seven of 10 reactions amplified full length inserts, with bands of the expected 935 bp size. For Library J, one reaction amplified no product and the remaining nine of 10 reactions

amplified full length inserts. There were no reactions which resulted in bands of 329 bp, the size of PCR product amplified from clones lacking a scFv insert.

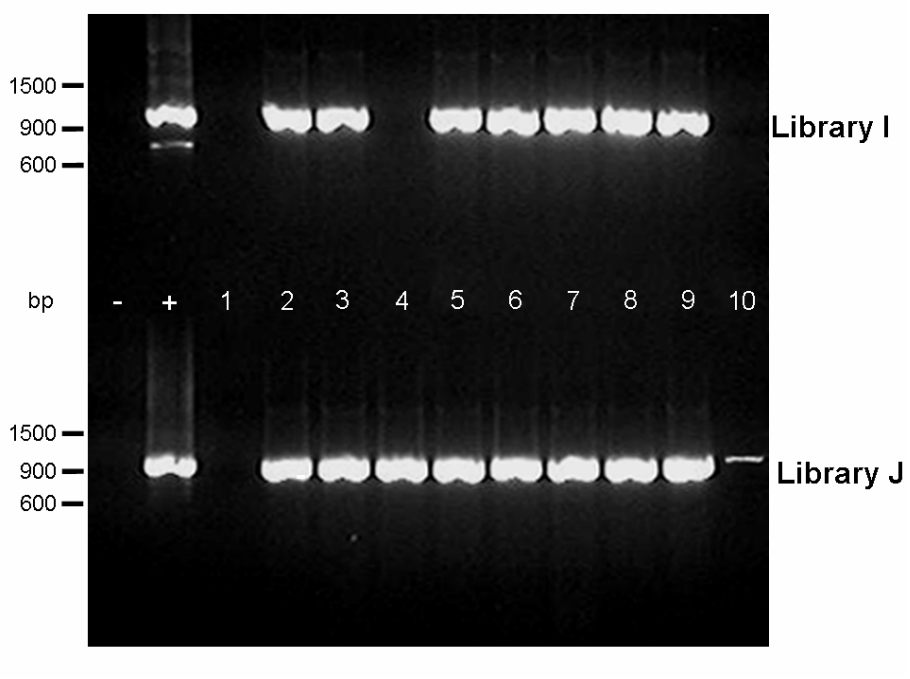

Figure 5.1: scFv inserts in Libraries I+J.
PCR screening of Library I and Library J clones (clones **1-10** in lanes 1-10) showed all clones which amplified products were of the expected 935bp full length size. No product was amplified from the no template control **(-)**. Positive control was unselected library phage **(+)**.

5.1.2 Selections with control phage

Next, test selections using controls supplied with the Tomlinson I+J libraries were carried out to ensure the phage display technology worked in our hands. Controls were TG1 bacteria infected with a polyclonal phage population which had been subjected to one round of selection against either BSA or ubiquitin by the supplier. Phage was made from the control aliquots, and a second round of selection performed using 100µg/ml BSA or ubiquitin as target. Polyclonal phage ELISA was used to assess enrichment of specific phage.

Both BSA and ubiquitin selections showed enrichment of specific phage (Figure 5.2). Absorbance (A) increased by at least two-fold in both populations, as was expected

from the supplier's instructions. There was minimal binding of phage to the non-selection antigen.

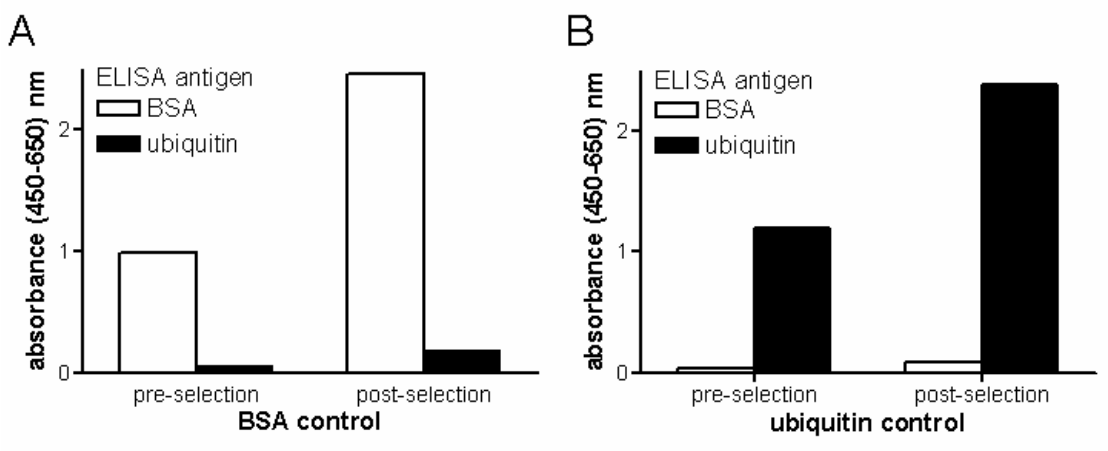

Figure 5.2: Selection with control phage.
Polyclonal ELISA analysis of one round of phage selection using previously selected phage controls for BSA **(A)** and ubiquitin **(B)**.

5.1.3 Selection with control targets

Test selection using a target protein (BSA) and peptide (c-myc) to which monoclonal antibodies have been produced (Apple *et al*, 1984; Evan *et al*, 1985) were also performed to verify that the unselected libraries could be enriched for specific clones. BSA and c-myc at 100µg/ml were used for three rounds of selection with Library J, with a polyclonal ELISA for assessment of specific phage enrichment.

For selection with BSA, after three rounds of panning a polyclonal ELISA showed the absorbance of phage bound to BSA was almost three-fold higher than the absorbance of the same phage population bound to the control antigen (Figure 5.3). There was also an enrichment of binders for c-myc, with absorbance increasing over the three rounds from 0.36 to 1.57. However, there was also a concomitant increase of phage binding to the control antigen, with a rise in absorbance from 0.15 in round 1 to 1.30 in round 3. Phage titres between the two selections were comparable, with no increase in phage output compared to controls (Table 5.1). Therefore, Tomlinson J could be enriched for clones specific for BSA but not c-myc.

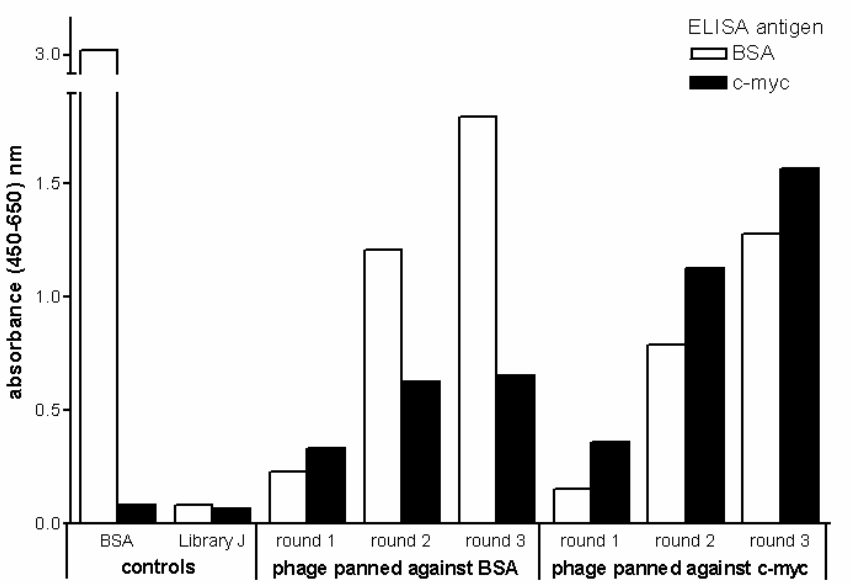

Figure 5.3: Library J selection using BSA and c-myc as targets. Polyclonal ELISA analysis of three rounds of Library J phage selection using BSA and c-myc as targets. ELISA controls are BSA specific phage and unselected Library J phage.

Table 5.1: Phage titres of Library J selection using BSA and c-myc as targets.

target	round	phage titre		
		input	output	control
BSA	1	$1x10^{13}$	$2.1x10^{7}$	$9.1x10^{6}$
	2	$1.1x10^{10}$	$1.5x10^{8}$	$1.6x10^{8}$
	3	$1.9x10^{10}$	$6.8x10^{9}$	$9.2x10^{9}$
c-myc	1	$1x10^{13}$	$6.2x10^{6}$	$9.1x10^{6}$
	2	$1.5x10^{10}$	$6.4x10^{7}$	$1.4x10^{8}$
	3	$1.6x10^{10}$	$4.4x10^{9}$	$4.8x10^{9}$

5.2 Panning the libraries

5.2.1 Target peptides

In order to identify target LMP2 peptides, the Swiss-Prot database at the Swiss Institute of Bioinformatics was searched (www.expasy.org). Input of LMP2 as the

keyword yielded sequence from Epstein Barr virus strain B95-8 (entry name: LMP2_EBV; primary accession number: P13285; reference: Baer *et al*, 1984). The feature aligner tool in Swiss-Prot gave six potential extracellular domains. These were compared with published sequence annotated with potential transmembrane domains (Sample *et al*, 1989). One extracellular sequence of four aa was discarded as too short to use for phage selection, as antibody epitopes are generally five to eight aa. The remaining five sequences were used to synthesise the peptides shown in Table 5.2 and indicated in Figure 1.5. To create the biotinylated (designated b) and biotinylated cyclised (designated bc) peptides, sequences were lengthened by three to six aa using the flanking protein sequences.

Table 5.2: Target peptides for phage library selections.
Peptides used as targets for phage library selections, together with label, configuration, sequence, length, and aa position in the LMP2 protein sequence from EBV B95-8 (Baer *et al*, 1984). [* designates point of cyclisation]

label	configuration and sequence	length	aa position
2.1	SCFTASVS	8	142-149
b2.1	biotin-ßAlaßAla-AASCFTASVSTV	12	140-151
bc2.1	biotin-ßAlaßAla-Q*AASCFTASVSTVK*	14	140-151
2.2	RIEDPPFNS	9	199-207
b2.2	biotin-ßAlaßAla-TWRIEDPPFNSLL	13	197-209
bc2.2	biotin-ßAlaßAla-Q*TWRIEDPPFNSLLK*	15	197-209
2.3	DAVLQLSP	8	260-267
b2.3	biotin-ßAlaßAla-IVDAVLQLSPL	11	258-268
bc2.3	biotin-ßAlaßAla-Q*IVDAVLQLSPLK*	13	258-268
2.5	SILQTNFKSLSSTEFIPN	18	374-391
b2.5	biotin-ßAlaßAla-SILQTNFKSLSSTEFIPN	18	374-391
bc2.5	biotin-ßAlaßAla-Q*SILQTNFKSLSSTEFIPNK*	20	374-391
2.6	SNTLLSA	7	444-450
b2.6	biotin-ßAlaßAla-VMSNTLLSAWI	11	442-452
bc2.6	biotin-ßAlaßAla-Q*VMSNTLLSAWIK*	13	442-452

5.2.2 Selections using unmodified peptides

Using the peptide panel (Table 5.2), two pools of unmodified peptides were used for the selection of Library I and Library J in parallel. Pool 1 contained peptides 2.1, 2.2 and 2.3, while pool 2 contained peptides 2.5 and 2.6. Three rounds of selection were

performed, with peptides at a final concentration of 100µg/ml. Polyclonal phage ELISA was used for assessment of specific phage enrichment, and monoclonal phage ELISA was used for screening of individual clone specificity.

Phage panned on pool 1 but not pool 2 showed a slight enrichment of binders by polyclonal ELISA (A=0.62) (Figure 5.4). However, this enrichment did not appear to be specific for the peptides as phage also bound to BSA (A=0.42). Phage titres for neither pool showed any increase in phage output compared to control (Table 5.3).

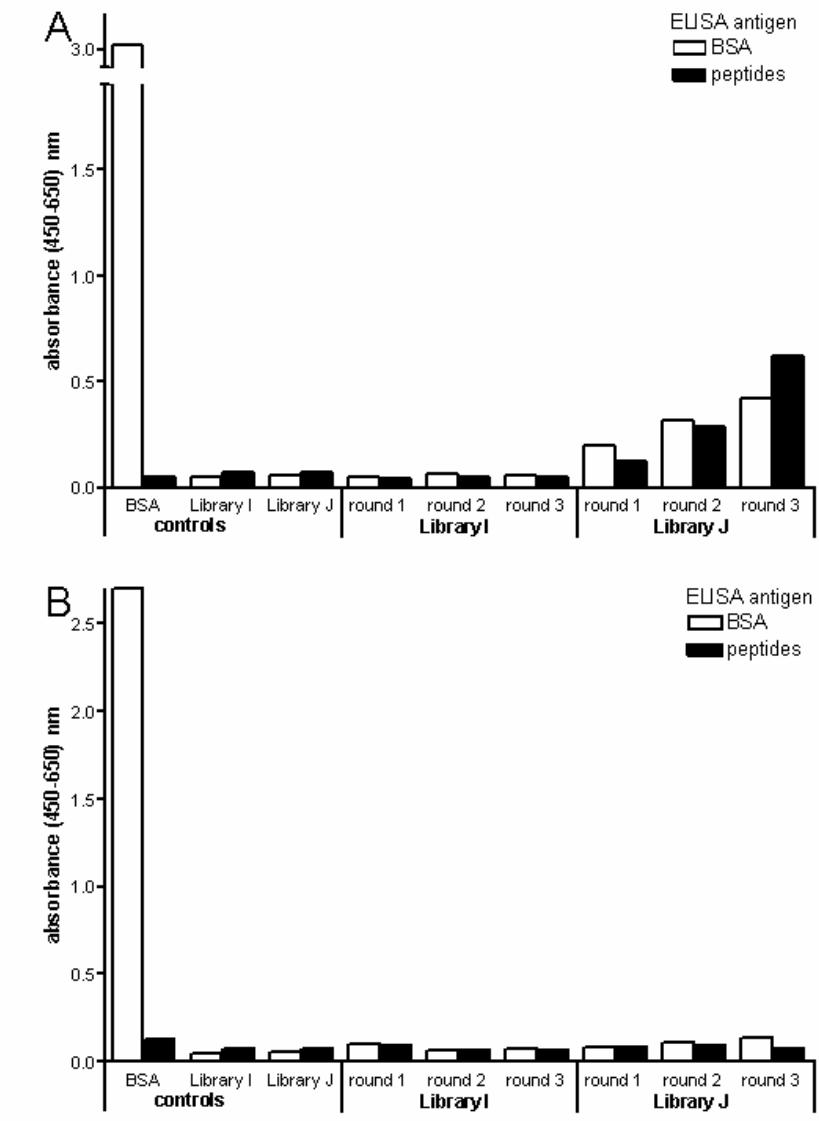

Figure 5.4: Library I and J selections using pools of unmodified peptides as targets.
Polyclonal phage ELISA analysis of three rounds of Library I and J selection using peptide pools of 2.1, 2.2 and 2.3 **(A)** or 2.5 and 2.6 **(B)** as targets. ELISA controls are BSA specific phage and unselected Library phage.

Table 5.3: Phage titres of Library I and J selections using pools of unmodified peptides.

targets	Library	round	phage titre		Library	round	phage titre	
			input	output			input	output
2.1, 2.2, 2.3	I	1	$1x10^{13}$	$5.6x10^{5}$	J	1	$1x10^{13}$	$1.5x10^{6}$
		2	$1.1x10^{10}$	$7x10^{8}$		2	$1.3x10^{10}$	$4.9x10^{8}$
		3	$1.1x10^{10}$	$3.3x10^{8}$		3	$2x10^{10}$	$1.8x10^{9}$
2.5, 2.6	I	1	$1x10^{13}$	$5.6x10^{5}$	J	1	$1x10^{13}$	$3.8x10^{6}$
		2	$1.x10^{10}$	$2.1x10^{8}$		2	$7.2x10^{9}$	$3.1x10^{8}$
		3	$1.3x10^{10}$	$5.4x10^{8}$		3	$4.8x10^{9}$	$6.8x10^{6}$

Monoclonal ELISA screening was performed on 80 round three output clones from each of the four selections. This yielded two clones with higher absorbance on target peptide compared with BSA. Clone G11 was from pool 1 and Library J selection, with absorbances of 2.13 on the peptides and 1.49 on BSA. Clone H10 was from pool 2 and Library J selection, with absorbances of 0.33 on the peptides and 0.16 on BSA. These clones were rescued, and their specificity tested by phage ELISA using BSA, ubiquitin, individual peptides and human serum as targets (Figure 5.5).

Clone G11 bound to all targets tested with absorbances greater than 2.0, except for BSA, against which it had an absorbance of 1.5 (Figure 5.5 panel B). On the individual antigens, clone H10 bound most strongly to peptide 2.5 (A=0.87), although it bound more strongly still to human sera (A=1.26) (Figure 5.5 panel C). The BSA positive control bound only to BSA of the individual antigens (A=2.77), although it did also bind though less strongly to human sera (A=1.12). Therefore neither clone H10 nor clone G11 was specific for any LMP2 peptide.

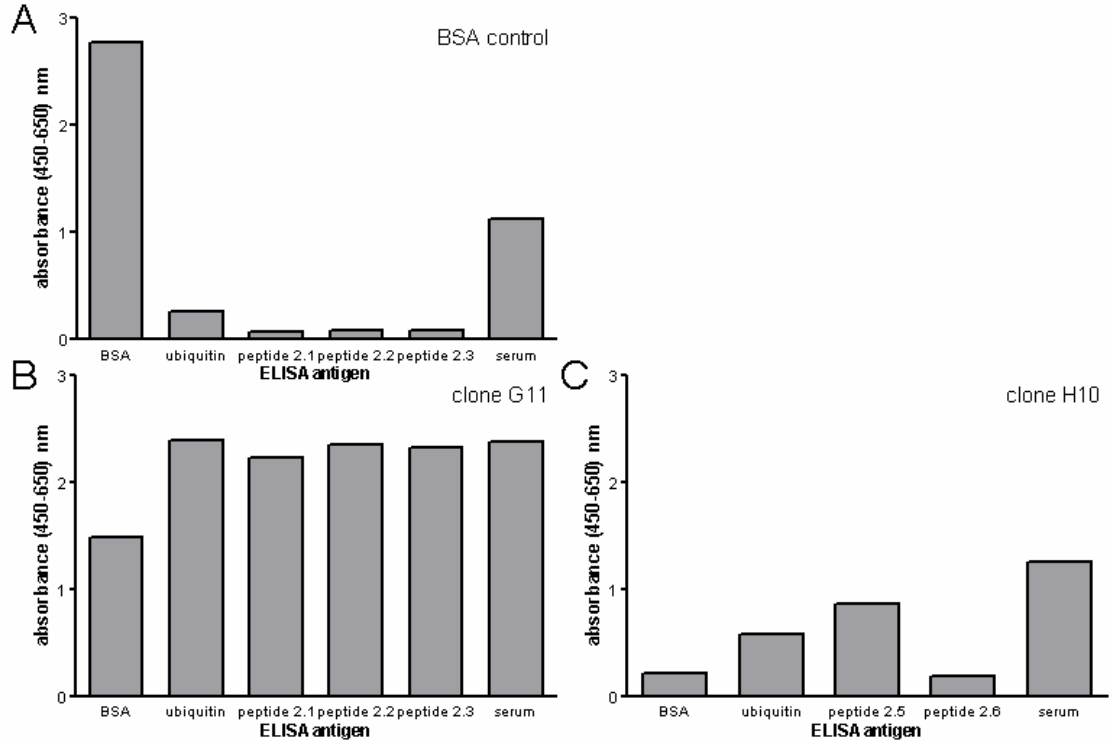

Figure 5.5: Specificity testing of clones from Library I and J selections using unmodified peptide pools.
BSA control **(A)**, and two clones from the third round of Library J phage selection using pools of peptides 2.1, 2.2 and 2.3 **(B)** or 2.5 and 2.6 **(C)** as target antigens.

5.2.3 Selections using biotinylated peptides

To make peptides more available to phage during the panning process, sequences were lengthened slightly and biotinylated (Table 5.1). The biotin tag would adhere to streptavidin or avidin pre-coated immunotubes, leaving peptides free for phage binding. Immunotubes were coated with 500ng/ml streptavidin or avidin, and 100µg/ml biotinylated peptide bound to this. Individual peptides b2.1, b2.2, b2.3, and b2.5 (Table 5.2) were used for three rounds of selection of Library I and Library J in parallel. Polyclonal phage ELISA was used for assessment of specific phage enrichment, and monoclonal phage ELISA for screening of individual clone specificity. A polyclonal phage population binding, but not specific, to streptavidin

was used as a positive control for ELISAs with streptavidin. Selections in this section were performed by Mr Matthew Seah (University of Edinburgh).

Selection experiments using Library I and Library J and peptides b2.1 and b2.2 showed enrichment of binders in a non-peptide-specific manner (Figure 5.6). After three rounds of selection, similar levels of absorbance were seen for phage binding to streptavidin and peptide (target), compared with streptavidin alone (control): Library I selected on peptide b2.1 - target A=1.91, control A=1.85; J+b2.1 - target A=1.20, control A=1.14; I+b2.2 - target A=2.37, control A=2.23; J+b2.2 - target A=1.84, control A=1.65. Peptide b2.3 also showed non-peptide-specific enrichment with Library I by round 3 (target A=2.65, control A=2.65), but no increase in binders with Library J. Peptide b2.5 showed no increase in binders with Library J. By round three with Library I, peptide b2.5 appears to have a substantial increase in specific peptide binders (target A=2.50, control A=0.10); however in this ELISA the no phage (A=1.45) and unselected Library I (A=1.12) also appeared reactive with the target peptides.

Monoclonal phage ELISA analysis was performed on the round three outputs shown in Figure 5.6. Results from the Library I and b2.5 screenings, which are representative of those seen for all library/peptide combinations, are shown in Figure 5.7. Target peptides b2.1, b2.2, b2.3, and b2.5 had 47, 80, 44 and 51 clones respectively positive for target binding in the screen, however all clones also bound to streptavidin alone. Therefore, no clone specific for biotinylated, linear LMP2 peptides was isolated from the Tomlinson I and J libraries.

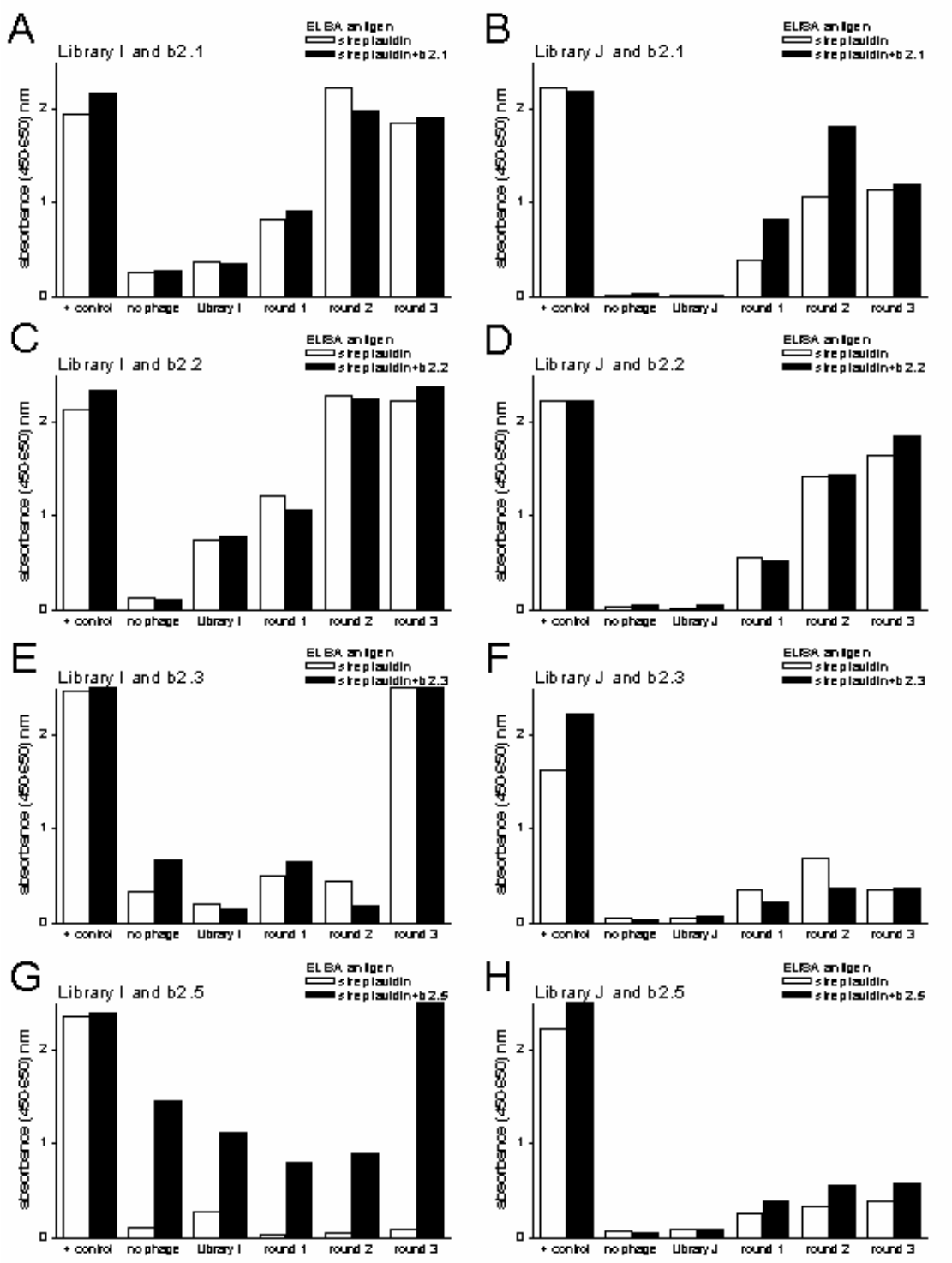

Figure 5.6: Library selection using biotinylated, linear peptides.
Polyclonal ELISA analysis of three rounds of Library I and J selection using biotinylated, linear peptides 2.1 **(A,B)**, 2.2 **(C,D)**, 2.3 **(E,F)** and 2.5 **(G,H)** as targets.

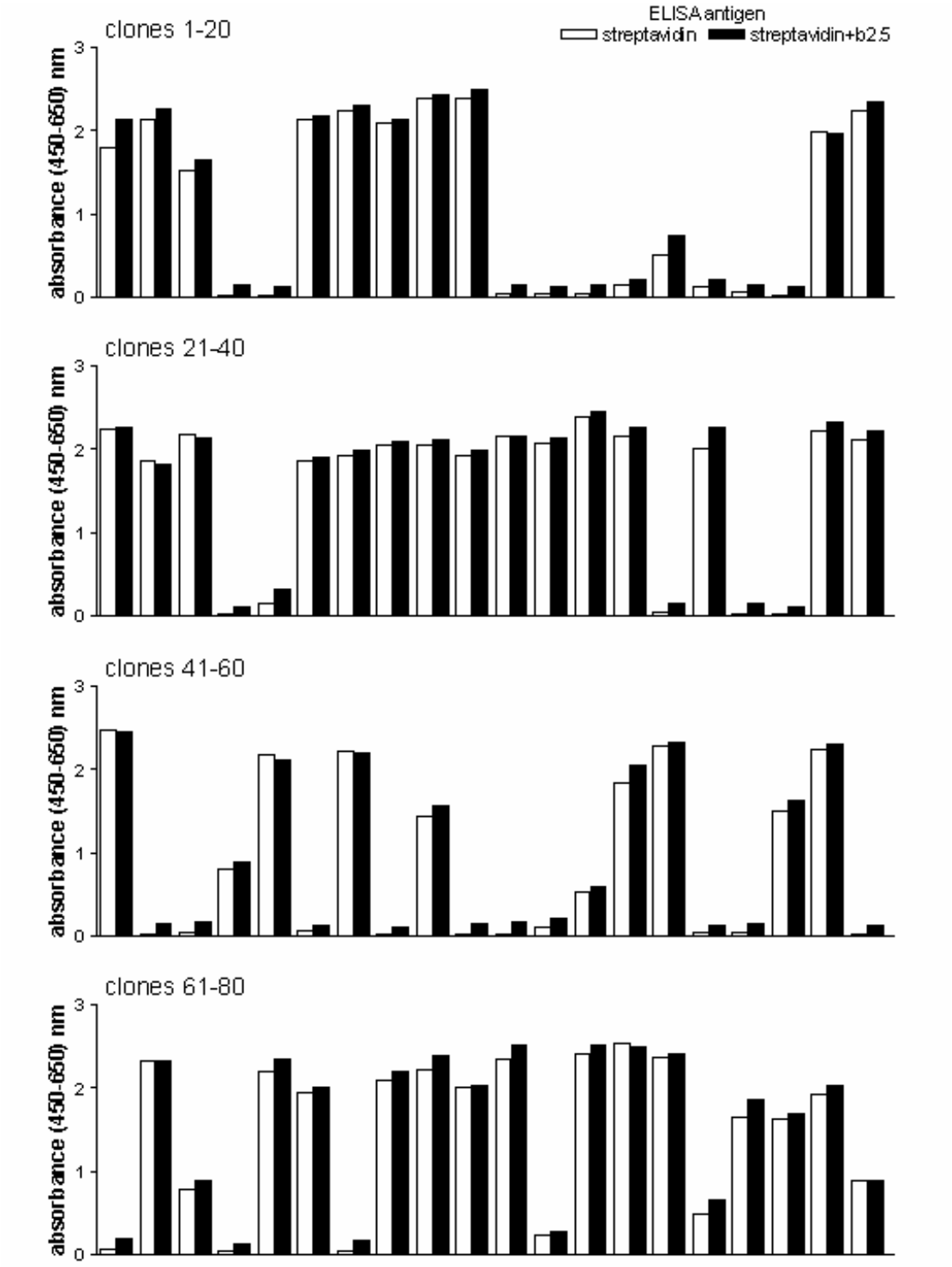

Figure 5.7: Screening of clones from selections using biotinylated, linear peptides.
Monoclonal ELISA screening of 80 clones from the third round output of Library I selection using biotinylated linear peptide b2.5 as a target.

5.2.4 Selections using biotinylated cyclised peptides

As the extracellular sequences of LMP2 in their natural configuration will be looped to allow insertion of the flanking domains into the cell membrane, the biotinylated peptides were cyclised in an effort to mimic this conformation. Individual peptides bc2.1, bc2.2, bc2.3, bc2.5 and bc2.6 (Table 5.2) were used for three rounds of selection of Library I or Library J. Polyclonal phage ELISA was used for assessment of specific phage enrichment, and monoclonal phage ELISA for screening of individual clone specificity.

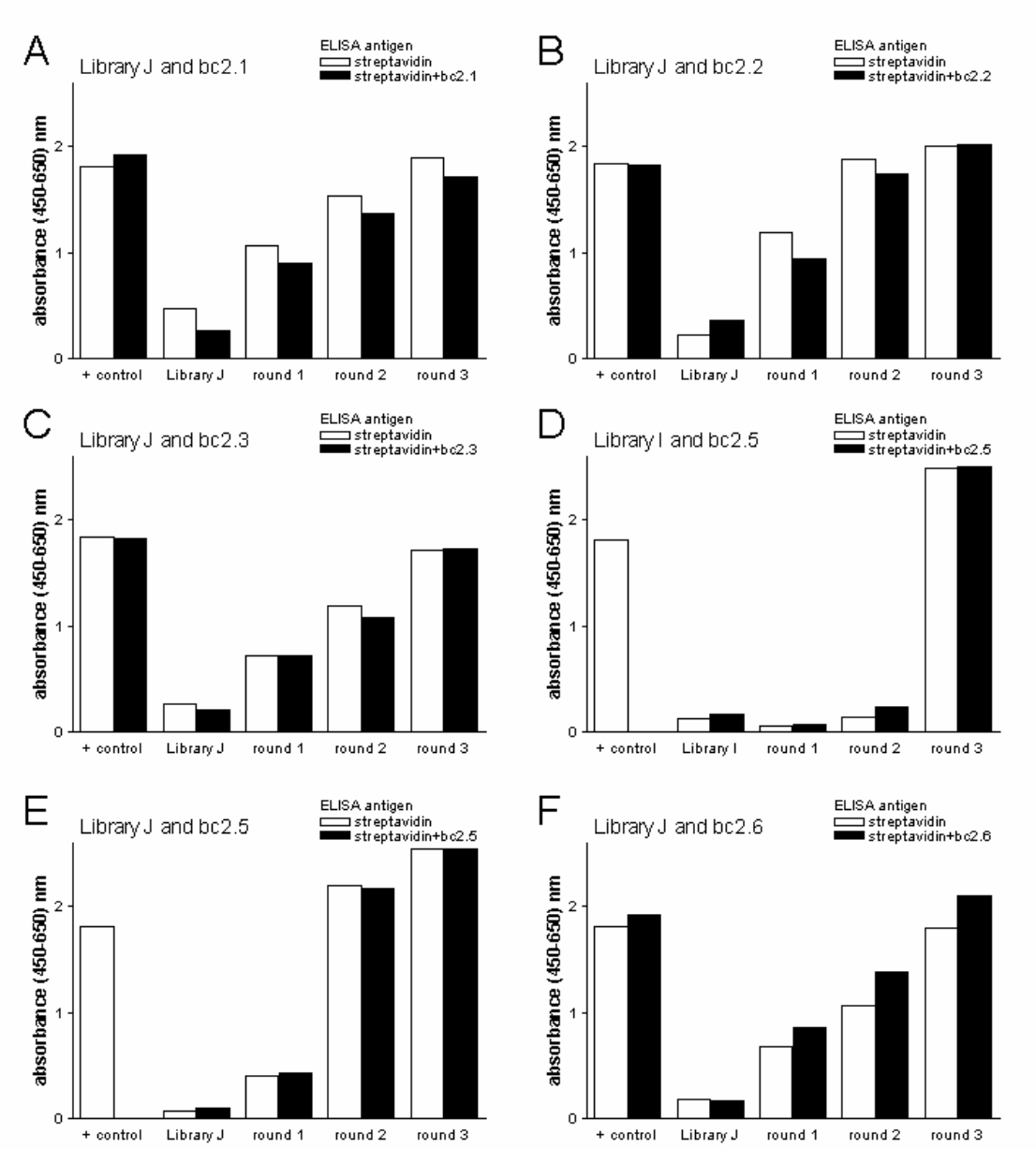

Figure 5.8: Library selection using biotinylated, cyclised peptides.
Polyclonal ELISA analysis of three rounds of selection using Library J and biotinylated, cyclised peptides 2.1 **(A)**, 2.2 **(B)**, 2.3 **(C)**, 2.5 **(E)** and 2.6 **(F)**, or Library I and 2.5 **(D)** as targets.

Selection experiments with all combinations of Library and peptide showed enrichment of binders in a non-peptide-specific manner (Figure 5.8). After three rounds, similar levels of absorbance were seen for phage binding to streptavidin and peptide (target), compared with streptavidin alone (control): Library J selected on peptide b2.1 - target A=1.71, control A=1.90; J+b2.2 - target A=2.01, control A=2.00; J+b2.3 - target A=1.72, control A=1.71; I+b2.5 - target A=2.50, control A=2.48; J+b2.5 - target A=2.54, control A=2.53; J+b2.6 - target A=2.09, control A=1.79. Phage titres for all combinations of Library and peptide showed no increase in phage output compared to controls (Table 5.4). However, the overall titre of both phage output and control did rise dramatically in the second and third rounds for all selections. If no selection was occurring, then the titres for both control and phage output would remain at the lower levels seen in the first round. If the selection was specific for the target peptides, there would be an increase in the phage output titres but no increase in the control titres. As there is an increase in both phage output and control titres, this suggests that selection pressure is resulting in the retention of strongly binding non-specific phage.

Table 5.4: Phage titres of Library I and J selections using biotinylated, cyclised peptides.

Library + target	round	phage titre input	phage titre output	phage titre control	Library + target	round	phage titre input	phage titre output	phage titre control
J+bc2.1	1	$1x10^{12}$	$4x10^{3}$	$4x10^{4}$	J+bc2.2	1	$1x10^{12}$	$2.4x10^{4}$	$4x10^{4}$
	2	$7.5x10^{10}$	$4x10^{8}$	$2.8x10^{9}$		2	$4x10^{9}$	$1x10^{9}$	$8x10^{9}$
	3	$1.3x10^{10}$	$5.2x10^{8}$	$7.6x10^{9}$		3	$9.6x10^{9}$	$1x10^{9}$	$8x10^{9}$
J+bc2.3	1	$1x10^{12}$	$1.8x10^{5}$	$5.2x10^{5}$	I+bc2.5	1	$1x10^{12}$	$1.2x10^{5}$	$2x10^{5}$
	2	$1.8x10^{10}$	$1.8x10^{8}$	$3.2x10^{9}$		2	$3.5x10^{10}$	$2x10^{7}$	$2.5x10^{8}$
	3	$2.2x10^{10}$	$4.4x10^{8}$	$1.1x10^{10}$		3	$5x10^{10}$	$8.4x10^{8}$	$3.6x10^{9}$
J+bc2.5	1	$1x10^{12}$	$1.3x10^{5}$	$3.6x10^{5}$	J+bc2.6	1	$1x10^{12}$	$1.2x10^{5}$	$5.2x10^{5}$
	2	$9.6x10^{9}$	$1.4x10^{8}$	$3x10^{8}$		2	$3x10^{10}$	$1.6x10^{8}$	$1.2x10^{9}$
	3	$1.7x10^{10}$	$2.4x10^{8}$	$5.x10^{8}$		3	$1.7x10^{10}$	$4.8x10^{8}$	$2.6x10^{10}$

Monoclonal phage ELISA analysis was performed on the round three outputs shown in Figure 5.8. Results from the Library J and bc2.6 screenings, which are representative of those seen for all library/peptide combinations, are shown in Figure 5.9. Target peptides bc2.1, bc2.2, bc2.3, bc2.5, and bc2.6 had 20, 45, 23, 7, and 17

clones respectively with A>0.5 for peptide binding in the screen, however all clones also bound to streptavidin alone. Therefore, no clone specific for biotinylated, cyclised LMP2 peptides was isolated from the Tomlinson I and J phage libraries.

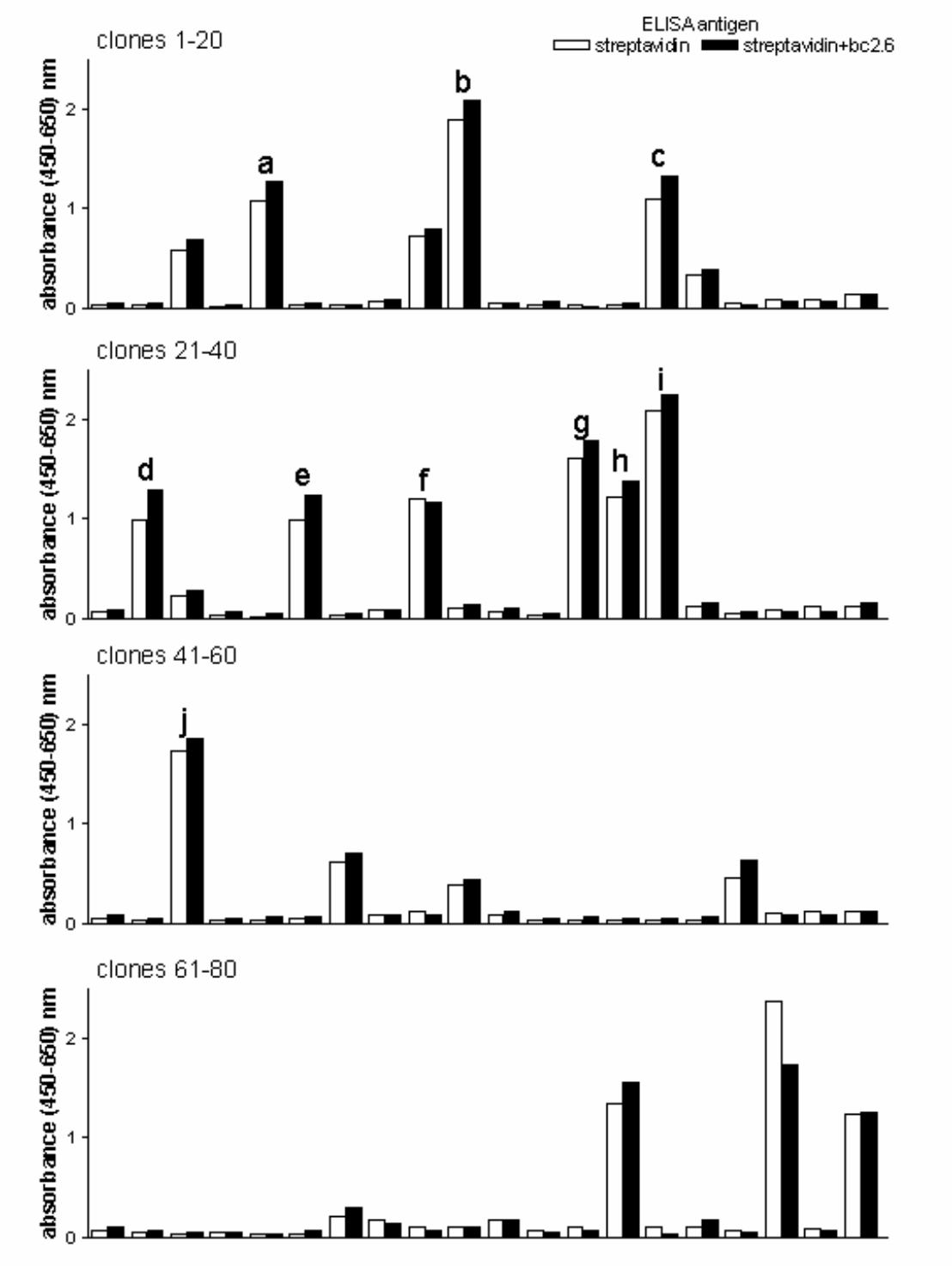

Figure 5.9: Screening of clones from selections using biotinylated, cyclised peptides. Monoclonal ELISA screening of 80 clones from the third round output of Library J selection using biotinylated cyclised peptide 2.6 as a target. Clones labelled **a-j** were taken for further analysis.

In light of the above results, 10 clones (designated a-j) were selected at random from the monoclonal screening of Library J and bc2.6 for further analysis of clone diversity. Clones were screened by PCR for full length inserts (Figure 5.10 panel A). Restriction enzyme digest fingerprinting of the PCR products was used as an indication of clone diversity (Figure 5.10 panel B), and sequencing reactions of the V_H and V_L regions of each of the clones were also performed.

DNA from all 10 clones amplified PCR products of the expected 935bp size, indicating full length scFv inserts, although clone g also had a second band of roughly equal intensity at approximately 700 bp (Figure 5.10 panel A). Nine of the 10 clones (a-h, j) had identical fingerprints, with clone i alone being unique. The secondary band from the clone g PCR did not distinguish its fingerprint from clones a-f, h and j.

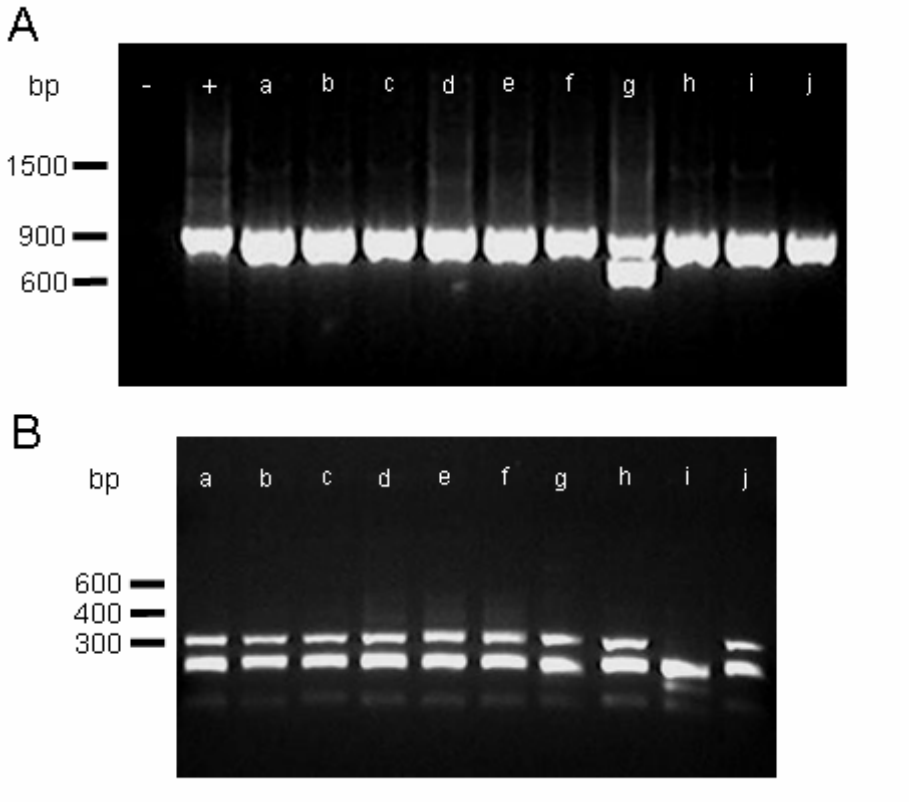

Figure 5.10: scFv inserts and clone diversity in bc2.6 selected phage. PCR screening for full length inserts **(A)** and restriction enzyme digest fingerprinting for diversity **(B)** of 10 clones **(a-j)** from the third round of Library J selection using biotinylated cyclised peptide bc2.6 as target antigen. PCR negative control **(-)** contained no template DNA and positive control **(+)** was unselected Library J phage.

Sequence alignment of nine clones identified four which were identical (a, c, h, j), while the remaining five were unique (b, d, e, f, i). The overrepresentation of a single clone after three rounds of panning suggests some form of selection is occurring, in line with the data from the selection titres. The sequence of clone g was of poor quality, presumably due to interference from the second PCR band, and hence was excluded from analysis.

5.2.5 Selection protocols incorporating negative selection for streptavidin binders

In order to discourage binding of streptavidin-specific clones, a negative selection step was incorporated at the beginning of each round of panning (see 2.6.5). Individual peptides bc2.1, bc2.2, bc2.3 and bc2.6 were used for two rounds of selection of a premixed population of Library I+J. Polyclonal phage ELISA was used for assessment of specific phage enrichment, and monoclonal phage ELISA for screening of individual clone specificity.

Selection experiments with all peptides showed enrichment of binders in a non-peptide-specific manner (Figure 5.11). After two rounds, similar levels of absorbance were seen for phage binding to streptavidin and peptide (target), compared with streptavidin alone (control) for bc2.2 (target A=0.95, control A=1.14), bc2.3 (target A=1.04, control A=1.12), and bc2.6 (target A=0.53, control A=0.47) and a higher level of absorbance for streptavidin alone compare to streptavidin and peptide for bc2.1 (target A=0.90, control A=1.66). Phage titres for all combinations of Library and peptide showed no increase in phage output compared to controls, and there was no enrichment of clones containing full length inserts (Table 5.5).

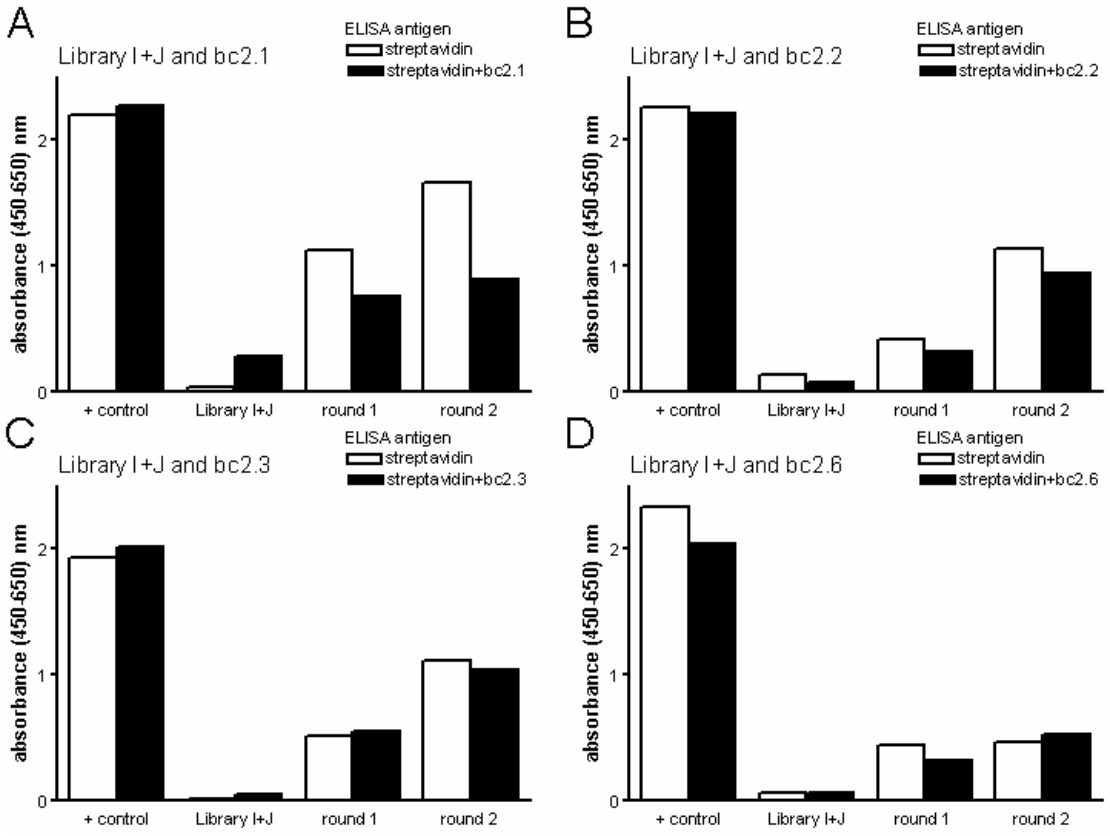

Figure 5.11: Library selection using biotinylated, cyclised peptides with negative selection for streptavidin binding phage.
Polyclonal ELISA analysis of two rounds of phage selection using Library I+J and biotinylated, cyclised peptide 2.1 **(A)**, 2.2 **(B)**, 2.3 **(C)**, or 2.6 **(E)** as targets.

Table 5.5: Phage titres and PCR screening of Library I+J selections using biotinylated, cyclised peptides with negative selection for streptavidin binding phage.

target	round	phage titre			PCR screening
		input	output	control	inserts / clones
bc2.1	1	$1x10^{12}$	$8x10^{3}$	$2x10^{4}$	6 / 8 (75%)
	2		$1.2x10^{9}$	$1.4x10^{9}$	8 / 8 (100%)
bc2.2	1	$1x10^{12}$	$1.6x10^{4}$	$2x10^{4}$	4 / 4 (100%)
	2		$1.4x10^{8}$	$2.1x10^{8}$	5 / 10 (50%)
bc2.3	1	$1x10^{12}$	$8x10^{3}$	$8x10^{3}$	7 / 10 (70%)
	2		$8.4x10^{7}$	$1x10^{8}$	3 / 8 (38%)
bc2.6	1	$1x10^{12}$	$4x10^{3}$	$8x10^{3}$	5 / 10 (50%)
	2		$2.2x10^{8}$	$1.5x10^{8}$	5 / 9 (56%)

Monoclonal phage ELISA analysis was performed on the round three outputs shown in Figure 5.11. No individual clone from selections on bc2.2, bc2.3, and b2.6 had an A>0.5 for either streptavidin alone or streptavidin and peptide. Nine clones from bc2.1 selections had A>0.5 on streptavidin and peptide, however all clones also bound to streptavidin alone. Therefore, although incorporating a negative selection step for streptavidin binders did appear to reduce the overall number of streptavidin binding phage in monoclonal ELISA analysis of selection, it did not appear to encourage selective enrichment of LMP2 binding phage, and no phage clone specific for biotinylated, cyclised LMP2 peptides was isolated.

5.2.6 Selections using streptavidin coated beads

In a parallel experiment also aimed at reducing the enrichment of streptavidin binding phage, selections using streptavidin-coated beads in place of immunotubes were performed. A μMACS Streptavidin Kit for Phage Display (Miltenyi Biotec) was used according to the manufacturer's instructions, with peptide bc2.5 as target for two rounds of Library I and Library J selection. Polyclonal phage ELISA was used for assessment of specific phage enrichment, and monoclonal phage ELISA for screening of individual clone specificity.

For Library I, selection using streptavidin coated beads had the effect of removing all binding phage, while the results for Library J once again showed enrichment in a non-peptide-specific manner (Figure 5.12). Similar levels of absorbance were seen after two rounds of selection for phage binding to streptavidin and peptide compared with streptavidin alone (peptide A=1.06, control A=1.24). Phage titres for the two libraries were also similar (Table 5.6).

Monoclonal ELISA analysis was performed on 80 round two output clones from each Library I and Library J selection. No individual clone showed an A>0.5 for either streptavidin alone or streptavidin and peptide bc2.5.

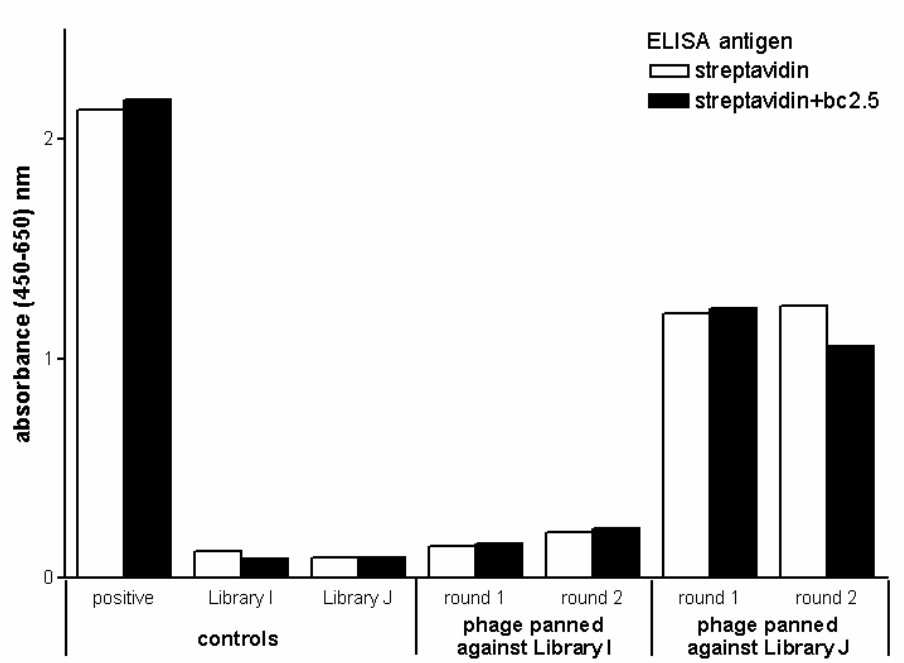

Figure 5.12: Library selection using a biotinylated, cyclised peptide with streptavidin coated beads.
Polyclonal ELISA analysis of two rounds of Library I or Library J selection using streptavidin coated beads and biotinylated, cyclised peptide 2.5 as target.

Table 5.6: Phage titres of Library I and J selections using streptavidin coated beads.

Library	round	phage titre	
		input	output
I	1	$1x10^{11}$	$4x10^{3}$
	2	$1.8x10^{10}$	$1.6x10^{7}$
J	1	$1x10^{11}$	$3.6x10^{4}$
	2	$1.6x10^{10}$	$9.6x10^{6}$

5.3 Selection experiments using alternate libraries

To test if phage libraries other than the Tomlinson I+J would yield specific clones after selection with LMP2 peptides, two new libraries were examined. Like the Tomlinson I+J, the ETH2Gold is a scFv phage library with a diversity of $3x10^9$ (Silacci *et al*, 2005). The RotMar library is in Fab format with a diversity of $5.36x10^9$.

5.3.1 ETH2Gold phage library

Selections using peptide bc2.1 and the ETH2Gold library were performed by Ms Lynda Robson at UCL, London, UK. After three rounds of selection, phage titres and PCR screening showed no specific enrichment of peptide binders compared with controls (Table 5.7).

Table 5.7: Phage titres of ETH2Gold phage library selection.

target	round	phage titre			PCR screening
		input	output	control	inserts / clones
2.1	1	$2x10^{12}$	$3.3x10^4$	$3x10^4$	5 / 10 (50%)
	2	$3x10^{12}$	$1.3x10^4$	$7x10^3$	0 / 9 (0%)
	3	$4.5x10^{12}$	$1x10^7$	$2.6x10^9$	1 / 9 (11%)

5.3.2 RotMar phage library

Selections using peptide bc2.5 were performed by Ms Karen McAulay (University of Edinburgh) and Dr Reno Debets (Erasmus-Daniel den Hoed Cancer Centre) at the Erasmus-Daniel den Hoed Cancer Centre, Rotterdam, Netherlands. After three rounds of selection monoclonal ELISA showed enrichment of binders in a non-peptide specific manner (Figure 5.13). Of the 96 clones screened, 70 had A>0.5, however all clones also bound to the streptavidin-bcLMP1 complex, and thus no phage clone specific for biotinylated, cyclised LMP2 peptide 2.5 was isolated from the RotMar library.

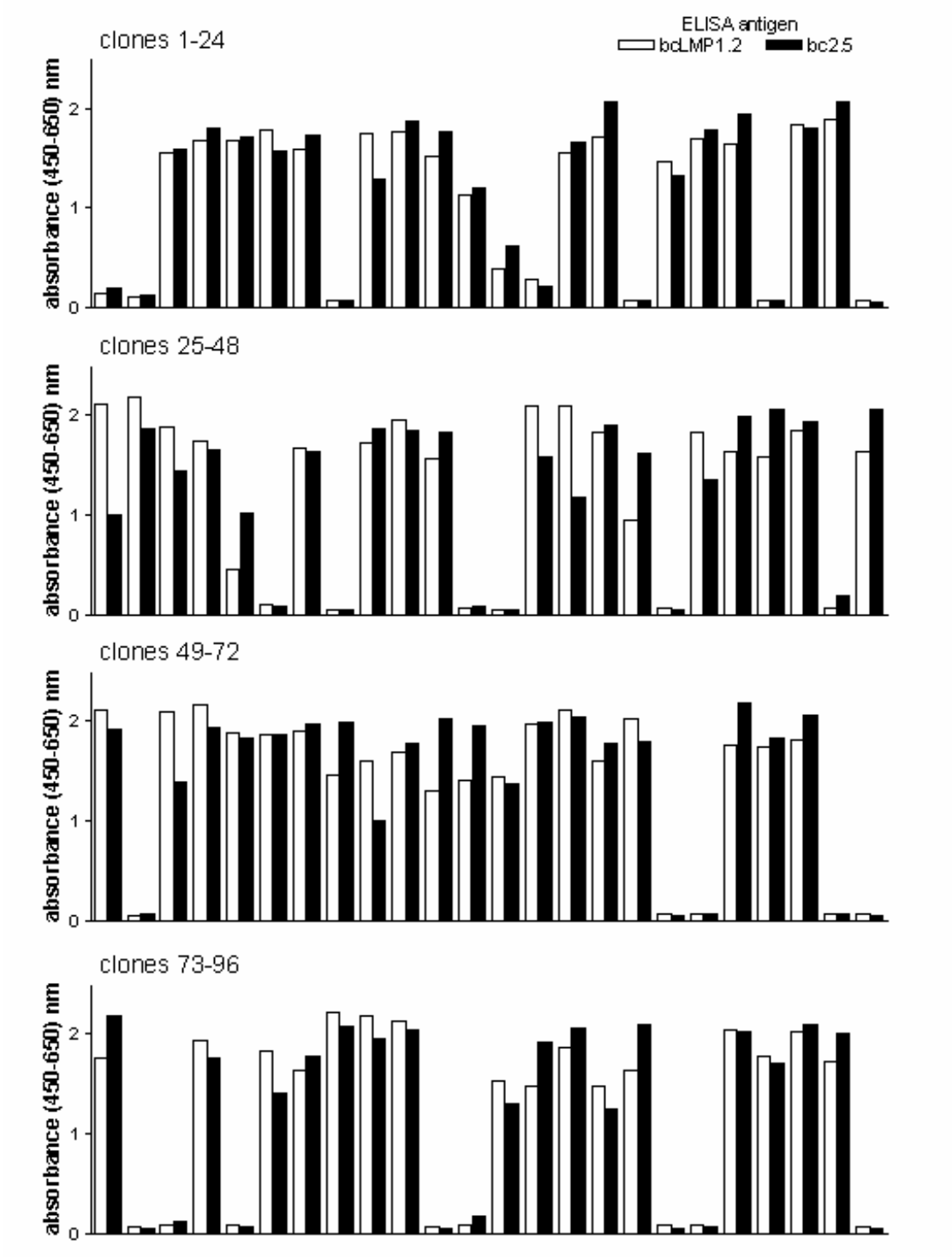

Figure 5.13: RotMar library selection using LMP2 peptide 2.5.
Monoclonal ELISA analysis of the third round output of RotMar phage library selection using biotinylated cyclised peptide 2.5 as target. bcLMP1 is the non-target peptide ELISA control.

5.4 Summary of results

- PCR screening showed at least 70% of Tomlinson I clones and 90% of Tomlinson J clones contained full length scFv inserts.
- After one round of selection, Tomlinson I+J were enriched for clones specific against target proteins BSA and ubiquitin.
- After three rounds of selection, Tomlinson J was enriched for clones specific for the target protein BSA. Enrichment for target peptide c-myc was non-specific.
- There was a small increase in the number of binding clones after three rounds of selection using pool 1 peptides and Library J, but no enrichment using pool 1 and Library I, or pool 2 and either library. Enrichment was not specific for the peptides when assessed by polyclonal ELISA.
- Two clones isolated from round 3 pool 1 and Library J selection displayed higher absorbance on target peptide compared with BSA in a monoclonal ELISA. Upon further analysis, one clone was non-specific and the other of low affinity for the target peptide.
- There was an increase in binding clones after three rounds of selection in 6 of 8 combinations using biotinylated linear peptides and Libraries I and J in parallel. Enrichment was not specific for the peptides when assessed by polyclonal or monoclonal ELISA.
- There was an increase in binding clones after three rounds of selection in all combinations using biotinylated cyclised peptides and Library I or J. Enrichment was not specific for the peptides when assessed by polyclonal or monoclonal ELISA.
- Of nine clones isolated from a round 3 Library J selection with a biotinylated cyclised peptide, all contained full length inserts; four represented a single clone, whilst the remaining five were unique.
- There was a comparatively small increase in binding clones after two rounds in all selections incorporating a negative selection step and using biotinylated cyclised peptides with Library I+J. Enrichment was not specific for the peptides when assessed by polyclonal or monoclonal ELISA.

- There was a small increase in binding clones after two rounds of selection using streptavidin coated beads and a biotinylated cyclised peptide with Library I and J in parallel. Enrichment was not specific for the peptides when assessed by polyclonal ELISA.
- There was no enrichment of specific clones after three rounds of selection using a biotinylated cyclised peptide and the ETH2Gold scFv Library when assessed by PCR.
- There was no enrichment of specific clones after three rounds of selection using a biotinylated cyclised peptide and the RotMar Fab Library when assessed by polyclonal ELISA.

5.5 Discussion

LMP2 was chosen as the target for phage display selections for two reasons; firstly, it is a membrane protein with external loops available for targeting via a cTCR, and secondly, it is expressed in the EBV latency II phenotype characteristic of HL and NPC as well as in a proportion of GC cases. Peptides identical in sequence to the extracellular loops of LMP2 were used as targets rather than cells expressing LMP2 as advice received had highlighted the difficulties of panning on whole cells (personal communication, Sir Gregory Winter, MRC Laboratory of Molecular Biology, Cambridge, UK). The abundance of antigens present on any cell means that a huge number of clones would need to be screened to identify LMP2-specific binders. Even using a panel of LMP2-positive and -negative cell lines over multiple rounds of positive and negative selection, it would be extremely difficult to isolate LMP2 specific binders. Peptides were used in preference to whole purified protein as computer modelling to predict antigenic sequences within the LMP2 protein returned predominantly transmembrane and intracellular hits (http://bio.dfci.harvard.edu/Tools/antigenic.pl). This suggested that selection using whole protein might result in the selective enrichment of clones binding to those domains, with clones specific for the external loop sequences lost over progressive rounds of selection. A scFv format was selected for the phage library, as the Tomlinson I+J library was readily available as the time this project commenced. Also, the scFv configuration was the format most relevant for cTCR construction, which was the anticipated initial use for the selected clone.

Standardisation experiments demonstrated that the Tomlinson libraries were functioning correctly. By PCR screening, at least 70% of Tomlinson I and 90% of Tomlinson J clones contained full length scFv inserts (Figure 5.1). The library specification sheet gave 96% and 88% as the percentage of full length clones in I and J respectively, thus the results were as expected. The remaining clones did not amplify any product, full length or otherwise. It is possible that the clones do contain full length inserts, and that the lack of product was a result of sub-optimal PCR conditions. One possibility is that insufficient DNA was added to the reaction mix when bacteria were picked directly from agar plates. Three rounds of selection using Library J and BSA as a target protein confirmed that the library could be enriched for phage specific for a target protein (Figure 5.3). At this point it was decided that 0.5A would be the level beneath which phage binding in an ELISA would be classed as background. This was the approximate absorbance value of the third round BSA-selected phage population binding to c-myc in a polyclonal ELISA (Figure 5.3).

An increase in binding clones was observed during selections using c-myc as target (Figure 5.3); however, phage also bound to BSA control wells in the polyclonal ELISA. As the c-myc epitope is 10 aa long and a mAb for c-myc is commercially available, c-myc was chosen as a target to test if the library was capable of selection against short peptides. In retrospect, this was not a good choice of target as phage in the Tomlinson libraries carry a myc tag for detection, purification or immobilisation of the scFv. Thus, it is possible that phage specific for myc would bind to other phage during panning, greatly reducing the selection pressure necessary for specific enrichment. However, this was not appreciated at the time, and selection experiments using a more appropriate peptide target were not performed. Given the slight but visible difference between control and test wells in the polyclonal ELISA it was decided to continue with the peptide approach (Figure 5.3).

Selections using pooled, unmodified peptides and the Tomlinson libraries in parallel did not result in a high enrichment of binding clones. Only two potential clones with clear differences in absorbance when binding to target compared with BSA were identified by monoclonal ELISA: clones G11 and H10. Upon rescue and further analysis, clone G11 proved to be an equally strong binder against the all three pool

peptides when each was assayed individually (Figure 5.5). It also returned high absorbances against ubiquitin, human sera and to a slightly lesser extent BSA, demonstrating that it was not specific for target peptides. Clone H10 bound specifically to peptide 2.5 but not 2.6 or BSA. However, it was also reactive against ubiquitin and human sera (Figure 5.5). Additionally, although the phage used in the ELISA had been PEG-precipitated and was therefore of high concentration, absorbance was still relatively low (peptide 2.5, A=0.87), suggesting a weak affinity for peptide 2.5. As high affinity scFv show better tumour delivery (at least in antibody format; Adams *et al*, 1998), no further analysis of H10 was performed.

Biotinylating peptides had the effect of increasing 'background' phage in selections using both linear and cyclised peptides (Figure 5.6 and Figure 5.8). That is, overall more binding phage were rescued during rounds of selection, as evidenced by increased absorbance levels in polyclonal ELISAs. However, these phage were reactive with both target peptides and the streptavidin used to adhere biotinylated peptides to immunotubes and ELISA plates. One polyclonal ELISA showed increased absorbance on target peptide compared to streptavidin (Library I and b2.5, Figure 5.6 panel G), although the no phage and unselected Library I controls also had raised absorbance. Thus, the most likely explanation for the ELISA results is cross-contamination with other samples, either in the sample aliquots or ELISA wells. Subsequent monoclonal ELISA analysis confirmed this was not a true positive result, as no specific individual clones were isolated from the 80 clones tested.

Sequence analysis of nine clones from a selection using Library J and bc2.6 showed that while five clones were unique, the remaining four clones selected represented a single scFv (see 5.2.4). This overrepresentation of a single clone after three rounds of panning, together with the high titres returned on both phage output and control tubes in the second and third rounds (Table 5.4),` suggests some form of selection is occurring, possibly on an epitope common to avidin and streptavidin. Avidin was used to bind target peptide in round 2 and streptavidin was used in rounds 1 and 3. Restriction enzyme digests were also used prior to sequencing as an initial screen for clone diversity (Figure 5.10 panel B). In retrospect this was not an appropriate choice as the Tomlinson library is based on a single antibody framework, with sequence diversity engineered only in the CDR3 and CDR2 regions. Thus BstNI cleavage

sites are not likely to vary even between clones with different specificities. Restriction enzyme digests are better suited to screening naïve libraries.

Some background is expected when using phage display, that is, rescue of phage clones not specific for the target may occur. Only a minority of phage particles display scFv. In the Tomlinson system, it is between 1 in 10 and 1 in 100 (Jensen *et al*, 2003a). However, these phage would be expected to be non-binders in monoclonal ELISAs given that they have no ligand with which to bind to targets. Some of the background yet binding clones may be reactive to the milk powder contained in the blocking buffer used for both ELISAs and panning. The problem of the streptavidin reactive background generally seen when using biotinylated target may have been compounded in this case by the lack of specific phage, with streptavidin reactive phage enriched over multiple rounds of selection as there was no competing enrichment of target-specific phage.

It remains an open question as to why LMP2 loops were unable to select out specific scFv. Although the peptides were comparatively short, they were long enough to be a target. With the c-myc epitope, only 10 aa are needed for specificity. The Tomlinson I+J are relatively old phage libraries, and newer, larger and therefore more diverse libraries are currently being constructed, such as the ETH2Gold and RotMar libraries. A major difference between the Tomlinson and ETH2Gold libraries compared with the RotMar library, is that the RotMar is a naïve library. This means that diversity is incorporated over the entire antibody fragment and not just in the CDR regions where antibody residues directly contact the antigen. Indeed, the Tomlinson and ETH use the same V_H framework (DP47). This may affect the size and shape of the antigen binding cleft of the antibody, with consequences for the range of targets able to be bound. As with the Tomlinson selections, panning using the ETH2Gold library and bc2.1 did not isolate peptide-specific clones (Figure 5.7). However, although a similar result was seen using the RotMar library and bc2.5 (Figure 5.13), parallel selections using a biotinylated cyclised LMP1 extracellular loop peptide (bcLMP1.2) were also performed, and these selections did result in specific enrichment (Figure 5.14). The bcLMP1 sequence is biotin-ßAlaßAla-LIALWNLHGQALFLG (Figure 1.4). Of the 96 clones screened after three rounds of selection, 72 specific clones were identified (peptide A>0.24, control A<0.1).

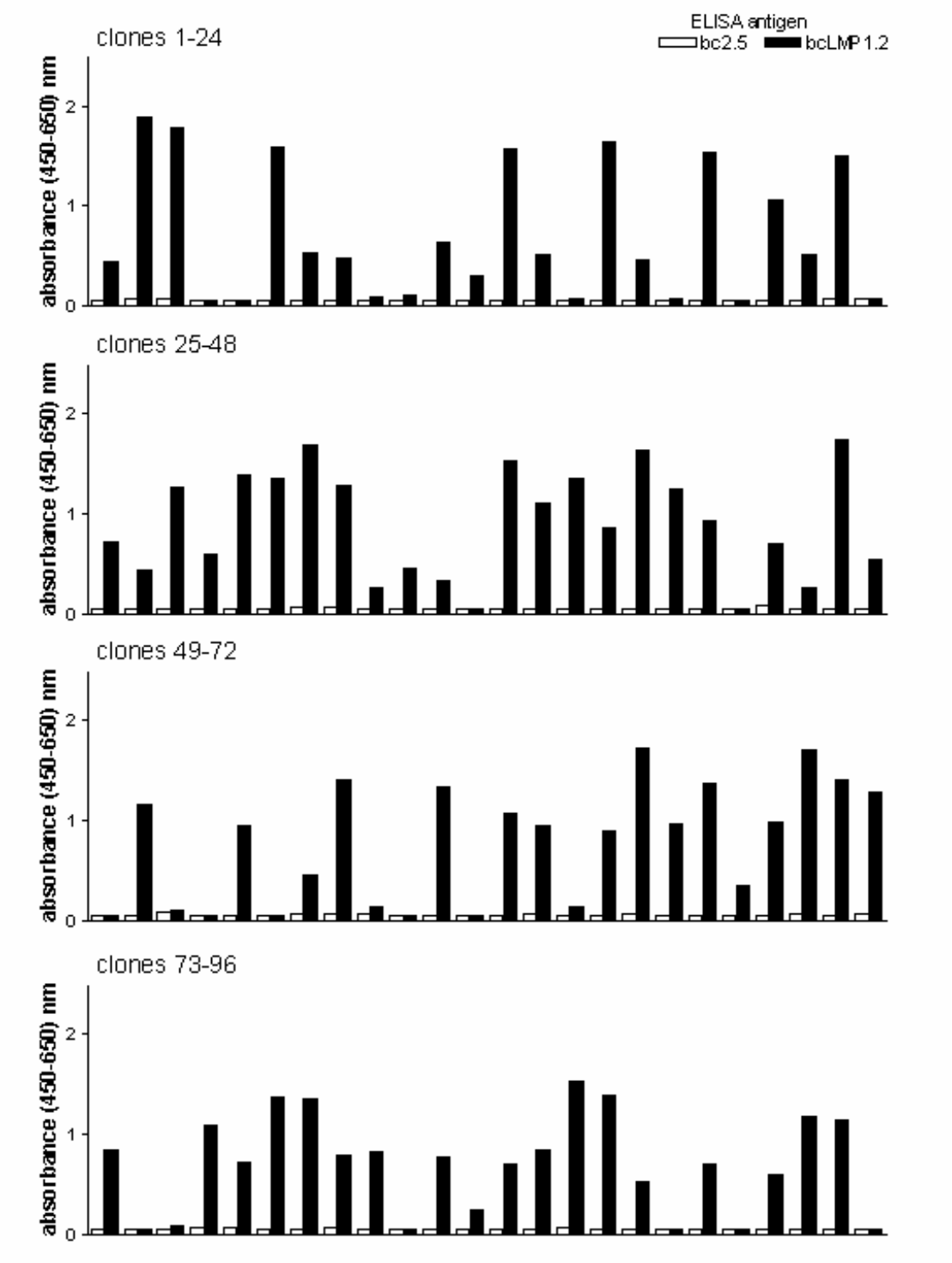

Figure 5.14: RotMar library selection using LMP1 peptide 1.2.
Monoclonal ELISA analysis of the third round output of RotMar phage library selection using biotinylated cyclised peptide LMP1.2 as target. bc2.5 is the non-target peptide ELISA control.

In addition to differences in library construction, the RotMar library is also in Fab format, compared to the scFv format of the Tomlinson and ETH2Gold libraries. Rather than a single recombinant antibody fragment fused to the pIII protein, the RotMar Fab library has only the antibody heavy chain fused to pIII. The antibody light chain is expressed as a separate molecule, which is secreted into the *E.coli* periplasm where it can pair with the heavy chain. Fabs tend to be expressed at lower levels on phage than scFv, leading to a lower display frequency and lower fraction of avid phage. Therefore, selections using Fab are governed more by affinity (the binding strength of an antigenic determinant to a single antigen-binding site) than avidity (the sum total binding strength of an antigenic particle to an antigen-binding molecule). Also, Fab do not form multimers when expressed as soluble fragments, in contrast with scFv which do tend to multimerise. Thus, Fab libraries are easier to use with respect to downstream affinity assays such as using surface plasmon resonance technology as crude protein fractions can be utilised without the need for purification. Also, and for the same reason, they are a better option when panning for fragments to be incorporated into whole antibody molecules.

Only one peptide each from LMP1 and LMP2 were used to screen the RotMar library (Figure 5.13 and Figure 5.14), so it is possible that a Fab specific for an LMP2 loop may yet be isolated. Logically, there is no reason why the LMP2 loops shouldn't retrieve specific scFv. LMP1 and LMP2 loops have been used previously to isolate Fab fragments from the de Haard library (personal communication, Professor Jaap Middeldorp; de Haard *et al*, 1999). Other possibilities for target manipulation which could be explored include synthesising peptide repeats to make targets longer, and branching peptides to display multiple copies of the same target or combinations of targets. The use of whole cells expressing LMP2 as targets has been discussed previously, and remains an option, albeit a difficult one. Colleagues in our laboratory are currently conducting further analysis on the LMP1 clones isolated in Rotterdam, and transferring the RotMar library to Edinburgh in order to continue selections using LMP1 and LMP2 peptides as targets. Initial results are encouraging, however further work evaluating the specificity and affinity of isolated clones is ongoing.

On a technical note, selections in our laboratory are now conducted using commercially available streptavidin coated beads to immobilise biotinylated targets, rather than the immunotube method described here. Although selections using streptavidin coated beads and a biotinylated cyclised peptide with Library I and J in parallel did not result in the isolation of an LMP2 specific clone during this project (Figure 5.12), this was a single experiment using only one peptide with no opportunity for optimisation or standardisation. As commercially available streptavidin coated beads undergo quality assurance testing prior to release from the supplier, this format reduces variability in streptavidin concentrations across selection experiments with obvious implications for the reliability of target concentration (personal communication, Dr Reno Debets). An additional advantage of this method is that it allows selections to be performed in smaller volumes than the immunotube format. This facilitates the binding of target and specific clone, which is presumably of low frequency in the initial library population, by bringing them into closer proximity.

In light of the unsuccessful nature of selections performed with the Tomlinson libraries and LMP2 peptides, an evaluation of the approach taken is warranted. The advantage of using the loop peptide targets is that they are able to be easily and relatively cheaply synthesised, and any phage binding to them is specific for the extracellular rather than intracellular or transmembrane portions of the LMP2 molecule, as required for cTCR construction. Conversely, the whole protein is considerably more difficult and expensive to synthesise or purify, and as it is a membrane protein it would not be in its native conformation. The major drawback to peptide selections is that in general they are not as successful those using whole protein targets. Also, scFv phage specific for peptides, or indeed whole purified proteins, do not necessarily bind targets in their native conformation and environment. ELISA screening using soluble scFv or Fab rather than fragments expressed on the surface of phage may give a more accurate indication of functionality, and in retrospect this assay should have been performed in the library control experiments (5.1.2 and 5.1.3). Nevertheless, as a starting point peptide targets were a reasonable choice.

With the benefit of additional time, it would have been interesting to also attempt selections on whole cells. Vaccinia constructs could have been assembled containing

LMP2, and the addition of a selectable marker would have allowed subtractive selection using FACS. With hindsight, a switch from the peptide target approach to whole cell selections, or to using a naïve library, should possibly been taken earlier. However given the time limits inherent in the project there is no guarantee that this would have led to the isolation of LMP2-specific scFv. Had a robust monoclonal antibody for LMP2 been available, the need for these selections may have been obviated, and the LMP2-specific scFv could have been obtained from this source. However, this lack is another argument for searching for LMP2-specific antibody fragments by phage display, as a specific LMP2 antibody would be a useful tool in EBV research.

6 Future Directions

"The history of cancer research has been a history of curing cancer in the mouse. We have cured mice of cancer for decades, and it simply didn't work in humans."

- Dr Richard Klausner
former director, US National Cancer Institute
Los Angeles Times, 6th May 1998

The above quote has been both a goal and a goad throughout this project. As yet, no mouse model has been a good predictor of the human response to immunotherapy (June, 2007) although the SCID model of PTLD is a possible exception. The divergent responses seen when using CTLA4-specific antibody blockade are one example highlighting the differences between the mouse and human situations. In mice, treatment is well tolerated and induces anti-tumour responses when administered in combination with a granulocyte/macrophage colony-stimulating factor (GM-CSF)-expressing tumour cell vaccine in a murine melanoma model (van Elsas *et al*, 1999). Although anti-tumour responses have also observed in humans, they were often accompanied by serious autoimmunity (Attia *et al*, 2005; Blansfield *et al*, 2005). The recent media furore which accompanied the hospitalisation of six men in Northwick Park as a result of a phase I immunotherapy trial also underscores the differences between model systems and the human situation (Suntharalingam *et al*, 2006). In this case the model animal was the rat, and a novel therapeutic anti-CD28 mAb (TGN1412) was well tolerated in this setting (Beyersdorf *et al*, 2005). Prior to the trial, the mAb was also tested on human PMBCs *in vitro*, as well as in cynomolgus macaques *in vivo* (whose CD28 molecule shares 100% homology with the intra- and extracellular domains of human CD28), with no adverse effects (Hanke, 2006). In fact, it was anticipated the antibody would preferentially expand T_{regs} (defined by a CD4+CD25^{high} phenotype) and be useful in the treatment of autoimmune disease. Instead, antibody administration initiated a rapid release of proinflammatory cytokines, a so called 'cytokine storm', leading to multiple organ failure in all six patients, although all eventually recovered (Suntharalingam *et al*, 2006). Whilst this is an extreme case, it emphasises the need for caution in

immunotherapy, as many aspects of the immune system have yet to be fully understood. Nonetheless, returning to the quote, curing cancer in a mouse is a considerable achievement. It provides proof-of-principle for novel therapies, and yet it falls short of the aim of the majority of cancer research, which is of course curing cancer in humans.

Evaluation of novel therapeutic agents requires complex, biologically relevant models in which to study interactions between agent and subject. Technical and ethical constraints limit the use of humans as test subjects, and consequently animals fill this niche. Current guidance from the International Conference on Harmonisation of Technical Requirements for Registration of Pharmaceuticals for Human Use (ICH), to which the European Union is a signatory, requires evaluation of preclinical data collected from animal experiments prior to the commencement of human trials. Non-human primates most closely represent human biology, yet they do not absolutely mimic the human situation, and as mentioned previously, the specialist requirements, high expense and adverse public attitude towards primate research means it is not feasible for large scale research in the UK. Due to their lack of functional T and B lymphocytes, SCID mice can be engrafted with human tissue. Such humanised animals are a useful tool in which to study the effects of targeted therapies for cancer, providing as it does the actual target cells in a microenvironment more akin to human malignancy than *in vitro* culture. Additionally, mouse models are relatively inexpensive and used on such a wide scale that mouse biology is well understood in comparison with other mammalian models (Hughes, 2003). Thus, the SCID models of HL, NPC and GC set up during this project may be valuable in future investigations of cancer therapy.

As a viral antigen associated with a number of tumours, some attention has been focused on LMP2 as a CTL target for immunotherapy of EBV-positive tumours. However, LCL-stimulated CTL cultures from healthy EBV-positive individuals usually contain less than 1% T cells recognizing LMP2A (Bollard *et al*, 2004). Although only subdominant and no immunodominant LMP2 specificities have been identified so far, these CTLs may still be immunologically relevant. Sun *et al* (2007) used an INF-γ capture assay to enrich CTL cultures for LMP2A-specific effector cells. *In vitro*, these polyclonal populations were able to specifically lyse fibroblasts

expressing LMP2A as well as LCLs expressing the full range of EBV latent antigens, and release Th1 cytokines such as INF-γ and GM-CSF following antigen stimulation (Sun *et al*, 2007). Bollard *et al* (2007) used an alternative method to enrich CTL populations for LMP2A-specific cells. Rather than use conventional EBV-positive LCLs for stimulation and expansion of CTLs, PBMCs were initially stimulated with dendritic cells engineered to express LMP2A from an adenovirus vector, with LCLs overexpressing LMP2A from the same vector used in subsequent stimulations. This approach resulted in a polyclonal population of LMP2A-specific CTLs, which were able to mediate four complete and one partial response, with one non-responder, in the six patients with relapsed HL or NHL treated using the LMP2A-specific cells (Bollard *et al*, 2007). This result validates the use of cellular therapies directed against LMP2 for the treatment of EBV-associated malignancies. However, a major disadvantage of the Bollard protocol is that the therapeutic CTLs are generated using PBMCs from the patient's own blood to derive the dendritic cells (DC), LCLs and T cells required. This means that the delay between decision to treat and actual therapy is prolonged, the patient must have LMP2 reactive T cells present in the periphery, and ideally PBMCs should not be numerically or functionally defective as a result of disease or treatment. One advantage of the cTCR approach undertaken in this project is that whilst a patient's PBMCs could be used as a T cell source if time and facilities permit (as outlined in Figure 1.8), a bank of best match CTLs transduced with the cTCR and expanded to clinically relevant numbers could also be created and stored, reducing treatment delay and obviating the need for functional patient cells.

Although immunotherapy using cTCRs to direct T cells against cancer cells has great potential, there are a number of issues which need to be addressed in order to facilitate the transfer of treatment from animal models into the clinic. Three phase I clinical trials using cTCR engineered T cells have been undertaken to date, and these studies have highlighted some of the key issues needing to be addressed by researchers in the engineered cellular immunotherapy field. The first study investigated cells targeting FBP found on ovarian cancers (Kershaw *et al*, 2006), and the second examined cells directed against the L1-cell adhesion molecule (CD171), which is overexpressed by neuroblastoma cells (Park *et al*, 2007). Both treatment regimes were well tolerated by patients. However, T cell persistence was poor and no clinical benefits were observed. Clinical responses have been correlated with T

cell persistence *in vivo*, at least in adoptive therapy of melanoma using unmodified melan-A-specific T cells, suggesting that persistence of therapeutic cells is crucial for successful treatment (Meidenbauer *et al*, 2003). Neither of the cTCRs used in the trials conducted by Kershaw *et al* or Park *et al* included a co-stimulatory domain. The lag time between laboratory and clinical studies can be as much as 10 years, making incorporation of the latest research unfeasible, and thus evaluation of safety was the main issue under investigation. Therefore, as there were no adverse events, the results of the trials are encouraging and pave the way for future trials using more advanced cTCRs incorporating co-stimulatory domains for improved T cell persistence and therapeutic efficacy. The third cTCR trial targeted carboxy anhydrase IX (CAIX), which is overexpressed in more than 90% of primary renal carcinoma (Lamers *et al*, 2006). Unfortunately, this trial was halted as a result of unexpected hepatic toxicity, most likely due to the engineered T-cells trafficking to and exerting cytotoxic effect against CAIX-expressing epithelial cells lining the bile ducts. Whilst this is an encouraging display of T cell migration and effect, it emphasises the need for careful selection of target antigens. Lamers *et al* (2006) also saw development of anti-scFv antibodies in patients, a situation which may need to be taken into consideration for future studies, although the mAb source of the scFv was in this case murine, and hence likely to be more immunogenic in patients than a fully human scFv. Taken together, the studies demonstrate that engineered T cells are capable of trafficking to and killing cells expressing the target antigen. When targets are carefully chosen, treatment is well tolerated by patients. However, safety and efficacy *in vivo* are areas in which more research is required.

A number of avenues are being explored to make T cells more efficacious, especially with regards to activation of therapeutic cells. The benefits of IL-2 on anti-tumour effect when co-administered systemically alongside tumour-specific T cells have long been known (Cheever *et al*, 1982). However, in the patient setting systemic IL-2 administration is toxic, and when used in conjunction with MART1, melan-A-specific or gp100-specific CTLs for the treatment of melanoma, minimal clinical benefits were observed (Yee *et al*, 2002). For a more specific IL-2 mediated T cell stimulation *in vivo*, therapeutic T cells could be transduced with a gene encoding IL-2. *In vitro*, this resulted in constitutive IL-2 expression and prolonged viability of T cells specific for a melanoma antigen in the absence of exogenous IL-2 (Liu &

Rosenberg, 2001). Alternatively, a chimeric GM-CSF/IL-2 receptor could be used, where stimulation of T cells results in GM-CSF secretion and initiation of an autocrine T cell growth loop (Cheng *et al*, 2002). Tumours may also secret or induce secretion of inhibitory cytokines, for example transforming growth factor (TGF)-β, creating a tumour microenvironment which prevents anti-tumour immune responses, as is the case in HL (Newcom & Gu, 1995; Gruss & Kadin, 1996). One strategy to defend therapeutic cells against tumour inhibitory factors is engineering them with a dominant negative TGF-βII receptor (Bollard *et al*, 2002). This has been shown to protect EBV-specific CTLs from TGF-β-mediated inhibition, whilst their phenotype, growth characteristic and ability to specifically lyse EBV-positive cells remained unaffected (Bollard *et al*, 2002).

As mentioned previously, safety is a major concern when designing engineered T cells for therapy. Although there has been no evidence so far of insertional mutagenesis in clinical testing of cells engineered using viral vectors, as seen with the CAIX-targeted trial mentioned above, cross-reactivity with healthy tissue is a real risk. Also, given the interest in the incorporation of additional costimulatory moieties intended to enhance T cell proliferation and persistence, uncontrolled lymphoproliferation is also a possibility. To guard against these and other unforeseen adverse events, inclusion of suicide genes is a prudent option. HSV-TK has been used for this, where expression of HSV-TK results in the phosphorylation of the non-toxic prodrug, ganciclovir. The active, phosphorylated analogue is incorporated into the DNA cells causing death by apoptosis. However, as it is a viral protein HSK-TK can provoke an immune response against therapeutic cells, greatly reducing efficacy (Ciceri *et al*, 2007). Thus, recent work has investigated the engineering of suicide genes using endogenous proteins such as caspase 9 (Tey *et al*, 2007). In the inducible caspase 9 system, administration of a synthetic drug (a chemical inducer of dimerisation) results in cross-linking and activation of the suicide gene product and subsequent apoptosis of the engineered cell (Straathof *et al*, 2005b).

Although this project has focused on the use of CD8+ CTLs as therapy, CD4+ T cell subsets also have an important role to play *in vivo*. The function of T_{regs} in cancer immunity has yet to be fully elucidated. T_{regs} are, however, enriched in TILs and

PBMCs of cancer patients, suggesting they contribute to the suppression of anti-tumour immune responses (Woo *et al*, 2001; Griffiths *et al*, 2007). CD4+ cells, nonetheless, are required together with CD8+ cells to generate an effective response *in vivo* (Dudley *et al*, 2001; Einsele *et al*, 2002), as well as for initiation and maintenance of CD8 memory (Bevan, 2004). Therefore, depletion of the entire CD4+ T cell subset from therapeutic populations is not an option. Further research is required to find a balance between CD4+ T cell help and suppression of CTL responses. Recent reports point to lymphodepletion prior to adoptive immunotherapy as a promising strategy in the clinic (Rosenberg & Dudley, 2004). The reasons why this approach enhances the efficacy of therapeutic T cells are not entirely clear. One possibility is that the creation of immune 'space' reduces competition between native and introduced cells for stimulatory cytokines, alternatively the removal of T_{regs} may reduce suppression of anti-tumour immunity (Wrzesinski & Restifo, 2005).

With so many alternatives potentially able to improve the efficacy of engineered T cells, the biggest challenge facing scientists is ascertaining which options are useful and complementary, and subsequently incorporating these into treatment regimes. Cancer immunotherapy treatments will need to be multifactorial in order to fully harness the enormously complex human immune system. However, there is much yet to be learned with regard to gene modified T cells, and hopefully the understanding gained will lead to superior and more effective therapies.

REFERENCES

Adams, G. P., Schier, R., Marshall, K., Wolf, E. J., McCall, A. M., Marks, J. D. & Weiner, L. M. (1998). Increased affinity leads to improved selective tumor delivery of single-chain Fv antibodies. *Cancer Res* **58**, 485-90.

Adler, B., Schaadt, E., Kempkes, B., Zimber-Strobl, U., Baier, B. & Bornkamm, G. W. (2002). Control of Epstein-Barr virus reactivation by activated CD40 and viral latent membrane protein 1. *Proc Natl Acad Sci U S A* **99**, 437-42.

Agathanggelou, A., Niedobitek, G., Chen, R., Nicholls, J., Yin, W. & Young, L. S. (1995). Expression of immune regulatory molecules in Epstein-Barr virus-associated nasopharyngeal carcinomas with prominent lymphoid stroma. Evidence for a functional interaction between epithelial tumor cells and infiltrating lymphoid cells. *Am J Pathol* **147**, 1152-60.

Akiyama, S., Amo, H., Watanabe, T., Matsuyama, M., Sakamoto, J., Imaizumi, M., Ichihashi, H., Kondo, T. & Takagi, H. (1988). Characteristics of three human gastric cancer cell lines, NU-GC-2, NU-GC-3 and NU-GC-4. *Japanese Journal of Surgery* **18**, 438-46.

Alfieri, C., Birkenbach, M. & Kieff, E. (1991). Early events in Epstein-Barr virus infection of human B lymphocytes. *Virology* **181**, 595-608.

Allan, G. J., Inman, G. J., Parker, B. D., Rowe, D. T. & Farrell, P. J. (1992). Cell growth effects of Epstein-Barr virus leader protein. *J Gen Virol* **73 (Pt 6)**, 1547-51.

Allday, M. J. & Farrell, P. J. (1994). Epstein-Barr virus nuclear antigen EBNA3C/6 expression maintains the level of latent membrane protein 1 in G1-arrested cells. *J Virol* **68**, 3491-8.

Anagnostopoulos, I., Herbst, H., Niedobitek, G. & Stein, H. (1989). Demonstration of monoclonal EBV genomes in Hodgkin's disease and Ki-1-positive anaplastic large cell lymphoma by combined Southern blot and in situ hybridization. *Blood* **74**, 810-6.

Apple, R., Knauper, B., Pesce, A. & Michael, G. (1984). Shared determinants of native and denatured bovine serum albumin are recognized by both B- and T-cells. *Molecular Immunology* **21**, 901-5.

Armstrong, R. W., Imrey, P. B., Lye, M. S., Armstrong, M. J., Yu, M. C. & Sani, S. (1998). Nasopharyngeal carcinoma in Malaysian Chinese: salted fish and other dietary exposures. *Int J Cancer* **77**, 228-35.

Attia, P., Phan, G. Q., Maker, A. V., Robinson, M. R., Quezado, M. M., Yang, J. C., Sherry, R. M., Topalian, S. L., Kammula, U. S., Royal, R. E., Restifo, N. P., Haworth, L. R., Levy, C., Mavroukakis, S. A., Nichol, G., Yellin, M. J. & Rosenberg, S. A. (2005). Autoimmunity correlates with tumor regression in patients with metastatic melanoma treated with anti-cytotoxic T-lymphocyte antigen-4. *J Clin Oncol* **23**, 6043-53.

Audouin, J., Diebold, J. & Pallesen, G. (1992). Frequent expression of Epstein-Barr virus latent membrane protein-1 in tumour cells of Hodgkin's disease in HIV-positive patients. *J Pathol* **167**, 381-4.

Babcock, G. J., Decker, L. L., Volk, M. & Thorley-Lawson, D. A. (1998). EBV persistence in memory B cells in vivo. *Immunity* **9**, 395-404.

Babcock, G. J., Hochberg, D. & Thorley-Lawson, A. D. (2000). The expression pattern of Epstein-Barr virus latent genes in vivo is dependent upon the differentiation stage of the infected B cell. *Immunity* **13**, 497-506.

Babcock, G. J. & Thorley-Lawson, D. A. (2000). Tonsillar memory B cells, latently infected with Epstein-Barr virus, express the restricted pattern of latent genes previously found only in Epstein-Barr virus-associated tumors. *Proc Natl Acad Sci U S A* **97**, 12250-5.

Baer, R., Bankier, A. T., Biggin, M. D., Deininger, P. L., Farrell, P. J., Gibson, T. J., Hatfull, G., Hudson, G. S., Satchwell, S. C., Seguin, C. & et al. (1984). DNA sequence and expression of the B95-8 Epstein-Barr virus genome. *Nature* **310**, 207-11.

Baichwal, V. R. & Sugden, B. (1989). The multiple membrane-spanning segments of the BNLF-1 oncogene from Epstein-Barr virus are required for transformation. *Oncogene* **4**, 67-74.

Bargou, R. C., Emmerich, F., Krappmann, D., Bommert, K., Mapara, M. Y., Arnold, W., Royer, H. D., Grinstein, E., Greiner, A., Scheidereit, C. & Dorken, B. (1997). Constitutive nuclear factor-kappaB-RelA activation is required for proliferation and survival of Hodgkin's disease tumor cells. *J Clin Invest* **100**, 2961-9.

Barranco, S. C., Townsend, C. M., Jr., Casartelli, C., Macik, B. G., Burger, N. L., Boerwinkle, W. R. & Gourley, W. K. (1983). Establishment and characterization of an in vitro model system for human adenocarcinoma of the stomach. *Cancer Research* **43**, 1703-9.

Baumforth, K. R., Flavell, J. R., Reynolds, G. M., Davies, G., Pettit, T. R., Wei, W., Morgan, S., Stankovic, T., Kishi, Y., Arai, H., Nowakova, M., Pratt, G., Aoki, J., Wakelam, M. J., Young, L. S. & Murray, P. G. (2005). Induction of autotaxin by the Epstein-Barr virus promotes the growth and survival of Hodgkin lymphoma cells. *Blood* **106**, 2138-46.

Berinstein, N. L., Grillo-Lopez, A. J., White, C. A., Bence-Bruckler, I., Maloney, D., Czuczman, M., Green, D., Rosenberg, J., McLaughlin, P. & Shen, D. (1998). Association of serum Rituximab (IDEC-C2B8) concentration and anti-tumor response in the treatment of recurrent low-grade or follicular non-Hodgkin's lymphoma. *Ann Oncol* **9**, 995-1001.

Bevan, M. J. (2004). Helping the CD8(+) T-cell response. *Nat Rev Immunol* **4**, 595-602.

Beyersdorf, N., Gaupp, S., Balbach, K., Schmidt, J., Toyka, K. V., Lin, C. H., Hanke, T., Hunig, T., Kerkau, T. & Gold, R. (2005). Selective targeting of regulatory T cells with CD28 superagonists allows effective therapy of experimental autoimmune encephalomyelitis. *J Exp Med* **202**, 445-55.

Blake, N., Lee, S., Redchenko, I., Thomas, W., Steven, N., Leese, A., Steigerwald-Mullen, P., Kurilla, M. G., Frappier, L. & Rickinson, A. (1997). Human CD8+ T cell responses to EBV EBNA1: HLA class I presentation of the (Gly-Ala)-containing protein requires exogenous processing. *Immunity* **7**, 791-802.

Blansfield, J. A., Beck, K. E., Tran, K., Yang, J. C., Hughes, M. S., Kammula, U. S., Royal, R. E., Topalian, S. L., Haworth, L. R., Levy, C., Rosenberg, S. A. & Sherry, R. M. (2005). Cytotoxic T-lymphocyte-associated antigen-4 blockage can induce autoimmune hypophysitis in patients with metastatic melanoma and renal cancer. *J Immunother (1997)* **28**, 593-8.

Blaskovic, D., Stancekova, M., Svobodova, J. & Mistrikova, J. (1980). Isolation of five strains of herpesviruses from two species of free living small rodents. *Acta Virol* **24**, 468.

Boder, E. T., Midelfort, K. S. & Wittrup, K. D. (2000). Directed evolution of antibody fragments with monovalent femtomolar antigen-binding affinity. *Proc Natl Acad Sci U S A* **97**, 10701-5.

Bollard, C. M., Aguilar, L., Straathof, K. C., Gahn, B., Huls, M. H., Rousseau, A., Sixbey, J., Gresik, M. V., Carrum, G., Hudson, M., Dilloo, D., Gee, A., Brenner, M. K., Rooney, C. M. & Heslop, H. E. (2004). Cytotoxic T lymphocyte therapy for Epstein-Barr virus+ Hodgkin's disease. *J Exp Med* **200**, 1623-33.

Bollard, C. M., Gottschalk, S., Leen, A. M., Weiss, H., Straathof, K. C., Carrum, G., Khalil, M., Wu, M. F., Huls, M. H., Chang, C. C., Gresik, M. V., Gee, A. P., Brenner, M. K., Rooney, C. M. & Heslop, H. E. (2007). Complete responses of relapsed lymphoma following genetic modification of tumor-antigen presenting cells and T-lymphocyte transfer. *Blood*.

Bollard, C. M., Rossig, C., Calonge, M. J., Huls, M. H., Wagner, H. J., Massague, J., Brenner, M. K., Heslop, H. E. & Rooney, C. M. (2002). Adapting a transforming growth factor beta-related tumor protection strategy to enhance antitumor immunity. *Blood* **99**, 3179-87.

Borza, C. M. & Hutt-Fletcher, L. M. (2002). Alternate replication in B cells and epithelial cells switches tropism of Epstein-Barr virus. *Nat Med* **8**, 594-9.

Bosma, G. C., Custer, R. P. & Bosma, M. J. (1983). A severe combined immunodeficiency mutation in the mouse. *Nature* **301**, 527-30.

Bosma, G. C., Fried, M., Custer, R. P., Carroll, A., Gibson, D. M. & Bosma, M. J. (1988). Evidence of functional lymphocytes in some (leaky) scid mice. *J Exp Med* **167**, 1016-33.

Bradbury, A. R. & Marks, J. D. (2004). Antibodies from phage antibody libraries. *J Immunol Methods* **290**, 29-49.

Brentjens, R. J., Latouche, J. B., Santos, E., Marti, F., Gong, M. C., Lyddane, C., King, P. D., Larson, S., Weiss, M., Riviere, I. & Sadelain, M. (2003). Eradication of systemic B-cell tumors by genetically targeted human T lymphocytes co-stimulated by CD80 and interleukin-15.[see comment]. *Nature Medicine* **9**, 279-86.

Brooks, G. F., Butel, J. S. & Morse, S. A. (2001). Medical Microbiology, 22nd edn. Chicago: Lange Medical Books.

Brooks, L., Yao, Q. Y., Rickinson, A. B. & Young, L. S. (1992). Epstein-Barr virus latent gene transcription in nasopharyngeal carcinoma cells: coexpression of EBNA1, LMP1, and LMP2 transcripts. *J Virol* **66**, 2689-97.

Buday, L. (1999). Membrane-targeting of signalling molecules by SH2/SH3 domain-containing adaptor proteins. *Biochim Biophys Acta* **1422**, 187-204.

Burkitt, D. (1958). A sarcoma involving the jaws in African children. *Br J Surg* **46**, 218-23.

Burkitt, D. (1962). A children's cancer dependent on climatic factors. *Nature* **194**, 232-4.

Burns, D. M. & Crawford, D. H. (2004). Epstein-Barr virus-specific cytotoxic T-lymphocytes for adoptive immunotherapy of post-transplant lymphoproliferative disease. *Blood Rev* **18**, 193-209.

Caldwell, R. G., Wilson, J. B., Anderson, S. J. & Longnecker, R. (1998). Epstein-Barr virus LMP2A drives B cell development and survival in the absence of normal B cell receptor signals. *Immunity* **9**, 405-11.

Callan, M. F., Steven, N., Krausa, P., Wilson, J. D., Moss, P. A., Gillespie, G. M., Bell, J. I., Rickinson, A. B. & McMichael, A. J. (1996). Large clonal

expansions of CD8+ T cells in acute infectious mononucleosis. *Nat Med* **2**, 906-11.

Carosella, E. D., Moreau, P., Le Maoult, J., Le Discorde, M., Dausset, J. & Rouas-Freiss, N. (2003). HLA-G molecules: from maternal-fetal tolerance to tissue acceptance. *Adv Immunol* **81**, 199-252.

Casey, J. L., Napier, M. P., King, D. J., Pedley, R. B., Chaplin, L. C., Weir, N., Skelton, L., Green, A. J., Hope-Stone, L. D., Yarranton, G. T. & Begent, R. H. (2002). Tumour targeting of humanised cross-linked divalent-Fab' antibody fragments: a clinical phase I/II study. *Br J Cancer* **86**, 1401-10.

Cen, H., Williams, P. A., McWilliams, H. P., Breinig, M. C., Ho, M. & McKnight, J. L. (1993). Evidence for restricted Epstein-Barr virus latent gene expression and anti-EBNA antibody response in solid organ transplant recipients with posttransplant lymphoproliferative disorders. *Blood* **81**, 1393-403.

Chang, Y., Tung, C. H., Huang, Y. T., Lu, J., Chen, J. Y. & Tsai, C. H. (1999). Requirement for cell-to-cell contact in Epstein-Barr virus infection of nasopharyngeal carcinoma cells and keratinocytes. *J Virol* **73**, 8857-66.

Cheadle, E. J., Gilham, D. E., Thistlethwaite, F. C., Radford, J. A. & Hawkins, R. E. (2005). Killing of non-Hodgkin lymphoma cells by autologous CD19 engineered T cells. *British Journal of Haematology* **129**, 322-32.

Cheever, M. A., Greenberg, P. D., Fefer, A. & Gillis, S. (1982). Augmentation of the anti-tumor therapeutic efficacy of long-term cultured T lymphocytes by in vivo administration of purified interleukin 2. *J Exp Med* **155**, 968-80.

Cheng, L. E., Ohlen, C., Nelson, B. H. & Greenberg, P. D. (2002). Enhanced signaling through the IL-2 receptor in CD8+ T cells regulated by antigen recognition results in preferential proliferation and expansion of responding CD8+ T cells rather than promotion of cell death. *Proc Natl Acad Sci U S A* **99**, 3001-6.

Cheung, S. T., Huang, D. P., Hui, A. B., Lo, K. W., Ko, C. W., Tsang, Y. S., Wong, N., Whitney, B. M. & Lee, J. C. (1999). Nasopharyngeal carcinoma cell line (C666-1) consistently harbouring Epstein-Barr virus. *International Journal of Cancer* **83**, 121-6.

Chevallier-Greco, A., Manet, E., Chavrier, P., Mosnier, C., Daillie, J. & Sergeant, A. (1986). Both Epstein-Barr virus (EBV)-encoded trans-acting factors, EB1 and EB2, are required to activate transcription from an EBV early promoter. *Embo J* **5**, 3243-9.

Chien, Y. C., Chen, J. Y., Liu, M. Y., Yang, H. I., Hsu, M. M., Chen, C. J. & Yang, C. S. (2001). Serologic markers of Epstein-Barr virus infection and nasopharyngeal carcinoma in Taiwanese men. *N Engl J Med* **345**, 1877-82.

Ciceri, F., Bonini, C., Marktel, S., Zappone, E., Servida, P., Bernardi, M., Pescarollo, A., Bondanza, A., Peccatori, J., Rossini, S., Magnani, Z., Salomoni, M., Benati, C., Ponzoni, M., Callegaro, L., Corradini, P., Bregni, M., Traversari, C. & Bordignon, C. (2007). Antitumor effects of HSV-TK-engineered donor lymphocytes after allogeneic stem-cell transplantation. *Blood* **109**, 4698-707.

Clay, T. M., Custer, M. C., Sachs, J., Hwu, P., Rosenberg, S. A. & Nishimura, M. I. (1999). Efficient transfer of a tumor antigen-reactive TCR to human peripheral blood lymphocytes confers anti-tumor reactivity. *Journal of Immunology* **163**, 507-13.

Cludts, I. & Farrell, P. J. (1998). Multiple functions within the Epstein-Barr virus EBNA-3A protein. *J Virol* **72**, 1862-9.

Coffey, A. J., Brooksbank, R. A., Brandau, O., Oohashi, T., Howell, G. R., Bye, J. M., Cahn, A. P., Durham, J., Heath, P., Wray, P., Pavitt, R., Wilkinson, J., Leversha, M., Huckle, E., Shaw-Smith, C. J., Dunham, A., Rhodes, S., Schuster, V., Porta, G., Yin, L., Serafini, P., Sylla, B., Zollo, M., Franco, B., Bolino, A., Seri, M., Lanyi, A., Davis, J. R., Webster, D., Harris, A., Lenoir, G., de St Basile, G., Jones, A., Behloradsky, B. H., Achatz, H., Murken, J., Fassler, R., Sumegi, J., Romeo, G., Vaudin, M., Ross, M. T., Meindl, A. & Bentley, D. R. (1998). Host response to EBV infection in X-linked lymphoproliferative disease results from mutations in an SH2-domain encoding gene. *Nat Genet* **20**, 129-35.

Cohen, C. J., Li, Y. F., El-Gamil, M., Robbins, P. F., Rosenberg, S. A. & Morgan, R. A. (2007). Enhanced antitumor activity of T cells engineered to express T-cell receptors with a second disulfide bond. *Cancer Res* **67**, 3898-903.

Comoli, P., Pedrazzoli, P., Maccario, R., Basso, S., Carminati, O., Labirio, M., Schiavo, R., Secondino, S., Frasson, C., Perotti, C., Moroni, M., Locatelli, F. & Siena, S. (2005). Cell therapy of stage IV nasopharyngeal carcinoma with autologous Epstein-Barr virus-targeted cytotoxic T lymphocytes. *Journal of Clinical Oncology* **23**, 8942-9.

Cooper, L. J., Al-Kadhimi, Z., Serrano, L. M., Pfeiffer, T., Olivares, S., Castro, A., Chang, W. C., Gonzalez, S., Smith, D., Forman, S. J. & Jensen, M. C. (2005). Enhanced antilymphoma efficacy of CD19-redirected influenza MP1-specific CTLs by cotransfer of T cells modified to present influenza MP1. *Blood* **105**, 1622-31.

Cooper, L. J., Topp, M. S., Serrano, L. M., Gonzalez, S., Chang, W. C., Naranjo, A., Wright, C., Popplewell, L., Raubitschek, A., Forman, S. J. & Jensen, M. C. (2003). T-cell clones can be rendered specific for CD19: toward the selective augmentation of the graft-versus-B-lineage leukemia effect. *Blood* **101**, 1637-44.

Cordier, M., Calender, A., Billaud, M., Zimber, U., Rousselet, G., Pavlish, O., Banchereau, J., Tursz, T., Bornkamm, G. & Lenoir, G. M. (1990). Stable transfection of Epstein-Barr virus (EBV) nuclear antigen 2 in lymphoma cells containing the EBV P3HR1 genome induces expression of B-cell activation molecules CD21 and CD23. *J Virol* **64**, 1002-13.

Cox, C., Chang, S., Karran, L., Griffin, B. & Wedderburn, N. (1996). Persistent Epstein-Barr virus infection in the common marmoset (Callithrix jacchus). *J Gen Virol* **77 (Pt 6)**, 1173-80.

Cox, M. A., Leahy, J. & Hardwick, J. M. (1990). An enhancer within the divergent promoter of Epstein-Barr virus responds synergistically to the R and Z transactivators. *J Virol* **64**, 313-21.

Crawford, D. H. (2001). Biology and disease associations of Epstein-Barr virus. *Philos Trans R Soc Lond B Biol Sci* **356**, 461-73.

Crawford, D. H. & Ando, I. (1986). EB virus induction is associated with B-cell maturation. *Immunology* **59**, 405-9.

Crawford, D. H., Macsween, K. F., Higgins, C. D., Thomas, R., McAulay, K., Williams, H., Harrison, N., Reid, S., Conacher, M., Douglas, J. & Swerdlow, A. J. (2006). A cohort study among university students: identification of risk factors for Epstein-Barr virus seroconversion and infectious mononucleosis. *Clin Infect Dis* **43**, 276-82.

Dawson, C. W., Rickinson, A. B. & Young, L. S. (1990). Epstein-Barr virus latent membrane protein inhibits human epithelial cell differentiation. *Nature* **344**, 777-80.

de-The, G., Geser, A., Day, N. E., Tukei, P. M., Williams, E. H., Beri, D. P., Smith, P. G., Dean, A. G., Bronkamm, G. W., Feorino, P. & Henle, W. (1978). Epidemiological evidence for causal relationship between Epstein-Barr virus and Burkitt's lymphoma from Ugandan prospective study. *Nature* **274**, 756-61.

de Haard, H. J., van Neer, N., Reurs, A., Hufton, S. E., Roovers, R. C., Henderikx, P., de Bruine, A. P., Arends, J. W. & Hoogenboom, H. R. (1999). A large non-immunized human Fab fragment phage library that permits rapid isolation and kinetic analysis of high affinity antibodies. *J Biol Chem* **274**, 18218-30.

de Kruif, J., Terstappen, L., Boel, E. & Logtenberg, T. (1995). Rapid selection of cell subpopulation-specific human monoclonal antibodies from a synthetic phage antibody library. *Proc Natl Acad Sci U S A* **92**, 3938-42.

Deacon, E. M., Pallesen, G., Niedobitek, G., Crocker, J., Brooks, L., Rickinson, A. B. & Young, L. S. (1993). Epstein-Barr virus and Hodgkin's disease: transcriptional analysis of virus latency in the malignant cells. *J Exp Med* **177**, 339-49.

Diehl, V., Kirchner, H. H., Burrichter, H., Stein, H., Fonatsch, C., Gerdes, J., Schaadt, M., Heit, W., Uchanska-Ziegler, B., Ziegler, A., Heintz, F. & Sueno, K. (1982). Characteristics of Hodgkin's disease-derived cell lines. *Cancer Treatment Reports* **66**, 615-32.

Diehl, V., Kirchner, H. H., Schaadt, M., Fonatsch, C., Stein, H., Gerdes, J. & Boie, C. (1981). Hodgkin's disease: establishment and characterization of four in vitro cell lines. *Journal of Cancer Research & Clinical Oncology* **101**, 111-24.

Diepstra, A., Niens, M., Vellenga, E., van Imhoff, G. W., Nolte, I. M., Schaapveld, M., van der Steege, G., van den Berg, A., Kibbelaar, R. E., te Meerman, G. J. & Poppema, S. (2005). Association with HLA class I in Epstein-Barr-virus-positive and with HLA class III in Epstein-Barr-virus-negative Hodgkin's lymphoma.[see comment]. *Lancet* **365**, 2216-24.

Dillner, J., Sternas, L., Kallin, B., Alexander, H., Ehlin-Henriksson, B., Jornvall, H., Klein, G. & Lerner, R. (1984). Antibodies against a synthetic peptide identify the Epstein-Barr virus-determined nuclear antigen. *Proc Natl Acad Sci U S A* **81**, 4652-6.

Dirmeier, U., Hoffmann, R., Kilger, E., Schultheiss, U., Briseno, C., Gires, O., Kieser, A., Eick, D., Sugden, B. & Hammerschmidt, W. (2005). Latent membrane protein 1 of Epstein-Barr virus coordinately regulates proliferation with control of apoptosis. *Oncogene* **24**, 1711-7.

Dooley, H. & Flajnik, M. F. (2005). Shark immunity bites back: affinity maturation and memory response in the nurse shark, Ginglymostoma cirratum. *Eur J Immunol* **35**, 936-45.

Dorshkind, K., Pollack, S. B., Bosma, M. J. & Phillips, R. A. (1985). Natural killer (NK) cells are present in mice with severe combined immunodeficiency (scid). *J Immunol* **134**, 3798-801.

Drexler, H. G. (1992). Recent results on the biology of Hodgkin and Reed-Sternberg cells. I. Biopsy material. *Leuk Lymphoma* **8**, 283-313.

Drexler, H. G. (1993). Recent results on the biology of Hodgkin and Reed-Sternberg cells. II. Continuous cell lines. *Leukemia & Lymphoma* **9**, 1-25.

Drexler, H. G., Gaedicke, G., Lok, M. S., Diehl, V. & Minowada, J. (1986). Hodgkin's disease derived cell lines HDLM-2 and L-428: comparison of morphology, immunological and isoenzyme profiles. *Leukemia Research* **10**, 487-500.

Drexler, H. G., Gignac, S. M., Hoffbrand, A. V., Leber, B. F., Norton, J., Lok, M. S. & Minowada, J. (1989). Characterization of Hodgkin's disease derived cell line HDLM-2. *Recent Results Cancer Res* **117**, 75-82.

Dudley, M. E., Wunderlich, J., Nishimura, M. I., Yu, D., Yang, J. C., Topalian, S. L., Schwartzentruber, D. J., Hwu, P., Marincola, F. M., Sherry, R., Leitman, S. F. & Rosenberg, S. A. (2001). Adoptive transfer of cloned melanoma-reactive T lymphocytes for the treatment of patients with metastatic melanoma. *J Immunother (1997)* **24**, 363-73.

Dudley, M. E., Wunderlich, J. R., Robbins, P. F., Yang, J. C., Hwu, P., Schwartzentruber, D. J., Topalian, S. L., Sherry, R., Restifo, N. P., Hubicki, A. M., Robinson, M. R., Raffeld, M., Duray, P., Seipp, C. A., Rogers-Freezer, L., Morton, K. E., Mavroukakis, S. A., White, D. E. & Rosenberg, S. A. (2002). Cancer regression and autoimmunity in patients after clonal repopulation with antitumor lymphocytes. *Science* **298**, 850-4.

Efstathiou, S., Ho, Y. M., Hall, S., Styles, C. J., Scott, S. D. & Gompels, U. A. (1990). Murine herpesvirus 68 is genetically related to the gammaherpesviruses Epstein-Barr virus and herpesvirus saimiri. *J Gen Virol* **71 (Pt 6)**, 1365-72.

Einsele, H., Roosnek, E., Rufer, N., Sinzger, C., Riegler, S., Loffler, J., Grigoleit, U., Moris, A., Rammensee, H. G., Kanz, L., Kleihauer, A., Frank, F., Jahn, G. & Hebart, H. (2002). Infusion of cytomegalovirus (CMV)-specific T cells for the treatment of CMV infection not responding to antiviral chemotherapy. *Blood* **99**, 3916-22.

Eliopoulos, A. G., Gallagher, N. J., Blake, S. M., Dawson, C. W. & Young, L. S. (1999). Activation of the p38 mitogen-activated protein kinase pathway by Epstein-Barr virus-encoded latent membrane protein 1 coregulates interleukin-6 and interleukin-8 production. *J Biol Chem* **274**, 16085-96.

Emini, E. A., Luka, J., Armstrong, M. E., Banker, F. S., Provost, P. J. & Pearson, G. R. (1986). Establishment and characterization of a chronic infectious mononucleosislike syndrome in common marmosets. *J Med Virol* **18**, 369-79.

Epstein, M. A., Achong, B. G. & Barr, Y. M. (1964). Virus Particles in Cultured Lymphoblasts from Burkitt's Lymphoma. *Lancet* **1**, 702-3.

Epstein, M. A. & Barr, Y. M. (1964). Cultivation in Vitro of Human Lymphoblasts from Burkitt's Malignant Lymphoma. *Lancet* **1**, 252-3.

Epstein, M. A., Morgan, A. J., Finerty, S., Randle, B. J. & Kirkwood, J. K. (1985). Protection of cottontop tamarins against Epstein-Barr virus-induced malignant lymphoma by a prototype subunit vaccine. *Nature* **318**, 287-9.

Erickson, K. D. & Martin, J. M. (1997). Early detection of the lytic LMP-1 protein in EBV-infected B-cells suggests its presence in the virion. *Virology* **234**, 1-13.

Eshhar, Z., Waks, T., Bendavid, A. & Schindler, D. G. (2001). Functional expression of chimeric receptor genes in human T cells. *J Immunol Methods* **248**, 67-76.

Eshhar, Z., Waks, T., Gross, G. & Schindler, D. G. (1993). Specific activation and targeting of cytotoxic lymphocytes through chimeric single chains consisting

of antibody-binding domains and the gamma or zeta subunits of the immunoglobulin and T-cell receptors. *Proc Natl Acad Sci U S A* **90**, 720-4.
Evan, G. I., Lewis, G. K., Ramsay, G. & Bishop, J. M. (1985). Isolation of monoclonal antibodies specific for human c-myc proto-oncogene product. *Molecular & Cellular Biology* **5**, 3610-6.
Fahraeus, R., Rymo, L., Rhim, J. S. & Klein, G. (1990). Morphological transformation of human keratinocytes expressing the LMP gene of Epstein-Barr virus. *Nature* **345**, 447-9.
Falkenburg, J. H., Wafelman, A. R., Joosten, P., Smit, W. M., van Bergen, C. A., Bongaerts, R., Lurvink, E., van der Hoorn, M., Kluck, P., Landegent, J. E., Kluin-Nelemans, H. C., Fibbe, W. E. & Willemze, R. (1999). Complete remission of accelerated phase chronic myeloid leukemia by treatment with leukemia-reactive cytotoxic T lymphocytes. *Blood* **94**, 1201-8.
Farrell, P. J., Hollyoake, M., Niedobitek, G., Agathanggelou, A., Morgan, A. & Wedderburn, N. (1997). Direct demonstration of persistent Epstein-Barr virus gene expression in peripheral blood of infected common marmosets and analysis of virus-infected tissues in vivo. *J Gen Virol* **78 (Pt 6)**, 1417-24.
Faulkner, G. C., Burrows, S. R., Khanna, R., Moss, D. J., Bird, A. G. & Crawford, D. H. (1999). X-Linked agammaglobulinemia patients are not infected with Epstein-Barr virus: implications for the biology of the virus. *J Virol* **73**, 1555-64.
Faulkner, G. C., Krajewski, A. S. & Crawford, D. H. (2000). The ins and outs of EBV infection. *Trends Microbiol* **8**, 185-9.
FDAOrangeBook (2007). Approved Drug Products With Therapeutic Equivalence Evaluations (Orange Book). Edited by CenterforDrugEvaluationandResearch. USA: Food and Drug Administration.
Fingeroth, J. D., Diamond, M. E., Sage, D. R., Hayman, J. & Yates, J. L. (1999). CD21-Dependent infection of an epithelial cell line, 293, by Epstein-Barr virus. *J Virol* **73**, 2115-25.
Fingeroth, J. D., Weis, J. J., Tedder, T. F., Strominger, J. L., Biro, P. A. & Fearon, D. T. (1984). Epstein-Barr virus receptor of human B lymphocytes is the C3d receptor CR2. *Proc Natl Acad Sci U S A* **81**, 4510-4.
Finney, H. M., Lawson, A. D., Bebbington, C. R. & Weir, A. N. (1998). Chimeric receptors providing both primary and costimulatory signaling in T cells from a single gene product. *J Immunol* **161**, 2791-7.
Fixman, E. D., Hayward, G. S. & Hayward, S. D. (1992). Trans-acting requirements for replication of Epstein-Barr virus ori-Lyt. *J Virol* **66**, 5030-9.
Floettmann, J. E. & Rowe, M. (1997). Epstein-Barr virus latent membrane protein-1 (LMP1) C-terminus activation region 2 (CTAR2) maps to the far C-terminus and requires oligomerisation for NF-kappaB activation. *Oncogene* **15**, 1851-8.
Fogh, J., Fogh, J. M. & Orfeo, T. (1977). One hundred and twenty-seven cultured human tumor cell lines producing tumors in nude mice. *J Natl Cancer Inst* **59**, 221-6.
Foss, H. D., Herbst, H., Hummel, M., Araujo, I., Latza, U., Rancso, C., Dallenbach, F. & Stein, H. (1994). Patterns of cytokine gene expression in infectious mononucleosis. *Blood* **83**, 707-12.
Frank, A., Andiman, W. A. & Miller, G. (1976). Epstein-Barr virus and nonhuman primates: natural and experimental infection. *Adv Cancer Res* **23**, 171-201.

Frech, B., Zimber-Strobl, U., Suentzenich, K. O., Pavlish, O., Lenoir, G. M., Bornkamm, G. W. & Mueller-Lantzsch, N. (1990). Identification of Epstein-Barr virus terminal protein 1 (TP1) in extracts of four lymphoid cell lines, expression in insect cells, and detection of antibodies in human sera. *J Virol* **64**, 2759-67.

Fulop, G. M. & Phillips, R. A. (1990). The scid mutation in mice causes a general defect in DNA repair. *Nature* **347**, 479-82.

Furlong, D., Swift, H. & Roizman, B. (1972). Arrangement of herpesvirus deoxyribonucleic acid in the core. *J Virol* **10**, 1071-4.

Garzelli, C., Taub, F. E., Scharff, J. E., Prabhakar, B. S., Ginsberg-Fellner, F. & Notkins, A. L. (1984). Epstein-Barr virus-transformed lymphocytes produce monoclonal autoantibodies that react with antigens in multiple organs. *J Virol* **52**, 722-5.

Geiger, T. L., Nguyen, P., Leitenberg, D. & Flavell, R. A. (2001). Integrated src kinase and costimulatory activity enhances signal transduction through single-chain chimeric receptors in T lymphocytes. *Blood* **98**, 2364-71.

Gerber, P., Lucas, S., Nonoyama, M., Perlin, E. & Goldstein, L. I. (1972). Oral excretion of Epstein-Barr virus by healthy subjects and patients with infectious mononucleosis. *Lancet* **2**, 988-9.

Gil, D., Schamel, W. W., Montoya, M., Sanchez-Madrid, F. & Alarcon, B. (2002). Recruitment of Nck by CD3 epsilon reveals a ligand-induced conformational change essential for T cell receptor signaling and synapse formation. *Cell* **109**, 901-12.

Gilham, D. E., O'Neil, A., Hughes, C., Guest, R. D., Kirillova, N., Lehane, M. & Hawkins, R. E. (2002). Primary polyclonal human T lymphocytes targeted to carcino-embryonic antigens and neural cell adhesion molecule tumor antigens by CD3zeta-based chimeric immune receptors. *Journal of Immunotherapy* **25**, 139-51.

Giulino, L. B., Bussel, J. B. & Neufeld, E. J. (2007). Treatment with rituximab in benign and malignant hematologic disorders in children. *J Pediatr* **150**, 338-44, 344 e1.

Glaser, R. & Nonoyama, M. (1974). Host cell regulation of induction of Epstein-Barr virus. *J Virol* **14**, 174-6.

Glaser, S. L., Clarke, C. A., Gulley, M. L., Craig, F. E., DiGiuseppe, J. A., Dorfman, R. F., Mann, R. B. & Ambinder, R. F. (2003). Population-based patterns of human immunodeficiency virus-related Hodgkin lymphoma in the Greater San Francisco Bay Area, 1988-1998. *Cancer* **98**, 300-9.

Glaser, S. L. & Jarrett, R. F. (1996). The epidemiology of Hodgkin's disease. *Baillieres Clin Haematol* **9**, 401-16.

Goletz, S., Christensen, P. A., Kristensen, P., Blohm, D., Tomlinson, I., Winter, G. & Karsten, U. (2002). Selection of large diversities of antiidiotypic antibody fragments by phage display. *Journal of Molecular Biology* **315**, 1087-97.

Gong, M. C., Latouche, J. B., Krause, A., Heston, W. D., Bander, N. H. & Sadelain, M. (1999). Cancer patient T cells genetically targeted to prostate-specific membrane antigen specifically lyse prostate cancer cells and release cytokines in response to prostate-specific membrane antigen. *Neoplasia* **1**, 123-7.

Gordon, L. I., Witzig, T., Molina, A., Czuczman, M., Emmanouilides, C., Joyce, R., Vo, K., Theuer, C., Pohlman, B., Bartlett, N., Wiseman, G., Darif, M. & White, C. (2004). Yttrium 90-labeled ibritumomab tiuxetan

radioimmunotherapy produces high response rates and durable remissions in patients with previously treated B-cell lymphoma. *Clin Lymphoma* **5**, 98-101.
Gottschalk, S., Rooney, C. M. & Heslop, H. E. (2005). Post-transplant lymphoproliferative disorders. *Annu Rev Med* **56**, 29-44.
Greenspan, D., De Souza, Y. G., Conant, M. A., Hollander, H., Chapman, S. K., Lennette, E. T., Petersen, V. & Greenspan, J. S. (1990). Efficacy of desciclovir in the treatment of Epstein-Barr virus infection in oral hairy leukoplakia. *J Acquir Immune Defic Syndr* **3**, 571-8.
Greenspan, J. S., Greenspan, D., Lennette, E. T., Abrams, D. I., Conant, M. A., Petersen, V. & Freese, U. K. (1985). Replication of Epstein-Barr virus within the epithelial cells of oral "hairy" leukoplakia, an AIDS-associated lesion. *N Engl J Med* **313**, 1564-71.
Gregory, C. D., Tursz, T., Edwards, C. F., Tetaud, C., Talbot, M., Caillou, B., Rickinson, A. B. & Lipinski, M. (1987). Identification of a subset of normal B cells with a Burkitt's lymphoma (BL)-like phenotype. *J Immunol* **139**, 313-8.
Griffiths, A. D., Malmqvist, M., Marks, J. D., Bye, J. M., Embleton, M. J., McCafferty, J., Baier, M., Holliger, K. P., Gorick, B. D., Hughes-Jones, N. C. & et al. (1993). Human anti-self antibodies with high specificity from phage display libraries. *Embo J* **12**, 725-34.
Griffiths, R. W., Elkord, E., Gilham, D. E., Ramani, V., Clarke, N., Stern, P. L. & Hawkins, R. E. (2007). Frequency of regulatory T cells in renal cell carcinoma patients and investigation of correlation with survival. *Cancer Immunol Immunother*.
Grossman, S. R., Johannsen, E., Tong, X., Yalamanchili, R. & Kieff, E. (1994). The Epstein-Barr virus nuclear antigen 2 transactivator is directed to response elements by the J kappa recombination signal binding protein. *Proc Natl Acad Sci U S A* **91**, 7568-72.
Gruss, H. J. & Kadin, M. E. (1996). Pathophysiology of Hodgkin's disease: functional and molecular aspects. *Baillieres Clin Haematol* **9**, 417-46.
Haan, K. M., Kwok, W. W., Longnecker, R. & Speck, P. (2000). Epstein-Barr virus entry utilizing HLA-DP or HLA-DQ as a coreceptor. *J Virol* **74**, 2451-4.
Hacein-Bey-Abina, S., Von Kalle, C., Schmidt, M., McCormack, M. P., Wulffraat, N., Leboulch, P., Lim, A., Osborne, C. S., Pawliuk, R., Morillon, E., Sorensen, R., Forster, A., Fraser, P., Cohen, J. I., de Saint Basile, G., Alexander, I., Wintergerst, U., Frebourg, T., Aurias, A., Stoppa-Lyonnet, D., Romana, S., Radford-Weiss, I., Gross, F., Valensi, F., Delabesse, E., Macintyre, E., Sigaux, F., Soulier, J., Leiva, L. E., Wissler, M., Prinz, C., Rabbitts, T. H., Le Deist, F., Fischer, A. & Cavazzana-Calvo, M. (2003). LMO2-associated clonal T cell proliferation in two patients after gene therapy for SCID-X1. *Science* **302**, 415-9.
Hamilton-Dutoit, S. J., Raphael, M., Audouin, J., Diebold, J., Lisse, I., Pedersen, C., Oksenhendler, E., Marelle, L. & Pallesen, G. (1993). In situ demonstration of Epstein-Barr virus small RNAs (EBER 1) in acquired immunodeficiency syndrome-related lymphomas: correlation with tumor morphology and primary site. *Blood* **82**, 619-24.
Hammerschmidt, W. & Sugden, B. (1988). Identification and characterization of oriLyt, a lytic origin of DNA replication of Epstein-Barr virus. *Cell* **55**, 427-33.

Hammerschmidt, W. & Sugden, B. (1989). Genetic analysis of immortalizing functions of Epstein-Barr virus in human B lymphocytes. *Nature* **340**, 393-7.
Hanke, T. (2006). Lessons from TGN1412. *Lancet* **368**, 1569-70; author reply 1570.
Hanto, D. W., Birkenbach, M., Frizzera, G., Gajl-Peczalska, K. J., Simmons, R. L. & Schubach, W. H. (1989). Confirmation of the heterogeneity of posttransplant Epstein-Barr virus-associated B cell proliferations by immunoglobulin gene rearrangement analyses. *Transplantation* **47**, 458-64.
Haque, T., Amlot, P. L., Helling, N., Thomas, J. A., Sweny, P., Rolles, K., Burroughs, A. K., Prentice, H. G. & Crawford, D. H. (1998). Reconstitution of EBV-specific T cell immunity in solid organ transplant recipients. *Journal of Immunology* **160**, 6204-9.
Haque, T., Wilkie, G. M., Jones, M. M., Higgins, C. D., Urquhart, G., Wingate, P., Burns, D., McAulay, K., Turner, M., Bellamy, C., Amlot, P. L., Kelly, D., Macgilchrist, A., Gandhi, M. K., Swerdlow, A. J. & Crawford, D. H. (2007). Allogeneic cytotoxic T cell therapy for EBV-positive post transplant lymphoproliferative disease: results of a phase II multicentre clinical trial. *Blood*.
Haque, T., Wilkie, G. M., Taylor, C., Amlot, P. L., Murad, P., Iley, A., Dombagoda, D., Britton, K. M., Swerdlow, A. J. & Crawford, D. H. (2002). Treatment of Epstein-Barr-virus-positive post-transplantation lymphoproliferative disease with partly HLA-matched allogeneic cytotoxic T cells. *Lancet* **360**, 436-42.
Harada, S. & Kieff, E. (1997). Epstein-Barr virus nuclear protein LP stimulates EBNA-2 acidic domain-mediated transcriptional activation. *J Virol* **71**, 6611-8.
Haynes, N. M., Trapani, J. A., Teng, M. W., Jackson, J. T., Cerruti, L., Jane, S. M., Kershaw, M. H., Smyth, M. J. & Darcy, P. K. (2002). Single-chain antigen recognition receptors that costimulate potent rejection of established experimental tumors.[erratum appears in Blood. 2003 May 15;101(10):3808]. *Blood* **100**, 3155-63.
Henderson, S., Huen, D., Rowe, M., Dawson, C., Johnson, G. & Rickinson, A. (1993). Epstein-Barr virus-coded BHRF1 protein, a viral homologue of Bcl-2, protects human B cells from programmed cell death. *Proc Natl Acad Sci U S A* **90**, 8479-83.
Henderson, S., Rowe, M., Gregory, C., Croom-Carter, D., Wang, F., Longnecker, R., Kieff, E. & Rickinson, A. (1991). Induction of bcl-2 expression by Epstein-Barr virus latent membrane protein 1 protects infected B cells from programmed cell death. *Cell* **65**, 1107-15.
Henle, G. & Henle, W. (1966). Studies on cell lines derived from Burkitt's lymphoma. *Trans N Y Acad Sci* **29**, 71-9.
Hennessy, K., Fennewald, S., Hummel, M., Cole, T. & Kieff, E. (1984). A membrane protein encoded by Epstein-Barr virus in latent growth-transforming infection. *Proc Natl Acad Sci U S A* **81**, 7207-11.
Herbst, H., Foss, H. D., Samol, J., Araujo, I., Klotzbach, H., Krause, H., Agathanggelou, A., Niedobitek, G. & Stein, H. (1996). Frequent expression of interleukin-10 by Epstein-Barr virus-harboring tumor cells of Hodgkin's disease. *Blood* **87**, 2918-29.
Herbst, H., Tippelmann, G., Anagnostopoulos, I., Gerdes, J., Schwarting, R., Boehm, T., Pileri, S., Jones, D. B. & Stein, H. (1989). Immunoglobulin and T-cell receptor gene rearrangements in Hodgkin's disease and Ki-1-positive

anaplastic large cell lymphoma: dissociation between phenotype and genotype. *Leuk Res* **13**, 103-16.

Heussinger, N., Buttner, M., Ott, G., Brachtel, E., Pilch, B. Z., Kremmer, E. & Niedobitek, G. (2004). Expression of the Epstein-Barr virus (EBV)-encoded latent membrane protein 2A (LMP2A) in EBV-associated nasopharyngeal carcinoma. *J Pathol* **203**, 696-9.

Hislop, A. D., Annels, N. E., Gudgeon, N. H., Leese, A. M. & Rickinson, A. B. (2002). Epitope-specific evolution of human CD8(+) T cell responses from primary to persistent phases of Epstein-Barr virus infection. *J Exp Med* **195**, 893-905.

Hitt, M. M., Allday, M. J., Hara, T., Karran, L., Jones, M. D., Busson, P., Tursz, T., Ernberg, I. & Griffin, B. E. (1989). EBV gene expression in an NPC-related tumour. *Embo J* **8**, 2639-51.

Hochberg, D., Middeldorp, J. M., Catalina, M., Sullivan, J. L., Luzuriaga, K. & Thorley-Lawson, D. A. (2004). Demonstration of the Burkitt's lymphoma Epstein-Barr virus phenotype in dividing latently infected memory cells in vivo. *Proc Natl Acad Sci U S A* **101**, 239-44.

Hodi, F. S., Mihm, M. C., Soiffer, R. J., Haluska, F. G., Butler, M., Seiden, M. V., Davis, T., Henry-Spires, R., MacRae, S., Willman, A., Padera, R., Jaklitsch, M. T., Shankar, S., Chen, T. C., Korman, A., Allison, J. P. & Dranoff, G. (2003). Biologic activity of cytotoxic T lymphocyte-associated antigen 4 antibody blockade in previously vaccinated metastatic melanoma and ovarian carcinoma patients. *Proc Natl Acad Sci U S A* **100**, 4712-7.

Holliger, P. & Hudson, P. J. (2005). Engineered antibody fragments and the rise of single domains. *Nat Biotechnol* **23**, 1126-36.

Hombach, A., Muche, J. M., Gerken, M., Gellrich, S., Heuser, C., Pohl, C., Sterry, W. & Abken, H. (2001). T cells engrafted with a recombinant anti-CD30 receptor target autologous CD30(+) cutaneous lymphoma cells. *Gene Ther* **8**, 891-5.

Hoogenboom, H. R. (2005). Selecting and screening recombinant antibody libraries. *Nat Biotechnol* **23**, 1105-16.

Hoogenboom, H. R., Griffiths, A. D., Johnson, K. S., Chiswell, D. J., Hudson, P. & Winter, G. (1991). Multi-subunit proteins on the surface of filamentous phage: methodologies for displaying antibody (Fab) heavy and light chains. *Nucleic Acids Res* **19**, 4133-7.

Hopwood, P. & Crawford, D. H. (2000). The role of EBV in post-transplant malignancies: a review. *Journal of Clinical Pathology* **53**, 248-54.

Howe, J. G. & Steitz, J. A. (1986). Localization of Epstein-Barr virus-encoded small RNAs by in situ hybridization. *Proc Natl Acad Sci U S A* **83**, 9006-10.

Hudson, G. S., Farrell, P. J. & Barrell, B. G. (1985). Two related but differentially expressed potential membrane proteins encoded by the EcoRI Dhet region of Epstein-Barr virus B95-8. *J Virol* **53**, 528-35.

Hudson, P. J. & Souriau, C. (2003). Engineered antibodies. *Nature Medicine* **9**, 129-34.

Huen, D. S., Henderson, S. A., Croom-Carter, D. & Rowe, M. (1995). The Epstein-Barr virus latent membrane protein-1 (LMP1) mediates activation of NF-kappa B and cell surface phenotype via two effector regions in its carboxy-terminal cytoplasmic domain. *Oncogene* **10**, 549-60.

Hughes, A. L. (2003). Genomes of mice and men. *Heredity* **90**, 115-7.

Hurwitz, H., Fehrenbacher, L., Novotny, W., Cartwright, T., Hainsworth, J., Heim, W., Berlin, J., Baron, A., Griffing, S., Holmgren, E., Ferrara, N., Fyfe, G., Rogers, B., Ross, R. & Kabbinavar, F. (2004). Bevacizumab plus irinotecan, fluorouracil, and leucovorin for metastatic colorectal cancer. *N Engl J Med* **350**, 2335-42.

IARC (1997). Working Group on the Evaluation of the Carcinogenic Risk of Chemicals to Humans: Epstein-Barr virus and Kaposi sarcoma herpesvirus/human herpesvirus 8. *IARC Monograph* **70**, 47-52.

Imai, C., Iwamoto, S. & Campana, D. (2005). Genetic modification of primary natural killer cells overcomes inhibitory signals and induces specific killing of leukemic cells. *Blood* **106**, 376-83.

Imai, S., Koizumi, S., Sugiura, M., Tokunaga, M., Uemura, Y., Yamamoto, N., Tanaka, S., Sato, E. & Osato, T. (1994). Gastric carcinoma: monoclonal epithelial malignant cells expressing Epstein-Barr virus latent infection protein. *Proc Natl Acad Sci U S A* **91**, 9131-5.

Imai, S., Nishikawa, J. & Takada, K. (1998). Cell-to-cell contact as an efficient mode of Epstein-Barr virus infection of diverse human epithelial cells. *Journal of Virology* **72**, 4371-8.

Jain, R. K. (2001). Delivery of molecular and cellular medicine to solid tumors. *Adv Drug Deliv Rev* **46**, 149-68.

Janz, A., Oezel, M., Kurzeder, C., Mautner, J., Pich, D., Kost, M., Hammerschmidt, W. & Delecluse, H. J. (2000). Infectious Epstein-Barr virus lacking major glycoprotein BLLF1 (gp350/220) demonstrates the existence of additional viral ligands. *J Virol* **74**, 10142-52.

Jarrett, R. F. (2006). Viruses and lymphoma/leukaemia. *J Pathol* **208**, 176-86.

Jensen, K. B., Jensen, O. N., Ravn, P., Clark, B. F. & Kristensen, P. (2003a). Identification of keratinocyte-specific markers using phage display and mass spectrometry. *Mol Cell Proteomics* **2**, 61-9.

Jensen, M. C., Cooper, L. J., Wu, A. M., Forman, S. J. & Raubitschek, A. (2003b). Engineered CD20-specific primary human cytotoxic T lymphocytes for targeting B-cell malignancy. *Cytotherapy* **5**, 131-8.

Johannessen, I., Asghar, M. & Crawford, D. H. (2000). Essential role for T cells in human B-cell lymphoproliferative disease development in severe combined immunodeficient mice. *British Journal of Haematology* **109**, 600-10.

Johannessen, I. & Crawford, D. H. (1999). In vivo models for Epstein-Barr virus (EBV)-associated B cell lymphoproliferative disease (BLPD). *Rev Med Virol* **9**, 263-77.

JointFormularyCommittee (2007). British National Formulary, 54 edn. London: British Medical Association and Royal Pharmaceutical Society of Great Britain.

June, C. H. (2007). Principles of adoptive T cell cancer therapy. *J Clin Invest* **117**, 1204-12.

Kalergis, A. M., Boucheron, N., Doucey, M. A., Palmieri, E., Goyarts, E. C., Vegh, Z., Luescher, I. F. & Nathenson, S. G. (2001). Efficient T cell activation requires an optimal dwell-time of interaction between the TCR and the pMHC complex. *Nat Immunol* **2**, 229-34.

Kanegane, H., Bhatia, K., Gutierrez, M., Kaneda, H., Wada, T., Yachie, A., Seki, H., Arai, T., Kagimoto, S., Okazaki, M., Oh-ishi, T., Moghaddam, A., Wang, F. & Tosato, G. (1998). A syndrome of peripheral blood T-cell infection with

Epstein-Barr virus (EBV) followed by EBV-positive T-cell lymphoma. *Blood* **91**, 2085-91.

Kanegane, H., Wado, T., Nunogami, K., Seki, H., Taniguchi, N. & Tosato, G. (1996). Chronic persistent Epstein-Barr virus infection of natural killer cells and B cells associated with granular lymphocytes expansion. *Br J Haematol* **95**, 116-22.

Kanzler, H., Hansmann, M. L., Kapp, U., Wolf, J., Diehl, V., Rajewsky, K. & Kuppers, R. (1996a). Molecular single cell analysis demonstrates the derivation of a peripheral blood-derived cell line (L1236) from the Hodgkin/Reed-Sternberg cells of a Hodgkin's lymphoma patient. *Blood* **87**, 3429-36.

Kanzler, H., Kuppers, R., Hansmann, M. L. & Rajewsky, K. (1996b). Hodgkin and Reed-Sternberg cells in Hodgkin's disease represent the outgrowth of a dominant tumor clone derived from (crippled) germinal center B cells. *J Exp Med* **184**, 1495-505.

Kaye, K. M., Izumi, K. M. & Kieff, E. (1993). Epstein-Barr virus latent membrane protein 1 is essential for B-lymphocyte growth transformation. *Proc Natl Acad Sci U S A* **90**, 9150-4.

Kennedy, G., Komano, J. & Sugden, B. (2003). Epstein-Barr virus provides a survival factor to Burkitt's lymphomas. *Proc Natl Acad Sci U S A* **100**, 14269-74.

Kenney, S., Kamine, J., Holley-Guthrie, E., Lin, J. C., Mar, E. C. & Pagano, J. (1989). The Epstein-Barr virus (EBV) BZLF1 immediate-early gene product differentially affects latent versus productive EBV promoters. *J Virol* **63**, 1729-36.

Kershaw, M. H., Westwood, J. A. & Hwu, P. (2002). Dual-specific T cells combine proliferation and antitumor activity. *Nat Biotechnol* **20**, 1221-7.

Kershaw, M. H., Westwood, J. A., Parker, L. L., Wang, G., Eshhar, Z., Mavroukakis, S. A., White, D. E., Wunderlich, J. R., Canevari, S., Rogers-Freezer, L., Chen, C. C., Yang, J. C., Rosenberg, S. A. & Hwu, P. (2006). A phase I study on adoptive immunotherapy using gene-modified T cells for ovarian cancer. *Clin Cancer Res* **12**, 6106-15.

Kessels, H. W., Wolkers, M. C., van den Boom, M. D., van der Valk, M. A. & Schumacher, T. N. (2001). Immunotherapy through TCR gene transfer.[see comment]. *Nature Immunology* **2**, 957-61.

Khan, G., Miyashita, E. M., Yang, B., Babcock, G. J. & Thorley-Lawson, D. A. (1996). Is EBV persistence in vivo a model for B cell homeostasis? *Immunity* **5**, 173-9.

Khanna, R., Bell, S., Sherritt, M., Galbraith, A., Burrows, S. R., Rafter, L., Clarke, B., Slaughter, R., Falk, M. C., Douglass, J., Williams, T., Elliott, S. L. & Moss, D. J. (1999). Activation and adoptive transfer of Epstein-Barr virus-specific cytotoxic T cells in solid organ transplant patients with posttransplant lymphoproliferative disease. *Proc Natl Acad Sci U S A* **96**, 10391-6.

Khanna, R. & Burrows, S. R. (2000). Role of cytotoxic T lymphocytes in Epstein-Barr virus-associated diseases. *Annu Rev Microbiol* **54**, 19-48.

Khanna, R., Burrows, S. R., Kurilla, M. G., Jacob, C. A., Misko, I. S., Sculley, T. B., Kieff, E. & Moss, D. J. (1992). Localization of Epstein-Barr virus cytotoxic T cell epitopes using recombinant vaccinia: implications for vaccine development. *J Exp Med* **176**, 169-76.

Kieff, E. & Rickinson, A. B. (2007). Epstein-Barr Virus and Its Replication. In *Fields Virology*, 5th edn, pp. 2603-2654. Edited by D. Knipe & P. Howley. Philadelphia: Lippincott Williams and Wilkins.

Kilger, E., Kieser, A., Baumann, M. & Hammerschmidt, W. (1998). Epstein-Barr virus-mediated B-cell proliferation is dependent upon latent membrane protein 1, which simulates an activated CD40 receptor. *Embo J* **17**, 1700-9.

Kis, L. L., Nishikawa, J., Takahara, M., Nagy, N., Matskova, L., Takada, K., Elmberger, P. G., Ohlsson, A., Klein, G. & Klein, E. (2005). In vitro EBV-infected subline of KMH2, derived from Hodgkin lymphoma, expresses only EBNA-1, while CD40 ligand and IL-4 induce LMP-1 but not EBNA-2. *International Journal of Cancer* **113**, 937-45.

Kitagawa, N., Goto, M., Kurozumi, K., Maruo, S., Fukayama, M., Naoe, T., Yasukawa, M., Hino, K., Suzuki, T., Todo, S. & Takada, K. (2000). Epstein-Barr virus-encoded poly(A)(-) RNA supports Burkitt's lymphoma growth through interleukin-10 induction. *Embo J* **19**, 6742-50.

Klein, G., Giovanella, B. C., Lindahl, T., Fialkow, P. J., Singh, S. & Stehlin, J. S. (1974). Direct evidence for the presence of Epstein-Barr virus DNA and nuclear antigen in malignant epithelial cells from patients with poorly differentiated carcinoma of the nasopharynx. *Proc Natl Acad Sci U S A* **71**, 4737-41.

Klein, G., Svedmyr, E., Jondal, M. & Persson, P. O. (1976). EBV-determined nuclear antigen (EBNA)-positive cells in the peripheral blood of infectious mononucleosis patients. *Int J Cancer* **17**, 21-6.

Klimm, B., Engert, A. & Diehl, V. (2005). First-line treatment of Hodgkin's lymphoma. *Curr Hematol Rep* **4**, 15-22.

Knox, P. G., Li, Q. X., Rickinson, A. B. & Young, L. S. (1996). In vitro production of stable Epstein-Barr virus-positive epithelial cell clones which resemble the virus:cell interaction observed in nasopharyngeal carcinoma. *Virology* **215**, 40-50.

Kohler, G. & Milstein, C. (1975). Continuous cultures of fused cells secreting antibody of predefined specificity. *Nature* **256**, 495-7.

Kolb, H. J., Mittermuller, J., Clemm, C., Holler, E., Ledderose, G., Brehm, G., Heim, M. & Wilmanns, W. (1990). Donor leukocyte transfusions for treatment of recurrent chronic myelogenous leukemia in marrow transplant patients. *Blood* **76**, 2462-5.

Komano, J., Maruo, S., Kurozumi, K., Oda, T. & Takada, K. (1999). Oncogenic role of Epstein-Barr virus-encoded RNAs in Burkitt's lymphoma cell line Akata. *J Virol* **73**, 9827-31.

Kovalchuk, A. L., Qi, C. F., Torrey, T. A., Taddesse-Heath, L., Feigenbaum, L., Park, S. S., Gerbitz, A., Klobeck, G., Hoertnagel, K., Polack, A., Bornkamm, G. W., Janz, S. & Morse, H. C., 3rd (2000). Burkitt lymphoma in the mouse. *J Exp Med* **192**, 1183-90.

Kristensen, P. & Winter, G. (1998). Proteolytic selection for protein folding using filamentous bacteriophages. *Folding & Design* **3**, 321-8.

Kuppers, R. (2003). B cells under influence: transformation of B cells by Epstein-Barr virus. *Nature Reviews. Immunology* **3**, 801-12.

Lacerda, J. F., Ladanyi, M., Louie, D. C., Fernandez, J. M., Papadopoulos, E. B. & O'Reilly, R. J. (1996). Human Epstein-Barr virus (EBV)-specific cytotoxic T lymphocytes home preferentially to and induce selective regressions of

autologous EBV-induced B cell lymphoproliferations in xenografted C.B-17 scid/scid mice. *J Exp Med* **183**, 1215-28.

Laichalk, L. L. & Thorley-Lawson, D. A. (2005). Terminal differentiation into plasma cells initiates the replicative cycle of Epstein-Barr virus in vivo. *J Virol* **79**, 1296-307.

Lalonde, A., Avila-Carino, J., Caruso, M. & de Campos-Lima, P. O. (2007). Rescue of the immunotherapeutic potential of a novel T cell epitope in the Epstein-Barr virus latent membrane protein 2. *Virology* **361**, 253-62.

Lam, K. M., Syed, N., Whittle, H. & Crawford, D. H. (1991). Circulating Epstein-Barr virus-carrying B cells in acute malaria. *Lancet* **337**, 876-8.

Lamers, C. H., Sleijfer, S., Vulto, A. G., Kruit, W. H., Kliffen, M., Debets, R., Gratama, J. W., Stoter, G. & Oosterwijk, E. (2006). Treatment of metastatic renal cell carcinoma with autologous T-lymphocytes genetically retargeted against carbonic anhydrase IX: first clinical experience. *J Clin Oncol* **24**, e20-2.

Larson, R. A., Sievers, E. L., Stadtmauer, E. A., Lowenberg, B., Estey, E. H., Dombret, H., Theobald, M., Voliotis, D., Bennett, J. M., Richie, M., Leopold, L. H., Berger, M. S., Sherman, M. L., Loken, M. R., van Dongen, J. J., Bernstein, I. D. & Appelbaum, F. R. (2005). Final report of the efficacy and safety of gemtuzumab ozogamicin (Mylotarg) in patients with CD33-positive acute myeloid leukemia in first recurrence. *Cancer* **104**, 1442-52.

Laux, G., Perricaudet, M. & Farrell, P. J. (1988). A spliced Epstein-Barr virus gene expressed in immortalized lymphocytes is created by circularization of the linear viral genome. *Embo J* **7**, 769-74.

Le Roux, A., Kerdiles, B., Walls, D., Dedieu, J. F. & Perricaudet, M. (1994). The Epstein-Barr virus determined nuclear antigens EBNA-3A, -3B, and -3C repress EBNA-2-mediated transactivation of the viral terminal protein 1 gene promoter. *Virology* **205**, 596-602.

Lee, M. A., Diamond, M. E. & Yates, J. L. (1999). Genetic evidence that EBNA-1 is needed for efficient, stable latent infection by Epstein-Barr virus. *J Virol* **73**, 2974-82.

Leen, A., Meij, P., Redchenko, I., Middeldorp, J., Bloemena, E., Rickinson, A. & Blake, N. (2001). Differential immunogenicity of Epstein-Barr virus latent-cycle proteins for human CD4(+) T-helper 1 responses. *J Virol* **75**, 8649-59.

Lennette, E. T., Winberg, G., Yadav, M., Enblad, G. & Klein, G. (1995). Antibodies to LMP2A/2B in EBV-carrying malignancies. *Eur J Cancer* **31A**, 1875-8.

Leung, E., Shenton, B. K., Jackson, G., Gould, F. K., Yap, C. & Talbot, D. (2002). Use of real-time PCR to measure Epstein-Barr virus genomes in whole blood. *Journal of Immunological Methods* **270**, 259-67.

Levitskaya, J., Coram, M., Levitsky, V., Imreh, S., Steigerwald-Mullen, P. M., Klein, G., Kurilla, M. G. & Masucci, M. G. (1995). Inhibition of antigen processing by the internal repeat region of the Epstein-Barr virus nuclear antigen-1. *Nature* **375**, 685-8.

Levitskaya, J., Sharipo, A., Leonchiks, A., Ciechanover, A. & Masucci, M. G. (1997). Inhibition of ubiquitin/proteasome-dependent protein degradation by the Gly-Ala repeat domain of the Epstein-Barr virus nuclear antigen 1. *Proc Natl Acad Sci U S A* **94**, 12616-21.

Li, Q., Turk, S. M. & Hutt-Fletcher, L. M. (1995). The Epstein-Barr virus (EBV) BZLF2 gene product associates with the gH and gL homologs of EBV and

carries an epitope critical to infection of B cells but not of epithelial cells. *J Virol* **69**, 3987-94.
Liebowitz, D., Wang, D. & Kieff, E. (1986). Orientation and patching of the latent infection membrane protein encoded by Epstein-Barr virus. *J Virol* **58**, 233-7.
Lindahl, T., Adams, A., Bjursell, G., Bornkamm, G. W., Kaschka-Dierich, C. & Jehn, U. (1976). Covalently closed circular duplex DNA of Epstein-Barr virus in a human lymphoid cell line. *J Mol Biol* **102**, 511-30.
Liu, C., Sista, N. D. & Pagano, J. S. (1996). Activation of the Epstein-Barr virus DNA polymerase promoter by the BRLF1 immediate-early protein is mediated through USF and E2F. *J Virol* **70**, 2545-55.
Liu, K. & Rosenberg, S. A. (2001). Transduction of an IL-2 gene into human melanoma-reactive lymphocytes results in their continued growth in the absence of exogenous IL-2 and maintenance of specific antitumor activity. *J Immunol* **167**, 6356-65.
Liu, Y. J. & Arpin, C. (1997). Germinal center development. *Immunol Rev* **156**, 111-26.
Lo, K. W. & Huang, D. P. (2002). Genetic and epigenetic changes in nasopharyngeal carcinoma. *Semin Cancer Biol* **12**, 451-62.
Lo, Y. M., Chan, L. Y., Chan, A. T., Leung, S. F., Lo, K. W., Zhang, J., Lee, J. C., Hjelm, N. M., Johnson, P. J. & Huang, D. P. (1999a). Quantitative and temporal correlation between circulating cell-free Epstein-Barr virus DNA and tumor recurrence in nasopharyngeal carcinoma. *Cancer Res* **59**, 5452-5.
Lo, Y. M., Chan, L. Y., Lo, K. W., Leung, S. F., Zhang, J., Chan, A. T., Lee, J. C., Hjelm, N. M., Johnson, P. J. & Huang, D. P. (1999b). Quantitative analysis of cell-free Epstein-Barr virus DNA in plasma of patients with nasopharyngeal carcinoma. *Cancer Res* **59**, 1188-91.
Longnecker, R. & Kieff, E. (1990). A second Epstein-Barr virus membrane protein (LMP2) is expressed in latent infection and colocalizes with LMP1. *J Virol* **64**, 2319-26.
Longnecker, R. & Miller, C. L. (1996). Regulation of Epstein-Barr virus latency by latent membrane protein 2. *Trends Microbiol* **4**, 38-42.
Lopes, V., Young, L. S. & Murray, P. G. (2003). Epstein-Barr virus-associated cancers: aetiology and treatment. *Herpes* **10**, 78-82.
Lozada-Nur, F., Robinson, J. & Regezi, J. A. (1994). Oral hairy leukoplakia in nonimmunosuppressed patients. Report of four cases. *Oral Surg Oral Med Oral Pathol* **78**, 599-602.
Lozzio, C. B. & Lozzio, B. B. (1975). Human chronic myelogenous leukemia cell-line with positive Philadelphia chromosome. *Blood* **45**, 321-34.
Macfarlane, G. J., Evstifeeva, T., Boyle, P. & Grufferman, S. (1995). International patterns in the occurrence of Hodgkin's disease in children and young adult males. *Int J Cancer* **61**, 165-9.
MacMahon, E. M., Glass, J. D., Hayward, S. D., Mann, R. B., Becker, P. S., Charache, P., McArthur, J. C. & Ambinder, R. F. (1991). Epstein-Barr virus in AIDS-related primary central nervous system lymphoma. *Lancet* **338**, 969-73.
Macsween, K. F. & Crawford, D. H. (2003). Epstein-Barr virus-recent advances. *Lancet Infect Dis* **3**, 131-40.
Maher, J., Brentjens, R. J., Gunset, G., Riviere, I. & Sadelain, M. (2002). Human T-lymphocyte cytotoxicity and proliferation directed by a single chimeric TCRzeta /CD28 receptor. *Nat Biotechnol* **20**, 70-5.

Maher, J. & Davies, E. T. (2004). Targeting cytotoxic T lymphocytes for cancer immunotherapy. *Br J Cancer* **91**, 817-21.

Mancao, C. & Hammerschmidt, W. (2007). Epstein-Barr virus latent membrane protein 2A is a B-cell receptor mimic and essential for B-cell survival. *Blood*.

Marshall, D. & Sample, C. (1995). Epstein-Barr virus nuclear antigen 3C is a transcriptional regulator. *J Virol* **69**, 3624-30.

Mayer, A., Francis, R. J., Sharma, S. K., Tolner, B., Springer, C. J., Martin, J., Boxer, G. M., Bell, J., Green, A. J., Hartley, J. A., Cruickshank, C., Wren, J., Chester, K. A. & Begent, R. H. (2006). A phase I study of single administration of antibody-directed enzyme prodrug therapy with the recombinant anti-carcinoembryonic antigen antibody-enzyme fusion protein MFECP1 and a bis-iodo phenol mustard prodrug. *Clin Cancer Res* **12**, 6509-16.

McCafferty, J., Griffiths, A. D., Winter, G. & Chiswell, D. J. (1990). Phage antibodies: filamentous phage displaying antibody variable domains. *Nature* **348**, 552-4.

McLaughlin, P., Grillo-Lopez, A. J., Link, B. K., Levy, R., Czuczman, M. S., Williams, M. E., Heyman, M. R., Bence-Bruckler, I., White, C. A., Cabanillas, F., Jain, V., Ho, A. D., Lister, J., Wey, K., Shen, D. & Dallaire, B. K. (1998). Rituximab chimeric anti-CD20 monoclonal antibody therapy for relapsed indolent lymphoma: half of patients respond to a four-dose treatment program. *J Clin Oncol* **16**, 2825-33.

Meggetto, F., Muller, C., Henry, S., Selves, J., Mariame, B., Brousset, P., Saati, T. A. & Delsol, G. (1996). Epstein-Barr virus (EBV)-associated lymphoproliferations in severe combined immunodeficient mice transplanted with Hodgkin's disease lymph nodes: implications of EBV-positive bystander B lymphocytes rather than EBV-infected Reed-Sternberg cells. *Blood* **87**, 2435-42.

Meidenbauer, N., Marienhagen, J., Laumer, M., Vogl, S., Heymann, J., Andreesen, R. & Mackensen, A. (2003). Survival and tumor localization of adoptively transferred Melan-A-specific T cells in melanoma patients. *J Immunol* **170**, 2161-9.

Miller, A. D., Garcia, J. V., von Suhr, N., Lynch, C. M., Wilson, C. & Eiden, M. V. (1991). Construction and properties of retrovirus packaging cells based on gibbon ape leukemia virus. *J Virol* **65**, 2220-4.

Miller, C. L., Burkhardt, A. L., Lee, J. H., Stealey, B., Longnecker, R., Bolen, J. B. & Kieff, E. (1995). Integral membrane protein 2 of Epstein-Barr virus regulates reactivation from latency through dominant negative effects on protein-tyrosine kinases. *Immunity* **2**, 155-66.

Miller, C. L., Lee, J. H., Kieff, E. & Longnecker, R. (1994). An integral membrane protein (LMP2) blocks reactivation of Epstein-Barr virus from latency following surface immunoglobulin crosslinking. *Proc Natl Acad Sci U S A* **91**, 772-6.

Miller, G., Niederman, J. C. & Andrews, L. L. (1973). Prolonged oropharyngeal excretion of Epstein-Barr virus after infectious mononucleosis. *N Engl J Med* **288**, 229-32.

Miller, G., Shope, T., Lisco, H., Stitt, D. & Lipman, M. (1972). Epstein-Barr virus: transformation, cytopathic changes, and viral antigens in squirrel monkey and marmoset leukocytes. *Proc Natl Acad Sci U S A* **69**, 383-7.

Minguet, S., Swamy, M., Alarcon, B., Luescher, I. F. & Schamel, W. W. (2007). Full activation of the T cell receptor requires both clustering and conformational changes at CD3. *Immunity* **26**, 43-54.

Miyazaki, T., Liu, Z. J., Kawahara, A., Minami, Y., Yamada, K., Tsujimoto, Y., Barsoumian, E. L., Permutter, R. M. & Taniguchi, T. (1995). Three distinct IL-2 signaling pathways mediated by bcl-2, c-myc, and lck cooperate in hematopoietic cell proliferation. *Cell* **81**, 223-31.

Moghaddam, A., Koch, J., Annis, B. & Wang, F. (1998). Infection of human B lymphocytes with lymphocryptoviruses related to Epstein-Barr virus. *J Virol* **72**, 3205-12.

Moghaddam, A., Rosenzweig, M., Lee-Parritz, D., Annis, B., Johnson, R. P. & Wang, F. (1997). An animal model for acute and persistent Epstein-Barr virus infection. *Science* **276**, 2030-3.

Molesworth, S. J., Lake, C. M., Borza, C. M., Turk, S. M. & Hutt-Fletcher, L. M. (2000). Epstein-Barr virus gH is essential for penetration of B cells but also plays a role in attachment of virus to epithelial cells. *J Virol* **74**, 6324-32.

Montagna, D., Maccario, R., Locatelli, F., Rosti, V., Yang, Y., Farness, P., Moretta, A., Comoli, P., Montini, E. & Vitiello, A. (2001). Ex vivo priming for long-term maintenance of antileukemia human cytotoxic T cells suggests a general procedure for adoptive immunotherapy. *Blood* **98**, 3359-66.

Montini, E., Cesana, D., Schmidt, M., Sanvito, F., Ponzoni, M., Bartholomae, C., Sergi Sergi, L., Benedicenti, F., Ambrosi, A., Di Serio, C., Doglioni, C., von Kalle, C. & Naldini, L. (2006). Hematopoietic stem cell gene transfer in a tumor-prone mouse model uncovers low genotoxicity of lentiviral vector integration. *Nat Biotechnol* **24**, 687-96.

Morgan, D. A., Ruscetti, F. W. & Gallo, R. (1976). Selective in vitro growth of T lymphocytes from normal human bone marrows. *Science* **193**, 1007-8.

Morgan, R. A., Dudley, M. E., Wunderlich, J. R., Hughes, M. S., Yang, J. C., Sherry, R. M., Royal, R. E., Topalian, S. L., Kammula, U. S., Restifo, N. P., Zheng, Z., Nahvi, A., de Vries, C. R., Rogers-Freezer, L. J., Mavroukakis, S. A. & Rosenberg, S. A. (2006). Cancer regression in patients after transfer of genetically engineered lymphocytes. *Science* **314**, 126-9.

Mosier, D. E., Gulizia, R. J., Baird, S. M. & Wilson, D. B. (1988). Transfer of a functional human immune system to mice with severe combined immunodeficiency. *Nature* **335**, 256-9.

Moss, D. J., Burrows, S. R., Silins, S. L., Misko, I. & Khanna, R. (2001). The immunology of Epstein-Barr virus infection. *Philos Trans R Soc Lond B Biol Sci* **356**, 475-88.

Murray, R. J., Kurilla, M. G., Brooks, J. M., Thomas, W. A., Rowe, M., Kieff, E. & Rickinson, A. B. (1992). Identification of target antigens for the human cytotoxic T cell response to Epstein-Barr virus (EBV): implications for the immune control of EBV-positive malignancies. *J Exp Med* **176**, 157-68.

Murray, R. J., Kurilla, M. G., Griffin, H. M., Brooks, J. M., Mackett, M., Arrand, J. R., Rowe, M., Burrows, S. R., Moss, D. J., Kieff, E. & et al. (1990). Human cytotoxic T-cell responses against Epstein-Barr virus nuclear antigens demonstrated by using recombinant vaccinia viruses. *Proc Natl Acad Sci U S A* **87**, 2906-10.

Nagy, Z. A., Hubner, B., Lohning, C., Rauchenberger, R., Reiffert, S., Thomassen-Wolf, E., Zahn, S., Leyer, S., Schier, E. M., Zahradnik, A., Brunner, C., Lobenwein, K., Rattel, B., Stanglmaier, M., Hallek, M., Wing, M., Anderson,

S., Dunn, M., Kretzschmar, T. & Tesar, M. (2002). Fully human, HLA-DR-specific monoclonal antibodies efficiently induce programmed death of malignant lymphoid cells. *Nat Med* **8**, 801-7.

Nakamura, S., Ueki, T., Yao, T., Ueyama, T. & Tsuneyoshi, M. (1994). Epstein-Barr virus in gastric carcinoma with lymphoid stroma. Special reference to its detection by the polymerase chain reaction and in situ hybridization in 99 tumors, including a morphologic analysis. *Cancer* **73**, 2239-49.

Nalesnik, M. A. (2001). The diverse pathology of post-transplant lymphoproliferative disorders: the importance of a standardized approach. *Transpl Infect Dis* **3**, 88-96.

Nanbo, A., Inoue, K., Adachi-Takasawa, K. & Takada, K. (2002). Epstein-Barr virus RNA confers resistance to interferon-alpha-induced apoptosis in Burkitt's lymphoma. *Embo J* **21**, 954-65.

Nemerow, G. R., Mold, C., Schwend, V. K., Tollefson, V. & Cooper, N. R. (1987). Identification of gp350 as the viral glycoprotein mediating attachment of Epstein-Barr virus (EBV) to the EBV/C3d receptor of B cells: sequence homology of gp350 and C3 complement fragment C3d. *J Virol* **61**, 1416-20.

Neri, A., Barriga, F., Inghirami, G., Knowles, D. M., Neequaye, J., Magrath, I. T. & Dalla-Favera, R. (1991). Epstein-Barr virus infection precedes clonal expansion in Burkitt's and acquired immunodeficiency syndrome-associated lymphoma. *Blood* **77**, 1092-5.

Newcom, S. R. & Gu, L. (1995). Transforming growth factor beta 1 messenger RNA in Reed-Sternberg cells in nodular sclerosing Hodgkin's disease. *J Clin Pathol* **48**, 160-3.

Nicholson, L. J., Hopwood, P., Johannessen, I., Salisbury, J. R., Codd, J., Thorley-Lawson, D. & Crawford, D. H. (1997). Epstein-Barr virus latent membrane protein does not inhibit differentiation and induces tumorigenicity of human epithelial cells. *Oncogene* **15**, 275-83.

Niederman, J. C., Evans, A. S., Subrahmanyan, L. & McCollum, R. W. (1970). Prevalence, incidence and persistence of EB virus antibody in young adults. *N Engl J Med* **282**, 361-5.

Oertel, S. H., Papp-Vary, M., Anagnostopoulos, I., Hummel, M. W., Jonas, S. & Riess, H. B. (2003). Salvage chemotherapy for refractory or relapsed post-transplant lymphoproliferative disorder in patients after solid organ transplantation with a combination of carboplatin and etoposide. *Br J Haematol* **123**, 830-5.

Ogden, C. A., Pound, J. D., Batth, B. K., Owens, S., Johannessen, I., Wood, K. & Gregory, C. D. (2005). Enhanced apoptotic cell clearance capacity and B cell survival factor production by IL-10-activated macrophages: implications for Burkitt's lymphoma. *J Immunol* **174**, 3015-23.

Oh, S. T., Cha, J. H., Shin, D. J., Yoon, S. K. & Lee, S. K. (2007). Establishment and characterization of an in vivo model for Epstein-Barr virus positive gastric carcinoma. *J Med Virol* **79**, 1343-8.

Okano, M., Matsumoto, S., Osato, T., Sakiyama, Y., Thiele, G. M. & Purtilo, D. T. (1991). Severe chronic active Epstein-Barr virus infection syndrome. *Clin Microbiol Rev* **4**, 129-35.

Orentas, R. J., Roskopf, S. J., Nolan, G. P. & Nishimura, M. I. (2001). Retroviral transduction of a T cell receptor specific for an Epstein-Barr virus-encoded peptide. *Clinical Immunology* **98**, 220-8.

OrthoGroup (1985). A randomized clinical trial of OKT3 monoclonal antibody for acute rejection of cadaveric renal transplants. Ortho Multicenter Transplant Study Group *N Engl J Med* **313**, 337-42.

Paludan, C., Bickham, K., Nikiforow, S., Tsang, M. L., Goodman, K., Hanekom, W. A., Fonteneau, J. F., Stevanovi, S. & Munz, C. (2002). Epstein-Barr nuclear antigen 1-specific CD4(+) Th1 cells kill Burkitt's lymphoma cells. *Journal of Immunology* **169**, 1593-603.

Papadopoulos, E. B., Ladanyi, M., Emanuel, D., Mackinnon, S., Boulad, F., Carabasi, M. H., Castro-Malaspina, H., Childs, B. H., Gillio, A. P., Small, T. N. & et al. (1994). Infusions of donor leukocytes to treat Epstein-Barr virus-associated lymphoproliferative disorders after allogeneic bone marrow transplantation. *N Engl J Med* **330**, 1185-91.

Park, J. R., Digiusto, D. L., Slovak, M., Wright, C., Naranjo, A., Wagner, J., Meechoovet, H. B., Bautista, C., Chang, W. C., Ostberg, J. R. & Jensen, M. C. (2007). Adoptive transfer of chimeric antigen receptor re-directed cytolytic T lymphocyte clones in patients with neuroblastoma. *Mol Ther* **15**, 825-33.

Paschke, M. (2006). Phage display systems and their applications. *Appl Microbiol Biotechnol* **70**, 2-11.

Pedneault, L., Lapointe, N., Alfieri, C., Ghadirian, P., Carpentier, L., Samson, J. & Joncas, J. (1996). Antibody responses to two Epstein-Barr virus (EBV) nuclear antigens (EBNA-1 and EBNA-2) during EBV primary infection in children born to mothers infected with human immunodeficiency virus. *Clin Infect Dis* **23**, 806-8.

Pegtel, D. M., Middeldorp, J. & Thorley-Lawson, D. A. (2004). Epstein-Barr virus infection in ex vivo tonsil epithelial cell cultures of asymptomatic carriers. *J Virol* **78**, 12613-24.

Pellett, P. & Roizman, B. (2007). The family Herpesviridae: A brief introduction. In *Fields Virology*, 5th edn, pp. 2479-2499. Edited by D. Knipe & P. Howley. Philadelphia: Lippincott Williams and Wilkins.

Perera, S. M., Thomas, J. A., Burke, M. & Crawford, D. H. (1998). Analysis of the T-cell micro-environment in Epstein-Barr virus-related post-transplantation B lymphoproliferative disease. *J Pathol* **184**, 177-84.

Perry, M. & Whyte, A. (1998). Immunology of the tonsils. *Immunol Today* **19**, 414-21.

Phan, G. Q., Yang, J. C., Sherry, R. M., Hwu, P., Topalian, S. L., Schwartzentruber, D. J., Restifo, N. P., Haworth, L. R., Seipp, C. A., Freezer, L. J., Morton, K. E., Mavroukakis, S. A., Duray, P. H., Steinberg, S. M., Allison, J. P., Davis, T. A. & Rosenberg, S. A. (2003). Cancer regression and autoimmunity induced by cytotoxic T lymphocyte-associated antigen 4 blockade in patients with metastatic melanoma. *Proc Natl Acad Sci U S A* **100**, 8372-7.

Pingel, S., Hannig, H., Matz-Rensing, K., Kaup, F. J., Hunsmann, G. & Bodemer, W. (1997). Detection of Epstein-Barr virus small RNAs EBER1 and EBER2 in lymphomas of SIV-infected rhesus monkeys by in situ hybridization. *Int J Cancer* **72**, 160-5.

Piro, L. D., White, C. A., Grillo-Lopez, A. J., Janakiraman, N., Saven, A., Beck, T. M., Varns, C., Shuey, S., Czuczman, M., Lynch, J. W., Kolitz, J. E. & Jain, V. (1999). Extended Rituximab (anti-CD20 monoclonal antibody) therapy for relapsed or refractory low-grade or follicular non-Hodgkin's lymphoma. *Ann Oncol* **10**, 655-61.

Pitcher, L. A. & van Oers, N. S. (2003). T-cell receptor signal transmission: who gives an ITAM? *Trends Immunol* **24**, 554-60.
Pope, J. H., Horne, M. K. & Scott, W. (1968). Transformation of foetal human keukocytes in vitro by filtrates of a human leukaemic cell line containing herpes-like virus. *Int J Cancer* **3**, 857-66.
Poppema, S. (2005). Immunobiology and pathophysiology of hodgkin lymphomas. *Hematology Am Soc Hematol Educ Program*, 231-8.
Precopio, M. L., Sullivan, J. L., Willard, C., Somasundaran, M. & Luzuriaga, K. (2003). Differential kinetics and specificity of EBV-specific CD4+ and CD8+ T cells during primary infection. *J Immunol* **170**, 2590-8.
Puglielli, M. T., Desai, N. & Speck, S. H. (1997). Regulation of EBNA gene transcription in lymphoblastoid cell lines: characterization of sequences downstream of BCR2 (Cp). *J Virol* **71**, 120-8.
Pule, M. A., Straathof, K. C., Dotti, G., Heslop, H. E., Rooney, C. M. & Brenner, M. K. (2005). A chimeric T cell antigen receptor that augments cytokine release and supports clonal expansion of primary human T cells. *Molecular Therapy: the Journal of the American Society of Gene Therapy* **12**, 933-41.
Pulvertaft, J. V. (1964). Cytology of Burkitt's Tumour (African Lymphoma). *Lancet* **39**, 238-40.
Raab-Traub, N. & Flynn, K. (1986). The structure of the termini of the Epstein-Barr virus as a marker of clonal cellular proliferation. *Cell* **47**, 883-9.
Radkov, S. A., Touitou, R., Brehm, A., Rowe, M., West, M., Kouzarides, T. & Allday, M. J. (1999). Epstein-Barr virus nuclear antigen 3C interacts with histone deacetylase to repress transcription. *J Virol* **73**, 5688-97.
Rasheed, S., Nelson-Rees, W. A., Toth, E. M., Arnstein, P. & Gardner, M. B. (1974). Characterization of a newly derived human sarcoma cell line (HT-1080). *Cancer* **33**, 1027-33.
Reedman, B. M. & Klein, G. (1973). Cellular localization of an Epstein-Barr virus (EBV)-associated complement-fixing antigen in producer and non-producer lymphoblastoid cell lines. *Int J Cancer* **11**, 499-520.
Rickinson, A. B. & Kieff, E. (2007). Epstein-Barr Virus. In *Fields Virology*, 5th edn, pp. 2655-2700. Edited by D. Knipe & P. Howley. Philadelphia
Lippincott Williams and Wilkins.
Rickinson, A. B. & Moss, D. J. (1997). Human cytotoxic T lymphocyte responses to Epstein-Barr virus infection. *Annu Rev Immunol* **15**, 405-31.
Rickinson, A. B., Young, L. S. & Rowe, M. (1987). Influence of the Epstein-Barr virus nuclear antigen EBNA 2 on the growth phenotype of virus-transformed B cells. *J Virol* **61**, 1310-7.
Riddell, S. R., Watanabe, K. S., Goodrich, J. M., Li, C. R., Agha, M. E. & Greenberg, P. D. (1992). Restoration of viral immunity in immunodeficient humans by the adoptive transfer of T cell clones. *Science* **257**, 238-41.
Robertson, E. S., Lin, J. & Kieff, E. (1996). The amino-terminal domains of Epstein-Barr virus nuclear proteins 3A, 3B, and 3C interact with RBPJ(kappa). *J Virol* **70**, 3068-74.
Roizman, B. & Baines, J. (1991). The diversity and unity of Herpesviridae. *Comp Immunol Microbiol Infect Dis* **14**, 63-79.
Roizman, B., Carmichael, L. E., Deinhardt, F., de-The, G., Nahmias, A. J., Plowright, W., Rapp, F., Sheldrick, P., Takahashi, M. & Wolf, K. (1981). Herpesviridae. Definition, provisional nomenclature, and taxonomy. The

Herpesvirus Study Group, the International Committee on Taxonomy of Viruses. *Intervirology* **16**, 201-17.

Roizman, B., Desrosiers, R. C., Fleckenstein, B., Lopez, C., Minson, A. C. & Studdert, M. J. (1992). The family Herpesviridae: an update. The Herpesvirus Study Group of the International Committee on Taxonomy of Viruses. *Arch Virol* **123**, 425-49.

Romond, E. H., Perez, E. A., Bryant, J., Suman, V. J., Geyer, C. E., Jr., Davidson, N. E., Tan-Chiu, E., Martino, S., Paik, S., Kaufman, P. A., Swain, S. M., Pisansky, T. M., Fehrenbacher, L., Kutteh, L. A., Vogel, V. G., Visscher, D. W., Yothers, G., Jenkins, R. B., Brown, A. M., Dakhil, S. R., Mamounas, E. P., Lingle, W. L., Klein, P. M., Ingle, J. N. & Wolmark, N. (2005). Trastuzumab plus adjuvant chemotherapy for operable HER2-positive breast cancer. *N Engl J Med* **353**, 1673-84.

Rooney, C. M., Smith, C. A., Ng, C. Y., Loftin, S., Li, C., Krance, R. A., Brenner, M. K. & Heslop, H. E. (1995). Use of gene-modified virus-specific T lymphocytes to control Epstein-Barr-virus-related lymphoproliferation. *Lancet* **345**, 9-13.

Rooney, C. M., Smith, C. A., Ng, C. Y., Loftin, S. K., Sixbey, J. W., Gan, Y., Srivastava, D. K., Bowman, L. C., Krance, R. A., Brenner, M. K. & Heslop, H. E. (1998). Infusion of cytotoxic T cells for the prevention and treatment of Epstein-Barr virus-induced lymphoma in allogeneic transplant recipients. *Blood* **92**, 1549-55.

Rosenberg, S. A. & Dudley, M. E. (2004). Cancer regression in patients with metastatic melanoma after the transfer of autologous antitumor lymphocytes. *Proc Natl Acad Sci U S A* **101 Suppl 2**, 14639-45.

Rowe, M., Lear, A. L., Croom-Carter, D., Davies, A. H. & Rickinson, A. B. (1992). Three pathways of Epstein-Barr virus gene activation from EBNA1-positive latency in B lymphocytes. *J Virol* **66**, 122-31.

Rowe, M., Young, L. S., Crocker, J., Stokes, H., Henderson, S. & Rickinson, A. B. (1991). Epstein-Barr virus (EBV)-associated lymphoproliferative disease in the SCID mouse model: implications for the pathogenesis of EBV-positive lymphomas in man. *J Exp Med* **173**, 147-58.

Rudolph, M. G., Stanfield, R. L. & Wilson, I. A. (2006). How TCRs bind MHCs, peptides, and coreceptors. *Annu Rev Immunol* **24**, 419-66.

Ruf, I. K., Rhyne, P. W., Yang, C., Cleveland, J. L. & Sample, J. T. (2000). Epstein-Barr virus small RNAs potentiate tumorigenicity of Burkitt lymphoma cells independently of an effect on apoptosis. *J Virol* **74**, 10223-8.

Ruggeri, L., Capanni, M., Urbani, E., Perruccio, K., Shlomchik, W. D., Tosti, A., Posati, S., Rogaia, D., Frassoni, F., Aversa, F., Martelli, M. F. & Velardi, A. (2002). Effectiveness of donor natural killer cell alloreactivity in mismatched hematopoietic transplants. *Science* **295**, 2097-100.

Russel, M., Kidd, S. & Kelley, M. R. (1986). An improved filamentous helper phage for generating single-stranded plasmid DNA. *Gene* **45**, 333-8.

Sample, J., Liebowitz, D. & Kieff, E. (1989). Two related Epstein-Barr virus membrane proteins are encoded by separate genes. *J Virol* **63**, 933-7.

Sausville, E. A. & Burger, A. M. (2006). Contributions of human tumor xenografts to anticancer drug development. *Cancer Res* **66**, 3351-4, discussion 3354.

Savard, M., Belanger, C., Tardif, M., Gourde, P., Flamand, L. & Gosselin, J. (2000). Infection of primary human monocytes by Epstein-Barr virus. *J Virol* **74**, 2612-9.

Savoldo, B., Rooney, C. M., Di Stasi, A., Abken, H., Hombach, A., Foster, A. E., Zhang, L., Heslop, H. E., Brenner, M. K. & Dotti, G. (2007). Epstein barr virus-specific cytotoxic T lymphocytes expressing the anti-CD30{zeta} artificial chimeric T-cell receptor for immunotherapy of Hodgkin's disease. *Blood*.

Sawyer, R. N., Evans, A. S., Niederman, J. C. & McCollum, R. W. (1971). Prospective studies of a group of Yale University freshmen. I. Occurrence of infectious mononucleosis. *J Infect Dis* **123**, 263-70.

Sayos, J., Wu, C., Morra, M., Wang, N., Zhang, X., Allen, D., van Schaik, S., Notarangelo, L., Geha, R., Roncarolo, M. G., Oettgen, H., De Vries, J. E., Aversa, G. & Terhorst, C. (1998). The X-linked lymphoproliferative-disease gene product SAP regulates signals induced through the co-receptor SLAM. *Nature* **395**, 462-9.

Schluns, K. S., Kieper, W. C., Jameson, S. C. & Lefrancois, L. (2000). Interleukin-7 mediates the homeostasis of naive and memory CD8 T cells in vivo. *Nat Immunol* **1**, 426-32.

Schmid, C., Pan, L., Diss, T. & Isaacson, P. G. (1991). Expression of B-cell antigens by Hodgkin's and Reed-Sternberg cells. *Am J Pathol* **139**, 701-7.

Scholle, F., Bendt, K. M. & Raab-Traub, N. (2000). Epstein-Barr virus LMP2A transforms epithelial cells, inhibits cell differentiation, and activates Akt. *J Virol* **74**, 10681-9.

Schuler, W., Weiler, I. J., Schuler, A., Phillips, R. A., Rosenberg, N., Mak, T. W., Kearney, J. F., Perry, R. P. & Bosma, M. J. (1986). Rearrangement of antigen receptor genes is defective in mice with severe combined immune deficiency. *Cell* **46**, 963-72.

Schwering, I., Brauninger, A., Klein, U., Jungnickel, B., Tinguely, M., Diehl, V., Hansmann, M. L., Dalla-Favera, R., Rajewsky, K. & Kuppers, R. (2003). Loss of the B-lineage-specific gene expression program in Hodgkin and Reed-Sternberg cells of Hodgkin lymphoma. *Blood* **101**, 1505-12.

Scott, A. M., Wiseman, G., Welt, S., Adjei, A., Lee, F. T., Hopkins, W., Divgi, C. R., Hanson, L. H., Mitchell, P., Gansen, D. N., Larson, S. M., Ingle, J. N., Hoffman, E. W., Tanswell, P., Ritter, G., Cohen, L. S., Bette, P., Arvay, L., Amelsberg, A., Vlock, D., Rettig, W. J. & Old, L. J. (2003). A Phase I dose-escalation study of sibrotuzumab in patients with advanced or metastatic fibroblast activation protein-positive cancer. *Clin Cancer Res* **9**, 1639-47.

Shannon-Lowe, C. D., Neuhierl, B., Baldwin, G., Rickinson, A. B. & Delecluse, H. J. (2006). Resting B cells as a transfer vehicle for Epstein-Barr virus infection of epithelial cells. *Proc Natl Acad Sci U S A* **103**, 7065-70.

Shaw, D. M., Connolly, N. B., Patel, P. M., Kilany, S., Hedlund, G., Nordle, O., Forsberg, G., Zweit, J., Stern, P. L. & Hawkins, R. E. (2007). A phase II study of a 5T4 oncofoetal antigen tumour-targeted superantigen (ABR-214936) therapy in patients with advanced renal cell carcinoma. *Br J Cancer* **96**, 567-74.

Shibata, D. & Weiss, L. M. (1992). Epstein-Barr virus-associated gastric adenocarcinoma. *Am J Pathol* **140**, 769-74.

Shimakage, M., Kimura, M., Yanoma, S., Ibe, M., Yokota, S., Tsujino, G., Kozuka, T., Dezawa, T., Tamura, S., Ohshima, A., Yutsudo, M. & Hakura, A. (1999). Expression of latent and replicative-infection genes of Epstein-Barr virus in macrophage. *Arch Virol* **144**, 157-66.

Shimizu, N., Yoshiyama, H. & Takada, K. (1996). Clonal propagation of Epstein-Barr virus (EBV) recombinants in EBV-negative Akata cells. *Journal of Virology* **70**, 7260-3.

Shope, T., Dechairo, D. & Miller, G. (1973). Malignant lymphoma in cottontop marmosets after inoculation with Epstein-Barr virus. *Proc Natl Acad Sci U S A* **70**, 2487-91.

Shultz, L. D., Schweitzer, P. A., Christianson, S. W., Gott, B., Schweitzer, I. B., Tennent, B., McKenna, S., Mobraaten, L., Rajan, T. V., Greiner, D. L. & et al. (1995). Multiple defects in innate and adaptive immunologic function in NOD/LtSz-scid mice. *J Immunol* **154**, 180-91.

Silacci, M., Brack, S., Schirru, G., Marlind, J., Ettorre, A., Merlo, A., Viti, F. & Neri, D. (2005). Design, construction, and characterization of a large synthetic human antibody phage display library. *Proteomics* **5**, 2340-50.

Silins, S. L. & Sculley, T. B. (1994). Modulation of vimentin, the CD40 activation antigen and Burkitt's lymphoma antigen (CD77) by the Epstein-Barr virus nuclear antigen EBNA-4. *Virology* **202**, 16-24.

Slamon, D. J., Clark, G. M., Wong, S. G., Levin, W. J., Ullrich, A. & McGuire, W. L. (1987). Human breast cancer: correlation of relapse and survival with amplification of the HER-2/neu oncogene. *Science* **235**, 177-82.

Smith, G. P. (1985). Filamentous fusion phage: novel expression vectors that display cloned antigens on the virion surface. *Science* **228**, 1315-7.

Smith, M. R. (2003). Rituximab (monoclonal anti-CD20 antibody): mechanisms of action and resistance. *Oncogene* **22**, 7359-68.

Spriggs, M. K., Armitage, R. J., Comeau, M. R., Strockbine, L., Farrah, T., Macduff, B., Ulrich, D., Alderson, M. R., Mullberg, J. & Cohen, J. I. (1996). The extracellular domain of the Epstein-Barr virus BZLF2 protein binds the HLA-DR beta chain and inhibits antigen presentation. *J Virol* **70**, 5557-63.

Steel, C. M., Philipson, J., Arthur, E., Gardiner, S. E., Newton, M. S. & McIntosh, R. V. (1977). Possibility of EB virus preferentially transforming a subpopulation of human B lymphocytes. *Nature* **270**, 729-31.

Steven, N. M., Annels, N. E., Kumar, A., Leese, A. M., Kurilla, M. G. & Rickinson, A. B. (1997). Immediate early and early lytic cycle proteins are frequent targets of the Epstein-Barr virus-induced cytotoxic T cell response. *J Exp Med* **185**, 1605-17.

Straathof, K. C., Bollard, C. M., Popat, U., Huls, M. H., Lopez, T., Morriss, M. C., Gresik, M. V., Gee, A. P., Russell, H. V., Brenner, M. K., Rooney, C. M. & Heslop, H. E. (2005a). Treatment of nasopharyngeal carcinoma with Epstein-Barr virus--specific T lymphocytes. *Blood* **105**, 1898-904.

Straathof, K. C., Bollard, C. M., Rooney, C. M. & Heslop, H. E. (2003). Immunotherapy for Epstein-Barr virus-associated cancers in children. *Oncologist* **8**, 83-98.

Straathof, K. C., Pule, M. A., Yotnda, P., Dotti, G., Vanin, E. F., Brenner, M. K., Heslop, H. E., Spencer, D. M. & Rooney, C. M. (2005b). An inducible caspase 9 safety switch for T-cell therapy. *Blood* **105**, 4247-54.

Sugden, B., Phelps, M. & Domoradzki, J. (1979). Epstein-Barr virus DNA is amplified in transformed lymphocytes. *J Virol* **31**, 590-5.

Sugiura, M., Imai, S., Tokunaga, M., Koizumi, S., Uchizawa, M., Okamoto, K. & Osato, T. (1996). Transcriptional analysis of Epstein-Barr virus gene expression in EBV-positive gastric carcinoma: unique viral latency in the tumour cells. *Br J Cancer* **74**, 625-31.

Sun, Q., Brewer, N., Dunham, K., Chen, L., Bao, L., Burton, R. & Lucas, K. G. (2007). Interferon-gamma expressing EBV LMP2A-specific T cells for cellular immunotherapy. *Cell Immunol* **246**, 81-91.

Sun, Q., Burton, R. L. & Lucas, K. G. (2002). Cytokine production and cytolytic mechanism of CD4(+) cytotoxic T lymphocytes in ex vivo expanded therapeutic Epstein-Barr virus-specific T-cell cultures. *Blood* **99**, 3302-9.

Sunil-Chandra, N. P., Efstathiou, S., Arno, J. & Nash, A. A. (1992a). Virological and pathological features of mice infected with murine gamma-herpesvirus 68. *J Gen Virol* **73 (Pt 9)**, 2347-56.

Sunil-Chandra, N. P., Efstathiou, S. & Nash, A. A. (1992b). Murine gammaherpesvirus 68 establishes a latent infection in mouse B lymphocytes in vivo. *J Gen Virol* **73 (Pt 12)**, 3275-9.

Suntharalingam, G., Perry, M. R., Ward, S., Brett, S. J., Castello-Cortes, A., Brunner, M. D. & Panoskaltsis, N. (2006). Cytokine storm in a phase 1 trial of the anti-CD28 monoclonal antibody TGN1412. *N Engl J Med* **355**, 1018-28.

Swaminathan, S., Tomkinson, B. & Kieff, E. (1991). Recombinant Epstein-Barr virus with small RNA (EBER) genes deleted transforms lymphocytes and replicates in vitro. *Proc Natl Acad Sci U S A* **88**, 1546-50.

Takada, K. (2000). Epstein-Barr virus and gastric carcinoma. *Mol Pathol* **53**, 255-61.

Tan, L. C., Gudgeon, N., Annels, N. E., Hansasuta, P., O'Callaghan, C. A., Rowland-Jones, S., McMichael, A. J., Rickinson, A. B. & Callan, M. F. (1999). A re-evaluation of the frequency of CD8+ T cells specific for EBV in healthy virus carriers. *J Immunol* **162**, 1827-35.

Tanner, J., Weis, J., Fearon, D., Whang, Y. & Kieff, E. (1987). Epstein-Barr virus gp350/220 binding to the B lymphocyte C3d receptor mediates adsorption, capping, and endocytosis. *Cell* **50**, 203-13.

Tao, Q., Robertson, K. D., Manns, A., Hildesheim, A. & Ambinder, R. F. (1998). Epstein-Barr virus (EBV) in endemic Burkitt's lymphoma: molecular analysis of primary tumor tissue. *Blood* **91**, 1373-81.

Taylor, A. L., Marcus, R. & Bradley, J. A. (2005). Post-transplant lymphoproliferative disorders (PTLD) after solid organ transplantation. *Crit Rev Oncol Hematol* **56**, 155-67.

Tey, S. K., Bollard, C. M. & Heslop, H. E. (2006). Adoptive T-cell transfer in cancer immunotherapy. *Immunol Cell Biol* **84**, 281-9.

Tey, S. K., Dotti, G., Rooney, C. M., Heslop, H. E. & Brenner, M. K. (2007). Inducible caspase 9 suicide gene to improve the safety of allodepleted T cells after haploidentical stem cell transplantation. *Biol Blood Marrow Transplant* **13**, 913-24.

Thomas, J. A., Felix, D. H., Wray, D., Southam, J. C., Cubie, H. A. & Crawford, D. H. (1991). Epstein-Barr virus gene expression and epithelial cell differentiation in oral hairy leukoplakia. *Am J Pathol* **139**, 1369-80.

Thomas, J. A., Hotchin, N. A., Allday, M. J., Amlot, P., Rose, M., Yacoub, M. & Crawford, D. H. (1990). Immunohistology of Epstein-Barr virus-associated antigens in B cell disorders from immunocompromised individuals. *Transplantation* **49**, 944-53.

Thompson, C. B. & Allison, J. P. (1997). The emerging role of CTLA-4 as an immune attenuator. *Immunity* **7**, 445-50.

Thorley-Lawson, D. A. & Geilinger, K. (1980). Monoclonal antibodies against the major glycoprotein (gp350/220) of Epstein-Barr virus neutralize infectivity. *Proc Natl Acad Sci U S A* **77**, 5307-11.

Thorley-Lawson, D. A. & Gross, A. (2004). Persistence of the Epstein-Barr virus and the origins of associated lymphomas.[see comment]. *New England Journal of Medicine* **350**, 1328-37.

Thorley-Lawson, D. A. & Poodry, C. A. (1982). Identification and isolation of the main component (gp350-gp220) of Epstein-Barr virus responsible for generating neutralizing antibodies in vivo. *J Virol* **43**, 730-6.

Timms, J. M., Bell, A., Flavell, J. R., Murray, P. G., Rickinson, A. B., Traverse-Glehen, A., Berger, F. & Delecluse, H. J. (2003). Target cells of Epstein-Barr-virus (EBV)-positive post-transplant lymphoproliferative disease: similarities to EBV-positive Hodgkin's lymphoma. *Lancet* **361**, 217-23.

Tomkinson, B., Robertson, E. & Kieff, E. (1993). Epstein-Barr virus nuclear proteins EBNA-3A and EBNA-3C are essential for B-lymphocyte growth transformation. *J Virol* **67**, 2014-25.

Tosato, G., Blaese, R. M. & Yarchoan, R. (1985). Relationship between immunoglobulin production and immortalization by Epstein Barr virus. *J Immunol* **135**, 959-64.

Tugizov, S., Herrera, R., Veluppillai, P., Greenspan, J., Greenspan, D. & Palefsky, J. M. (2007). Epstein-Barr virus (EBV)-infected monocytes facilitate dissemination of EBV within the oral mucosal epithelium. *J Virol* **81**, 5484-96.

Tugizov, S. M., Berline, J. W. & Palefsky, J. M. (2003). Epstein-Barr virus infection of polarized tongue and nasopharyngeal epithelial cells. *Nat Med* **9**, 307-14.

Uchida, J., Yasui, T., Takaoka-Shichijo, Y., Muraoka, M., Kulwichit, W., Raab-Traub, N. & Kikutani, H. (1999). Mimicry of CD40 signals by Epstein-Barr virus LMP1 in B lymphocyte responses. *Science* **286**, 300-3.

van den Berg, A., Visser, L. & Poppema, S. (1999). High expression of the CC chemokine TARC in Reed-Sternberg cells. A possible explanation for the characteristic T-cell infiltratein Hodgkin's lymphoma. *Am J Pathol* **154**, 1685-91.

van Elsas, A., Hurwitz, A. A. & Allison, J. P. (1999). Combination immunotherapy of B16 melanoma using anti-cytotoxic T lymphocyte-associated antigen 4 (CTLA-4) and granulocyte/macrophage colony-stimulating factor (GM-CSF)-producing vaccines induces rejection of subcutaneous and metastatic tumors accompanied by autoimmune depigmentation. *J Exp Med* **190**, 355-66.

Vanhoutte, V. J. (2006). The characterisation of ex vivo generated Epstein-Barr virus-specific cytotoxic T-cell lines. In *Department of Medical Microbiology*. Edinburgh: University of Edinburgh.

Verschuuren, E. A., Stevens, S. J., van Imhoff, G. W., Middeldorp, J. M., de Boer, C., Koeter, G., The, T. H. & van Der Bij, W. (2002). Treatment of posttransplant lymphoproliferative disease with rituximab: the remission, the relapse, and the complication. *Transplantation* **73**, 100-4.

Vockerodt, M., Belge, G., Kube, D., Irsch, J., Siebert, R., Tesch, H., Diehl, V., Wolf, J., Bullerdiek, J. & Staratschek-Jox, A. (2002). An unbalanced translocation involving chromosome 14 is the probable cause for loss of potentially functional rearranged immunoglobulin heavy chain genes in the Epstein-Barr virus-positive Hodgkin's lymphoma-derived cell line L591. *Br J Haematol* **119**, 640-6.

Vogel, C. L., Cobleigh, M. A., Tripathy, D., Gutheil, J. C., Harris, L. N., Fehrenbacher, L., Slamon, D. J., Murphy, M., Novotny, W. F., Burchmore,

M., Shak, S., Stewart, S. J. & Press, M. (2002). Efficacy and safety of trastuzumab as a single agent in first-line treatment of HER2-overexpressing metastatic breast cancer. *J Clin Oncol* **20**, 719-26.

von Kalle, C., Wolf, J., Becker, A., Sckaer, A., Munck, M., Engert, A., Kapp, U., Fonatsch, C., Komitowski, D., Feaux de Lacroix, W. & et al. (1992). Growth of Hodgkin cell lines in severely combined immunodeficient mice. *Int J Cancer* **52**, 887-91.

Voo, K. S., Fu, T., Heslop, H. E., Brenner, M. K., Rooney, C. M. & Wang, R. F. (2002). Identification of HLA-DP3-restricted peptides from EBNA1 recognized by CD4(+) T cells. *Cancer Res* **62**, 7195-9.

Walling, D. M., Ray, A. J., Nichols, J. E., Flaitz, C. M. & Nichols, C. M. (2007). Epstein-Barr virus infection of Langerhans cell precursors as a mechanism of oral epithelial entry, persistence, and reactivation. *J Virol* **81**, 7249-68.

Wang, D., Liebowitz, D., Wang, F., Gregory, C., Rickinson, A., Larson, R., Springer, T. & Kieff, E. (1988). Epstein-Barr virus latent infection membrane protein alters the human B-lymphocyte phenotype: deletion of the amino terminus abolishes activity. *J Virol* **62**, 4173-84.

Wang, F., Gregory, C., Sample, C., Rowe, M., Liebowitz, D., Murray, R., Rickinson, A. & Kieff, E. (1990a). Epstein-Barr virus latent membrane protein (LMP1) and nuclear proteins 2 and 3C are effectors of phenotypic changes in B lymphocytes: EBNA-2 and LMP1 cooperatively induce CD23. *J Virol* **64**, 2309-18.

Wang, F., Kikutani, H., Tsang, S. F., Kishimoto, T. & Kieff, E. (1991). Epstein-Barr virus nuclear protein 2 transactivates a cis-acting CD23 DNA element. *J Virol* **65**, 4101-6.

Wang, F., Rivailler, P., Rao, P. & Cho, Y. (2001). Simian homologues of Epstein-Barr virus. *Philos Trans R Soc Lond B Biol Sci* **356**, 489-97.

Wang, F., Tsang, S. F., Kurilla, M. G., Cohen, J. I. & Kieff, E. (1990b). Epstein-Barr virus nuclear antigen 2 transactivates latent membrane protein LMP1. *J Virol* **64**, 3407-16.

Wang, X. & Hutt-Fletcher, L. M. (1998). Epstein-Barr virus lacking glycoprotein gp42 can bind to B cells but is not able to infect. *J Virol* **72**, 158-63.

Wedderburn, N., Edwards, J. M., Desgranges, C., Fontaine, C., Cohen, B. & de The, G. (1984). Infectious mononucleosis-like response in common marmosets infected with Epstein-Barr virus. *J Infect Dis* **150**, 878-82.

Wei, W. I. & Sham, J. S. (2005). Nasopharyngeal carcinoma. *Lancet* **365**, 2041-54.

Weijtens, M. E., Hart, E. H. & Bolhuis, R. L. (2000). Functional balance between T cell chimeric receptor density and tumor associated antigen density: CTL mediated cytolysis and lymphokine production. *Gene Ther* **7**, 35-42.

Weis, J. J., Tedder, T. F. & Fearon, D. T. (1984). Identification of a 145,000 Mr membrane protein as the C3d receptor (CR2) of human B lymphocytes. *Proc Natl Acad Sci U S A* **81**, 881-5.

Whittle, H. C., Brown, J., Marsh, K., Greenwood, B. M., Seidelin, P., Tighe, H. & Wedderburn, L. (1984). T-cell control of Epstein-Barr virus-infected B cells is lost during P. falciparum malaria. *Nature* **312**, 449-50.

Wilkie, G. M., Taylor, C., Jones, M. M., Burns, D. M., Turner, M., Kilpatrick, D., Amlot, P. L., Crawford, D. H. & Haque, T. (2004). Establishment and characterization of a bank of cytotoxic T lymphocytes for immunotherapy of epstein-barr virus-associated diseases. *Journal of Immunotherapy* **27**, 309-16.

Willemsen, R. A., Debets, R., Hart, E., Hoogenboom, H. R., Bolhuis, R. L. & Chames, P. (2001). A phage display selected fab fragment with MHC class I-restricted specificity for MAGE-A1 allows for retargeting of primary human T lymphocytes. *Gene Ther* **8**, 1601-8.

Willemsen, R. A., Weijtens, M. E., Ronteltap, C., Eshhar, Z., Gratama, J. W., Chames, P. & Bolhuis, R. L. (2000). Grafting primary human T lymphocytes with cancer-specific chimeric single chain and two chain TCR. *Gene Ther* **7**, 1369-77.

Williams, H. & Crawford, D. H. (2006). Epstein-Barr virus: the impact of scientific advances on clinical practice. *Blood* **107**, 862-9.

Williams, H., McAulay, K., Macsween, K. F., Gallacher, N. J., Higgins, C. D., Harrison, N., Swerdlow, A. J. & Crawford, D. H. (2005). The immune response to primary EBV infection: a role for natural killer cells. *British Journal of Haematology* **129**, 266-74.

Wilson, J. B., Bell, J. L. & Levine, A. J. (1996). Expression of Epstein-Barr virus nuclear antigen-1 induces B cell neoplasia in transgenic mice. *Embo J* **15**, 3117-26.

Wilson, J. B., Weinberg, W., Johnson, R., Yuspa, S. & Levine, A. J. (1990). Expression of the BNLF-1 oncogene of Epstein-Barr virus in the skin of transgenic mice induces hyperplasia and aberrant expression of keratin 6. *Cell* **61**, 1315-27.

Winkler, U., Gottstein, C., Schon, G., Kapp, U., Wolf, J., Hansmann, M. L., Bohlen, H., Thorpe, P., Diehl, V. & Engert, A. (1994). Successful treatment of disseminated human Hodgkin's disease in SCID mice with deglycosylated ricin A-chain immunotoxins. *Blood* **83**, 466-75.

Winter, G. & Milstein, C. (1991). Man-made antibodies. *Nature* **349**, 293-9.

Woisetschlaeger, M., Strominger, J. L. & Speck, S. H. (1989). Mutually exclusive use of viral promoters in Epstein-Barr virus latently infected lymphocytes. *Proc Natl Acad Sci U S A* **86**, 6498-502.

Woisetschlaeger, M., Yandava, C. N., Furmanski, L. A., Strominger, J. L. & Speck, S. H. (1990). Promoter switching in Epstein-Barr virus during the initial stages of infection of B lymphocytes. *Proc Natl Acad Sci U S A* **87**, 1725-9.

Wolf, J., Kapp, U., Bohlen, H., Kornacker, M., Schoch, C., Stahl, B., Mucke, S., von Kalle, C., Fonatsch, C., Schaefer, H. E., Hansmann, M. L. & Diehl, V. (1996). Peripheral blood mononuclear cells of a patient with advanced Hodgkin's lymphoma give rise to permanently growing Hodgkin-Reed Sternberg cells. *Blood* **87**, 3418-28.

Woo, E. Y., Chu, C. S., Goletz, T. J., Schlienger, K., Yeh, H., Coukos, G., Rubin, S. C., Kaiser, L. R. & June, C. H. (2001). Regulatory CD4(+)CD25(+) T cells in tumors from patients with early-stage non-small cell lung cancer and late-stage ovarian cancer. *Cancer Res* **61**, 4766-72.

Woodcock-Mitchell, J., Eichner, R., Nelson, W. G. & Sun, T. T. (1982). Immunolocalization of keratin polypeptides in human epidermis using monoclonal antibodies. *J Cell Biol* **95**, 580-8.

Wrzesinski, C. & Restifo, N. P. (2005). Less is more: lymphodepletion followed by hematopoietic stem cell transplant augments adoptive T-cell-based anti-tumor immunotherapy. *Curr Opin Immunol* **17**, 195-201.

Wu, A. M. & Senter, P. D. (2005). Arming antibodies: prospects and challenges for immunoconjugates. *Nat Biotechnol* **23**, 1137-46.

Wu, H., Beuerlein, G., Nie, Y., Smith, H., Lee, B. A., Hensler, M., Huse, W. D. & Watkins, J. D. (1998). Stepwise in vitro affinity maturation of Vitaxin, an alphav beta3-specific humanized mAb. *Proc Natl Acad Sci U S A* **95**, 6037-42.

Wu, T. C., Mann, R. B., Charache, P., Hayward, S. D., Staal, S., Lambe, B. C. & Ambinder, R. F. (1990). Detection of EBV gene expression in Reed-Sternberg cells of Hodgkin's disease. *Int J Cancer* **46**, 801-4.

Yao, Q. Y., Rickinson, A. B. & Epstein, M. A. (1985). A re-examination of the Epstein-Barr virus carrier state in healthy seropositive individuals. *Int J Cancer* **35**, 35-42.

Yao, Q. Y., Rowe, M., Martin, B., Young, L. S. & Rickinson, A. B. (1991). The Epstein-Barr virus carrier state: dominance of a single growth-transforming isolate in the blood and in the oropharynx of healthy virus carriers. *J Gen Virol* **72 (Pt 7)**, 1579-90.

Yates, J. L., Warren, N. & Sugden, B. (1985). Stable replication of plasmids derived from Epstein-Barr virus in various mammalian cells. *Nature* **313**, 812-5.

Yee, C., Thompson, J. A., Byrd, D., Riddell, S. R., Roche, P., Celis, E. & Greenberg, P. D. (2002). Adoptive T cell therapy using antigen-specific CD8+ T cell clones for the treatment of patients with metastatic melanoma: in vivo persistence, migration, and antitumor effect of transferred T cells. *Proc Natl Acad Sci U S A* **99**, 16168-73.

Yoshiyama, H., Imai, S., Shimizu, N. & Takada, K. (1997). Epstein-Barr virus infection of human gastric carcinoma cells: implication of the existence of a new virus receptor different from CD21. *J Virol* **71**, 5688-91.

Young, L., Alfieri, C., Hennessy, K., Evans, H., O'Hara, C., Anderson, K. C., Ritz, J., Shapiro, R. S., Rickinson, A., Kieff, E. & et al. (1989a). Expression of Epstein-Barr virus transformation-associated genes in tissues of patients with EBV lymphoproliferative disease. *N Engl J Med* **321**, 1080-5.

Young, L. S., Dawson, C. W., Clark, D., Rupani, H., Busson, P., Tursz, T., Johnson, A. & Rickinson, A. B. (1988). Epstein-Barr virus gene expression in nasopharyngeal carcinoma. *J Gen Virol* **69 (Pt 5)**, 1051-65.

Young, L. S., Finerty, S., Brooks, L., Scullion, F., Rickinson, A. B. & Morgan, A. J. (1989b). Epstein-Barr virus gene expression in malignant lymphomas induced by experimental virus infection of cottontop tamarins. *J Virol* **63**, 1967-74.

Young, L. S. & Murray, P. G. (2003). Epstein-Barr virus and oncogenesis: from latent genes to tumours. *Oncogene* **22**, 5108-21.

Young, L. S. & Rickinson, A. B. (2004). Epstein-Barr virus: 40 years on. *Nature Reviews. Cancer* **4**, 757-68.

Zeng, R., Spolski, R., Finkelstein, S. E., Oh, S., Kovanen, P. E., Hinrichs, C. S., Pise-Masison, C. A., Radonovich, M. F., Brady, J. N., Restifo, N. P., Berzofsky, J. A. & Leonard, W. J. (2005). Synergy of IL-21 and IL-15 in regulating CD8+ T cell expansion and function. *J Exp Med* **201**, 139-48.

Zimber-Strobl, U., Suentzenich, K. O., Laux, G., Eick, D., Cordier, M., Calender, A., Billaud, M., Lenoir, G. M. & Bornkamm, G. W. (1991). Epstein-Barr virus nuclear antigen 2 activates transcription of the terminal protein gene. *J Virol* **65**, 415-23.

Zimber, U., Adldinger, H. K., Lenoir, G. M., Vuillaume, M., Knebel-Doeberitz, M. V., Laux, G., Desgranges, C., Wittmann, P., Freese, U. K., Schneider, U. & et

al. (1986). Geographical prevalence of two types of Epstein-Barr virus. *Virology* **154**, 56-66.

Zur Hausen, A., van Rees, B. P., van Beek, J., Craanen, M. E., Bloemena, E., Offerhaus, G. J., Meijer, C. J. & van den Brule, A. J. (2004). Epstein-Barr virus in gastric carcinomas and gastric stump carcinomas: a late event in gastric carcinogenesis. *J Clin Pathol* **57**, 487-91.